

Copyright  
by  
Justin Martin Keen  
2013

**The Dissertation Committee for Justin Martin Keen Certifies that this is the approved version of the following dissertation:**

**Novel Formulations and Thermal Processes for Bioavailability  
Enhancement of Soluble and Poorly Soluble Drugs**

**Committee:**

---

Robert O. Williams III, Co-Supervisor

---

James W. McGinity, Co-Supervisor

---

Hugh D. C. Smyth

---

Zhengrong Cui

---

Christian P. Whitman

**Novel Formulations and Thermal Processes for Bioavailability  
Enhancement of Soluble and Poorly Soluble Drugs**

**by**

**Justin Martin Keen, B.S.Ch.E**

**Dissertation**

Presented to the Faculty of the Graduate School of

The University of Texas at Austin

in Partial Fulfillment

of the Requirements

for the Degree of

**Doctor of Philosophy**

**The University of Texas at Austin**

**December, 2013**

## **Dedication**

To my wife, Kelly, who has been a constant source of encouragement and support, and to my daughter and source of inspiration, Kinsley.

## **Acknowledgements**

I would like to thank Professors James W. McGinity and Robert. O. Williams III for introducing me to the pharmaceutical sciences as an undergraduate engineering student and helping me secure an internship at a pharmaceutical company. That internship was a stepping stone to my career in the pharmaceutical industry, where I was mentored by a number of excellent scientists, Dr. Lei Shi, Jerry Kimbrough, Tom Shank, Cynthia Jewett, Robert Espinoza, Dr. John J. Koleng, Dr. Michael M. Crowley, Dr. Jason Vaughn and Dr. Feng Zhang; and engineers, Stephen Lermer and Stephen Miller. I would like to acknowledge Dr. James C. DiNunzio, Stephen Miller and Dr. Marcelo Omelczuk for their encouragement to leave industry and continue my education. I would like to thank my friends and former graduates of the program, Dr. Dave A. Miller and Dr. James C. DiNunzio, with whom our many conversations were extremely useful as I narrowed my research goals. I want to thank my supervisors and committee members, Dr. James W. McGinity, Dr. Robert O. Williams III, Dr. Hugh D. C. Smyth, Dr. Zhengrong Cui, and Dr. Christian P. Whitman for their confidence and support. I'm also thankful for Claudia McClelland and Yolanda Abasta for their assistance over the last few years.

I must acknowledge my parents, Charles and Velda Keen, who instilled the values and work ethic that have enabled me to reach my goals. My brother, Jonathan Keen, for his encouragement. I would like to thank my parents and my in-laws, Dr. Karl Kutch, and Dr. Denise Kutch, for all their tremendous and unwavering support. Which came in many forms, including entertaining my daughter when Kelly and I were traveling to conferences or when I was busy in the lab and Kelly needed a break. My wife, Kelly, has

consistently supported and encouraged me during this journey. While completing my research, I have not been around to cover my fair share of tasks associated with raising our young daughter, Kinsley. Yet her strength and love for Kinsley and I are truly wonderful (especially considering she is 9 months pregnant with our son at the time of writing).

To my fellow graduate students in the College of Pharmacy who have come and gone, I would like to thank you. In particular, Dr. Justin R. Hughey who spent considerable time helping me establish my research early on and provided a constant sounding board for ideas. I would also like to acknowledge Justin LaFontaine and Connor J. Foley for all of their research assistance, and Leena Prasad for her enthusiasm involving a yet to be named collaboration. Other current and former students/visiting scientists who I would like to acknowledge include Ryan Bennett, Matt Herpin, Chris Brough, Dr. Kevin O'Donnell, Dr. Bo Lang, Dr. Nicole Nelson, Dr. Helen Dugas, Dr. Simone Carvalho, Dr. Thiago Carvalho, Siyuan Huang, Soraya Hengsawas, Dr. Javier Morales, Askan Yazdi, Youseff Naquib, Michael Sandoval, Dr. Ikumasa Ohno, Dr. Stephanie Bosselmann, Ju Du, Ping Du, Sha Liu, Dr. Alan Watts, Julien Maincent, Nihal Bandara, and Dr. Amit Kumar. You were all great people to work with and to be around.

I would also like to thank my research benefactors with whom I have had many scientific discussions. Dr. Vincent Jannin, Delphine Marchaud, and Yvonne Cuppok from Gattefosse SAS, who also sponsored one of my presentations outside the college. Dr. Kenneth Anderson from Celanese. Dr. James C. DiNunzio from Hoffman La Roche. Charlie Martin from Leistritz America, who contributed equipment and facilities and sponsored an outside presentation. Finally, Dr. Gershon Yaniv, Chris Brough and Dr.

Dave A Miller from DisperSol Technologies deserve a special thanks for their financial support and providing me with post-graduate employment. Not to mention use of their facilities for my research. I would also like to thank Stephanie Mareth, Amy Kimbro, Devin Sarkady, Devon MacDonald, Daniel Ellenberger and Marshall Cisneros for their encouragement and help.

# **Novel Formulations and Thermal Processes for Bioavailability Enhancement of Soluble and Poorly Soluble Drugs**

Justin Martin Keen, Ph.D.

The University of Texas at Austin, 2013

Supervisors: James W. McGinity and Robert O. Williams III

Formulation intervention, through the application of processing technologies, is a requirement for enabling therapy for the vast majority of drugs. Without these enabling technologies, poorly soluble drugs may not achieve therapeutic concentrations in the blood or tissue of interest. Conversely, freely soluble and/or rapidly cleared drugs may require frequent dosing resulting in highly cyclic tissue concentrations. During the last several years, thermal processing techniques, such as melt mixing, spray congealing, sintering, and hot-melt extrusion (HME), have evolved rapidly. Several new technologies, specifically dry powder coating, injection molding, and KinetiSol® dispersing (KSD), have been adapted to the pharmaceutical arena.

Co-rotating twin screw extrusion is routinely applied for the purposes of dissolving poorly soluble drugs into glassy polymers to prepare amorphous solid dispersions, which create supersaturated drug concentrations in the gastro-intestinal tract. A potentially more advantageous alternate geometry, counter-rotating twin screw extrusion was evaluated for preparation of model amorphous solid dispersion and was observed to be more efficient in forming a solid solution and reduced the thermal stress on the drug.

HME and KSD processes were utilized to prepare two phase systems consisting of a lipid, glyceryl behenate, and a polymeric amorphous solid dispersion intended to provide both controlled release of drug and supersaturated drug concentrations in the release medium. Such systems are challenging due to the potential for crystallization of the drug within the dosage form during release, which was observed to be influenced by lipophilicity and porosity of the formulation, as well as the surface area to volume ratio of the system.

High molecular weight cellulose based glassy dispersions were prepared using a weakly basic model drug by KSD, which when formulated into tablets were optimized to provide either immediate or approximately 2 hours of controlled release under the pH conditions simulating the environment of the stomach. Without formulation intervention in the external phase of the tablet, these compositions gel, muting drug release and missing the drug absorption window. Compositions optimized by an *in vitro* dissolution test were compared to a lower molecular weight HME prepared commercial product in a beagle dog model and observed to have statistically similar bioavailability, and in one case improved variability.

A modified twin screw extrusion machine was utilized to develop a continuous granulation process capable of producing granules that do not require subsequent grinding or sizing. This novel process, which employs previously un-reported temperature profiles, produces lipid based granules that when compressed into tablets produce a controlled release of tramadol hydrochloride, which were not susceptible to alcohol induced dose dumping.

## Table of Contents

List of Tables .....	xv
List of Figures .....	xvii
Chapter 1: Enhancing Bioavailability through Thermal Processing.....	1
1.1 Abstract.....	1
1.2 Introduction.....	1
1.3 Thermal Processing Techniques .....	4
1.3.1 Melt Mixing .....	4
1.3.2 Spray Congealing.....	9
1.3.3 Sintering/Curing.....	11
1.3.4 Dry Powder Coating .....	14
1.3.5 Melt Granulation.....	18
1.3.6 Hot Melt Extrusion .....	21
1.3.7 Injection Molding.....	32
1.3.8 KinetiSol <sup>®</sup> Dispersing.....	36
1.4 Conclusions.....	38
1.5 References.....	40
Chapter 2: Research Objectives .....	53
2.1 Overall Objectives .....	53
2.2 Supporting Objectives.....	53
2.2.1 Investigation of Process Temperature and Screw Speed on Properties of a Pharmaceutical Solid Dispersion using Co-rotating and Counter-rotating Twin Screw Extruders.....	53
2.2.2 Controlled Release Supersaturating Solid Dispersions Containing Glyceryl Behenate.....	54
2.2.3 Development of Itraconazole Tablets Containing Viscous KinetiSol <sup>®</sup> Solid Dispersions: <i>in vitro</i> and <i>in vivo</i> Analysis in Dogs.....	54

2.2.4 Continuous Twin Screw Melt Granulation of Glyceryl Behenate: Evaluation of Critical Process Parameters and Development of Controlled Release Tramadol Hydrochloride Tablets for Improved Safety .....	55
2.3 Summary .....	55
Chapter 3: Investigation of Process Temperature and Screw Speed on Properties of a Pharmaceutical Solid Dispersion using Co-rotating and Counter-rotating Twin Screw Extruders .....	56
3.1 Abstract .....	56
3.2 Introduction .....	57
3.3 Materials and Methods .....	60
3.3.1 Materials .....	60
3.3.2 Methods .....	60
3.3.2.1 Hot Melt Extrusion .....	60
3.3.2.2 X-Ray Powder Diffraction .....	63
3.3.2.3 Shear Cell Analysis .....	63
3.3.2.4 Thermal Analysis .....	64
3.3.2.5 Rheology .....	65
3.3.2.6 Dissolution .....	65
3.3.2.7 High Performance Liquid Chromatography .....	66
3.3.2.8 Flory-Huggins Theory .....	66
3.3.2.9 Residence Time Distribution .....	69
3.4 Results and Discussion .....	71
3.4.1 Thermal analysis and construction of the phase diagram .....	71
3.4.2 Effect of Processing Modes and Processing Conditions on Griseofulvin/Copovidone Solid Dispersions .....	75
3.4.3 Residence time distribution .....	83
3.5 Conclusions .....	87
3.6 References .....	88
Chapter 4: Controlled Release Supersaturating Solid Dispersions Containing Glyceryl Behenate .....	94
4.1 Abstract .....	94

4.2 Introduction.....	94
4.3 Materials and Methods.....	96
4.3.1 Materials .....	96
4.3.2 Methods.....	97
4.3.2.1 Hot-Melt Extrusion .....	97
4.3.2.2 Milling and Compression.....	97
4.3.2.3 KinetiSol <sup>®</sup> Dispersing.....	98
4.3.2.4 Thermal Analysis .....	98
4.3.2.5 Powder X-Ray Diffraction.....	99
4.3.2.6 High Performance Liquid Chromatography .....	99
4.3.2.7 Non-Sink Dissolution Testing.....	99
4.4 Results and Discussion .....	101
4.4.1 Hot Melt Extrusion .....	101
4.4.2 Thermal Analysis.....	103
4.4.3 X-Ray Diffraction .....	105
4.4.4 <i>In Vitro</i> Release Studies.....	107
4.5 Conclusions.....	117
4.6 References.....	118
Chapter 5: Development of Itraconazole Tablets Containing Viscous KinetiSol <sup>®</sup> Solid Dispersions: <i>in vitro</i> and <i>in vivo</i> Analysis in Dogs.....	
5.1 Abstract.....	121
5.2 Introduction.....	121
5.3 Materials and Methods.....	125
5.3.1 Materials .....	125
5.3.2 Methods.....	126
5.3.2.1 KinetiSol <sup>®</sup> Dispersing.....	126
5.3.2.2 Milling and Sizing.....	126
5.3.2.3 Blending and Compression .....	127
5.3.2.4 Differential Scanning Calorimetry.....	127
5.3.2.5 Powder X-Ray Diffraction.....	128

5.3.2.6 Non-Sink Dissolution Analysis.....	128
5.3.2.7 High Performance Liquid Chromatography .....	129
5.3.2.8 In Vivo Analysis .....	130
5.4 Results and Discussion .....	131
5.4.1 Highly Viscous Solid Dispersions .....	131
5.4.2 Tablet Compositions and <i>in Vitro</i> Analysis .....	135
5.4.3 <i>In Vivo</i> Analysis in Beagle Dogs .....	146
5.5 Conclusions.....	150
5.6 References.....	151
Chapter 6: Continuous Twin Screw Melt Granulation of Glyceryl Behenate: Evaluation of Critical Process Parameters and Development of Controlled Release Tramadol Hydrochloride Tablets for Improved Safety .....	159
6.1 Abstract.....	159
6.2 Introduction.....	160
6.3 Materials and Methods.....	162
6.3.1 Materials .....	162
6.3.2 Methods.....	163
6.3.2.1 Milling.....	163
6.3.2.2 Continuous Twin Screw Granulation.....	163
6.3.2.3 Melt Mixing Granulation .....	163
6.3.2.4 Blending and Compression .....	164
6.3.2.5 Particle Size Characterization .....	164
6.3.2.6 Scanning Electron Microscopy .....	164
6.3.2.7 Thermal Analysis .....	165
6.3.2.8 Powder X-Ray Diffraction.....	165
6.3.2.9 Sink Dissolution Analysis.....	165
6.3.2.10 Stability .....	166
6.4 Results and Discussion .....	166
6.4.1 Continuous Granulation Process Development .....	166
6.4.2 Granule Characterization and Stability.....	171

6.4.3 Mechanism of Granulation .....	175
6.4.4 Tablet Formulation and Stability .....	181
6.5 Conclusions.....	188
6.6 References.....	189
Chapter 7: Concluding Remarks .....	194
7.1 Dissertation Conclusion.....	194
Bibliography .....	195
Vita	222

## List of Tables

Table 1.1	Bioavailability of an experimental drug molecule when dosed as a micronized powder in capsule, an oral solution, or as a melt mixed solid dispersion in capsule (Joshi et al., 2004) in beagle dogs, reproduced with permission.....	9
Table 1.2	Pharmacokinetic parameters of atenolol following sublingual administration (Monti et al., 2010), reproduced with permission.....	10
Table 1.3	Median pore radius, percent porosity and tortuosity of matrix tablets prepared by direct compression (D) and hot melt extrusion (HME) containing 30% guaifenesin and 70% ethylcellulose measured before and after dissolution (Crowley et al., 2004), reproduced with permission.....	23
Table 3.1	Extrusion test conditions.....	63
Table 3.2	Dissolution attributes .....	82
Table 3.3	Moments of the residence time distributions for the co-rotating and counter-rotating 27 mm twin screw extrusion trials as measured at 180 °C and 450 rpm following a 1 g indigo carmine tracer charged to a 30% w/w GRIS in copovidone extrusion process operating at 4 kg/hr. ....	86
Table 5.1	Properties of hydroxypropyl methylcellulose Type 2910 (Methocel™ E).....	124

Table 5.2	ITZ solid dispersion containing tablet compositions.....	136
Table 5.3	Area under the dissolution curves for ITZ solid dispersion containing tablet compositions, n=3.....	142
Table 5.4	Pharmacokinetic parameters for ITZ solid dispersion containing tablet compositions following oral administration to beagle dogs, n=4.....	149
Table 6.1	Granulation temperature profiles used in the NANO16 twin screw extruder.....	169
Table 6.2	Tablet Formulations.....	181

## List of Figures

- Figure 1.1 Ibuprofen plasma concentrations in rats following oral administration of neat drug, a physical mixture, and two solid dispersions. 25mg ibuprofen per kg, n=5 (Newa et al., 2007), reproduced with permission.....7
- Figure 1.2 Images of a water droplet in contact with Compritol® 888 ATO matrix tablets a) unsintered tablet, b) sintered tablet (Rao et al., 2009), reproduced with permission.....13
- Figure 1.3 Scanning electron micrographs of surface of free films prepared from Eudragit® E PO powder cured at 80 °C for 1 h (A), 2 h (B), 4 h (C), 8 h (D), 12 h (E), and 24 h (F) (Cerea et al., 2004), reproduced with permission.....15
- Figure 1.4 Plasma concentration–time curves of VAL following oral administration of valsartan suspension, core (F2) and coated (F2C3) pellets in rats, respectively. F2 was the core pellet incorporated with poloxamer 188 and NaOH in core composition. F2C3 was the coted pellet with a mixture of HPMC and CB (1:2, w/w) as coating material and the coating level was 15%. Each data point represents the mean ± S.D. of six separate determinations (Cao et al., 2012), reproduced with permission.....17

Figure 1.5 Plasma concentrations of theophylline for Theo-Dur<sup>®</sup>, melt granulated compositions using PEG 6000 and glycerol monostearate as thermal binders and compared to IV administration (Ochoa et al., 2010), reproduced with permission.....21

Figure 1.6 Mean metoprolol tartrate (■) and hydrochlorothiazide (▲) plasma concentration-time profiles (+/-, n=6) after oral administration of 200 mg metoprolol tartrate and 25 mg hydrochlorothiazide to dogs: Zok-Zid<sup>®</sup> (2 tablets) (dotted line), experimental co-extruded mini-matrices with a core consisting of 45% (w/w) metoprolol tartrate and coat consisting of 10% (w/w) hydrochlorothiazide (full line) (Dierickx et al., 2012), reproduced with permission. ....25

Figure 1.7 Supersaturation dissolution testing of the ITZ-HPMC and ITZ-PVP micronized particle extrudate formulations by a pH change method according to the USP 29 specifications for the Method A enteric test. Approximately 100 mg of ITZ was added to each dissolution vessel (n¼6). Testing was conducted for 2 h in 750 mL of 0.1 N HCl followed by pH adjustment with 250 mL of 0.2Msodium phosphate tribasic at 378C and a paddle speed of 50 rpm (Miller et al., 2007), reproduced with permission.....29

Figure 1.8	Dissolution profiles in pH 1.2 buffer solution of runs at: (o) 100% INM; (●) physical mixture; (◇) 100 °C 20 RPM; (Δ) 110 °C 20 rpm; (□) 100 °C 100 rpm; (◆) 110 °C 100 rpm; (■) 140 °C 20 rpm (Liu et al., 2010), reproduced with permission.....	30
Figure 1.9	Ritonavir bioequivalence studies, dog versus human (Garren et al., 2010), reproduced with permission.....	32
Figure 1.10	A) A digital photo of a molded microneedle and the background is an US coin of a dime B) top view SEM micrograph of the microneedle with an open-channel design and the width of the T-shape channel is 100 μm C) a close-up SEM micrograph showing the tip region (Sammoura et al., 2007), reproduced with permission. ....	34
Figure 1.11	Mean plasma concentration–time profiles (+/-SD, n = 6) normalised for the difference in dose after oral administration to dogs: (◆) half tablet Slow-Lopressor <sup>®</sup> 200 Divitabs <sup>®</sup> , (■) formulation F2 [30% (w/w) MPT, 27.5% XG, and 42.5% EC], and (▲) formulation F8 [50% (w/w) MPT, 19.64% XG, and 30.35% EC] (Quinten et al., 2011), reproduced with permission.....	36

Figure 1.12	Total and reversing DSC thermograms for itraconazole, HPMC, and solid dispersions (DiNunzio et al., 2010c), reproduced with permission.....	38
Figure 3.1	Screw design employed in the Leistritz 27 mm twin screw extruder for A) co-rotating configuration (GL) and the counter-rotating configuration (GG).....	62
Figure 3.2	Differential scanning calorimetry thermograms for physical mixtures of GRIS:Copovidone over the range of 100:0 to 80:20 by volume demonstrating the melting point depression as observed scanning at 1 °C/min.....	72
Figure 3.3	A) Thermal phase diagram of the GRIS/copovidone representing the boundaries between thermodynamically unstable, metastable and stable regions as bounded by the spinodal and binodal curves along with the glass transition boundary. B) Free energy diagram of the GRIS/copovidone system as determined using Flory-Huggins Theory. ....	73
Figure 3.4	Powder X-ray Diffractograms of GRIS, copovidone and selected test samples over the range of 10° to 50° 2θ. ....	80
Figure 3.5	Non-sink dissolution of 20% by weight GRIS solid dispersions and a physical mixture of GRIS and copovidone. N=3, 50 mg GRIS per vessel in 1000 mL of 0.1 N HCl at 37 °C and 50 rpm.....	81

Figure 3.6	Non-sink dissolution of 30% by weight GRIS solid dispersions and a physical mixture of GRIS and copovidone. N=3, 50 mg GRIS per vessel in 1000 mL of 0.1 N HCl at 37 °C and 50 rpm.....	82
Figure 3.7	Viscosity of copovidone as measured at 155 °C in the presence of the tracer, indigo carmine, used in the residence time distribution study. ....	84
Figure 3.8	Residence time distribution of 30% GRIS solid dispersion at 4 kg/hr, 450 rpm, 180 °C for (◆) co-rotating and (▲) counter-rotating configurations in a Leistritz 27 mm extruder, boxed area shown in inset.....	86
Figure 4.1	Extrusion torque values of PVP, Kollidon 30 and a PVP, Kollidon 30/Compritol 888 ATO mixture as determined at different temperatures.....	102
Figure 4.2	DSC thermograms of A) CBZ and B) ITZ solid dispersion systems.....	104
Figure 4.3	Powder x-ray diffractograms of A) CBZ and B) ITZ solid dispersion systems. ....	106

Figure 4.4	Non-sink dissolution of A)CBZ and B)ITZ solid dispersions in 1000 mL of purified water, USP Apparatus II at 50 RPM. Each vessel contains approximately 100 mg of drug. Weights indicate total tablet weight, with multiple tablets added as necessary to achieve target drug loading. ....	108
Figure 4.5	A cartoon depiction of the fate of drug in an amorphous solid dispersion containing tablet. A) A porous compressed tablet. B) A monolithic, molded tablet. ....	110
Figure 4.6	A) Molded tablet containing CBZ and PVP, B) Molded tablet containing CBZ, PVP and C888. C-F) Dissolution of granules (small blue dot), compressed tablets (red x) and molded tablets (large green circle), C) CBZ and PVP formulations below the solubility of CBZ (0.2 mg/ml) D) CBZ and PVP formulations above the solubility of CBZ (0.4 mg/ml) as compared to a solution spike of CBZ (black line) E) CBZ, PVP and C888 at 0.2 mg/ml F) CBZ, PVP and C888 at 0.4 mg/ml. USP I apparatus, 100 rpm, 37 °C in purified water (volume adjusted to dosage form weight).....	112
Figure 4.7	A) ITZ dissolution rates measured by USP Method II at 50rpm at 37 °C in 0.1 N HCl A) ITZ and PVP solid dispersions at 0.2mg/ml ITZ concentration B) ITZ, PVP and C888 solid dispersions at 0.2mg/ml ITZ concentration.....	116

Figure 5.1	KSD processing profiles for ITZ and HPMC viscous solid dispersions. ....	132
Figure 5.2	DSC thermograms of ITZ and HPMC viscous solid dispersions. ....	134
Figure 5.3	X-Ray diffractograms of ITZ and HPMC viscous solid dispersions. ....	135
Figure 5.4	<i>In vitro</i> release profiles of non-disintegrating tablets containing viscous ITZ solid dispersions. USP Apparatus II 750 ml of 0.1 N HCL for 2 hours and 4 hours in 1000 pH 6.8 phosphate buffer at 37 °C, 100 rpm n=3.....	138
Figure 5.5	<i>In vitro</i> release profiles of slow and rapidly disintegrating tablets containing viscous ITZ solid dispersions. USP Apparatus II 750 ml of 0.1 N HCL for 2 hours and 4 hours in 1000 pH 6.8 phosphate buffer at 37 °C, 100 rpm n=3.....	141
Figure 5.6	Small volume pH dilution model. <i>In vitro</i> release profiles of 200 mg ITZ tablets containing viscous solid dispersions. Initial conditions 30 ml pH 2 HCl at 37 °C, rotated at 100 rpm in an orbital shaker. ....	144
Figure 5.7	<i>In vivo</i> plasma concentrations of ITZ following oral administration of tablets in beagle dogs, n=4 dose = 200 mg ITZ. ....	148

Figure 6.1	A) Continuous twin screw granulation temperatures encountered by the granulation while traversing the extruder barrel. B) Particle size distributions of granules produced at each temperature profile. C) Granulation output from temperature profile 1. D) Granulation output from temperature profile 3.....	168
Figure 6.2	Cumulative particle size distributions of the pre-blend and 35% tramadol hydrochloride granulations prepared using temperature profile 3 at various throughput rates.....	170
Figure 6.3	Scanning electron micrographs of 15% tramadol hydrochloride in glyceryl behenate granules prepared by A) continuous twin screw granulation B) melt mixing and grinding.....	172
Figure 6.4	DSC thermograms of 35% tramadol HCl granules during 3 months of storage at 40 °C 75% relative humidity conditions in induction sealed HDPE bottles.....	174

Figure 6.6	Impact of binder (glyceryl behenate) feed particle size. Cumulative particle size distributions of 35% tramadol hydrochloride blends and granulations prepared using neat glyceryl behenate and pre-processed glyceryl behenate of various sieve cuts. A) Pre-blends prior to granulation B) granules prepared at 4.8 g/minute using temperature profile 3. ....	178
Figure 6.7	Sink dissolution of 35% tramadol hydrochloride granules prepared by continuous twin screw granulation and melt mixing. n=3, USP Apparatus I, 75 rpm, 900 ml 0.1N HCl at 37 °C. ....	180
Figure 6.8	Sink dissolution profiles of 100 mg tramadol hydrochloride tablets. n=3, USP Apparatus I, 75 rpm, 900 ml 0.1N HCl at 37 °C. ....	183
Figure 6.9	Hydroalcoholic dissolution profiles of 100 mg tramadol hydrochloride tablets prepared by A) direct compression (Formulation 1) or B) continuous twin screw granulation and compression (Formulation 3). n=3, USP Apparatus I, 75 rpm, 900 ml 0.1N HCl containng 0%, 5%, 20% or 40% ethanol at 37 °C. ....	185

Figure 6.10 Dissolution profiles of 100 mg tramadol hydrochloride tablets (formulation 2) during 3 months storage at 40 °C/75%RH A) uncured tablets or B) tablets cured for 24 hours at 50 °C. n=3, USP Apparatus I, 75 rpm, 900 ml 0.1N HCl.....187

# **Chapter 1: Enhancing Bioavailability through Thermal Processing**

## **1.1 ABSTRACT**

Formulation intervention, through the application of processing technologies, is a requirement for enabling therapy for the vast majority of drugs. Without these enabling technologies, poorly soluble drugs may not achieve therapeutic concentrations in the blood or tissue of interest. Conversely, freely soluble and/or rapidly cleared drugs may require frequent dosing resulting in highly cyclic tissue concentrations. During the last several years, thermal processing techniques, such as melt mixing, spray congealing, sintering, and hot-melt extrusion, have evolved rapidly and several new technologies, specifically dry powder coating, injection molding, and KinetiSol® dispersing, have been adapted to the pharmaceutical arena. An examination of the contemporary literature is reported in this review to summarize the variety and utility of thermal processing technologies employed for solubility enhancement and controlled release. In particular, the impact of these processing technologies on bioavailability, considered in terms of both rate and extent, has been reviewed.

## **1.2 INTRODUCTION**

Thermal processing, also known as fusion processing, technologies are instrumental tools for formulation scientists to use when attempting to control the release or improve the solubility of a medicament, and their use has increased over the last few years due to advancements in processing. The development approach for any drug should take into account its physical and chemical properties, the classification of which

will likely drive the choice of processing techniques for evaluation (Kawabata et al., 2011). For example, the processing options available to a formulator of an insoluble, high melting point drug that degrades in the amorphous state are limited when compared to a freely soluble drug exhibiting thermally stability and a low melting point. Furthermore, the properties of excipients that benefit the dosage form or are desirable for drug release may not be particularly amenable to a particular processing technique. The available processing technologies must be understood by formulation scientists in order to balance the physicochemical properties of the drug, the excipients and the capabilities of the process in order to achieve the desired rate and extent of drug bioavailability.

The two key aspects of controlling bioavailability, according to the biopharmaceutics classification system, are intestinal permeability and solubility of the drug molecule (Amidon et al., 1995). In the case of non-neutral drugs, the solubility of the drug in the gastrointestinal tract may vary along its length. A particular challenging case is that of basic drugs that exhibit substantially greater solubility in the acidic gastric juices than in the intestines. In this case, the drug may release from the dosage form in the stomach and then precipitate in the intestines prior to being absorbed. Furthermore, absorption may also be complicated by site specific permeability along the gastrointestinal tract (Davis, 2005).

Formulation scientists develop processes, excipient networks and structures with the ultimate goal of sustaining the rate of drug release (Hoffman, 2008), altering the physical state of a drug to improve solubility (Blagden et al., 2007), and/or otherwise affecting the presentation of a drug to the body in order to address bioavailability constraints. During the last decade, applications of thermal processing technologies have

advanced and several new technologies have entered the pharmaceutical arena to enable the formation of these structures and/or facilitate a solid state transformation of the drug. The objective of this review is to evaluate thermal processing over roughly the last 8 years to summarize the impact the various techniques have demonstrated on bioavailability.

The scope of this review does not consider solvent based processes, whose importance in drug delivery should not be understated. Based on the state of industrial pharmaceutical development and evidence in the literature, it is clear that improving the bioavailability of poorly water-soluble drugs has been a major focus over the last decade. As such, investigations into the application of solid dispersions for enabling drug therapy have steadily increased (Bikiaris, 2011a, b). While thermal processes are useful for forming solid dispersions (Vasconcelos et al., 2007), solution based processes such as spray drying are also more than suitable and have considerably advanced our understanding of the key aspects of their utility, both in achieving a stable amorphous state and exploiting the resulting supersaturated drug concentrations for improved absorption (Friesen et al., 2008). However, the excipients commonly employed to produce controlled release compositions and solid dispersions are increasingly difficult to process in an aqueous environment and require the use of organic solvents, which carry safety and environmental concerns.

Many recent reviews have focused on solid dispersions, including the current understanding of their physical chemistry (Janssens and Van den Mooter, 2009) and the importance of their ability to supersaturate gastrointestinal fluids (Brouwers et al., 2009). The focus on thermal processing techniques reflects perceived benefits to the

manufacture of solid dispersions at a large scale (Leuner and Dressman, 2000) and in a cost effective manner. We believe the recent body of evidence and availability of recently marketed drug therapies prepared by thermal processes, in particular hot melt extrusion, reflects this. Moving forward, as solid dispersion technology becomes more commonplace, thermal processing techniques will likely offer new approaches to producing formulations for the sustained release of poorly water soluble compounds, the approaches for which have recently been reviewed (Tran et al., 2011).

### **1.3 THERMAL PROCESSING TECHNIQUES**

#### **1.3.1 Melt Mixing**

One of the simplest methods of thermally processing drugs is to liquefy an excipient, typically a lipid or low molecular weight polymer, using heat and a simple mixing apparatus, such as a stir bar or impeller, and combine with a drug and/or other adjuvants. The liquefied excipient may act as a solvent for the drug, resulting in improved dissolution characteristics. The addition of diclofenac pyrrolidine to molten Gelucire<sup>®</sup> 50/13 resulted in amorphous solid dispersions at concentrations of up to 20% drug (Fini et al., 2005). Melt mixed and crushed compositions of these two materials, containing up to 40% diclofenac, resulted in rapid dissolution of 20% to 55% of diclofenac in aqueous non-sink conditions. The rate and extent of drug release for this system is a direct result of the thermal treatment, as physical mixtures of the same compositions resulted in approximately 5 to 15% dissolution under the same conditions. Dissolution improvement following thermal treatment was most evident for the amorphous compositions containing less than 20% drug, but a minimum of 2-fold

improvement was observed for the crystalline compositions. This exemplifies both the utility of solid dispersions and the importance of the arrangement of the drug in the matrix at the molecular level. The various types of solid dispersions were summarized by Chiou and Riegelman (1971), who noted that solid dispersions may take the form of a molecularly dispersed solid solution (commonly termed amorphous solid dispersion) or contain crystalline dispersed drug. Solid dispersions may also contain multiple amorphous phases or contain a fraction of the drug in an amorphous phase and a fraction as a separate crystalline phase.

Similarly, melt mixed compositions of desloratadine in the synthetic triblock copolymer poloxamer, were found to increase the intrinsic dissolution rate by 10-80 times over the pure drug (Kolašinac et al., 2012). The authors observed a higher increase in intrinsic dissolution rate for poloxamer 188 than for poloxamer 407, which was attributed to the lower molecular weight and higher hydrophilic proportion contained in the poloxamer 188 grade. For this polymer chemistry, which gels at body temperature, the drug release rate was fastest for 1:1 compositions of drug to polymer. At higher polymer loadings, 1:2 and 1:3, the release rate was slower indicating the gel layer was acting as a diffusion barrier for drug release.

The improved dissolution rates and ability of these formulations to improve the solubility of poorly soluble drugs relates to improved bioavailability. Newa et al. (2007) studied an ibuprofen solid dispersion in poloxamer 188 in a rat model. The compositions studied were not completely amorphous and contained some form of crystalline ibuprofen that varied with the drug loading. The impact of the melt mixing process was evident from an increase in AUC of the rat plasma concentrations, Figure 1.1. Poloxamer

was observed to improve the solubility of ibuprofen in distilled water following melt mixing. A 1:10 ibuprofen to poloxamer 188 physical mixture resulted in an ibuprofen solubility of 0.057 mg/ml, while the melt mixed composition yielded 4.31 mg/ml in solution. In this case, the melt mixing process resulted in a solution of drug and polymer during processing, which upon cooling resulted in recrystallization of ibuprofen to form a crystalline solid dispersion. The improvement in bioavailability observed from the melt mixed compositions was attributed to a number of factors including the production of microfine crystalline particles of ibuprofen and improved wetting from the surface active polymer.

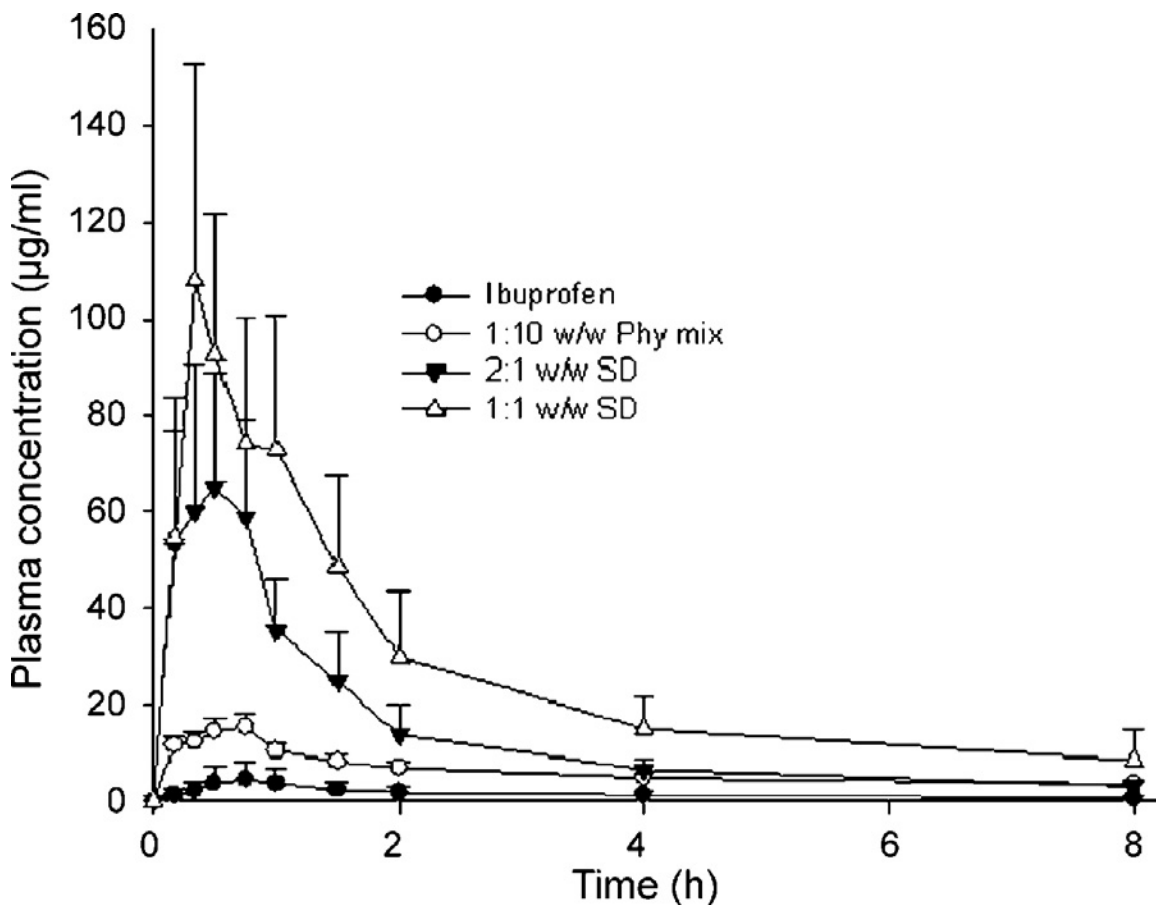


Figure 1.1 Ibuprofen plasma concentrations in rats following oral administration of neat drug, a physical mixture, and two solid dispersions. 25mg ibuprofen per kg, n=5 (Newa et al., 2007), reproduced with permission.

A disadvantage of melt mixing processes arises from the viscosity limitations of simple mixing processes, which precludes the use of high molecular weight polymers in high concentrations. Upon dissolution of a drug in a low molecular melt, conditions must be thermodynamically favorable following cooling for the composition to be stable. Otherwise, recrystallization of the drug is inevitable, which may alter the dissolution characteristics on storage. Given that the kinetics of recrystallization and the drug solubility in carriers are both temperature dependent, the rate of cooling after

incorporation may alter the active pharmaceutical ingredient (API) morphology. Urbanetz and Lippold (2005) studied the impact of recrystallization of nimodipine from a melt mixed formulation with polyethylene glycol (PEG) 2000 by rapidly cooling the melted solution to -20 °C followed by storage at -20 °C and 25 °C for 4 weeks. Nimodipine dissolution from this system, as measured under non-sink conditions, was minimal when the melt was cooled to 25 °C. However, rapid solidification to -20 °C resulted in an amorphous composition exhibiting greater than 4-fold saturation concentrations of nimodipine in the dissolution media, which recrystallized after several hours. Following storage at 25 °C for 4 weeks, during which time nimodipine was determined to recrystallize, the formulation no longer supersaturated in dissolution media. Furthermore, the rate and duration of supersaturation changed during storage at -20 °C for 4 weeks, indicating the kinetics of recrystallization were still significant at the reduced temperature.

The application of melt mixing processing is popular for preparing self-emulsifying drug delivery systems (SEDDs) (Tang et al., 2008). Solid SEDDs are commonly prepared by mixing a drug with molten surface active polymers or lipids, filling the molten mixture into capsules and cooling. Joshi et al. (2004) demonstrated the utility of surface active compounds in a beagle dog model. The authors found that during non-sink dissolution testing of their formulations containing an experimental drug molecule, a milky emulsion was formed from dispersed drug stabilized by polysorbate 80. These conditions mimic the *in vivo* conditions for the drug, which was compared to a capsule filled with micronized drug. A greater than 30-fold improvement of absolute bioavailability for the melt mixed solid dispersion was observed when compared to a micronized drug in a capsule, Table 1.1. A self-microemulsifying drug delivery system

(SMEDD) formulation containing ketoconazole, prepared by melt mixing and rapid cooling, was found to improve the area under the curve (AUC) in rats by 7-fold. In comparison, a simple melt mixed formulation of ketoconazole in polyethylene glycol (PEG) that did not self-emulsify, only doubled the AUC of the neat drug. Taken in conjunction with the previously presented investigations, it is clear that the solid state of the formulation following melt mixing as well as the physical form of the species formed following dissolution may significantly impact the bioavailability of poorly water soluble drugs.

Table 1.1 Bioavailability of an experimental drug molecule when dosed as a micronized powder in capsule, an oral solution, or as a melt mixed solid dispersion in capsule (Joshi et al., 2004) in beagle dogs, reproduced with permission.

Formulation	Dose (mg)	C <sub>max</sub> <sup>a</sup> (ng/ml)	AUC <sup>a</sup> (ng h/ml)	Absolute <sup>a</sup> bioavailability
IV solution	25	10681 (1252)	9782 (1071)	-
Oral capsule (powder)	50	39.2 (6.9)	326 (153)	1.7 (1.0)
Oral solution	100	2558 (1386)	23769 (10023)	59.6 (21.4)
Oral capsule (solid dispersion)	100 <sup>b</sup>	1206 (319)	14004 (2611)	35.8 (5.2)

<sup>a</sup> Mean (standard deviation) for n=3

<sup>b</sup> Two 50 mg capsules formulate in 3:1 PEG 3350-polysorbate 80 mixture

### 1.3.2 Spray Congealing

Spray congealing is a thermal processing technique that can result in spherical microparticles (Jannin et al., 2008). It is typically a downstream process to melt mixing and relies on the congealing of discrete droplets of the melt. The droplets may be formed by a variety of atomizers, most commonly in the form of an ultrasonic atomizer. The rate of cooling for each microsphere is similar and more controlled than would be observed

from cooling a melt mixed composition in a vessel. Microparticles produced by spray congealing with a two fluid atomizing nozzle were prepared having controllable median sizes from 58 to 278  $\mu\text{m}$ , depending on the flow rate of the molten feed and pressure of the atomizing air (Ilić et al., 2009). Similar to crushed melt mixed compositions, the microspheres had improved the dissolution characteristics when compared to neat drug.

Spray congealed particles using ultrasonic assisted atomization have been prepared for dissolution enhancement (Cavallari et al., 2005) as well as for controlled release applications (Passerini et al., 2006). A controlled release composition of atenolol, prepared by ultrasonic spray congealing, improved the bioavailability when compared to a commercial tablet, Table 1.2 (Monti et al., 2010). The melt mixing process, is particularly suited for low melting surface active materials, such as poloxamer, which may act as a permeation enhancer. Permeation enhancers act by a variety of mechanisms to improve transport of drugs across the intestinal or other epithelial membrane which may occur either paracellularly or transcellularly (Aungst, 2000). When administered sublingually to anaesthetized rabbits, the spray congealed microspheres approximately doubled the absolute bioavailability when compared to the reference formulation.

Table 1.2 Pharmacokinetic parameters of atenolol following sublingual administration (Monti et al., 2010), reproduced with permission.

Formulation	AUC <sub>0-24 h</sub> ( $\mu\text{g}/\text{ml h}$ )	C <sub>max</sub> ( $\mu\text{g}/\text{ml}$ )	T <sub>max</sub> (h)	C <sub>24 h</sub> (mg/ml)	A.B. (%)
Market Tablet	21.91 $\pm$ 6.89	2.77 $\pm$ 0.67	3.00	0.2 $\pm$ 0.1	17.42
Spray Congealed Microspheres	30.51 $\pm$ 3.09	2.63 $\pm$ 0.05	6.00	0.75 $\pm$ 0.10*	33.07

\* Significantly different from market tablet ( $p < 0.05$ , unpaired two tailed t-test).

A commercially approved product, Zmax, which is prepared by a rotary atomization process, releases azithromycin in a controlled manner over approximately 3 hours (Lo et al., 2009). The release profile was optimized to balance bioavailability and gastrointestinal (GI) targeting due to gastric irritation related to exposure of azithromycin to the early portion of the gastrointestinal tract. This formulation and process highlights the utility of spray congealing for improving drug therapy through modifying release. In addition, this process highlights a major potential disadvantage of melt mixing processes related to drug stability during processing. During scale-up, mixing and heating times increase due to surface area/volume efficiencies, which is problematic for thermally sensitive drugs. In the case of Zmax, a melt extruder was employed to reduce the thermal exposure of azithromycin, in order to prevent thermal degradation prior to spray congealing (Appel et al., 2011). The application of a melt extruder as a precursor to spray congealing allowed for continuous melting and pumping of the formulation to a rotary atomizer. The reduced residence time of the formulation in the extruder compared to a continuously stirred tank allowed for limiting the drug degradation to an acceptable level.

### **1.3.3 Sintering/Curing**

Sintering is a thermal treatment process, also referred to as curing, resulting in the fusion of particles or powder. Pellets containing finely divided carnauba wax, compounded into pellets with theophylline and microcrystalline cellulose, were sintered at 100 °C for up to 240 seconds resulting in a redistribution of the carnauba wax (Singh et al., 2007). Following sintering, drug release was markedly reduced, with the rate dependent on the sintering time. Tablets compressed from a 1:1 mixture of ketorolac

tromethamine and Compritol<sup>®</sup> 888 ATO were found to release 40% drug during the initial burst release phase of dissolution (Rao et al., 2009). Sintering for 3 hours reduced the burst effect to 20%, but did not change the rate of drug release following the burst phase. The heat treatment redistributed the Compritol<sup>®</sup> 888 ATO to form a surface film on the tablet, which drastically altered the contact angle of water, Table 1.2. In both of these cases, sintering was performed at temperature exceeding the melting point of the lipophilic matrix former. Dave et al. (2012) systematically studied the impact of temperature on the sintering process, which was performed above and below the glass transition temperature of the acrylic polymers Eudragit<sup>®</sup> RSPO and RLPO when incorporated into granules and tablets. The sintering process was found to improve hardness and reduce the dissolution rate from the matrices. However, the addition of plasticizer, which resulted in a lowered glass transition temperature of the Eudragit<sup>®</sup> RSPO system to 36°C, was found to have sustained release properties without sintering. This indicates the polymer matrix former was able to sufficiently redistribute itself during compaction and storage at ambient conditions, which highlights the temperature dependence of molecular mobility. When the matrix is softened sufficiently to rearrange, the porosity of the tablets is observed to decrease. Hasanzadeh et al. (2009) evaluated ibuprofen release from Eudragit RS and RL matrix tablets and observed a reduction in release rate with a corresponding reduction in porosity. The extent of release rate reduction at a given sintering temperature was dependent on the relationship between the glass transition temperatures of the system.

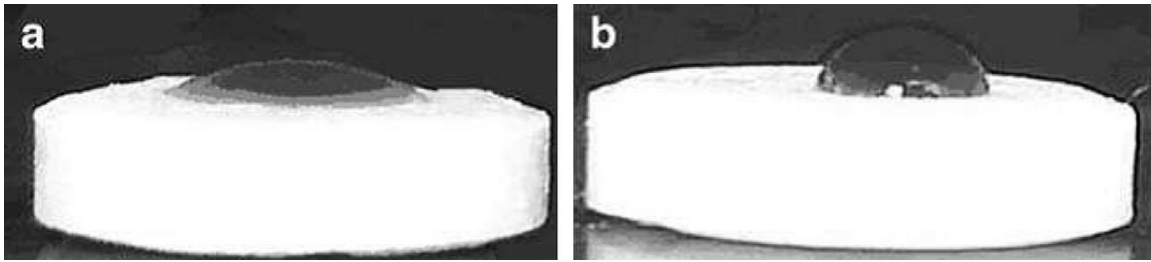


Figure 1.2 Images of a water droplet in contact with Compritol® 888 ATO matrix tablets a) unsintered tablet, b) sintered tablet (Rao et al., 2009), reproduced with permission.

Very few publications are available in the recent literature studying sintering, and no sintered oral dosage forms have recently been evaluated in vivo. Perhaps the lack of literature reflects the understanding of thermal treatment gained in the 20th century, or more likely researchers are opting for melt granulation or melt mixing techniques for greater control. Ghimire et al. (2011) investigated the erosion rate of tablets in vivo using gamma scintigraphy and observed the rates of erosion to be slowest for tablets directly solidified following melt mixing when compared to melt granulated and directly compressed tablets. Sudha et al. (2010) observed that wax matrix tablets containing tramadol HCl prepared by a melt mixing method retarded the drug release to a greater extent than other methods. Carcaboso et al. (2008) developed a compression sintered implant for the slow release of gabapentin from a poly( $\epsilon$ -caprolactone) (PCL) matrix. The matrix was implanted subcutaneously in mice, yielding the target gabapentin plasma concentrations over the course of 7 days. The implant was prepared as a cylindrical tablet, which required an impermeable coating on the tablet faces to reduce the burst effect and drug release rate. PCL matrices undergo hydrolytic degradation, which cleaves the polymer backbone. The matrix degradation process enables molecular mobility, both for diffusion of water into the matrix and drug release out of the matrix.

Gabapentin release from this PCL matrix was controlled by diffusion following the initial burst, which is the release of drug that is at or near the surface of the matrix. The addition of an impermeable coating on the top and bottom surfaces of the implant reduced the initial burst of drug by approximately half.

#### **1.3.4 Dry Powder Coating**

Dry powder coating processes require a sintering process to produce a solvent free film following powder coating of a surface. In these processes, the powder is applied to the surface and must adhere sufficiently for the sintering process to yield a film. Adhesion can be achieved through heating the substrate, spraying of a plasticizer during powder application, electrostatic charging of the powder or through a combination of these mechanisms(Luo et al., 2008).

Cerea et al. (2004) developed a heat only deposition process employing a modified spheronizer, which mobilized tablets for heating and coating. The process was initially developed using Eudragit<sup>®</sup> E PO, which has a low glass transition temperature allowing the coating process to occur at 55 °C to 60 °C. The progression of the sintering process, which was performed at 80 °C, is depicted in Figure 1.3. Enteric coated tablets have also been prepared(Sauer et al., 2007). Eudragit<sup>®</sup> L100-55 was compounded with triethyl citrate, using hot melt extrusion, to soften the acrylic polymer prior to the coating process. The resulting dry powder coated tablets met USP enteric requirements and were observed to be stable at 40 °C/75 %RH during storage for 12 weeks.

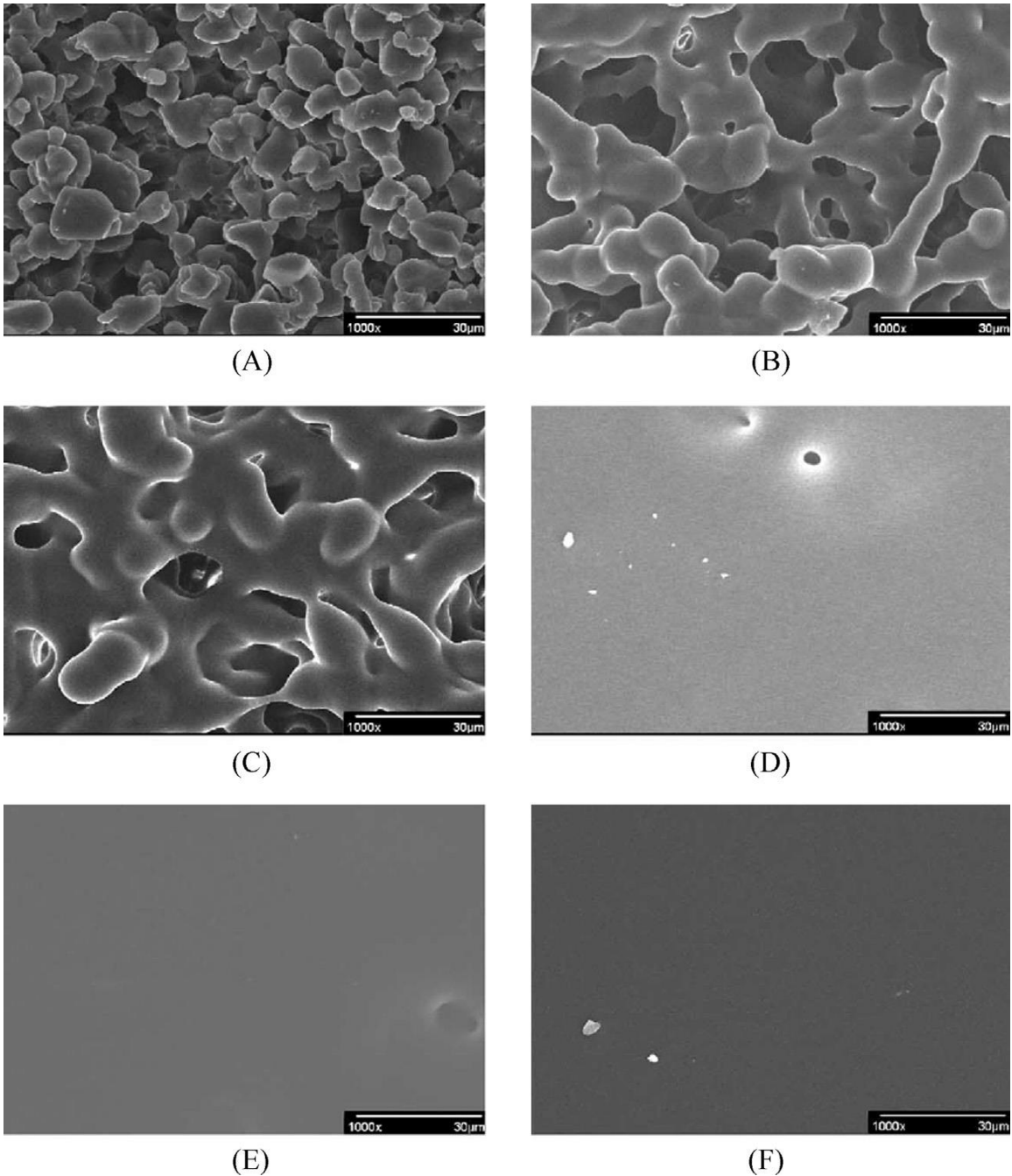


Figure 1.3 Scanning electron micrographs of surface of free films prepared from Eudragit® E PO powder cured at 80 °C for 1 h (A), 2 h (B), 4 h (C), 8 h (D), 12 h (E), and 24 h (F) (Cerea et al., 2004), reproduced with permission.

Kablitz et al. adapted plasticizer assisted powder deposition to a rotary fluid bed granulator (Kablitz et al., 2006). The process employed a three way nozzle, applying fluidizing air, plasticizer and powder in the direction of the substrate rotation. The utility of the process was originally demonstrated by achieving an effective enteric coating. A subsequent study and rigorous analysis of the coating and curing temperatures elucidated the key parameter of the process to be the glass transition temperature of the resulting film, based on which, the curing temperature should be selected (Kablitz and Urbanetz, 2007).

The most recent technology for solvent-less coating employs electrostatic deposition. Electrostatic powder coating has recently been adapted to a traditional pan coater (Qiao et al., 2010). The electrostatically charged particles adhere to the tablet surface, provided that the electrical resistivity of the tablet surface is sufficient. In practice, a liquid plasticizer was sprayed onto the tablet surface was utilized to improve the resistivity as well as lower the glass transition temperature of the powder to facilitate curing. In the case of a metallic substrate, the resistivity is not a concern and deposition may be readily achieved. Nukala et al. (Nukala et al., 2010) demonstrated the utility of electrostatic coating using microspheres, previously compounded by supercritical aerosol solvent extraction, to coat a stent. The coating was cured using infrared heating over the course of 60 seconds. The coating was successful in releasing sirolimus over several weeks in vitro.

Dry powder coating techniques have only recently been explored and in vivo studies are lacking in the literature. Cao et al. (Cao et al., 2012) developed a mucoadhesive particulate coating, which was applied by plasticizer assisted deposition in

a spheronizer. The particles were developed to prolong the duration of the dosage form, via mucoadhesion, and pH modulation to enhance absorption of valsartan in the upper GI tract. The thermal coating process allowed the incorporation of a high concentration of carbomer in the coating, which would generate a high viscosity, making solvent coating of this composition problematic. The coating, comprised mainly of a 1:2 ratio of hydroxypropyl methylcellulose and carbomer, substantially improved adhesion to mucin. Following administration to rats, a valsartan suspension was calculated to have an AUC of 6.80  $\mu\text{g h/ml}$ , compared to 12.18  $\mu\text{g h/ml}$  for the formulated pellet and 23.51  $\mu\text{g h/ml}$  for the dry powder coated pellet, Figure 1.4.

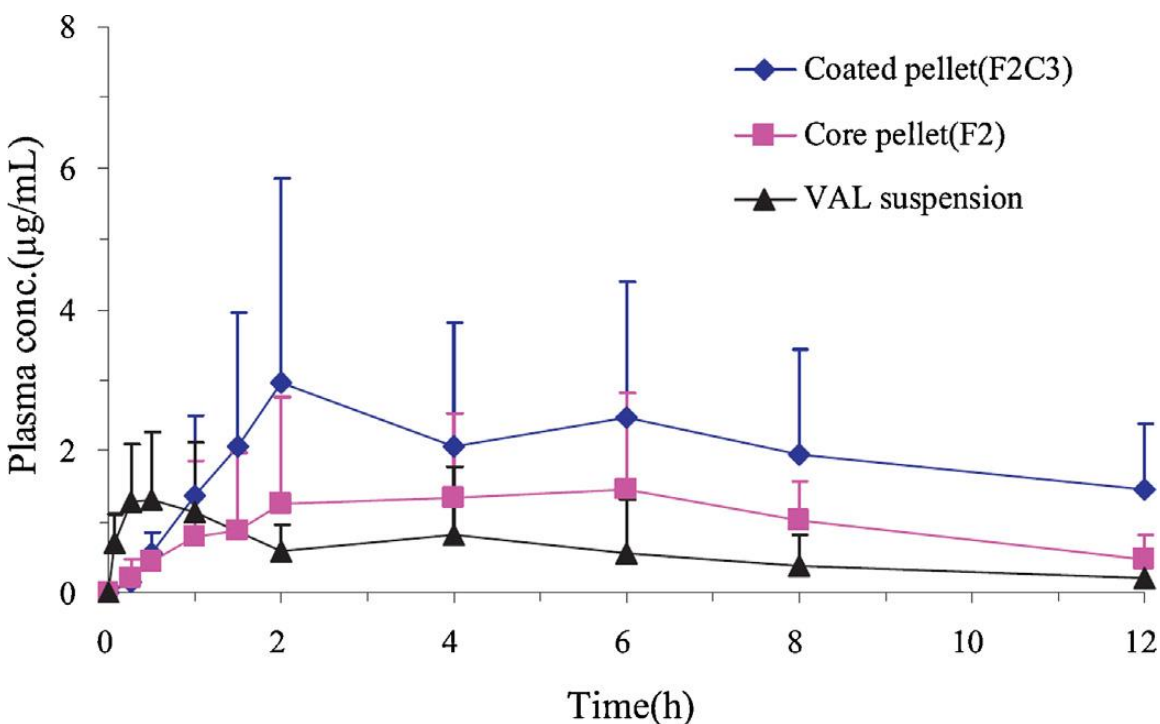


Figure 1.4 Plasma concentration–time curves of VAL following oral administration of valsartan suspension, core (F2) and coated (F2C3) pellets in rats, respectively. F2 was the core pellet incorporated with poloxamer 188 and NaOH in core composition. F2C3 was the coated pellet with a mixture of HPMC and CB (1:2, w/w) as coating material and

the coating level was 15%. Each data point represents the mean  $\pm$  S.D. of six separate determinations (Cao et al., 2012), reproduced with permission.

### **1.3.5 Melt Granulation**

Melt granulation is the process of agglomerating powders through the application of heat, either directly or through frictional heating, in the presence of a melting substance. High shear granulators form granules either by immersion or distribution and coalescence mechanisms, which is a function of the binder domain size and method of addition (Vilhelmsen and Schæfer, 2005). The binder can be pre-melted and sprayed/dripped into the granulator or included as a powder in the blend then melted during the process. In fluidized melt granulation, the binder is melted and atomized primarily forming granules through distribution and coalescence (Abberger et al., 2002). However, if the binder droplet size is larger than the powder size, the immersion mechanism will be dominant. The immersion granulation mechanism results in a denser granule, which depending on the composition, may be impact drug release.

The solid state of ibuprofen and ketoprofen, when granulated with lactose and PEG 6000, was determined to be independent of granulation methodology, despite differences in granulation mechanism (Passerini et al., 2010). Dissolution characteristics from this system were also similar, despite differences in particle size and morphology. Recently, open discharge twin screw extrusion has been demonstrated as an effective melt granulation technique (Mu and Thompson, 2012). Mu and Thompson studied the effects of binder viscosity and particle size and concluded that the immersion nucleation mechanism was dominant. In addition, they demonstrated the utility of the twin screw

extrusion screw configurability, which allowed alteration of the granule density through addition of mixing zones in the screw design.

The effect of thermal processing on the drug release and bioavailability of several drugs is evident from previously described research investigations applying simple heating processes. The impact of the process on in vivo outcomes confounds the already difficult formulation development process for a drug therapy. Compritol<sup>®</sup> 888 ATO and low substituted hydroxypropyl cellulose (LH-21) tablets, prepared at a ratio of 65:35, were studied in humans to determine the in vivo disintegration profile (Ghimire et al., 2011). The results demonstrated a potential benefit of melt granulation over direct compression and melt mixing processes. Disintegration of tablets compressed from melt granules was less variable and correlated well with in vivo results, as measured by gamma scintigraphy, when compared to tablets prepared following melt mixing. In addition, disintegration times were prolonged versus directly compressed tablets.

Sublingual tablets were prepared by the melt granulation of sugar with PEG, which was subsequently blended with ketotifen fumarate and other compression and dissolution aids. PEG was incorporated at a 4:6 ratio of MW 400 and 6000 in order to melt at body temperature (Tayel et al., 2010). The final composition of sugar, PEG and other adjuvants was optimized to balance tablet friability, compression characteristics, water absorption (sugar and super-disintegrant) and tablet disintegration. The tablets were evaluated in albino rabbits and compared to a marketed oral sublingual solution. The ability of the tablets to slowly disintegrate between 1 and 10 minutes, solubilize the drug and promote permeation through the mucosa resulted in a relative bioavailability of 164% when compared to the marketed solution. The tablet demonstrated a reduction in

T<sub>max</sub>, an increase in C<sub>max</sub>, and higher concentrations of drug were present during the elimination phase when compared to the marketed solution.

Yang et al. (2007) described the benefits of melt granulation using meltable binders with hydrophilic character, such as Gelucire<sup>®</sup> and PEG. The process allowed intimate contact of these dissolution enhancing binders with drug particles, but did not affect the solid state of the drug, in this case griseofulvin. Dissolution was performed on granulations comprising various drug loadings and including either hydroxypropyl methylcellulose (HPMC) or starch in the granules. In all reported cases, the melt granulation compositions were superior to physical mixtures.

Due to the effectiveness of dissolution enhancement observed in the presence of even small amounts of binder, melt granulation has been explored for high drug loading compositions. Vasanthavada et al. (2011) developed a melt granulated dosage form containing 90% imatinib mesylate that exhibited controlled release characteristics. The polymeric binders, hydroxypropyl cellulose and ethylcellulose, were utilized in the formulation, which required incorporation using a twin screw extruder. One tablet formulation prepared from the melt granules was determined to match the oral bioavailability of a bid IR tablet when administered as a single dose. Melt granulation has also been described as a less costly alternative in developing conventional matrix tablets. Theophylline was granulated with HPMC using PEG and glycerol monostearate as thermal binders resulting in plasma concentrations similar to marketed products, Figure 1.5 (Ochoa et al., 2010).

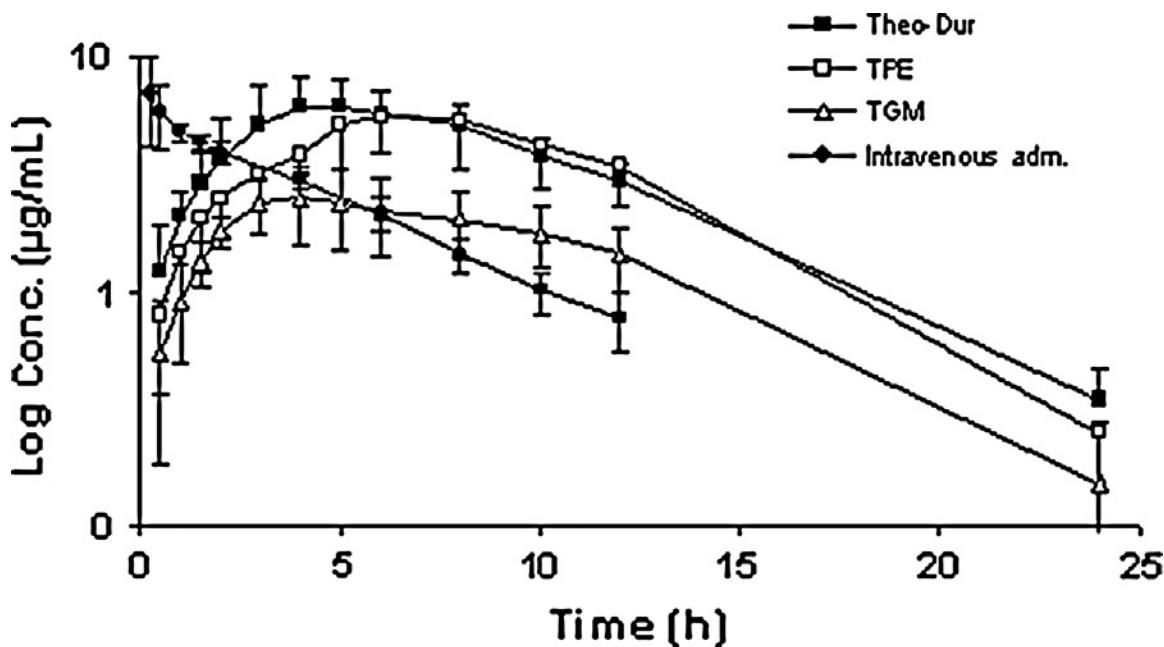


Figure 1.5 Plasma concentrations of theophylline for Theo-Dur<sup>®</sup>, melt granulated compositions using PEG 6000 and glycerol monostearate as thermal binders and compared to IV administration (Ochoa et al., 2010), reproduced with permission.

### 1.3.6 Hot Melt Extrusion

Hot melt extrusion is a thermal process by which a material is pumped by a rotating screw through a shaped die under elevated temperatures (Crowley et al., 2007). Extruders are produced in a variety of forms and can be configured to perform multiple unit operations. Configuration for pharmaceutical dosage forms typically involves designing the extruder length and screw configuration in order to convey, mix, compress, melt, devolatilize and pump the composition. In advanced applications, extruders are used for chemical reactions, foaming, wet granulation, and melt granulation. Based on a review of the published literature, extruders entered the pharmaceutical research space as a means to combine drugs with polymers for controlled release applications. More recently, hot melt extrusion has an ever increasing role in bioavailability enhancement as

a tool to produce amorphous solid dispersions. As such, hot melt extrusion is the subject of numerous reviews (Breitenbach, 2002, Crowley et al., 2007, Repka et al., 2007, Repka et al., 2008). In this section, literature from the last 8 years has been reviewed with a focus on applications for bioavailability enhancement.

One of the simplest shapes formed by an extrusion process is a rodform, which upon cutting may be administered directly as a matrix tablet. Crowley et al. (2004) studied the impact of melting, mixing and compacting ethylcellulose on the release characteristics of guaifenesin. The impact of intimate mixing and compaction as a result of the extrusion process was observed in the reduced porosity and increased tortuosity of the extruded matrices when compared to a directly compressed formulation. In addition, the study highlighted the impact of the solid state of the drug in matrix systems. When the extrusion temperature occurred above the melting point of guaifenesin, 85.6 °C a dramatic increase in the tortuosity of the matrix was observed. The results are summarized in Table 1.3.

Table 1.3 Median pore radius, percent porosity and tortuosity of matrix tablets prepared by direct compression (D) and hot melt extrusion (HME) containing 30% guaifenesin and 70% ethylcellulose measured before and after dissolution (Crowley et al., 2004), reproduced with permission.

Processing conditions	Median pore radius (Å)		Percent porosity		Tortuosity	
	Before	After	Before	After	Before	After
“Fine” ethyl cellulose (325-80 mesh)						
DC 10kN	529 ± 24		4.1 ± 0.3		4.7 ± 1.1	
DC 30 kN	476 ± 26		3.8 ± 0.2		6.0 ± 0.6	
DC 50 kN	475 ± 17		3.1 ± 0.2		6.9 ± 0.9	
HME 80, 85, 85, 90°C	264 ± 8	575 ± 51	1.0 ± 0.2	8.1 ± 1.8	53.2 ± 8.1	4.7 ± 0.6
HME 90, 105, 105, 110°C	137 ± 6	521 ± 65	0.4 ± 0.2	7.8 ± 2.2	321 ± 22	5.2 ± 0.9
“Coarse” ethyl cellulose (8-300 mesh)						
DC 10kN	1439 ± 42		6.5 ± 0.2		1.3 ± 0.7	
DC 30 kN	906 ± 23		5.7 ± 0.3		2.1 ± 0.6	
DC 50 kN	710 ± 25		5.2 ± 0.2		2.8 ± 0.5	
HME 80, 85, 85, 90°C	392 ± 11	642 ± 48	2.3 ± 0.4	4.1 ± 1.4	41.8 ± 5.5	4.4 ± 0.3
HME 90, 105, 105, 110°C	351 ± 13	588 ± 57	0.7 ± 0.1	4.1 ± 1.1	125 ± 16	5.0 ± 1.1

Each point represents mean ± standard deviation. N=3.

Drug release from insoluble matrices, such as ethylcellulose, occurs through diffusion mechanisms. Due to the stochastic nature of this process, the drug release rate tails at the end of the release process (Baker, 1987) and complete drug release may not be achieved in a physiologically relevant time frame. The addition of a soluble and swellable excipient, such as xanthan gum, to an ethylcellulose matrix was shown to allow for complete release of ibuprofen from extruded mini matrices (Verhoeven et al., 2006). In vivo evaluation of this system in dogs demonstrated the capability of the system to sustain the release. However, aggregation of the mini matrices confounded the release kinetics reducing the bioavailability relative to existing commercial tablets.

A subsequent study of this system using metoprolol tartrate was undertaken and compared the water soluble release modifiers xanthan gum and polyethylene oxide (PEO) (Verhoeven et al., 2009). The in vivo profiles in dogs confirmed the impact of the matrix aggregation on plasma peak concentrations of the xanthan gum containing mini matrices, which was significantly reduced when compared to the non-aggregating PEO containing mini matrices. Both of these systems demonstrated controlled release utility, having improved bioavailability relative to a marketed controlled release tablet. Furthermore, controlled release mini matrices from this research group have been developed for the simultaneous delivery for a fixed dose combination of metoprolol tartrate and hydrochlorothiazide (Dierickx et al., 2012). The system consisted of a core comprised of metoprolol tartrate in polycaprolactone contained in a coextruded skin layer containing hydrochlorothiazide in a polyethylene oxide matrix. This system was determined to be statistically bioequivalent to a commercial fixed dose combination product. In addition, the mean plasma concentration profile for metoprolol tartrate from this system did not exhibit the lag associated with the marketed product, Figure 1.6.

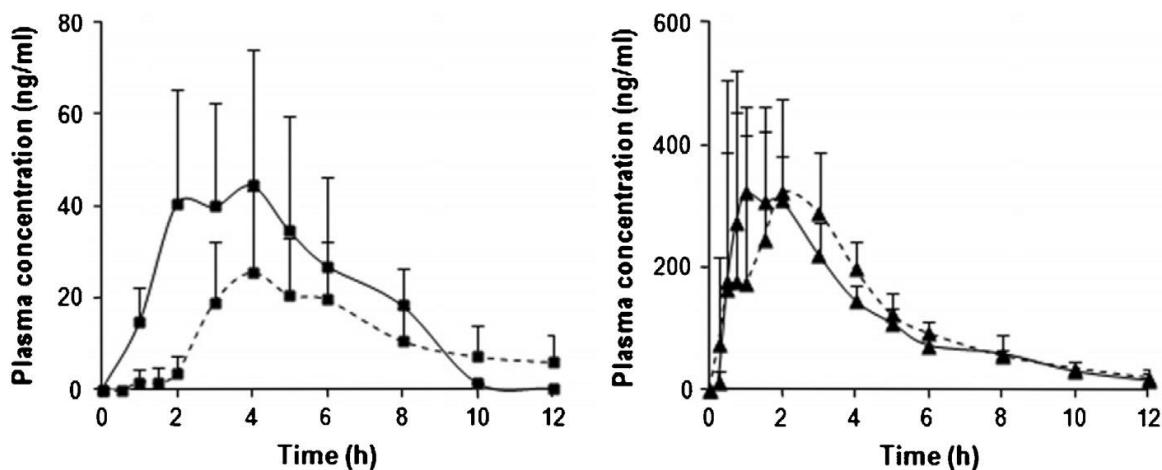


Figure 1.6 Mean metoprolol tartrate (■) and hydrochlorothiazide (▲) plasma concentration-time profiles (+/-, n=6) after oral administration of 200 mg metoprolol tartrate and 25 mg hydrochlorothiazide to dogs: Zok-Zid<sup>®</sup> (2 tablets) (dotted line), experimental co-extruded mini-matrices with a core consisting of 45% (w/w) metoprolol tartrate and coat consisting of 10% (w/w) hydrochlorothiazide (full line) (Dierickx et al., 2012), reproduced with permission.

A variety of dosage forms, other than simple oral matrices, have been described in the recent literature. Repka et al. (2005) demonstrated the feasibility of controlled release to the oral cavity using lidocaine in solid solution with hydroxypropyl cellulose (HPC) and HPMC. The composition was extruded as a film that exhibited a burst release followed by a controlled release phase, a profile which would be desirable for pain management. An erosion controlled system formed by filling an extruded ethylcellulose cylinder with a melt mixed composition of propranolol, Gelucire<sup>®</sup>, and HPC (Mehuys et al., 2004b). The extruded ethylcellulose shell shielded the core from hydrodynamic effects. The system achieved a 4-fold improvement in bioavailability compared to a commercial product in dogs (Mehuys et al., 2004a). A follow up study in humans also demonstrated a bioavailability improvement of the system, albeit not as significant

(Mehuys et al., 2005). Hot melt extrusion is well known to have utility in the preparation of commercially available vaginal products intended for contraception.

Recently, significant efforts have been applied in the development of microbicide products for prevention of human immunodeficiency virus (HIV) and herpes infections (Malcolm et al., 2010). These rings, which are prepared commonly for ethylene vinyl acetate (EVA) and silicon are capable of zero order release of low dose drugs over the course of several weeks or more (Clark et al., 2011).

Several investigations have highlighted the utility of lipophilic materials for extrusion at low temperatures (Reitz and Kleinebudde, 2007, Windbergs et al., 2009, Windbergs et al., 2010). These studies demonstrate the feasibility for preparing solid matrices using extrusion and the capacity for controlled release. However, in vivo results are not available to understand the impact of this technique on bioavailability. This approach has also been described for the sustained release of macromolecules (Schulze and Winter, 2009). Following stabilization of interferon  $\alpha$ -2a in the solid state with hydroxypropyl  $\beta$ -cyclodextrin, extrusion with Dynasan D118 and Dynasan H12 at 40 °C was performed. The protein structure was verified to be unaffected and the macromolecule was released over 15, 40 or 60 days by altering the diameter of the rodform extrudate to 0.5 mm, 1.0 mm, or 1.9 mm, respectively. Using single molecule tracking techniques, Sax et al. (2012) observed the release of the macromolecule from the system to occur as two populations. As expected, diffusion through pores in the matrix formed from a water soluble additive. However, diffusion also occurred in a molten lipid phase present as a portion of the lipid matrix at 37°C.

Foam extrusion has also been demonstrated *in vitro* to have properties with potential in improving bioavailability. Foam extrusion involves dispersing a gaseous agent at high pressure in the extruder, which upon transitioning to lower pressure at the die outlet, the gas expands and creates a foam structure that results in increased specific surface area and porosity of the extrudate (Verreck et al., 2005). Fukuda et al. (2006) developed foam extrudates, in which the gas phase was formed during off gassing of sodium bicarbonate resulting from the thermal decomposition reaction during the extrusion process. The porous tablets, comprised of Eudragit<sup>®</sup> EPO, were observed to float and sustain the release of chlorpheniramine maleate. Although sensitive to the fed state of the patient *in vivo*, floating dosage forms are a promising approach for gastroretention, which is desirable for targeting drugs to the upper small intestine (Davis, 2005, Streubel et al., 2006). Foam extrusion using supercritical carbon dioxide has been evaluated recently and shows promise for further enhancing the dissolution characteristics of supersaturating solid dispersions. Terife et al. (2012) developed a foamed solid solution of indomethacin in Soluplus<sup>®</sup>. The increase in surface area resulting from the cellular structure improved the dissolution rate of indomethacin from the solid dispersion.

Hot melt extruded compositions are known to improve the dissolution characteristics of poorly water soluble drugs, regardless of the API morphology. In the case of dispersed particles, polymeric matrices are beneficial for separating and stabilizing particles. Miller et al. (2007) stabilized microparticles, prepared from a flash evaporation process, by dispersing the particles in low molecular weight PEO using a low temperature extrusion process. The particles themselves contained amorphous itraconazole in either HPMC or polyvinyl pyrrolidone (PVP) that remained intact during

the extrusion process. The particle extrudate formulations released significantly faster than the particles themselves, due to the wetting action of PEO which prevented agglomeration of the particles in media. When studied in non-sink conditions, the HPMC particle extrudate formulation showed superior levels of supersaturation and a delay in precipitation when compared to PVP. This correlated well with in vivo results in rats, where both microparticle extrudate formulations allowed itraconazole to absorb at a faster rate and to a greater extent than the crystalline drug, Figure 1.7.

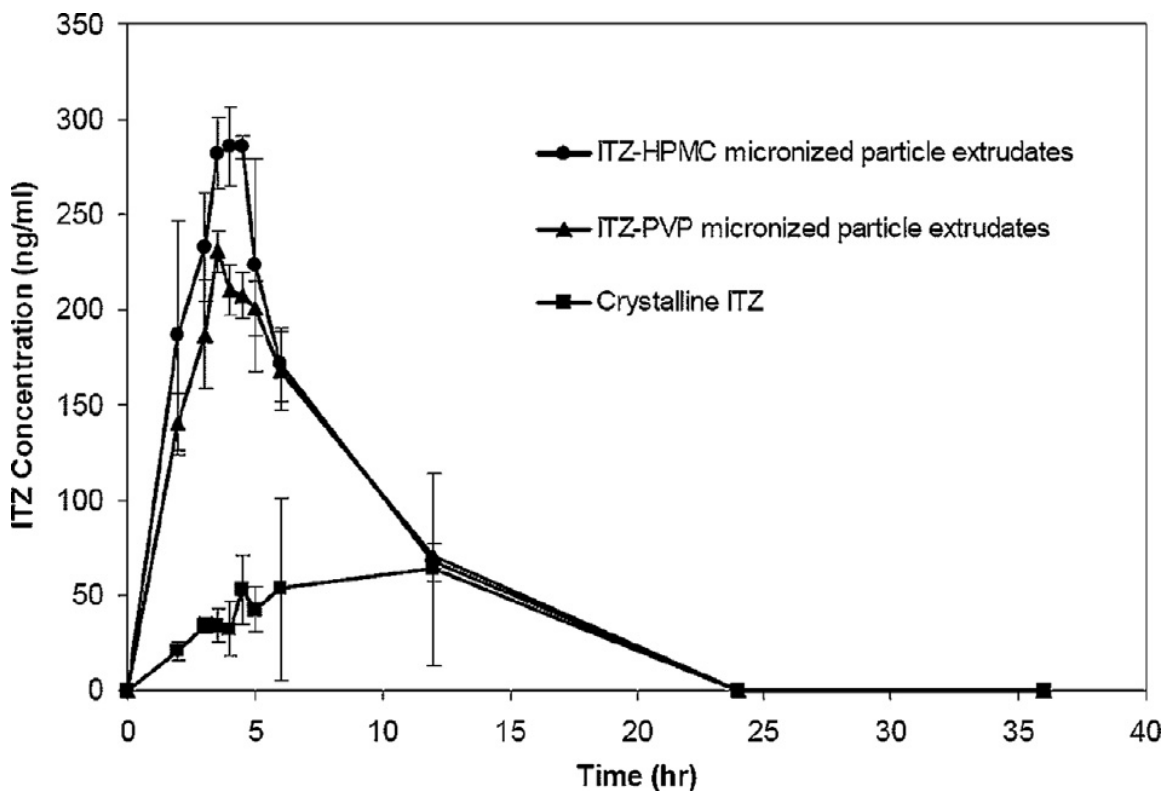


Figure 1.7 Supersaturation dissolution testing of the ITZ-HPMC and ITZ-PVP micronized particle extrudate formulations by a pH change method according to the USP 29 specifications for the Method A enteric test. Approximately 100 mg of ITZ was added to each dissolution vessel (n=6). Testing was conducted for 2 h in 750 mL of 0.1 N HCl followed by pH adjustment with 250 mL of 0.2M sodium phosphate tribasic at 37°C and a paddle speed of 50 rpm (Miller et al., 2007), reproduced with permission.

The temperature and mixing capability of the extruder may also be tuned in order to dissolve the drug in the polymer melt during the extrusion process. Liu et al. (2010) highlighted the importance of the shear rate and temperature in the dissolution of indomethacin in molten Eudragit® EPO. The results of both a higher shear and higher temperature increase the amount of indomethacin dissolved, which directly affects the dissolution profile of the solid dispersion, Figure 1.8. At higher temperatures, the

saturation solubility of the drug in the melt is elevated, increasing the driving force for dissolution. At higher shear rates, the boundary layer at the particle-melt interface is decreased.

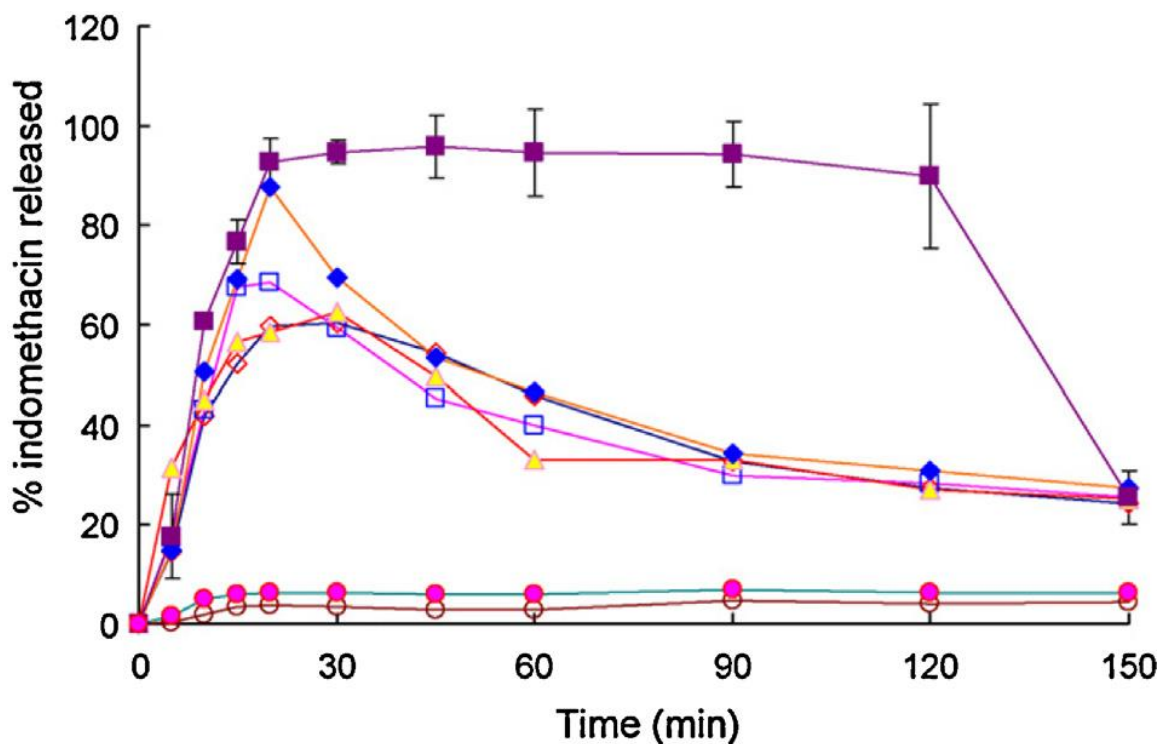


Figure 1.8 Dissolution profiles in pH 1.2 buffer solution of runs at: (○) 100% INM; (●) physical mixture; (◇) 100 °C 20 RPM; (Δ) 110 °C 20 rpm; (□) 100 °C 100 rpm; (◆) 110 °C 100 rpm; (■) 140 °C 20 rpm (Liu et al., 2010), reproduced with permission.

Conversely, if the active ingredient is stable following melting and the melting temperature is lower than the decomposition temperature of the polymer, the shear rate is not critical and the extruder needs only to melt and distribute the two materials together. Solid dispersions of nimodipine, processed above the melting temperature, were evaluate in a dog model by Zheng et al (2007). Solid dispersions with HPMC, Eudragit® EPO and

polyvinyl pyrrolidone-co-vinyl acetate (PVPVA) all significantly outperformed their representative physical mixtures. The solid dispersions performed as well as the commercial reference formulation. The differences between the solid dispersions of the various polymers were not statistically different. Itraconazole solid dispersions, prepared in several polymers by extrusion above the melting point of itraconazole, were developed by Six et al. (Six et al., 2005) and studied in humans. Itraconazole bioavailability was determined to be comparable to the commercial product for all the solid dispersions. Although not statistically different, the C<sub>max</sub> and AUC for solid dispersions prepared from HPMC, Eudragit<sup>®</sup> E100 and PVPVA were compared to in vitro dissolution profiles. Although the dissolution profiles for itraconazole from the three polymers were discriminating, the rank order did not agree with the in vivo results.

Based on a review of the literature performed by Newman et al. (Newman et al., 2012), the utility of in vitro dissolution testing for prediction of in vivo is not yet clear. Solid dispersions prepared from poorly soluble compounds are not always evaluated under sink and non-sink conditions, although the authors recommend evaluating both. In any case, pharmacokinetics in animal models present the best opportunity for developing lead candidates. A study by Garren et al. (Garren et al., 2010) evaluated the ability of a dog model to predict human bioequivalence of generic ritonavir formulations when compared to the hot melt extruded innovator product. The authors concluded that the dog model tended to over predict human bioequivalence. However, in all cases where bioequivalence was not achieved in the dog, it was also not achieved in humans, indicating bioequivalence in the animal model could be viewed as a prerequisite. The results of the comparison are summarized in Figure 1.9.

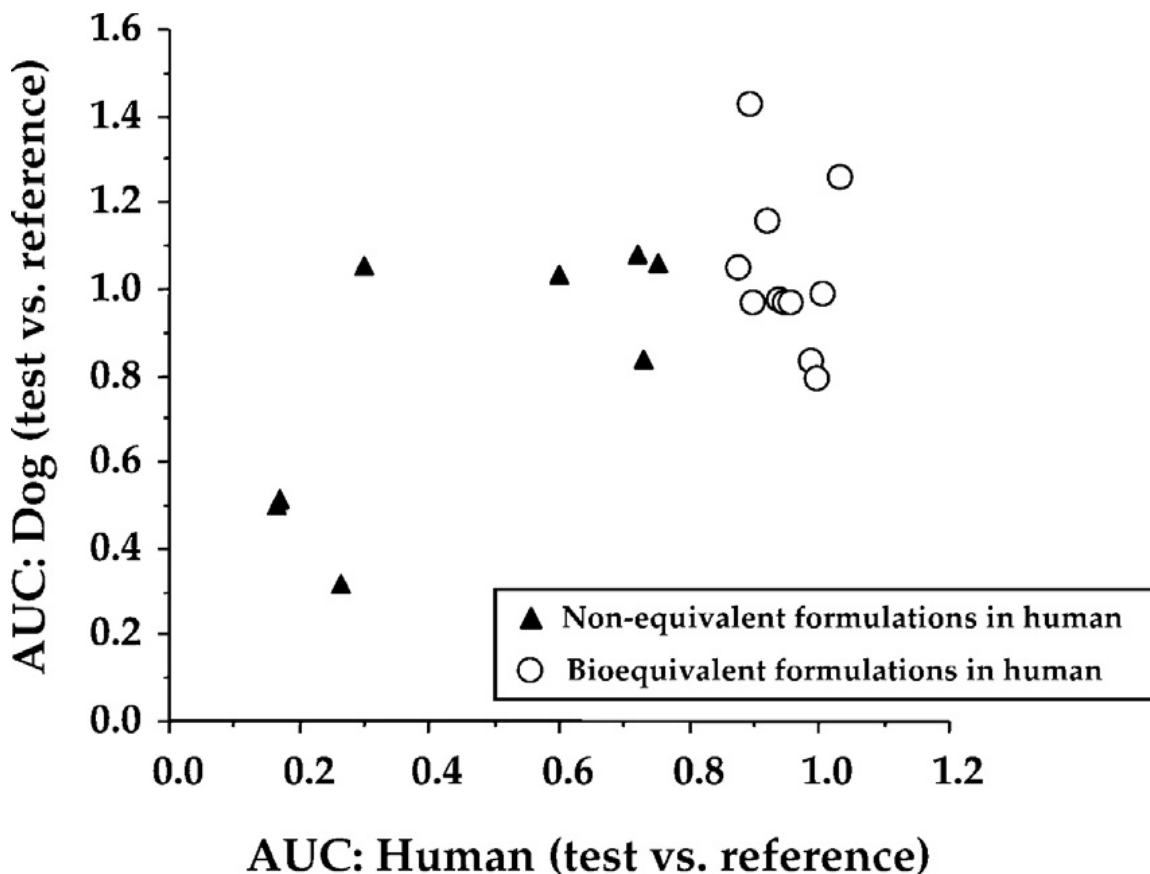


Figure 1.9 Ritonavir bioequivalence studies, dog versus human (Garren et al., 2010), reproduced with permission.

### 1.3.7 Injection Molding

Injection molding is a technique that can prepare objects from thermoplastic or thermoset materials using high pressure and temperature to inject a melt into a closed mold (Zema et al., 2012). The melt is typically formed by a plasticating screw and heater, which in some cases may be a compounding extruder. Recently, this technology has garnered interest for preparation of oral dosage forms and biomedical devices. Injection molding is capable of producing small and intricate shapes, such as microneedles, Figure 1.10 (Sammoura et al., 2007). Injection molded intravaginal rings

have been studied for zero order delivery of UC781, a microbicide for preventing transmission of HIV-1 (Clark et al., 2011). Injection molded ring segments prepared from silicon elastomer, as well as extruded rods prepared with ethylene vinyl acetate, were evaluated in female rabbits. Plasma levels of UC781 were followed for 28 days and observed to be very stable over that timescale.

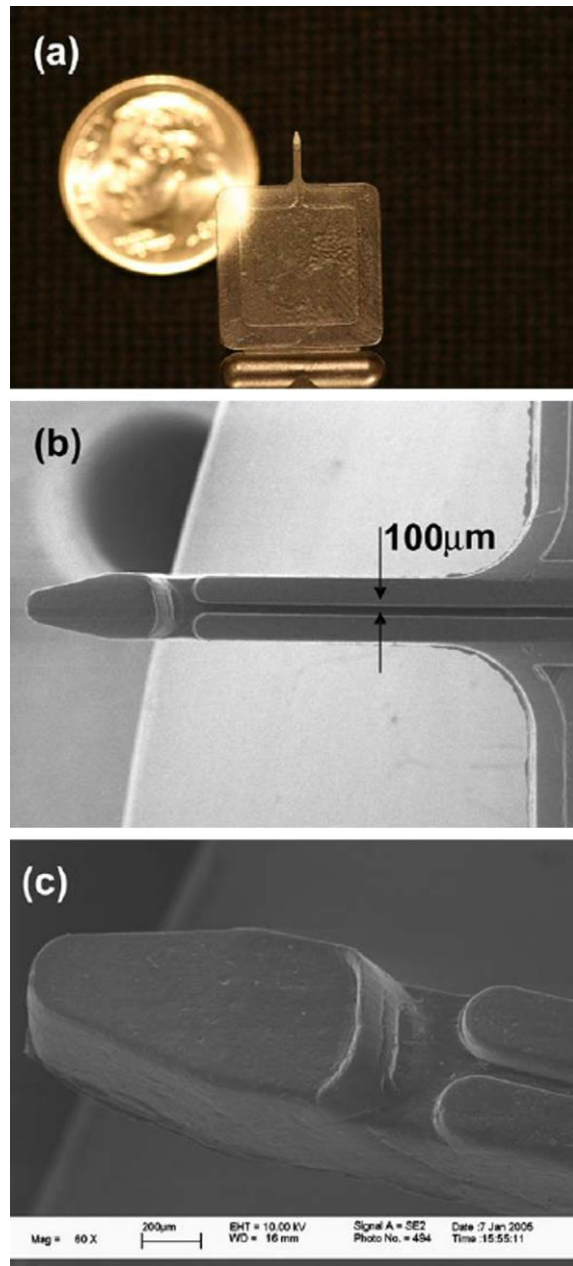


Figure 1.10 A) A digital photo of a molded microneedle and the background is an US coin of a dime B) top view SEM micrograph of the microneedle with an open-channel design and the width of the T-shape channel is 100 μm C) a close-up SEM micrograph showing the tip region (Sammoura et al., 2007), reproduced with permission.

Two piece capsules, formed from HPC (Klucel™ LF) plasticized with PEG, were developed using injection molding for pulsatile release (Gazzaniga et al., 2011). The thickness of the capsules was used to introduce a lag release, followed by a rapid release of the encapsulated drug. Using the same approach, enteric capsules have also been demonstrated using hydroxypropyl methylcellulose acetate succinate (HPMCAS) as the capsule shell material (Zema et al., 2012).

Quinten et al. (2009b) developed an oral therapy of metoprolol tartrate using injection molding. The drug was mixed in a compounding extruder with L-HPC, and ethylcellulose plasticized with dibutyl sebacate prior to forming tablets with an injection molder. The tablets were found to release drug in a controlled manner. The authors prepared a similar tablet using metoprolol tartrate and HPMC (Quinten et al., 2009a). In this system, the drug was determined to be partially crystalline and partially amorphous in the final tablets, in which small drug clusters were detected by Raman spectral mapping. A more recent study from this research group evaluated metoprolol tartrate in ethylcellulose and xanthan gum microparticles in vivo (Quinten et al., 2011). This system was also determined to contain the drug in both amorphous and crystalline phases. When studied in a crossover study with dogs, an injection molded composition was found to have equivalent bioavailability to a marketed product Figure 1.11. However, the injection molded formulation demonstrated a reduction in  $C_{max}$ , which would be desirable for a daily controlled release dosage form due to a reduction in plasma concentration fluctuation throughout the day.

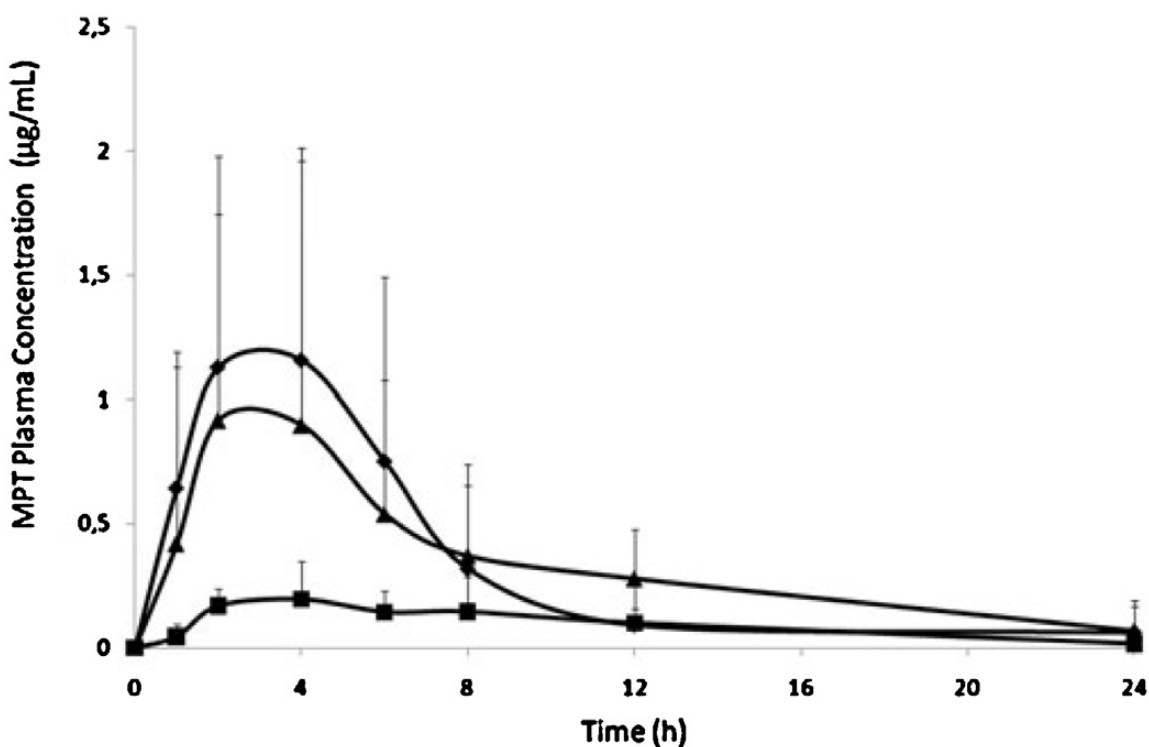


Figure 1.11 Mean plasma concentration–time profiles (+/-SD, n = 6) normalised for the difference in dose after oral administration to dogs: (◆) half tablet Slow-Lopressor® 200 Divitabs®, (■) formulation F2 [30% (w/w) MPT, 27.5% XG, and 42.5% EC], and (▲) formulation F8 [50% (w/w) MPT, 19.64% XG, and 30.35% EC] (Quinten et al., 2011), reproduced with permission.

### 1.3.8 KinetiSol® Dispersing

KinetiSol® Dispersing (KSD) is a thermal processing technique in which paddles rapidly rotate within a cylindrical chamber, generating heat through a combination of shear and friction (DiNunzio et al., 2010c). The process occurs rapidly, generating elevated temperatures in a matter of seconds before ejection of the solid dispersion when a target temperature is achieved. The benefit of rapid processing was demonstrated by developing amorphous solid dispersions with the thermo labile drug hydrocortisone

(DiNunzio et al., 2010a) and with an investigational drug, ROA (Hughey et al., 2010). In the latter case, the drug could not be rendered amorphous by HME into a solid dispersion without substantial degradation. The increased shear imparted by KSD was also effective in dissolving a high molecular weight compound, meloxicam (Hughey et al., 2011), which melts at 270 °C while minimizing thermal degradation. Drugs exhibiting a melting point substantially higher than 200 °C to 220 °C must be dissolved into the polymer carrier and not melted to ensure stability of the polymer. In addition, these high melting point compounds present a challenge in thermal processes, often degrading at elevated temperature once liberated from their crystalline structure, likely related to their structural complexity and size. Meloxicam was rendered amorphous in Soluplus<sup>®</sup> at 118 °C following processing for less than 25 seconds. However, the same composition required recirculation in the extruder for several minutes at 175 °C prior to dissolving. The potency of resulting solid dispersions from these trials were 97.7% and 87.1% for KSD and HME, respectively.

DiNunzio et al. (2010c) studied an itraconazole and HPMC system (1:2) prepared by both KSD and HME. Based on the results of thermal characterization, Figure 1.12, the solid dispersion prepared by HME contained two phases, a polymer rich phase and a drug rich phase. This difference in the solid state of the compositions by the two processes can be attributed to the poor viscous flow properties of HPMC (Methocel<sup>™</sup> E5), the high viscosity and lack of thermoplasticity prevent direct extrusion of this material. The KSD composition was determined to have a single phase, which resulted in a more rapid supersaturation of dissolution media when compared to the HME composition. When evaluated in a rat model, the composition as prepared by both processes was not statistically different following oral administration. However, both

resulted in plasma profiles that were significantly improved when compared to crystalline itraconazole in the same rat model. Further investigation of ITZ and HPMC in vitro by Hughey et al. (2012), which was performed with a higher molecular weight grade of the polymer (Methocel™ E50) utilizing KSD and HME, indicated that the polymer stability was affected by the choice of thermal process. Optimization of the KSD process yielded a reduction in molecular weight degradation, a reduction in polymer chemical degradation and a reduced level of residual medals in the processed compositions compared to those prepared using a HAAKE Minilab II Micro-compounder extruder.

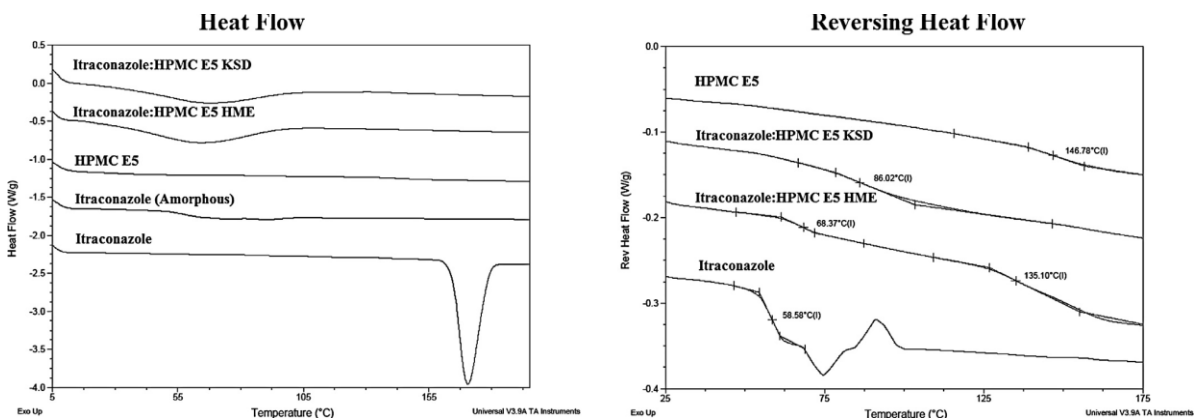


Figure 1.12 Total and reversing DSC thermograms for itraconazole, HPMC, and solid dispersions (DiNunzio et al., 2010c), reproduced with permission.

#### 1.4 CONCLUSIONS

A contemporary review of the literature related to thermal processing yielded a large number of investigations reporting bioavailability enhancement. Fusion processes can be characterized by the method of heat application in addition to the magnitude and duration of heat exposure. In some cases, thermal treatment simply promotes intimate contact of the API with adjuvants to improve solubility, dissolution or membrane

penetration with the final result of enhanced drug absorption. In other cases, thermal treatment allows configuration of dosage forms to modify the onset of drug release or control the rate of release to target absorption windows. Alternatively, the solid state of the drug may be altered, in many cases drastically improving solubility in the intestinal lumen and enabling drug therapy.

Based on this body of evidence, certain processes appear to have strengths either in shaping, forming controlled release structures or forming solid dispersions for solubility enhancement. Some general statements are warranted, yet each technology would likely find application in all these areas. Furthermore, applications for some of the technologies new to the pharmaceutical arena, like dry powder coating, injection molding and KinetiSol<sup>®</sup> dispersing, are still being explored. Shaping of drug delivery vehicles appears to be readily accomplished with injection molding, hot melt extrusion and spray congealing, yielding dosage forms having decreasing shape complexity in the order listed. Melt extrusion, dry powder coating and spray congealing appear well suited for forming controlled release matrices, yet basic melt mixing, melt granulation, and sintering processes have been explored. Solubility enhancing compositions resulting from melt mixing processes have been demonstrated effective in many investigations. However, a trend towards the formation of amorphous solid dispersions using high molecular weight glassy polymers position hot-melt extrusion and KinetiSol<sup>®</sup> dispersing as thermal processes of choice due to their ability to manage the viscosity of these systems in their rubbery or molten state.

## 1.5 REFERENCES

Abberger T, Seo A, and Schæfer T (2002) The effect of droplet size and powder particle size on the mechanisms of nucleation and growth in fluid bed melt agglomeration. *International Journal of Pharmaceutics* **249**, 185-97.

Amidon GL, Lennernäs H, Shah VP, and Crison JR (1995) A Theoretical Basis for a Biopharmaceutic Drug Classification: The Correlation of in Vitro Drug Product Dissolution and in Vivo Bioavailability. *Pharmaceutical Research* **12**, 413-20.

Appel LE, Ray RJR, Lyon DK, West JB, McCray SB, Crew MD et al. (2011) Multiparticulate crystalline drug compositions having controlled release profiles. US7887844B2.

Aungst BJ (2000) Intestinal permeation enhancers. *Journal of Pharmaceutical Sciences* **89**, 429-42.

Baker R (1987) In *Controlled Release of Biologically Active Agents*. Vol. pp. John Wiley & Sons, New York.

Bikiaris DN (2011a) Solid dispersions, Part I: recent evolutions and future opportunities in manufacturing methods for dissolution rate enhancement of poorly water-soluble drugs. *Expert Opinion on Drug Delivery* **8**, 1501-19.

Bikiaris DN (2011b) Solid dispersions, Part II: new strategies in manufacturing methods for dissolution rate enhancement of poorly water-soluble drugs. *Expert Opinion on Drug Delivery* **8**, 1663-80.

Blagden N, de Matas M, Gavan PT, and York P (2007) Crystal engineering of active pharmaceutical ingredients to improve solubility and dissolution rates. *Advanced Drug Delivery Reviews* **59**, 617-30.

Breitenbach J (2002) Melt extrusion: from process to drug delivery technology. *European Journal of Pharmaceutics & Biopharmaceutics* **54**, 107-17.

Brouwers J, Brewster ME, and Augustijns P (2009) Supersaturating drug delivery systems: The answer to solubility-limited oral bioavailability? *Journal of Pharmaceutical Sciences* **98**, 2549-72.

Cao Q-R, Liu Y, Xu W-J, Lee B-J, Yang M, and Cui J-H (2012) Enhanced oral bioavailability of novel mucoadhesive pellets containing valsartan prepared by a dry powder-coating technique. *International Journal of Pharmaceutics* **434**, 325-33.

Carcaboso ÁM, Chiappetta DA, Höcht C, Blake MG, Boccia MM, Baratti CM et al. (2008) In vitro/in vivo characterization of melt-molded gabapentin-loaded poly(epsilon-caprolactone) implants for sustained release in animal studies. *European Journal of Pharmaceutics & Biopharmaceutics* **70**, 666-73.

Cavallari C, Rodriguez L, Albertini B, Passerini N, Rosetti F, and Fini A (2005) Thermal and fractal analysis of diclofenac/Gelucire 50/13 microparticles obtained by ultrasound-assisted atomization. *Journal of Pharmaceutical Sciences* **94**, 1124-34.

Cerea M, Zheng W, Young CR, and McGinity JW (2004) A novel powder coating process for attaining taste masking and moisture protective films applied to tablets. *International Journal of Pharmaceutics* **279**, 127-39.

Chiou WL and Riegelman S (1971) Pharmaceutical applications of solid dispersion systems. *Journal of Pharmaceutical Sciences* **60**, 1281-302.

Clark M, Kiser P, Loxley A, McConville C, Malcolm R, and Friend D (2011) Pharmacokinetics of UC781-loaded intravaginal ring segments in rabbits: a comparison of polymer matrices. *Drug Delivery and Translational Research* **1**, 238-46.

Crowley MM, Schroeder B, Fredersdorf A, Obara S, Talarico M, Kucera S et al. (2004) Physicochemical properties and mechanism of drug release from ethyl cellulose matrix tablets prepared by direct compression and hot-melt extrusion. *International Journal of Pharmaceutics* **269**, 509-22.

Crowley MM, Zhang F, Repka MA, Thumma S, Upadhye SB, Kumar Battu S et al. (2007) Pharmaceutical Applications of Hot-Melt Extrusion: Part I. *Drug Development & Industrial Pharmacy* **33**, 909-26.

Dave VS, Fahmy RM, Bensley D, and Hoag SW (2012) Eudragit® RS PO/RL PO as rate-controlling matrix-formers via roller compaction: Influence of formulation and process variables on functional attributes of granules and tablets. *Drug Development & Industrial Pharmacy* **0**, 1-14.

Davis SS (2005) Formulation strategies for absorption windows. *Drug Discovery Today* **10**, 249-57.

Dierickx L, Saerens L, Almeida A, De Beer T, Remon JP, and Vervaet C (2012) Co-extrusion as manufacturing technique for fixed-dose combination mini-matrices. *European Journal of Pharmaceutics & Biopharmaceutics* **81**, 683-9.

DiNunzio JC, Brough C, Hughey JR, Miller DA, Williams Iii RO, and McGinity JW (2010a) Fusion production of solid dispersions containing a heat-sensitive active ingredient by hot melt extrusion and Kinetisol® dispersing. *European Journal of Pharmaceutics & Biopharmaceutics* **74**, 340-51.

DiNunzio JC, Brough C, Miller DA, Williams RO, and McGinity JW (2010c) Fusion processing of itraconazole solid dispersions by kinetisol® dispersing: A comparative study to hot melt extrusion. *Journal of Pharmaceutical Sciences* **99**, 1239-53.

Fini A, Moyano JR, Ginés JM, Perez-Martinez JI, and Rabasco AM (2005) Diclofenac salts, II. Solid dispersions in PEG6000 and Gelucire 50/13. *European Journal of Pharmaceutics & Biopharmaceutics* **60**, 99-111.

Friesen DT, Shanker R, Crew M, Smithey DT, Curatolo WJ, and Nightingale JAS (2008) Hydroxypropyl Methylcellulose Acetate Succinate-Based Spray-Dried Dispersions: An Overview. *Molecular Pharmaceutics* **5**, 1003-19.

Fukuda M, Peppas NA, and McGinity JW (2006) Floating hot-melt extruded tablets for gastroretentive controlled drug release system. *Journal of Controlled Release* **115**, 121-9.

Garren KW, Rahim S, Marsh K, and Morris JB (2010) Bioavailability of generic ritonavir and lopinavir/ritonavir tablet products in a dog model. *Journal of Pharmaceutical Sciences* **99**, 626-31.

Gazzaniga A, Cerea M, Cozzi A, Foppoli A, Maroni A, and Zema L (2011) A Novel Injection-Molded Capsular Device for Oral Pulsatile Delivery Based on Swellable/Erodible Polymers. *AAPS PharmSciTech* **12**, 295-303.

Ghimire M, Hodges LA, Band J, Lindsay B, O'Mahony B, McInnes FJ et al. (2011) Correlation between in vitro and in vivo erosion behaviour of erodible tablets using gamma scintigraphy. *European Journal of Pharmaceutics & Biopharmaceutics* **77**, 148-57.

Hasanzadeh D, Ghaffari S, Monajjemzadeh F, Al-Hallak M-K, Soltani G, and Azarmi S (2009) Thermal Treating of Acrylic Matrices as a Tool for Controlling Drug Release. *Chemical & Pharmaceutical Bulletin* **12**, 1356-62.

Hoffman AS (2008) The origins and evolution of “controlled” drug delivery systems. *Journal of Controlled Release* **132**, 153-63.

Hughey J, DiNunzio J, Bennett R, Brough C, Miller D, Ma H et al. (2010) Dissolution Enhancement of a Drug Exhibiting Thermal and Acidic Decomposition Characteristics by Fusion Processing: A Comparative Study of Hot Melt Extrusion and KinetiSol® Dispersing. *AAPS PharmSciTech* **11**, 760-74.

Hughey JR, Keen JM, Brough C, Saeger S, and McGinity JW (2011) Thermal processing of a poorly water-soluble drug substance exhibiting a high melting point: The utility of KinetiSol® Dispersing. *International Journal of Pharmaceutics* **419**, 222-30.

Hughey JR, Keen JM, Miller DA, Brough C, and McGinity JW (2012) Preparation of Viscous Solid Dispersion Systems by Hot-Melt Extrusion and KinetiSol® Dispersing: Polymer Screening and Thermal Stability. *International Journal of Pharmaceutics* **438**, 11-9.

Ilić I, Dreu R, Burjak M, Homar M, Kerč J, and Srčić S (2009) Microparticle size control and glimepiride microencapsulation using spray congealing technology. *International Journal of Pharmaceutics* **381**, 176-83.

Jannin V, Musakhanian J, and Marchaud D (2008) Approaches for the development of solid and semi-solid lipid-based formulations. *Advanced Drug Delivery Reviews* **60**, 734-46.

Janssens S and Van den Mooter G (2009) Review: physical chemistry of solid dispersions. *Journal of Pharmacy & Pharmacology* **61**, 1571-86.

Joshi HN, Tejwani RW, Davidovich M, Sahasrabudhe VP, Jemal M, Bathala MS et al. (2004) Bioavailability enhancement of a poorly water-soluble drug by solid dispersion in polyethylene glycol–polysorbate 80 mixture. *International Journal of Pharmaceutics* **269**, 251-8.

Kablitz CD, Harder K, and Urbanetz NA (2006) Dry coating in a rotary fluid bed. *European Journal of Pharmaceutical Sciences* **27**, 212-9.

Kablitz CD and Urbanetz NA (2007) Characterization of the film formation of the dry coating process. *European Journal of Pharmaceutics & Biopharmaceutics* **67**, 449-57.

Kawabata Y, Wada K, Nakatani M, Yamada S, and Onoue S (2011) Formulation design for poorly water-soluble drugs based on biopharmaceutics classification system: Basic approaches and practical applications. *International Journal of Pharmaceutics* **420**, 1-10.

Kolašinac N, Kachrimanis K, Homšek I, Grujić B, Đurić Z, and Ibrić S (2012) Solubility enhancement of desloratadine by solid dispersion in poloxamers. *International Journal of Pharmaceutics* **436**, 161-70.

Leuner C and Dressman J (2000) Improving drug solubility for oral delivery using solid dispersions. *European Journal of Pharmaceutics & Biopharmaceutics* **50**, 47-60.

Liu H, Wang P, Zhang X, Shen F, and Gogos CG (2010) Effects of extrusion process parameters on the dissolution behavior of indomethacin in Eudragit® E PO solid dispersions. *International Journal of Pharmaceutics* **383**, 161-9.

Lo JB, Appel LE, Herbig SM, McCray SB, and Thombre AG (2009) Formulation design and pharmaceutical development of a novel controlled release form of azithromycin for single-dose therapy. *Drug Development & Industrial Pharmacy* **35**, 1522-9.

Luo Y, Zhu J, Ma Y, and Zhang H (2008) Dry coating, a novel coating technology for solid pharmaceutical dosage forms. *International Journal of Pharmaceutics* **358**, 16-22.

Malcolm RK, Edwards K-L, Kiser P, Romano J, and Smith TJ (2010) Advances in microbicide vaginal rings. *Antiviral Research* **88, Supplement**, S30-S9.

Mehuys E, Remon JP, Korst A, Van Bortel L, Mols R, Augustijns P et al. (2005) Human bioavailability of propranolol from a matrix-in-cylinder system with a HPMC-Gelucire® core. *Journal of Controlled Release* **107**, 523-36.

Mehuys E, Vervaet C, Gielen I, Van Bree H, and Remon JP (2004a) In vitro and in vivo evaluation of a matrix-in-cylinder system for sustained drug delivery. *Journal of Controlled Release* **96**, 261-71.

Mehuys E, Vervaet C, and Remon JP (2004b) Hot-melt extruded ethylcellulose cylinders containing a HPMC-Gelucire® core for sustained drug delivery. *Journal of Controlled Release* **94**, 273-80.

Miller DA, McConville JT, Yang W, Williams RO, and McGinity JW (2007) Hot-melt extrusion for enhanced delivery of drug particles. *Journal of Pharmaceutical Sciences* **96**, 361-76.

Monti D, Burgalassi S, Rossato MS, Albertini B, Passerini N, Rodriguez L et al. (2010) Poloxamer 407 microspheres for orotransmucosal drug delivery. Part II: In vitro/in vivo evaluation. *International Journal of Pharmaceutics* **400**, 32-6.

Mu B and Thompson MR (2012) Examining the mechanics of granulation with a hot melt binder in a twin-screw extruder. *Chemical Engineering Science* **81**, 46-56.

Newa M, Bhandari KH, Li DX, Kwon T-H, Kim JA, Yoo BK et al. (2007) Preparation, characterization and in vivo evaluation of ibuprofen binary solid dispersions with poloxamer 188. *International Journal of Pharmaceutics* **343**, 228-37.

Newman A, Knipp G, and Zografi G (2012) Assessing the performance of amorphous solid dispersions. *Journal of Pharmaceutical Sciences* **101**, 1355-77.

Nukala R, Boyapally H, Slipper I, Mendham A, and Douroumis D (2010) The Application of Electrostatic Dry Powder Deposition Technology to Coat Drug-Eluting Stents. *Pharmaceutical Research* **27**, 72-81.

Ochoa L, Igartua M, Hernández RM, Solinís MÁ, Gascón AR, and Pedraz JL (2010) In vivo evaluation of two new sustained release formulations elaborated by one-step melt

granulation: Level A in vitro–in vivo correlation. *European Journal of Pharmaceutics & Biopharmaceutics* **75**, 232-7.

Passerini N, Albertini B, Perissutti B, and Rodriguez L (2006) Evaluation of melt granulation and ultrasonic spray congealing as techniques to enhance the dissolution of praziquantel. *International Journal of Pharmaceutics* **318**, 92-102.

Passerini N, Calogerà G, Albertini B, and Rodriguez L (2010) Melt granulation of pharmaceutical powders: A comparison of high-shear mixer and fluidised bed processes. *International Journal of Pharmaceutics* **391**, 177-86.

Qiao M, Zhang L, Ma Y, Zhu J, and Chow K (2010) A novel electrostatic dry powder coating process for pharmaceutical dosage forms: Immediate release coatings for tablets. *European Journal of Pharmaceutics & Biopharmaceutics* **76**, 304-10.

Quinten T, Beer TD, Vervaet C, and Remon JP (2009a) Evaluation of injection moulding as a pharmaceutical technology to produce matrix tablets. *European Journal of Pharmaceutics & Biopharmaceutics* **71**, 145-54.

Quinten T, De Beer T, Onofre FO, Mendez-Montecalvo G, Wang YJ, Remon JP et al. (2011) Sustained-release and swelling characteristics of xanthan gum/ethylcellulose-based injection moulded matrix tablets: in vitro and in vivo evaluation. *Journal of Pharmaceutical Sciences* **100**, 2858-70.

Quinten T, Gonnissen Y, Adriaens E, Beer TD, Cnudde V, Masschaele B et al. (2009b) Development of injection moulded matrix tablets based on mixtures of ethylcellulose and low-substituted hydroxypropylcellulose. *European Journal of Pharmaceutical Sciences* **37**, 207-16.

Rao M, Ranpise A, Borate S, and Thanki K (2009) Mechanistic Evaluation of the Effect of Sintering on Compritol® 888 ATO Matrices. *AAPS PharmSciTech* **10**, 355-60.

Reitz C and Kleinebudde P (2007) Solid lipid extrusion of sustained release dosage forms. *European Journal of Pharmaceutics & Biopharmaceutics* **67**, 440-8.

Repka MA, Battu SK, Upadhye SB, Thumma S, Crowley MM, Zhang F et al. (2007) Pharmaceutical Applications of Hot-Melt Extrusion: Part II. *Drug Development & Industrial Pharmacy* **33**, 1043-57.

Repka MA, Gutta K, Prodduturi S, Munjal M, and Stodghill SP (2005) Characterization of cellulosic hot-melt extruded films containing lidocaine. *European Journal of Pharmaceutics & Biopharmaceutics* **59**, 189-96.

Repka MA, Majumdar S, Kumar Battu S, Srirangam R, and Upadhye SB (2008) Applications of hot-melt extrusion for drug delivery. *Expert Opinion on Drug Delivery* **5**, 1357-76.

Sammoura F, Kang J, Heo Y-M, Jung T, and Lin L (2007) Polymeric microneedle fabrication using a microinjection molding technique. *Microsystem Technologies* **13**, 517-22.

Sauer D, Zheng W, Coots LB, and McGinity JW (2007) Influence of processing parameters and formulation factors on the drug release from tablets powder-coated with Eudragit® L 100-55. *European Journal of Pharmaceutics & Biopharmaceutics* **67**, 464-75.

Sax G, Feil F, Schulze S, Jung C, Bräuchle C, and Winter G (2012) Release pathways of interferon  $\alpha$ 2a molecules from lipid twin screw extrudates revealed by single molecule fluorescence microscopy. *Journal of Controlled Release*

Schulze S and Winter G (2009) Lipid extrudates as novel sustained release systems for pharmaceutical proteins. *Journal of Controlled Release* **134**, 177-85.

Singh R, Poddar S, and Chivate A (2007) Sintering of wax for controlling release from pellets. *AAPS PharmSciTech* **8**, E175-E83.

Six K, Daems T, de Hoon J, Van Hecken A, Depre M, Bouche M-P et al. (2005) Clinical study of solid dispersions of itraconazole prepared by hot-stage extrusion. *European Journal of Pharmaceutical Sciences* **24**, 179-86.

Streubel A, Siepmann J, and Bodmeier R (2006) Drug delivery to the upper small intestine window using gastroretentive technologies. *Current Opinion in Pharmacology* **6**, 501-8.

Sudha B, Sridhar B, and Srinatha A (2010) Modulation of Tramadol Release from a Hydrophobic Matrix: Implications of Formulations and Processing Variables. *AAPS PharmSciTech* **11**, 433-40.

Tang B, Cheng G, Gu J-C, and Xu C-H (2008) Development of solid self-emulsifying drug delivery systems: preparation techniques and dosage forms. *Drug Discovery Today* **13**, 606-12.

Tayel S, Soliman I, and Louis D (2010) Formulation of Ketotifen Fumarate Fast-Melt Granulation Sublingual Tablet. *AAPS PharmSciTech* **11**, 679-85.

Terife G, Wang P, Faridi N, and Gogos CG (2012) Hot melt mixing and foaming of soluplus® and indomethacin. *Polymer Engineering & Science* **52**, 1629-39.

Tran P, Tran T, Park J, and Lee B-J (2011) Controlled Release Systems Containing Solid Dispersions: Strategies and Mechanisms. *Pharmaceutical Research* **28**, 2353-78.

Urbanetz NA and Lippold BC (2005) Solid dispersions of nimodipine and polyethylene glycol 2000: dissolution properties and physico-chemical characterisation. *European Journal of Pharmaceutics & Biopharmaceutics* **59**, 107-18.

Vasanthavada M, Wang Y, Haefele T, Lakshman JP, Mone M, Tong W et al. (2011) Application of melt granulation technology using twin-screw extruder in development of high-dose modified-release tablet formulation. *Journal of Pharmaceutical Sciences* **100**, 1923-34.

Vasconcelos T, Sarmento B, and Costa P (2007) Solid dispersions as strategy to improve oral bioavailability of poor water soluble drugs. *Drug Discovery Today* **12**, 1068-75.

Verhoeven E, De Beer TRM, Schacht E, Van den Mooter G, Remon JP, and Vervaet C (2009) Influence of polyethylene glycol/polyethylene oxide on the release characteristics of sustained-release ethylcellulose mini-matrices produced by hot-melt extrusion: in vitro and in vivo evaluations. *European Journal of Pharmaceutics & Biopharmaceutics* **72**, 463-70.

Verhoeven E, Vervaet C, and Remon JP (2006) Xanthan gum to tailor drug release of sustained-release ethylcellulose mini-matrices prepared via hot-melt extrusion: in vitro and in vivo evaluation. *European Journal of Pharmaceutics & Biopharmaceutics* **63**, 320-30.

Verreck G, Decorte A, Heymans K, Adriaensen J, Cleeren D, Jacobs A et al. (2005) The effect of pressurized carbon dioxide as a temporary plasticizer and foaming agent on the hot stage extrusion process and extrudate properties of solid dispersions of itraconazole with PVP-VA 64. *European Journal of Pharmaceutical Sciences* **26**, 349-58.

Vilhelmsen T and Schæfer T (2005) Agglomerate formation and growth mechanisms during melt agglomeration in a rotary processor. *International Journal of Pharmaceutics* **304**, 152-64.

Windbergs M, Haaser M, McGoverin CM, Gordon KC, Kleinebudde P, and Strachan CJ (2010) Investigating the relationship between drug distribution in solid lipid matrices and dissolution behaviour using raman spectroscopy and mapping. *Journal of Pharmaceutical Sciences* **99**, 1464-75.

Windbergs M, Strachan CJ, and Kleinebudde P (2009) Understanding the solid-state behaviour of triglyceride solid lipid extrudates and its influence on dissolution. *European Journal of Pharmaceutics & Biopharmaceutics* **71**, 80-7.

Yang D, Kulkarni R, Behme RJ, and Kotiyan PN (2007) Effect of the melt granulation technique on the dissolution characteristics of griseofulvin. *International Journal of Pharmaceutics* **329**, 72-80.

Zema L, Loreti G, Melocchi A, Maroni A, and Gazzaniga A (2012) Injection Molding and its application to drug delivery. *Journal of Controlled Release* **159**, 324-31.

Zheng X, Yang R, Zhang Y, Wang Z, Tang X, and Zheng L (2007) Part II: Bioavailability in Beagle Dogs of Nimodipine Solid Dispersions Prepared by Hot-Melt Extrusion. *Drug Development & Industrial Pharmacy* **33**, 783-9.

## **Chapter 2: Research Objectives**

### **2.1 OVERALL OBJECTIVES**

This work was undertaken to investigate novel thermal processing technologies and formulation techniques intended to enhance the bioavailability of drugs, both soluble and insoluble. Thermal processes were developed to exploit various material properties to alter the geometries of particles and the molecular arrangement therein to safely control drug release, improve solubility or both. In some cases, these particles were formulated into and characterized as final dosage forms. In one formulation, *in vitro* analysis was insufficient to determine utility as a medicament, *in vivo* analysis was performed to assess bioavailability directly in a dog model.

### **2.2 SUPPORTING OBJECTIVES**

#### **2.2.1 Investigation of Process Temperature and Screw Speed on Properties of a Pharmaceutical Solid Dispersion using Co-rotating and Counter-rotating Twin Screw Extruders**

In this study, a counter-rotating geometry of hot-melt extrusion, which is unexplored for the preparation of glassy supersaturating solid dispersions, was applied to determine if the process presents efficiencies suitable for the preparation of solubility enhancing amorphous dispersions of high melting point drugs. These drugs must be dissolved in the polymer melt below their melting temperatures and due to their size and molecular complexity are often thermo labile. This extrusion mode was applied to a model system and compared to the often applied co-rotating extrusion mode and compared in for solubilization efficiency as a function of temperature. In addition, total

thermal exposure was assessed through modeling of the residence times. These results were compared to thermodynamic predictions of Flory Huggins theory.

### **2.2.2 Controlled Release Supersaturating Solid Dispersions Containing Glycerol Behenate**

Two thermal processes, hot-melt extrusion and KinetiSol<sup>®</sup> Dispersing were evaluated in the preparation of glassy amorphous systems containing a lipid and a high molecular weight polymer with two poorly water soluble drugs, carbamazepine and itraconazole. The impact of the lipid on the extrusion process was evaluated. The properties of the resulting matrices were studied to understand the mechanism of release so that factors suitable to allow for a controlled release in non-sink and sink conditions can be controlled. Specifically, the porosity, hydrophobicity, geometry of the matrices and media volume were varied to understand when the amorphous drugs crystallized within the dosage forms prior to release.

### **2.2.3 Development of Itraconazole Tablets Containing Viscous KinetiSol<sup>®</sup> Solid Dispersions: *in vitro* and *in vivo* Analysis in Dogs**

KinetiSol<sup>®</sup> Dispersing was utilized for the development of immediate and controlled release tablets of itraconazole. High molecular weight hydroxypropyl methylcellulose solid dispersions were prepared and the formulation variables required to create controlled release in acid or immediate release profiles of itraconazole were investigated. The impact of these variables on the solubility of itraconazole in fasted simulated intestinal fluid and neutral buffers were investigated *in vitro*. Finally, pharmacokinetics of lead formulations were studied in beagle dogs and compared to a hot-melt extruded commercial control.

#### **2.2.4 Continuous Twin Screw Melt Granulation of Glyceryl Behenate: Evaluation of Critical Process Parameters and Development of Controlled Release Tramadol Hydrochloride Tablets for Improved Safety**

A novel melt granulation process utilizing a staged and reduced temperature profile in a modified twin screw extruder was developed for continuous granulation using a lipid. The critical process parameters for producing a desirable granulation particle size distribution were determined. The resulting granules were formulated into tablets exhibiting a controlled, yet complete release of tramadol hydrochloride. The formulated tablets were observed to yield a safe, unaltered release of drug in the presence of alcohol. In addition, the mechanisms of granulation and drug release were evaluated.

### **2.3 SUMMARY**

This work investigates the utility of combining materials having a broad range of properties with medicaments using existing and novel thermal processing techniques to alter the molecular arrangement and macro scale geometry of dosage forms to improve the bioavailability of drugs. Lipids and polymers were carefully formulated using novel processes to improve the solubility of poorly soluble drugs and to develop controlled release dosage forms of poorly soluble and water soluble drugs. Bioavailability enhancement of a supersaturating, controlled release composition containing a poorly water soluble drug was demonstrated in a beagle dog model.

## **Chapter 3: Investigation of Process Temperature and Screw Speed on Properties of a Pharmaceutical Solid Dispersion using Co-rotating and Counter-rotating Twin Screw Extruders**

### **3.1 ABSTRACT**

The use of co-rotating twin screw hot-melt extruders to prepare amorphous drug/polymer systems has become commonplace. As small molecule drug candidates exiting discovery pipelines trend towards higher molecular weight and become more structurally complicated, the acceptable operating space shifts below the drug melting point. Understanding of the process space, which should be selected to ensure the drug is solubilized in the polymer with minimal thermal exposure, is critical to ensuring the performance, stability and purity of the solid dispersion. The properties of a model solid dispersion were investigated using both co-rotating and counter-rotating hot melt twin screw extruders operated at various temperatures and screw speeds. The solid state and dissolution performance of the resulting solid dispersions was investigated and evaluated in context of thermodynamic predictions from Flory-Huggins Theory. In addition, the residence time distribution of both extrusion modes was measured using a tracer, modeled and characterized. The amorphous content in the resulting solid dispersions was dependent on the combination of screw speed, temperature and operating mode. The counter-rotating extruder was observed to form amorphous solid dispersions at a slightly lower temperature and with a narrower residence time distribution, which also exhibited a more desirable shape.

### 3.2 INTRODUCTION

Hot-melt extrusion (HME) has emerged as a robust processing technology in the pharmaceutical industry where it is used to produce a variety of dosage forms including granules, pellets, tablets, transdermal laminates, implants, and process intermediates for controlled release and solubility enhancement of therapeutics (Repka et al., 2007, Dierickx et al., 2012, Feng et al., 2012, Terife et al., 2012). Twin screw extruders are routinely employed due to their ability to form intimate mixtures of drugs and polymers. Co-rotating and counter-rotating twin screw extruders are both used to melt, shear and pump polymeric materials. However, their differing geometries change the relative amounts of positive displacement and shear. In terms of plastics processing and broadly speaking, co-rotating extruders are widely employed to mix plastic formulations for subsequent use in injection molding or subsequent extrusion processes. Counter-rotating extruders are often, but not exclusively, employed for processes requiring stable and/or high pressure output, such as forming continuous profiles or sheets. The counter-rotating extruder provides a greater degree of positive displacement and extensional shear occurs along the entire length of the screw, even in the conveying sections (Tadmor and Gogos, 2006). On the other hand, co-rotating extruders are perceived to offer a wider range of mixing capabilities (Crowley et al., 2007). However, there is a great deal of overlap in the processing capabilities of the two extrusion modes as screw designs can be designed for either mode to accomplish a wide range of pressure and shear profiles.

Co-rotating twin screw extruders are routinely employed for solubility enhancement of BCS Class II and IV drugs. The properties of small molecule drugs emerging from development pipelines during the last decade indicate a trend towards higher molecular weight, increasing lipophilicity and lower solubility (Keseru and

Makara, 2009). With this trend in drug molecule properties, the configuration of the extruder and its operating conditions becomes more critical to ensuring these drugs are solubilized in the polymer during the residence time in the extruder. In particular, as higher molecular weights correspond to higher melting points, melting the drug during the process may become prohibited by the operating range of the polymer. Keserü and Makara (2009) also observed that drug candidates are becoming more complex; having increased numbers of heavy atoms, rotors, and rings. Undoubtedly, these attributes lead to increased sensitivity to degradation in the amorphous state and/or upon melting further pressuring the process to operate at lower temperatures.

For thermally sensitive high molecular weight drugs, the balance between mixing efficiency and thermal exposure must be evaluated and controlled to ensure safety and efficacy of the final product. In theory, counter-rotating extruders may offer an advantage for this application, for two reasons: 1) counter-rotating extruders impart extensional flow along the entire length of the screw due to the diverging geometry at the intermesh, and 2) counter-rotating extruders can be designed to provide a greater degree of positive displacement.

The flow profiles in twin screw extruders are complex, yet there are a few key distinctions. Maximum velocity occurs at the intermeshing region of a counter-rotating extruder and at the tips of the screws in the co-rotating extruder (Shah and Gupta, 2004). In the counter-rotating extruder, material is stretched and elongated at the interface as the surfaces of the screws diverge. The resulting extensional flow increases the interfacial area exponentially with time, while in a simple shear field interfacial area grows linearly with time (Manas-Zloczower, 2009, Tucker III, 2009). From the perspective of a drug

particle dissolving in a polymer melt, this flow profile may prove important in reducing the boundary layer thickness and increasing the dissolution rate of the drug. The dissolution process of crystalline drugs in polymer melts has been demonstrated as a critical aspect of producing amorphous solid dispersions below the melting point of the drug (Liu et al., 2010, Hughey et al., 2011).

Another important consequence of the screw geometries of counter-rotating versus co-rotating twin screw extruders is that the counter-rotation configuration, depending on screw design, provides positive displacement instead of semi-drag flow that is indicative of co-rotating extruders (Martin, 2004). In practical terms, counter-rotation designs can be configured more like a pump and can have a narrower residence time distribution (RTD). During solid dispersion development as with all pharmaceutical products, low level impurities from thermal degradation must be monitored to ensure safety and efficacy of the final dosage form (FDA, 2008). Impurity formation during thermal processing is a known function of residence time (DiNunzio et al., 2010a).

The objective of this study was to investigate the properties of a model solid dispersion system of griseofulvin and copovidone (Kollidon<sup>®</sup> VA 64) in a Leistritz 27mm twin screw extruder operated in the co-rotating and counter-rotating mode. Griseofulvin was selected due to its poor solubility, molecular weight of 353 Da, and a melting point >200 °C; properties which are in-line with pipeline molecules that require solubility enhancement. Relative to hot-melt extrusion, these properties indicate that the drug will require solubilization in the polymer and will not be melted during extrusion. This initial investigation focuses on the extrusion mode and parameters required to dissolve crystalline griseofulvin into the solid dispersion and to quantify the RTD of the two

geometries. The temperature, screw speed and concentration of griseofulvin in the solid dispersion were varied for each extrusion mode to compare and contrast the factors leading to an amorphous solid dispersion. These factors were considered in parallel to the thermodynamic predictions of Flory-Huggins Theory for this system. The *in vitro* performance of the amorphous solid dispersions and the solid state were investigated. Finally, the residence time distributions for each extruder configuration were determined, modeled and characterized.

### **3.3 MATERIALS AND METHODS**

#### **3.3.1 Materials**

Copovidone, Kollidon VA 64, was kindly donated by BASF Corporation (Florham Park, NJ). Micronized griseofulvin (GRIS) was purchased from Letco Medical (Decatur, AL). Indigo carmine was obtained from Acros Organics (Geel, Belgium). High performance liquid chromatography grade acetonitrile, and tetrahydrofuran were purchased from Fisher Scientific (Pittsburg, PA). All materials were used as supplied.

#### **3.3.2 Methods**

##### ***3.3.2.1 Hot Melt Extrusion***

GRIS and copovidone were simultaneously fed, at a combined feed rate of 4 kg/hr, from two separate gravimetric twin screw feeders, (K-Tron, Pitman, NJ), to a 27mm twin screw extruder, Leistritz Micro 27 (Leistritz, Somerville, NJ). The composition of the feed was varied based on the test condition between 20% and 40% by

weight GRIS. Experiments were conducted both with the gear box and screws configured for co-rotation (GL) and for counter-rotation (GG). The screw designs, both 40:1 Length:Diameter (L/D), are included in Figure 3.1 for reference. The barrel temperature, starting at the first mixing zone, was set at the test temperature. The extruder was equipped with a 5 mm diameter die that was maintained at 160 °C for all experiments. The screw RPM, along with the feed composition, and barrel temperature were varied to investigate the conditions that yielded amorphous extruded, based on visual observation. The test conditions evaluated are listed in Table 3.1. The total feed rate for all tests was 4 kg/hr and the extrudate was air cooled on a conveyor. Collected samples were ground using a coffee mill to transform to powder. The size fraction between 90 µm and 180 µm, which is a suitable particle size for the intended analytical evaluations and ease of handling, was collected for further analysis.

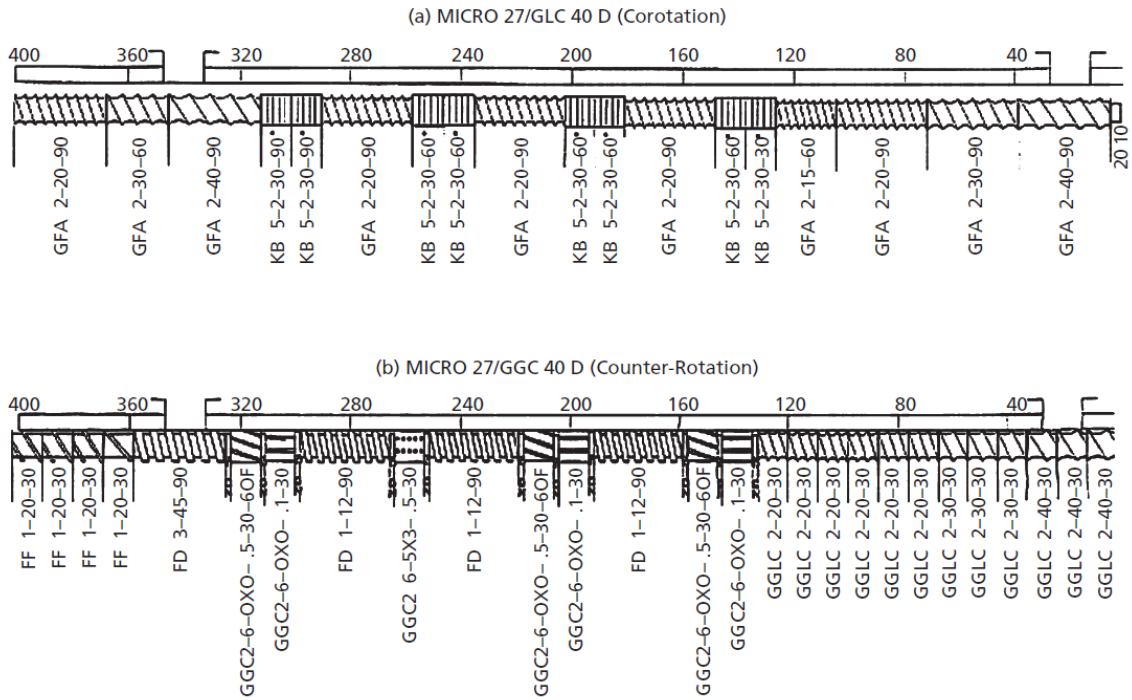


Figure 3.1 Screw design employed in the Leistritz 27 mm twin screw extruder for A) co-rotating configuration (GL) and the counter-rotating configuration (GG).

Table 3.1 Extrusion test conditions

Test No.	Extruder Configuration	Drug Load (%)	Temperature (°C)	Screw Speed (rpm)	Visual Assessment of Extrudate
1	Co-Rotating	20	160	150	Crystalline
2	Co-Rotating	20	180	150	Amorphous
3	Co-Rotating	30	170	300	Crystalline
4	Co-Rotating	30	170	450	Crystalline
5	Co-Rotating	30	180	150	Crystalline
6	Co-Rotating	30	180	300	Crystalline
7	Co-Rotating	30	180	450	Amorphous
8	Co-Rotating	40	180	450	Crystalline
9	Counter-Rotating	20	160	150	-
10	Counter-Rotating	20	160	300	Amorphous
11	Counter-Rotating	30	160	300	Crystalline
12	Counter-Rotating	30	170	300	Crystalline
13	Counter-Rotating	30	170	450	Amorphous
14	Counter-Rotating	30	180	300	Crystalline
15	Counter-Rotating	30	180	450	Amorphous

### 3.3.2.2 X-Ray Powder Diffraction

An Equinox 100 standalone bench top X-ray diffractometer (INEL, Inc., Stratham NH) was used to analyze the milled extrudate samples for the presence of crystallinity. Samples were placed in an aluminum crucible and loaded in a rotating sample holder. Samples were analyzed for 300 seconds using a Cu K radiation source ( $\lambda = 1.5418 \text{ \AA}$ ) operating at 42 kV and 0.81 mA.

### 3.3.2.3 Shear Cell Analysis

To evaluate the powder flow behavior of the GRIS/copovidone system, 20% and 30% GRIS by weight were blended and analyzed using a RST-XS Ring Shear Tester (Dietmar Schulze, Wolfenbüttel, Germany). The shear stress of both blends was

evaluated under load ranging from 0.3 to 1.2 kPa. The flow-function coefficient (FFC) was determined using RSV 95 software (Dietmar Schulze).

#### ***3.3.2.4 Thermal Analysis***

Thermal analysis was performed using a model Q20 modulated differential scanning calorimeter (TA Instruments, New Castle, Delaware) to determine the influence of copovidone on the onset melting temperature and the melting enthalpy of griseofulvin and investigate the glass transition temperature of test samples. Physical mixtures of 100, 95, 90, 85, and 80% GRIS by volume were prepared, stored in a desiccator, and tested in triplicate.  $6.0 \pm 0.1$  mg samples were analyzed under a nitrogen atmosphere (50 mL/min). The samples were equilibrated at 35 °C for 5 minutes followed by a 1.00 °C/min ramp to 250 °C. The glass transition temperature of the test samples was determined on  $6.0 \pm 1$  mg samples. The samples were equilibrated at 35 °C for 5 minutes followed by a 5 °C/min ramp to 250 °C modulating every 60 s at an amplitude of 1 °C. Glass transition temperatures were measured similarly for determining the concentration Tg profile with the exception that samples were pretreated by heating to 250 °C and quench cooled to remove thermal history.

A Thermogravimetric Analyzer 7 (Perkin-Elmer, Norwalk, CT) was used to investigate the thermal stability of GRIS. Sample pans were placed in the chamber and equilibrated at 50 °C under a constant flow of nitrogen (65 mL/min). Once equilibrated, the sample mass was monitored as the temperature was increased from 50 °C to 350 °C at a rate of 10 °C/min.

### **3.3.2.5 Rheology**

The viscosity of copovidone as a function of indigo carmine concentration (0.00, 0.25, 0.50 and 1.00% w/w indigo carmine) was determined using an Advanced Rheometer 2000 (TA Instruments, New Castle, Delaware) equipped with a smooth parallel plate assembly. Samples were prepared by blending copovidone and indigo carmine, then extruding at 160 °C and 360 rpm using a HAAKE Minilab II Microcompounder (Thermo Electron Corporation, Newington, New Hampshire). Ground samples were raised to 155 °C and incrementally squeezed to a gap clearance of 2000 µm in the rheometer. The system was equilibrated for 10 minutes before reducing the clearance to 1000 µm, followed by additional 10 minutes of equilibration. Testing was performed in Oscillatory Frequency Sweep mode with a frequency range of 0.1-100 Hz at a constant strain amplitude in the linear viscoelastic region. Samples attained steady state to allow for the decay of transient phenomena prior to measurement. Data was transformed using the Cox Merz rule within the TA Advantage Software.

### **3.3.2.6 Dissolution**

Non-sink dissolution analysis was performed using a VK 7010 dissolution testing apparatus (Varian Inc., Palo Alto, California) configured according to USP XXXIX Method A (paddle method). Sieved extrudate was weighed to achieve  $50 \pm 1$  mg GRIS and added to dissolution vessels containing 1000 mL 0.1N HCl. The vessels were maintained at  $37.0 \pm 0.5$  °C with paddles rotating at 50 rpm. Test samples were studied in triplicate, with 5 mL samples collected from the vessels at 5, 10, 15, 30, 45, 60, 90 and 120 minutes. Immediately following sampling, the samples were filtered through 0.2 µm, 17 mm, PVDF syringe filters (Fisher Scientific, Pittsburgh, PA) and diluted 1:1 with 50:50 acetonitrile:water and transferred to HPLC vials for analysis.

### 3.3.2.7 High Performance Liquid Chromatography

High performance liquid chromatography (HPLC) was used to analyze the potency of selected test samples as well as to quantitate the dissolution samples. A 717 autosampler (Waters Corporation, Milford, MA) configured with a Luna 5  $\mu\text{m}$  CN 100 Å, 150 x 4.6 mm column (Phenomenex, Torrance, CA). The mobile phase was a mixture of acetonitrile:water:tetrahydrofuran 65:35:5 flowing at 1.00 mL/min. Potency samples were prepared to contain 0.1 mg/mL in acetonitrile:water 50:50. Potency and dissolution samples were injected at volume of 20  $\mu\text{L}$ . A Waters 2996 photodiode array detector, extracting at 292 nm, was used to quantify the results. The retention time of GRIS was approximately 4 min. All analyses maintained linearity ( $R^2 = 0.999$ ) in the range tested and a relative standard deviation of less than 2.0%. Empower Version 5.0 was utilized to process all chromatography data.

### 3.3.2.8 Flory-Huggins Theory

The phase diagram for the GRIS and copovidone system was generated using Flory-Huggins theory, as described previously (Flory, 1942, Huggins, 1942, Marsac et al., 2009, Lin and Huang, 2010, Zhao et al., 2011, Bellantone et al., 2012, Tian et al., 2012). The Gibbs free energy of mixing function that results from application of the Flory-Huggins model is dependent on the volume fraction of the drug,  $\phi$ , a constant indicative of the relative size of the polymer in relation to the drug,  $m$ , and the interaction parameter,  $\chi$ .

$$\frac{\Delta G_{mix}}{RT} = \phi \ln \phi + \frac{(1-\phi)}{m} \ln(1-\phi) + \phi(1-\phi)\chi \quad \text{Equation 3.1}$$

DSC experiments to determine the melting enthalpy of the drug,  $\Delta H$ , and either the melting temperature (Marsac et al., 2009, Lin and Huang, 2010), onset of melting (Zhao et al., 2011), or ending of melting (Tian et al., 2012) have been applied by various authors to determine  $\chi$ , which is a function of temperature (Marsac et al., 2006). For the GRIS/copovidone system, melting temperature was selected based on the reproducibility of this value in experimental trials. The equation to determine  $\chi$  in the drugs melting range is:

$$\frac{1}{T_m} - \frac{1}{T_m^o} = -\frac{R}{\Delta H} \left[ \ln(\phi) + \left(1 - \frac{1}{m}\right)(1 - \phi) + \chi(1 - \phi)^2 \right] \text{Equation 3.2}$$

Where  $T_m^o$  is the melting point of GRIS and  $T_m$  is the melting point of GRIS in the presence of copovidone at each concentration studied. The constant,  $m$ , was determined from the molecular weights of GRIS and copovidone along with their density,  $\rho$ ,

$$m = \frac{\frac{MW_{\text{copovidone}}}{\rho_{\text{copovidone}}}}{\frac{MW_{\text{GRIS}}}{\rho_{\text{GRIS}}}} \text{Equation 3.3}$$

The temperature dependency of  $\chi$  can be extrapolated to room temperature with the application of solubility parameters (Zhao et al., 2011). Literature values for the Hoftyzer and Van Krevelen solubility parameters,  $\delta$ , for GRIS, 29.54 (J/cm<sup>3</sup>)<sup>1/2</sup> (Nair et al., 2001), and copovidone, 23.91 (J/cm<sup>3</sup>)<sup>1/2</sup> (Zhao et al., 2011), along with the molar volume per Flory-Huggins lattice site,  $v$ , taken to be the molar volume of GRIS, 255.1 cm<sup>3</sup>/mol (Al-Obaidi et al., 2011, Bellantone et al., 2012),

$$\chi = \frac{v(\delta_{\text{GRIS}} - \delta_{\text{copovidone}})^2}{RT} \text{Equation 3.4}$$

The results from Equations 3.2 and 3.4 were combined to determine the overall dependence of  $\chi$  from 25 °C to the melting point for the drug.

$$\chi(T) = A + \frac{B}{T} \quad \text{Equation 3.5}$$

It is notable that for this analysis  $\chi$  is assumed to be only a function of temperature. Any dependency on composition is neglected; this assumption is in line with that made by previous authors (Marsac et al., 2009, Lin and Huang, 2010, Zhao et al., 2011, Tian et al., 2012). With the solution to Equation 3.5, a Gibbs free energy diagram at selected temperatures can be produced.

Setting the second derivative of Equation 3.1 equal to zero and determining  $\phi$  as a function of  $\chi$  allows for the determination of the boundary between unstable and metastable regions, the spinodal curve.

$$\frac{1}{\phi} + \frac{1}{m(1-\phi)} - 2\chi = 0 \quad \text{Equation 3.6}$$

Furthermore, the boundary between the metastable and stable regions can be formed by constructing the common tangents between minima on the free energy diagram. This corresponds to points in which the chemical potentials of two phases are in equilibrium.

$$\left( \frac{\partial \frac{G}{RT}}{\partial \phi} \right)^{\text{Phase 1}} = \left( \frac{\partial \frac{G}{RT}}{\partial \phi} \right)^{\text{Phase 2}} \quad \text{Equation 3.7}$$

and

$$\left( \frac{\partial \frac{G}{RT}}{\partial (1-\phi)} \right)^{\text{Phase 1}} = \left( \frac{\partial \frac{G}{RT}}{\partial (1-\phi)} \right)^{\text{Phase 2}} \quad \text{Equation 3.8}$$

The binodal curve resulting from the solution to Equations 3.7 and 3.8, which is solved numerically, will intersect the spinodal curve at the critical point, the third derivative of Equation 3.1.

$$\frac{\partial^3 \frac{G}{RT}}{\partial \phi^3} = 0 \quad \text{Equation 3.9}$$

However, it is notable that in the case of a small molecule drug and a high molecular weight polymer (large value of  $m$ ), the free energy curves and spinodal curve are highly asymmetrical. Consequently, a real solution to Equations 3.7 and 3.8 may not exist. From a physical perspective, this situation arises when the metastable form separates into two phases in which one phase consists of pure drug. In this case, the binodal curve in the region of interest can be constructed from the single minimum observed on the free energy curves.

### ***3.3.2.9 Residence Time Distribution***

The RTD was determined for the co-rotating and counter-rotating extrusion configurations by charging 1 g of indigo carmine into the extruder feed hopper. The charge was selected based the results of preliminary studies performed with copovidone on a 16mm NANO 16 co-rotating twin screw extruder (Leistritz, Somerville, NJ). The time at which material was charged into the feed zone was denoted as  $t = 0$  and a calibrated timer utilized to determine the time. The time at which colored extrudate emerged from the die was noted and samples were subsequently collected every 15 seconds for 2 minutes after the initial coloring was visually observed. After that point, sampling frequency was reduced to 1 minute intervals for a total of 10 minutes. Approximately 50 cm of extrudate was collected at each time point. Samples were

evaluated in triplicate by dissolving  $150 \text{ mg} \pm 50 \text{ mg}$  of neat extrudate in 20 mL of acetonitrile:water 50:50 and quantified using a UV spectrometer ( $\mu$ Quant, BIO-TEK<sup>®</sup> Instruments, Inc., Winooski, VT) at 610 nm. The UV response of indigo carmine in this analysis was linear over the concentration range studied ( $R^2 > 0.9999$ ) and the limit of detection was  $0.25 \text{ } \mu\text{g/ml}$ .

The data was fit according to the Zusatz residence time distribution function (Poulesquen et al., 2003, Zhang et al., 2008).

$$E(t) = at^{-c-1}b^{c+1}e^{(b^c t^c - 1)\left(\frac{-c-1}{c}\right)} \quad \text{Equation 3.10}$$

Where a, b and c are fitted parameter for the system. Mu and Thompson (2012) recently demonstrated the applicability of this approach to modeling complex screw geometry where mixing sections result in axial dispersion observed as tailing of the RTD. The RTD in this case was fitted assuming additive contributions from the conveying and mixing zones. Mathematically, the RTD equation is fitted by deconvoluting a modified form of Equation 3.10, which is modified to be a summation of each contributor,  $n=3$  was used for our analysis.

$$E(t) = \sum_i^n \left( at^{-c-1}b^{c+1}e^{(b^c t^c - 1)\left(\frac{-c-1}{c}\right)} \right)_i \quad \text{Equation 3.11}$$

The mean residence time is calculated from the first moment of the distribution,

$$t_{mean} = \int_0^\infty tE(t)dt \quad \text{Equation 3.12}$$

and the variance is calculated from the second moment.(Poulesquen and Vergnes, 2003)

$$\sigma^2 = \int_0^\infty (t - t_{mean})^2 E(t)dt \quad \text{Equation 3.13}$$

The skewness(Minnich et al., 2011) is calculated to describe the asymmetry of the RTD.

$$S = \sigma^{-3} \int_0^{\infty} (t - t_{mean})^3 E(t) dt \quad \text{Equation 3.14}$$

## 3.4 RESULTS AND DISCUSSION

### 3.4.1 Thermal analysis and construction of the phase diagram

The GRIS melting point was observed to decrease with increasing concentration of copovidone, Figure 3.2. The Flory Huggins interaction parameter,  $\chi$ , was calculated by melting point depression data at elevated temperature (Equation 3.2) and by solubility parameter estimation at 25 °C, resulting in values of  $0.4 \pm 0.08$  and 3.6, respectively. The decrease of  $\chi$  at elevated temperature indicated mixing of GRIS and copovidone becomes more favorable with increasing temperature. Examination of free energy diagrams presented in Figure 3.3(a) and generated by the solving the free energy relationship (Equation 3.1) at specific temperatures further highlight this behavior, with thermodynamic favorability for systems greater than 60% v/v at 150 °C. Conversely, at low temperatures only limited thermodynamic favorability is observed, with systems less than 5% v/v being favored at room temperature.

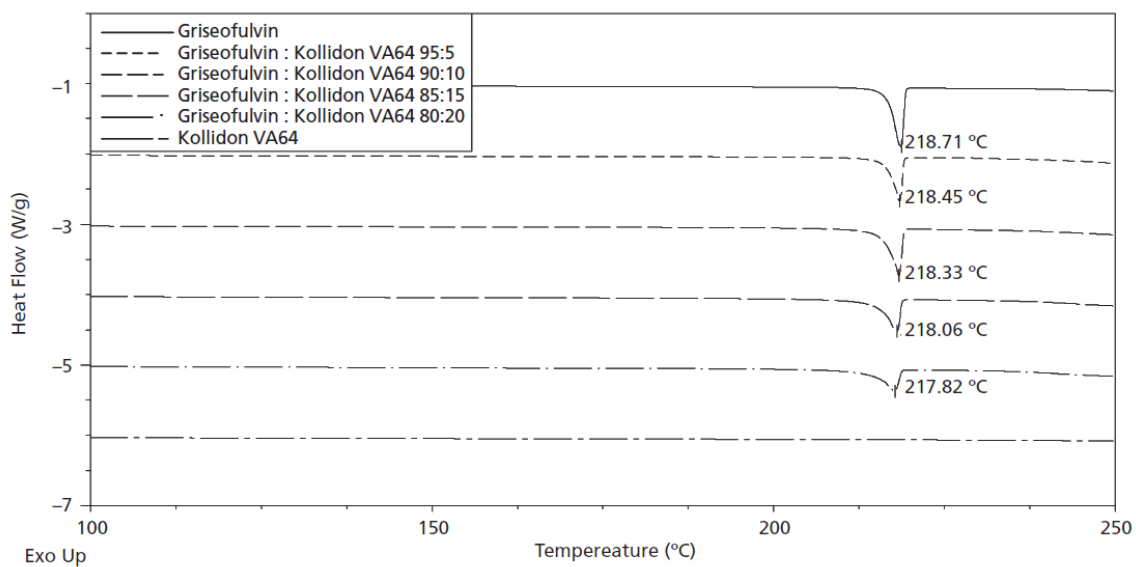


Figure 3.2 Differential scanning calorimetry thermograms for physical mixtures of GRIS:Copovidone over the range of 100:0 to 80:20 by volume demonstrating the melting point depression as observed scanning at 1 °C/min.

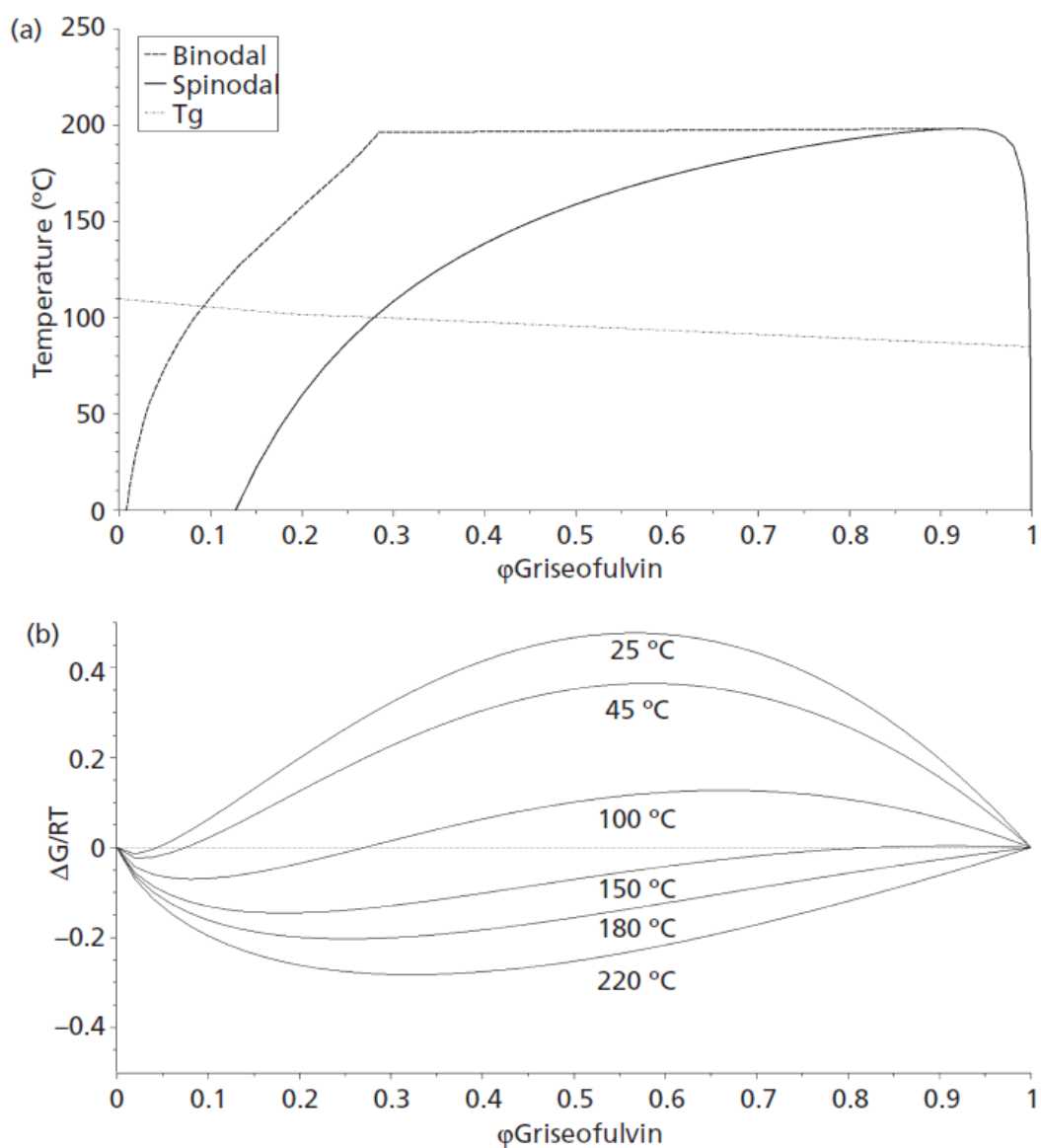


Figure 3.3 A) Thermal phase diagram of the GRIS/copovidone representing the boundaries between thermodynamically unstable, metastable and stable regions as bounded by the spinodal and binodal curves along with the glass transition boundary. B) Free energy diagram of the GRIS/copovidone system as determined using Flory-Huggins Theory.

The free energy diagram, presented in Figure 3.3(b), was used to generate a phase diagram for the GRIS:copovidone system, illustrating the stable, metastable and unstable regions of the system as a function of temperature. In addition to the binodal and spinodal curves, the glass transition temperature curve serves as an indicator of a drastic change in viscosity (Craig et al., 1999), where below this line reduced molecular motion of the system kinetically hinders mixing of thermodynamically favorable systems and demixing of thermodynamically unfavorable systems on experimentally relevant time scales (Hancock et al., 1995). As temperature increases, viscosity decreases, driving an increase of molecular motion within the system that reduces kinetic barriers to attaining thermodynamic equilibrium. While rates to achieve equilibrium can be reduced from months to minutes by increasing molecular mobility, when considering processes on extrusion relevant timescales kinetic factors cannot be neglected. For pharmaceutical applications, residence times generally range from 5 s to 10 min depending on extruder process design and operating conditions. To successfully develop amorphous dispersions by HME it is necessary to identify drug loadings that do not lie in the unstable region at the target processing conditions. From the phase diagram, 20% and 30% w/w GRIS concentration are projected to be obtained at melt temperatures of 159 °C and 198 °C, respectively. Noting that the melting point of the drug substance is 219 °C, the phase diagram estimates establish the lower bound for melt temperature that can achieve the target drug loading in the solubilization regime.

Thermal stability of a compound is also a critical property that can establish an upper bound to allowable melt temperature. During thermal analysis GRIS was observed to be thermally stable in comparison to similar size molecules we have encountered in development. GRIS degradation beyond 0.1% was observed at temperatures greater than

200 °C (data not presented), with an increasing rate of decomposition noted as temperature increased. Copovidone decomposition has also been reported at temperatures exceeding 230 °C (Kolter et al., 2010). Based on these results, all efforts should be made to minimize melt temperatures to less than 200 °C. As such, processing above the GRIS melting temperature is not possible and the extrusion process must dissolve the drug in the polymer melt. In this case, the processing conditions and mixing modalities control dissolution of drug in the molten polymer (Liu et al., 2010, Hughey et al., 2011).

#### **3.4.2 Effect of Processing Modes and Processing Conditions on Griseofulvin/Copovidone Solid Dispersions**

Different processing modalities have been utilized in twin screw extrusion, but the application of counter-rotating extruders for pharmaceutical systems remains limited. In order to make a direct assessment of the performance of co-rotating extruders and counter-rotating extruders in a head-to-head comparison, process geometries were developed in a similar fashion. Across the length of each screw, four major sections of dispersive and distributive elements were placed having a total common length across both systems to reduce equipment setup bias during the comparative trials. To further assess the impact of process parameters on the performance of the system, systems containing 20% and 30% GRIS were extruded under the conditions shown in Table 3.1.

At-line visual observations were made about the appearance of the dispersions, noting the well documented tendency of amorphous dispersions to form a clear glass during the extrusion process. For simple systems, an amorphous solid dispersion will have a transparent appearance and significant levels of crystallinity impart an opaque

appearance to the solid dispersion (Forster et al., 2001). Using the co-rotating extruder, opaque, semi-crystalline solid dispersions were produced at processing temperatures of 160 °C and 150 rpm. Under similar conditions with the counter-rotating extruder it was not possible to achieve sufficient feed into the extruder, preventing a direct comparison between the systems for generating solid dispersions. However, comparison between feed intake behaviors can be made. For the counter-rotating mode, the screws rotate outward on top and inward at the bottom, this maximizes the free volume for intake (Eise et al., 1981). The powder must flow down into the lower wedge formed by the screws and conveyed. In the co-rotating mode, powder is transferred from one screw towards the other where it is further conveyed. In this mode, the wedge area provides a twist restraint, which reduces the tendency of rotation in the channel and increases particle conveyance in the axial direction. The difference of intake mechanism based on equipment geometry most likely contributed to the observed performance difference.

Micronized GRIS and copovidone used in these trials have specific attributes that can impact flow into the feed section of the extruder. The low particle size of the drug substance presents a problem for powder flow, providing a high specific surface area for interaction and low individual particle mass that reduce flowability into the open area of the screw flights for transport into the closed barrel. Copovidone also exhibits characteristics that can impact flow, particularly the moisture content of the material and tendency to form sticky gels in high moisture environments. Characterization of flow properties was performed using shear cell analysis of the 20% and 30% by weight GRIS blends, although the materials were fed independently. FFC values of 8.04 and 6.37, respectively, were noted which indicated moderate flow for a pharmaceutical system. Based on the trend of the FFC, increasing the GRIS concentration degrades the

flowability of the formulation, indicating the particle size may heavily influence the feed intake. Given the common properties of this system with many pharmaceutical systems, the poor intake performance on a counter-rotating extruder may occur with a range of pharmaceutical systems.

Increasing screw speed to 300 rpm enhanced the conveyance of the counter-rotating feed section to support a feed rate of 4 kg/hr, indicating that greater screw speed could be used to compensate for lower conveying efficiency of the counter-rotating system. Furthermore, it was observed that a clear glass was formed, indicating amorphous extrudate at 160 °C. In comparison to the co-rotating extruder which required a process section temperature of 180 °C, an amorphous form was achieved at a process section temperature 20 °C lower with the counter-rotating unit. This suggested a potential benefit in solubilization of high melting point APIs in the molten polymer, although the contribution of greater screw speed in the counter-rotating system to this performance is likely significant. Performance differences between the two systems were also investigated using a 30% GRIS formulation. A similar procedure of incremental temperature and screw speed increases were followed to identify the conditions under which an amorphous form was produced. For operating conditions at or below 170 °C process section temperature and 300 rpm, an opaque, semi-crystalline extrudate was observed. Further increasing the screw speed for both systems to 450 rpm allowed the counter-rotating system to achieve a transparent glass, while the co-rotating system remained opaque. For the co-rotating configuration, increasing process temperature to 180 °C was necessary to establish an amorphous form while maintaining a screw speed of 450 rpm. Interestingly, operation of the counter-rotating extruder at 180 °C and 450 rpm resulted in an amorphous system; however, by reducing the screw speed to 300 rpm

a semi-crystalline system was observed. By lowering the speed the energy imparted by the screws for dissolution was decreased. This suggested that mechanical energy input was the more dominant factor in solubilizing the high melting point compound in the molten polymer when compared to process section temperature. This result was not entirely unexpected, as it is well known in extrusion that mechanical energy contributes to the majority of heat energy produced in the system (Breitenbach, 2002), with the process section functioning as a sink to remove thermal energy. Furthermore, the mechanical energy input varies based on the aggressiveness of the screw elements selected and their distribution along the screw. It should also be noted that the dissolution process of drug in molten polymer is a kinetic phenomenon tied to the residence time distribution of the process and the boundary layer thickness at the drug-polymer interface, which is a function of mixing and driving force for dissolution as determined by the equilibrium solubility of drug in polymer. Although not possible to identify the primary mechanism which limited dissolution at the lower screw speed, it is clear that screw speed had a more dominant influence on achieving complete melt solubilization than process section temperature.

Direct comparison of the co-rotating and counter-rotating extruders operated at 180 °C and 450 rpm produced dispersions with similar visual characteristics, yielding clear amorphous glasses. Pressure build-up and viscous dissipation have been reported to contribute to localized heating in the extruder. To better characterize local heating in these systems, the melt temperature was measured directly by placement of a thermocouple into the screw tip region near die outlet. The observed melt temperatures for the counter-rotating and co-rotating extruders were 196 °C ± 4 °C and 204 °C ± 4 °C, respectively. Comparing the process section temperature for the 20% drug loading

formulation and melt temperatures measured for the 30% drug loading formulation to the phase diagram, Figure 3(b), show that the compositions lie in close proximity to the binodal curve. This suggests that the maximum attainable drug loading of a high melting point compound in a specific system is given by the binodal boundary at the operating melt temperature.

Upon cooling, the solid dispersion transitions the metastable region and T<sub>g</sub> boundary shown in the phase diagram, to where both 20% and 30% GRIS dispersions exist in the unstable region where the high viscosity of the polymer provides kinetic stabilization. The T<sub>g</sub> boundary was generated from second run mDSC analysis of copovidone, GRIS and X-ray amorphous compositions of 20% and 30% w/w, the slope of the line indicates that the GRIS:copovidone system lacks significant specific interactions and exhibits volume additivity (Hancock and Zografi, 1994). Over time, this system will eventually relax (Hancock et al., 1995) and establish an equilibrium defined by the binodal curve, with a component of pure crystalline drug. To investigate the amorphous nature of the extrudates powder X-ray diffraction analysis was performed on representative test samples shown in Figure 3.4. The results of the cooled extrudates corroborated the results observed from visually observing the melt with one exception. Test 14 was observed to have opaque character during extrusion trials, yet no peaks were observed by X-ray. The most likely explanation is that the amount of crystalline material was below the limit of detection, which was determined by serial dilution of physical mixtures of GRIS and copovidone to be < 1.25% w/w of crystalline material in the sample.

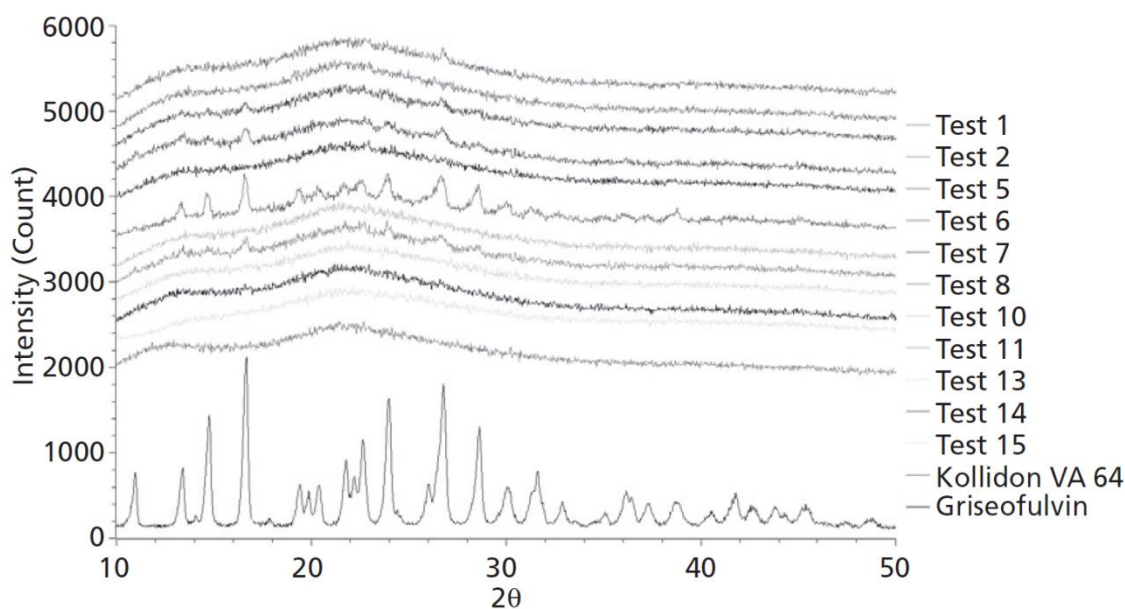


Figure 3.4 Powder X-ray Diffractograms of GRIS, copovidone and selected test samples over the range of 10° to 50° 2θ.

Non-sink dissolution was performed on the extrudates from selected tests to ascertain if the process geometry affected the drug release behavior of the dispersions. In some cases, the supersaturating capability of solid dispersions *in vitro* is an indicator of *in vivo* exposure (Newman et al., 2012). This type of testing can also be used as a quality metric to assess levels of residual crystallinity within formulations. The 20% by weight compositions, Figure 3.5, and the 30% by weight compositions, Figure 3.6, that were determined to be amorphous both visually and by X-ray were found to exhibit similar rates and extent of supersaturation. Properties of the dissolution curves are summarized in Table 3.2. Solution concentrations greater than 2-fold improvements over the physical mixtures were observed. In addition, a sample from Test 11, which was observed to be crystalline by X-ray was investigated and included along with the X-ray amorphous compositions in Figure 6. The results indicate that the presence of crystalline GRIS slowed the rate of supersaturation, while the maximum level of supersaturation was

similar to that of the amorphous compositions. Furthermore, the 90 and 120 minute data points indicate that the crystalline GRIS induced a greater degree of precipitation. All samples tested for dissolution were also confirmed to have acceptable potency, similar purity to that of the standard, similar glass transition temperature, and loss on drying values (data not shown).

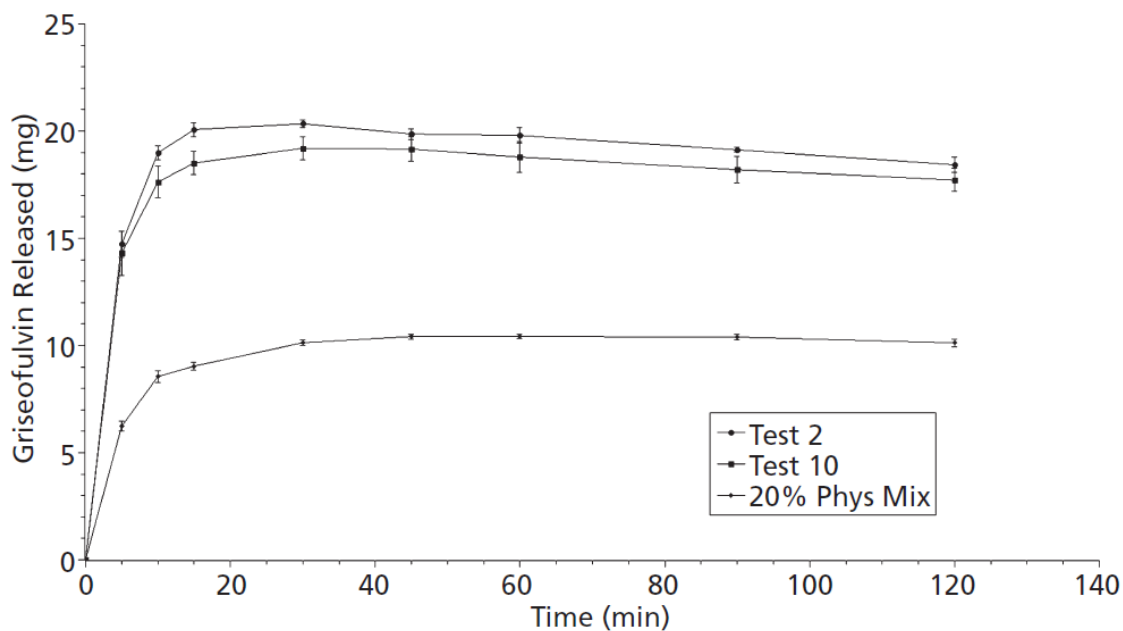


Figure 3.5 Non-sink dissolution of 20% by weight GRIS solid dispersions and a physical mixture of GRIS and copovidone. N=3, 50 mg GRIS per vessel in 1000 mL of 0.1 N HCl at 37 °C and 50 rpm.

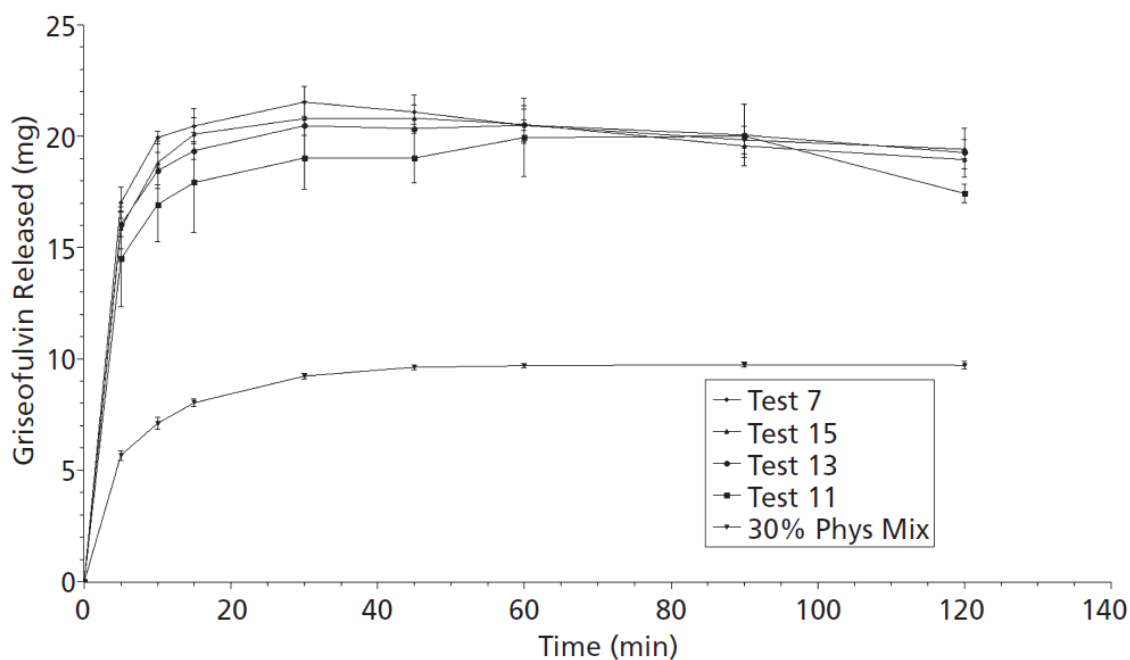


Figure 3.6 Non-sink dissolution of 30% by weight GRIS solid dispersions and a physical mixture of GRIS and copovidone. N=3, 50 mg GRIS per vessel in 1000 mL of 0.1 N HCl at 37 °C and 50 rpm.

Table 3.2 Dissolution attributes

Sample Description	S <sub>max</sub>	Initial Dissolution Rate <sub>0-5 min</sub> (mg/min)	AUDC <sub>0-120 min</sub> (mg min)
Test 2	1.95 ± 0.01	2.94 ± 0.12	2267 ± 31
Test 10	1.84 ± 0.05	2.86 ± 0.20	2154 ± 74
20% Physical Mixture	-	1.24 ± 0.09	1170 ± 38
Test 7	2.20 ± 0.07	3.40 ± 0.14	2375 ± 76
Test 11	2.05 ± 0.04	2.90 ± 0.42	2217 ± 137
Test 13	2.10 ± 0.04	3.20 ± 0.11	2329 ± 78
Test 15	2.13 ± 0.06	3.17 ± 0.18	2331 ± 78
30% Physical Mixture	-	1.13 ± 0.04	1083 ± 14

### **3.4.3 Residence time distribution**

Residence time of continuous operations are often characterized through the use of a tracer, which in the case of extrusion is a material added as a single bolus charge into the feed zone where the concentration of tracer in the extrudate is measured as a function of time on leaving the die. The tracer selected for the RTD tests, indigo carmine, has a large chromophore, allowing detection by UV even at low solution concentration and at a wavelength that does not overlap with GRIS or copovidone. This enables charging the tracer at a low mass compared to the feed rate of the solid dispersion. Indigo carmine is a crystalline material, with a high melting point ( $>235\text{ }^{\circ}\text{C}$ ) that dissolves in the polymer at the extrusion temperatures employed, mimicking the behavior of GRIS in the system. Furthermore, indigo carmine allows for visual observation of the RTD, which transitions from a dark indigo, to blue, to a light green hue as the concentration decreases, allowing accurate sample collection and determination of the minimum exit time. While these attributes of the tracer are ideal, there is still a possibility that a small molecule tracer could act as a plasticizer and alter the melt viscosity such that the normal flow profiles are disturbed. To rule this out, the rheology of copovidone in the presence of up to 1% indigo carmine was measured, Figure 3.7. Based on these results, indigo carmine is not a plasticizer for copovidone and is acceptable for the intended purpose.

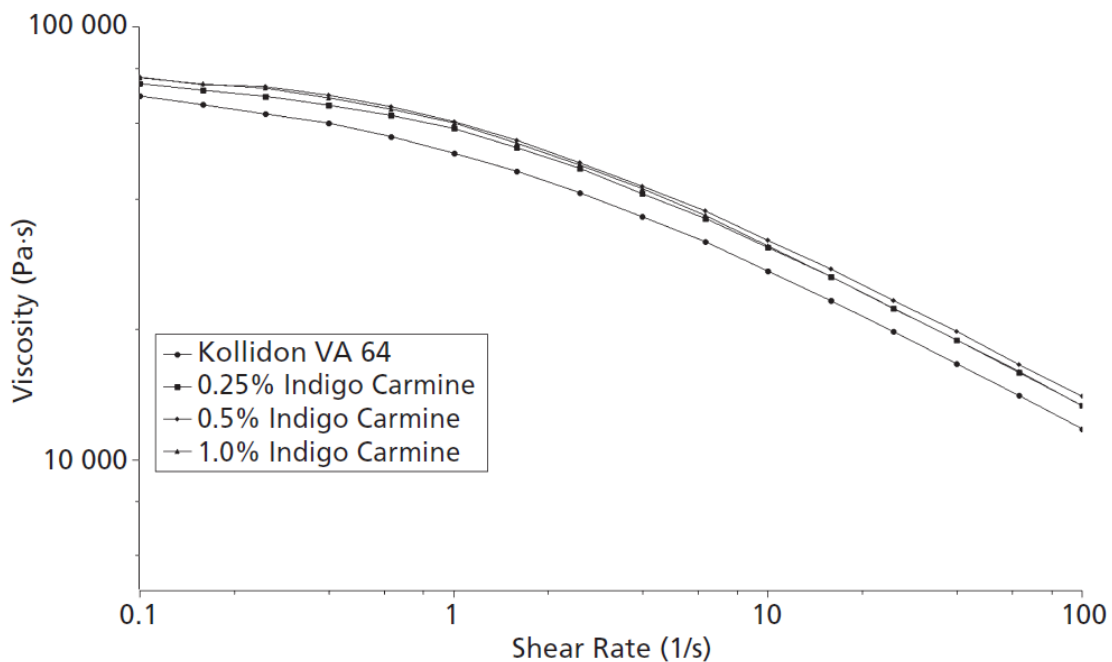


Figure 3.7 Viscosity of copovidone as measured at 155 °C in the presence of the tracer, indigo carmine, used in the residence time distribution study.

According to Poulesquen and Vergnes (2003), the RTD of an extrusion system can be summarized by three attributes, the minimum exit time, the mean residence time and the variance of the distribution. However, in the case of thermally sensitive materials, it may also be important to look at the third moment of distribution for the purpose of characterizing the skewness, which is often characterized for plug flow reactors (Minnich et al., 2011) and in this case provides a value to describe the asymmetry of the RTD. The primary parameters affecting the mean residence time are the feed rate, screw design and the internal free volume of the extruder. For a given extruder volume and feed rate, the skewness gives an indication to the propensity for tailing, which should be minimized to reduce drug exposure to high temperatures to a minimum.

Test conditions 7 and 15, representing the 30% w/w GRIS solid dispersions produced at 180 °C and 450 rpm for the co-rotating and counter-rotating configurations, respectively, were selected for the RTD trials. The results are plotted in Figure 3.8 along with the non-linear least squares fit to Equation 3.11. The results for the moments for the distribution and other key statistics are summarized in Table 3.3. Based on these results, the RTD of the solid dispersion for both configurations exhibited similar minimum exit times, within 5 s of each other. The mean residence time, variance and asymmetry were all reduced for the counter-rotation configuration when compared to the co-rotating configuration. The counter-rotating extruder also provided shorter  $t_{90}$  and  $t_{99}$  values, which denote the time that 90% and 99% of the charge has passed through the extruder. Together, these values represent a potential benefit for using a counter-rotating extruder when working with heat sensitive and/or high melting point compounds. The narrower distribution presented by the counter-rotating platform allows for more uniform processing of material. For high melting point compounds where the drug must be solubilized in the molten polymer, this helps to ensure that dissolution is achieved with minimal excess energy input. Similarly, for high melting point compounds where decomposition occurs as a function of time and temperature, the narrow distribution and more uniform time exposures seen in the counter-rotating system should minimize impurity formation. This suggests a potential underutilized benefit of counter-rotating extruders for the production of solid dispersions.

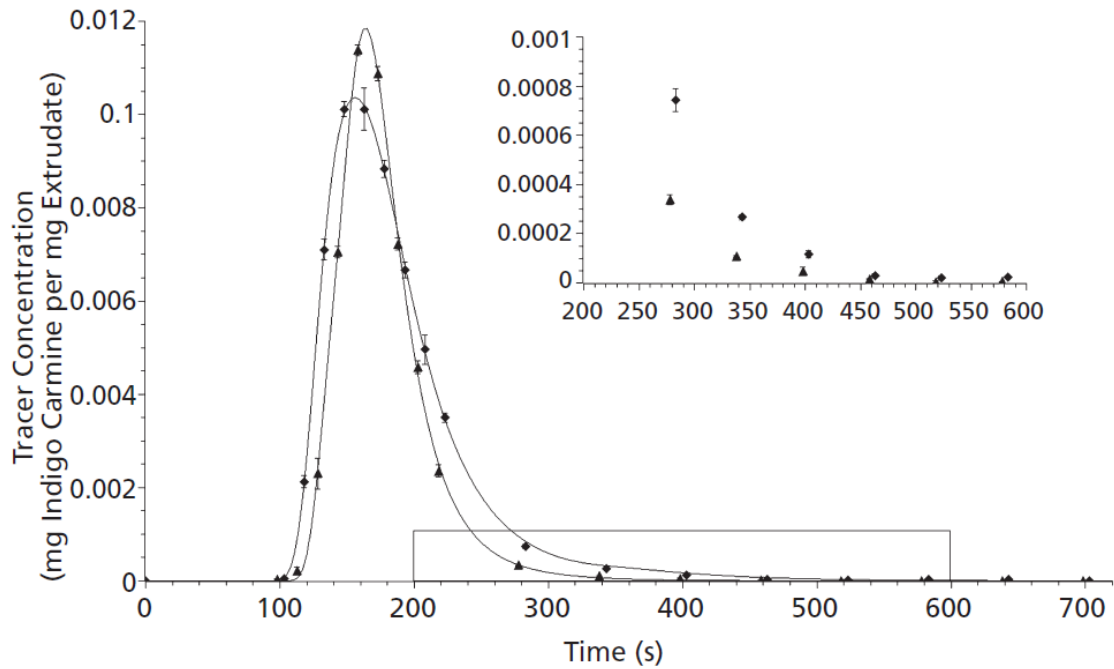


Figure 3.8 Residence time distribution of 30% GRIS solid dispersion at 4 kg/hr, 450 rpm, 180 °C for (◆) co-rotating and (▲) counter-rotating configurations in a Leistritz 27 mm extruder, boxed area shown in inset.

Table 3.3 Moments of the residence time distributions for the co-rotating and counter-rotating 27 mm twin screw extrusion trials as measured at 180 °C and 450 rpm following a 1 g indigo carmine tracer charged to a 30% w/w GRIS in copovidone extrusion process operating at 4 kg/hr.

<b>RTD Attribute</b>	<b>Co-rotation</b>	<b>Counter-Rotation</b>
Minimum Exit Time	103 s	98 s
Mean Residence Time	189 s	178 s
Variance	3473 s <sup>2</sup>	1265 s <sup>2</sup>
Skewness	2.40	2.14
T90	252 s	219 s
T99	417 s	300 s

### **3.5 CONCLUSIONS**

In this investigation, a counter-rotating and co-rotating twin screw extrusion comparison was performed with a focus on the impact of the critical attributes of the solid dispersion. Both configurations produced visually and X-ray amorphous solid dispersions of up to 30% griseofulvin in copovidone having similar supersaturating capability. However, under the parameters of this study, the counter-rotating configuration produced the solid dispersion at a reduced temperature and with a residence time distribution that minimized the mean residence time, variance and skewness when compared to the co-rotating configuration. Using these attributes of counter-rotating extruders it may be possible to address challenging poorly soluble drug candidates where uniformity and/or minimization of thermal exposure are critical to the processing strategy.

### 3.6 REFERENCES

Al-Obaidi H, Ke P, Brocchini S, and Buckton G (2011) Characterization and stability of ternary solid dispersions with PVP and PHPMA. *International Journal of Pharmaceutics* **419**, 20-7.

Bellantone RA, Patel P, Sandhu H, Choi DS, Singhal D, Chokshi H et al. (2012) A method to predict the equilibrium solubility of drugs in solid polymers near room temperature using thermal analysis. *Journal of Pharmaceutical Sciences* **101**, 4549-58.

Breitenbach J (2002) Melt extrusion: from process to drug delivery technology. *European Journal of Pharmaceutics & Biopharmaceutics* **54**, 107-17.

Craig DQM, Royall PG, Kett VL, and Hopton ML (1999) The relevance of the amorphous state to pharmaceutical dosage forms: glassy drugs and freeze dried systems. *International Journal of Pharmaceutics* **179**, 179-207.

Crowley MM, Zhang F, Repka MA, Thumma S, Upadhye SB, Kumar Battu S et al. (2007) Pharmaceutical Applications of Hot-Melt Extrusion: Part I. *Drug Development & Industrial Pharmacy* **33**, 909-26.

Dierickx L, Saerens L, Almeida A, De Beer T, Remon JP, and Vervaet C (2012) Co-extrusion as manufacturing technique for fixed-dose combination mini-matrices. *European Journal of Pharmaceutics & Biopharmaceutics* **81**, 683-9.

DiNunzio JC, Brough C, Hughey JR, Miller DA, Williams Iii RO, and McGinity JW (2010a) Fusion production of solid dispersions containing a heat-sensitive active

ingredient by hot melt extrusion and Kinetisol® dispersing. *European Journal of Pharmaceutics & Biopharmaceutics* **74**, 340-51.

Eise K, Herrmann H, Jakopin S, Burkhardt U, and Werner H (1981) An analysis of twin-screw extruder mechanisms. *Advances in Polymer Technology* **1**, 18-39.

FDA (2008) Guidance for Industry: Q3A Impurities in New Drug Substances. In *Revision 2*. (ed.), Vol. pp. Center for Drug Evaluation and Research (CDER).

Feng J, Xu L, Gao R, Luo Y, and Tang X (2012) Evaluation of polymer carriers with regard to the bioavailability enhancement of bifendate solid dispersions prepared by hot-melt extrusion. *Drug Development & Industrial Pharmacy* **38**, 735-43.

Flory PJ (1942) Thermodynamics of High Polymer Solutions. *Journal of Chemical Physics* **10**, 51-61.

Forster A, Hemenstall J, and Rades T (2001) Characterization of glass solutions of poorly water-soluble drugs produced by melt extrusion with hydrophilic amorphous polymers. *Journal of Pharmacy & Pharmacology* **53**, 303-15.

Hancock BC, Shamblin SL, and Zografi G (1995) Molecular Mobility of Amorphous Pharmaceutical Solids Below Their Glass Transition Temperatures. *Pharmaceutical Research* **12**, 799-806.

Hancock BC and Zografi G (1994) The Relationship Between the Glass Transition Temperature and the Water Content of Amorphous Pharmaceutical Solids. *Pharmaceutical Research* **11**, 471-7.

Huggins ML (1942) Thermodynamics Properties of Solutions of Long-Chain Compounds. *Annals of the New York Academy of Sciences* **43**, 1-32.

Hughey JR, Keen JM, Brough C, Saeger S, and McGinity JW (2011) Thermal processing of a poorly water-soluble drug substance exhibiting a high melting point: The utility of KinetiSol® Dispersing. *International Journal of Pharmaceutics* **419**, 222-30.

Keseru GM and Makara GM (2009) The influence of lead discovery strategies on the properties of drug candidates. *Nature Reviews. Drug Discovery* **8**, 203-12.

Kolter K, Karl M, Nalawade S, and Rottmann N (2010) Hot-Melt Extrusion with BASF Pharma Polymers: Extrusion Compendium. In BASF (ed.), (ed.), Vol. pp. Ludwigshafen, Germany.

Lin D and Huang Y (2010) A thermal analysis method to predict the complete phase diagram of drug-polymer solid dispersions. *International Journal of Pharmaceutics* **399**, 109-15.

Liu H, Wang P, Zhang X, Shen F, and Gogos CG (2010) Effects of extrusion process parameters on the dissolution behavior of indomethacin in Eudragit® E PO solid dispersions. *International Journal of Pharmaceutics* **383**, 161-9.

Manas-Zloczower I (2009) Continuous Process Visualization: Visual Observation, On-Line Monitoring, Model-Fluid Extrusion and Simulation. In *Mixing and Compounding of Polymers*. Manas-Zloczower I (ed.), 2nd Edition (ed.), Vol. pp. 473-572. Hanser Publications, Munich.

Marsac P, Li T, and Taylor L (2009) Estimation of Drug–Polymer Miscibility and Solubility in Amorphous Solid Dispersions Using Experimentally Determined Interaction Parameters. *Pharmaceutical Research* **26**, 139-51.

Marsac P, Shamblin S, and Taylor L (2006) Theoretical and Practical Approaches for Prediction of Drug–Polymer Miscibility and Solubility. *Pharmaceutical Research* **23**, 2417-26.

Martin C (2004) Counter-Rotating Twin-Screw Extruders. In (ed.), Vol. pp. 101-6, RonJon Publishing, Denton, TX, SPE Plastics Technician’s Toolbox – Extrusion, Drawer 4: Single & Twin-Screw Extruders, Section: Twin Screw Extruders.

Minnich CB, Greiner L, Reimers C, Uerdingen M, and Liauw MA (2011) Bridging the gap: A nested-pipe reactor for slow reactions in continuous flow chemical synthesis. *Chemical Engineering Journal* **168**, 759-64.

Mu B and Thompson MR (2012) Examining the mechanics of granulation with a hot melt binder in a twin-screw extruder. *Chemical Engineering Science* **81**, 46-56.

Nair R, Nyamweya N, Gönen S, Martínez-Miranda LJ, and Hoag SW (2001) Influence of various drugs on the glass transition temperature of poly(vinylpyrrolidone): a thermodynamic and spectroscopic investigation. *International Journal of Pharmaceutics* **225**, 83-96.

Newman A, Knipp G, and Zografi G (2012) Assessing the performance of amorphous solid dispersions. *Journal of Pharmaceutical Sciences* **101**, 1355-77.

Poulesquen A and Vergnes B (2003) A study of residence time distribution in co-rotating twin-screw extruders. Part I: Theoretical modeling. *Polymer Engineering & Science* **43**, 1841-8.

Poulesquen A, Vergnes B, Cassagnau P, Michel A, Carneiro OS, and Covas JA (2003) A study of residence time distribution in co-rotating twin-screw extruders. Part II: Experimental validation. *Polymer Engineering & Science* **43**, 1849-62.

Repka MA, Battu SK, Upadhye SB, Thumma S, Crowley MM, Zhang F et al. (2007) Pharmaceutical Applications of Hot-Melt Extrusion: Part II. *Drug Development & Industrial Pharmacy* **33**, 1043-57.

Shah A and Gupta M (2004) Comparison of the Flow in Co-Rotating and Counter-Rotating Twin-Screw Extruders. In *ANTEC, Conference Proceedings*. (ed.), Vol. 1, pp. 443-7,

Tadmor Z and Gogos CG (2006) Principles of Polymer Processing. In 2 (ed.), Vol. pp. Wiley-Interscience, Hoboken.

Terife G, Wang P, Faridi N, and Gogos CG (2012) Hot melt mixing and foaming of soluplus® and indomethacin. *Polymer Engineering & Science* **52**, 1629-39.

Tian Y, Booth J, Meehan E, Jones DS, Li S, and Andrews GP (2012) Construction of Drug–Polymer Thermodynamic Phase Diagrams Using Flory–Huggins Interaction Theory: Identifying the Relevance of Temperature and Drug Weight Fraction to Phase Separation within Solid Dispersions. *Molecular Pharmaceutics* **10**, 236-48.

Tucker III C (2009) Mixing of Miscible Liquids. In *Mixing and Compounding of Polymers*. Manas-Zloczower I (ed.), 2nd Edition (ed.), Vol. pp. 5-38. Hanser Publications, Munich.

Zhang X-M, Feng L-F, Hoppe S, and Hu G-H (2008) Local residence time, residence revolution, and residence volume distributions in twin-screw extruders. *Polymer Engineering & Science* **48**, 19-28.

Zhao Y, Inbar P, Chokshi HP, Malick AW, and Choi DS (2011) Prediction of the thermal phase diagram of amorphous solid dispersions by flory–huggins theory. *Journal of Pharmaceutical Sciences* **100**, 3196-207.

## **Chapter 4: Controlled Release Supersaturating Solid Dispersions Containing Glyceryl Behenate**

### **4.1 ABSTRACT**

The objective of this study was to evaluate the use of glyceryl behenate as a plasticizer and release modifier in solid dispersion systems containing itraconazole and carbamazepine. Amorphous solid dispersions of high molecular weight polyvinylpyrrolidone were prepared by hot-melt extrusion, the processing of which was improved by the inclusion of glyceryl behenate. Dispersions were milled and subsequently compressed into tablets. Solid dispersions were also prepared by Kinetisol<sup>®</sup> Dispersing which allowed for the manufacture of monolithic tablets of the same composition as compressed tablets. Tablets without glyceryl behenate and all compressed tablets were observed to have an incomplete release profile likely due to drug crystallization within the tablet as this occurred at sink conditions. Monolithic tablets formulated to be more hydrophobic, by including glyceryl behenate, allowed for sustained release at sink and non-sink conditions.

### **4.2 INTRODUCTION**

An abundance of poorly soluble BCS Class II and IV drug candidates are in development. These drug candidates may have high therapeutic value, but solubility limitations must be overcome during development for effective oral therapy. Amorphous solid dispersion technologies, the promise of which was originally recognized by Chou and Riegelman (Chiou and Riegelman, 1971), are commonly applied to overcome solubility limitations as the result of an increased understanding of carrier systems,

preparation technologies and characterization techniques (Hancock et al., 1997, Hancock and Zografi, 1997, Serajuddin, 1999, Breitenbach, 2002, Craig, 2002, Crowley et al., 2007, Repka et al., 2007, Vasconcelos et al., 2007, Friesen et al., 2008, Janssens and Van den Mooter, 2009).

Such amorphous solid dispersions create supersaturated solutions upon dissolution that exhibit improved bioavailability *in vivo* (DiNunzio et al., 2008, Miller et al., 2008a, Miller et al., 2008b). The bulk of research to date has focused on the development of immediate release dosage forms. The focus of previous work is understandable as manipulation of the kinetics and thermodynamics of recrystallization on storage as well as precipitation inhibition during dissolution must initially be understood. However, for BCS Class II drugs with short half-lives, it may be desirable to prepare sustained release compositions (Tran et al., 2011). Sustained release of drugs from solid dispersions may also be advantageous for delivering drug to the small intestines where the majority of drug absorption occurs, as opposed to generating high concentration of drug in the stomach. In addition, reducing the rate of release in the lumen may reduce the extent of supersaturation and therefore the driving force for precipitation. This would be especially true for drugs that rapidly permeate the gastrointestinal membranes. Controlled release amorphous solid dispersions must also be formulated to prevent drug precipitation within the dosage form to ensure the drug is liberated from the dosage form following administration.

The purpose of this study was to develop and evaluate a controlled release amorphous solid dispersion system suitable for thermal processing. A high molecular weight water soluble glassy polymer, such as polyvinyl pyrrolidone (PVP), is of interest

due to potential to provide solid state stability related to its high glass transition temperature (Hancock et al., 1995) and due to its potential as a precipitation inhibitor (Brouwers et al., 2009). However, fusion processing of high molecular weight PVP is problematic due to the high viscosity in its rubbery state (Kolter et al., 2010). Due to loading limitations, the incorporation of a separate plasticizer along with the drug and release modifier is undesirable. Glycerol behenate, commonly used in controlled release matrix tablets, was evaluated as a dual function excipient, functioning as a plasticizer and release modifier. In addition to compressed tablets containing milled dispersion, monolithic dosage forms were also evaluated. Monoliths were included to understand if intergranular pores, present in compressed tablets play a role of precipitation within tablets during dissolution. KinetiSol<sup>®</sup> Dispersing (KSD) was utilized to produce large masses of solid dispersions that were suitable for molding into a tablet that matched the major and minor axis dimensions of the compressed tablets. KSD is a fusion process that is capable of producing large masses solid dispersions in time scales of 5 to 10 seconds that can subsequently be shaped during cooling (DiNunzio et al., 2010b, Hughey et al., 2012).

## **4.3 MATERIALS AND METHODS**

### **4.3.1 Materials**

Carbamazepine (CBZ) and Itraconazole (ITZ) were purchased from Letco Medical (Decatur, Alabama). Glyceryl behenate (C888, Compritol<sup>®</sup> 888 ATO) was provided by Gattefossé (Saint Priest, France). Polyvinyl pyrrolidone (PVP, Kollidon<sup>®</sup>

30) was provided by BASF (Tarrytown, NY). Analytical reagents were of ACS grade or higher and purchased from Fisher Scientific (Pittsburg, PA).

## **4.3.2 Methods**

### ***4.3.2.1 Hot-Melt Extrusion***

Screening studies were performed with a Haake Minilab (ThermoFisher) conical twin screw extruder. CBZ, PVP and Compritol<sup>®</sup> 888 ATO (C888) were pre-blended and hand forced using a push rod into the extruder inlet. The extruder was operated at 300 RPM without a die. Solid dispersions containing C888 were prepared at 170 °C. Solid dispersions not containing C888 were processed at 180 - 200 °C as processing below this temperature caused vitrification within the flow channels. Processing torque values were determined in recirculating mode with 10 g batches at a range of temperatures.

### ***4.3.2.2 Milling and Compression***

For analysis, the solid dispersions were milled with a Fitzmill L1A hammer mill (Fitzpatrick) operating at 9000 RPM with knives forward. A 0.020” screen was installed in the milling chamber and the powder fraction passing a 60 mesh screen was collected for further analysis or compression. Compressed tablets were prepared using a MTCM-I tablet press (Globe Pharma) at 20 KN compression force using various sizes of tooling as appropriate for the tablet weight.

#### ***4.3.2.3 KinetiSol® Dispersing***

Monolithic matrices were formed using a KinetiSol® compounder (DisperSol Technologies) and a platen press (DisperSol Technologies) containing tablet shaped cavities. Blends were hand mixed in a polyethylene bag and loaded into the processing chamber of the compounder. A shaft within the processing chamber, having protruding blades, was rotated at a controlled rotational speed with an online control module. Through a combination of high frictional and shearing forces imparted by the rotating blades, without the use of external heat, the temperature of the composition was rapidly increased until a molten mass was achieved. Realtime temperature of the material within the processing chamber was monitored. Once reaching the desired temperature, the mass was automatically ejected from the processing chamber and immediately transferred to the platen press and quenched under pressure to form tablets. Excess material was milled as described in the previous section. A portion of milled material was retained and the remainder compressed into tablets.

#### ***4.3.2.4 Thermal Analysis***

Modulated differential scanning calorimetry (mDSC) was used to evaluate the presence of crystalline C888 and CBZ in the solid dispersions. mDSC was performed with a model 2920 mDSC (TA Instruments) using a sample size of 6 to 10 mg. The temperature was ramped from 50 °C to 200 °C with a ramp rate of 10°C/min, a 0.5°C amplitude and 40 s period. The samples were contained in crimped aluminum pans under a flow of nitrogen at 40mL/min.

A Perkin Elmer TGA 7 was used for thermogravimetric (TGA) analysis to detect weight loss from thermal degradation. Approximately 10 mg of sample was placed in

aluminum crucibles and evaluated isothermally or ramped at 10 °C/min over the range 50 °C to 350 °C.

#### ***4.3.2.5 Powder X-Ray Diffraction***

A model 1710 X-Ray Diffractometer (Phillips) using a Cu K radiation source ( $\lambda = 1.5418 \text{ \AA}$ ) operating at 40 kV and 30mA was used to analyze powder samples and detect the presence of crystalline refractions from both C888 and CBZ. The  $2\theta$  range of  $5^\circ$  to  $45^\circ$  was scanned with a step size of  $0.05^\circ$  and 3 s dwell time using a Cu K radiation source ( $\lambda = 1.5418 \text{ \AA}$ ).

#### ***4.3.2.6 High Performance Liquid Chromatography***

High performance liquid chromatography (HPLC) was employed to analyze the potency of the solid dispersions and to quantitate the amount of drug release following dissolution. A Waters HPLC system including a 717 Autosampler, dual 515 pumps and a 996 Photodiode Array Detector fitted with a Phenomenex<sup>®</sup> Luna 5  $\mu\text{m}$  C18 (2) 100  $\text{\AA}$ , 150 x 4.6 mm column was used. The mobile phase for CBZ analysis and ITZ analysis were 60:40 acetonitrile:water and 70:30:0.05 acetonitrile:water:diethanolamine respectively. 30  $\mu\text{L}$  samples were injected at a flow rate of 1 mL/min. Empower Version 4.0 was used to extract chromatograms at 288 nm and 254 nm for analysis of CBZ and ITZ, respectively.

#### ***4.3.2.7 Non-Sink Dissolution Testing***

Initial solid dispersions were evaluated under non-sink conditions per USP II, Method A, utilizing a VK 7000 dissolution tester with a VK 8000 Autosampler, n=3.

Granules or matrix tablets, added in sufficient amount equivalent to approximately 100 mg API, were studied in 1000 mL purified water (CBZ) or 0.1 N HCl (ITZ) media at 50 RPM. Alternatively, pH change dissolution testing was performed in 750 mL of 0.1 N HCl for two hours and then diluted with 250 mL of 0.2M Na<sub>3</sub>PO<sub>4</sub> to reach pH 6.8. Samples of 5 mL were collected at each time point and analyzed by HPLC. At the time of sampling, samples were filtered through 0.2 μm PVDF Target2 syringe filters (Thermo Scientific, Waltham, MA) and diluted 1:1 with mobile phase. In order to determine if the amorphous drug would crystallize in the tablets during the dissolution process, tablet compacts were prepared at various sizes and multiple tablets added to the dissolution vessels. Due to the initial study design and the variety of tablets, the amount of API added to the vessels slightly varied from the target concentration of 100 mg (± 8 mg).

Follow-up studies designed to probe the mechanism of drug release and recrystallization in the tablet were evaluated using the same dissolution conditions with free drug content being directly measured in the dissolution vessel with a fiber optic Spectra instrument (Pion) fitted with 1mm path length Pion Probes. The equilibrium concentration of CBZ was determined at the conditions studied, 100 rpm in USP apparatus 1, purified water and 500 mL of purified water at 37 °C by spiking excess CBZ dissolved in acetonitrile and observing the precipitation with the UV probe. Follow on studies were performed above and below this concentration at 0.2 mg/ml and 0.4 mg/ml respectively by adjusting the volume of purified water to accommodate the dose of the material being evaluated. ITZ was studied similarly, only the non-sink concentration was evaluated in 0.1N HCl.

## **4.4 RESULTS AND DISCUSSION**

### **4.4.1 Hot Melt Extrusion**

Neat PVP and binary mixtures of PVP and C888 at a 4:1.5 ratio were extruded at various temperatures ranging from 120 °C to 200 °C. The Haake Minilab extruder was unable to process Kollidon 30 at temperatures lower than 180°C due to high viscosity and lack of flow in the outlet channel. The inclusion of C888 reduced the torque load from 475 N cm for pure PVP to 125 N cm at 180 °C (Figure 4.1). In addition, the extrusion torque for the mixture was less than 400 N cm when processed as low as 120 °C.

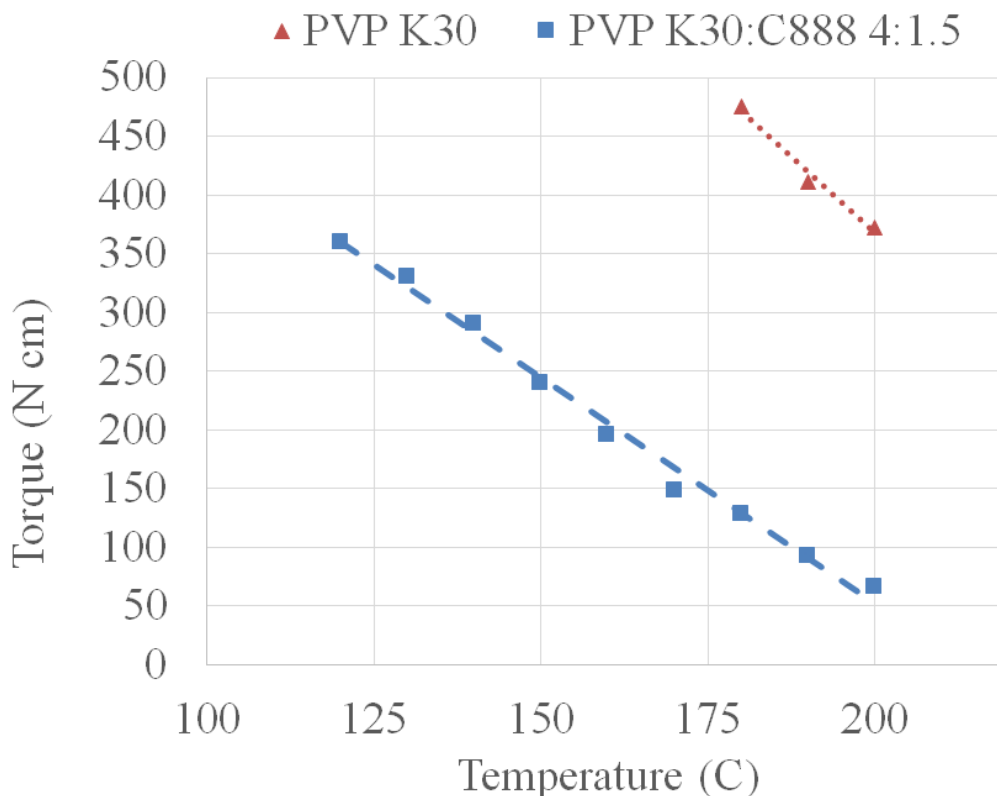


Figure 4.1 Extrusion torque values of PVP, Kollidon 30 and a PVP, Kollidon 30/Compritol 888 ATO mixture as determined at different temperatures.

Active comparator batches containing either carbamazepine (CBZ:PVP[1:4]) and itraconazole (ITZ:PVP[1:4]) were extruded at 180 °C to 200 °C and were found unsuitable for continuous processing. Sufficient material for characterization was collected by opening the extruder and collecting the solid dispersion from the melt channel and end of the screw. The solid dispersion was transparent with a yellow color. Active batches containing either carbamazepine (CBZ:PVP:C888[1:4:1.5]) or itraconazole (ITZ:PVP:C888[1:4:1.5/0.5]) were extruded at 170 °C. The extrudates appeared almost translucent exiting from the die channel and upon cooling developed a milky white color indicating the presence of a crystalline phase.

#### 4.4.2 Thermal Analysis

Thermogravimetric analysis indicated that degradation of the drugs, PVP and C888 did not significantly occur below 225 °C (data not shown). However, CBZ was found to be sensitive at the processing temperature, characterized by 0.5% degradation after six minutes of exposure to 180°C. The mean residence time within the extruder is typically on the order of two minutes (DiNunzio et al., 2010a, Keen et al., 2013). Rapid extrusion of CBZ-based compositions at temperatures lower than 180 °C is unlikely to result in substantial degradation.

Solid dispersions and their individual components were studied by differential scanning calorimetry to evaluate the effect of processing on the crystallinity of the drugs and C888 (Figure 4.2). The solid dispersions containing both CBZ and ITZ did not exhibit melting endotherms, indicating they were rendered amorphous during the extrusion process. The melting endotherm for C888 was not apparent in the solid dispersion containing CBZ indicating that the Compritol was dispersed within the PVP. The reduced melting endotherm in the ITZ solid dispersion identified that a fraction of the C888 material was able to recrystallize as a separate phase before PVP vitrified. The DSC curves and visually observations of the extrudate indicate that C888 was substantially molecularly dispersed within the PVP, yet a crystalline phase of C888 was present.

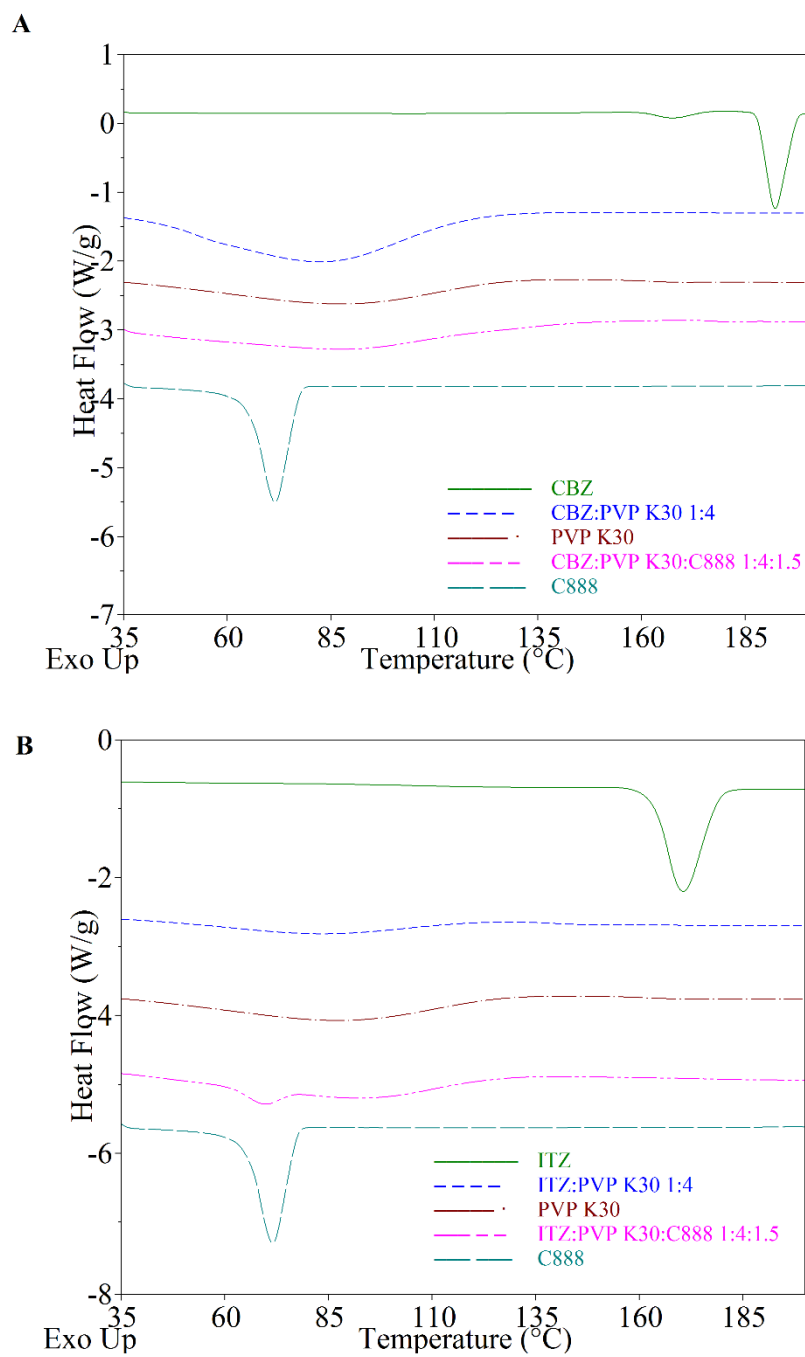


Figure 4.2 DSC thermograms of A) CBZ and B) ITZ solid dispersion systems.

#### **4.4.3 X-Ray Diffraction**

Milled solid dispersion samples were also evaluated by powder X-Ray Diffraction to evaluate crystalline character (Figure 4.3). The model drugs as well as C888 have distinct diffraction patterns when analyzed in their crystalline forms. The characteristic peaks for crystalline CBZ and ITZ were not present in the solid dispersions, indicating they are present primarily in an amorphous form. A slight peak for C888 was present at approximately  $21^\circ 2\theta$  in the solid dispersions. These results confirm the results from DSC in that C888 is substantially, but not completely, amorphous in the solid dispersions.

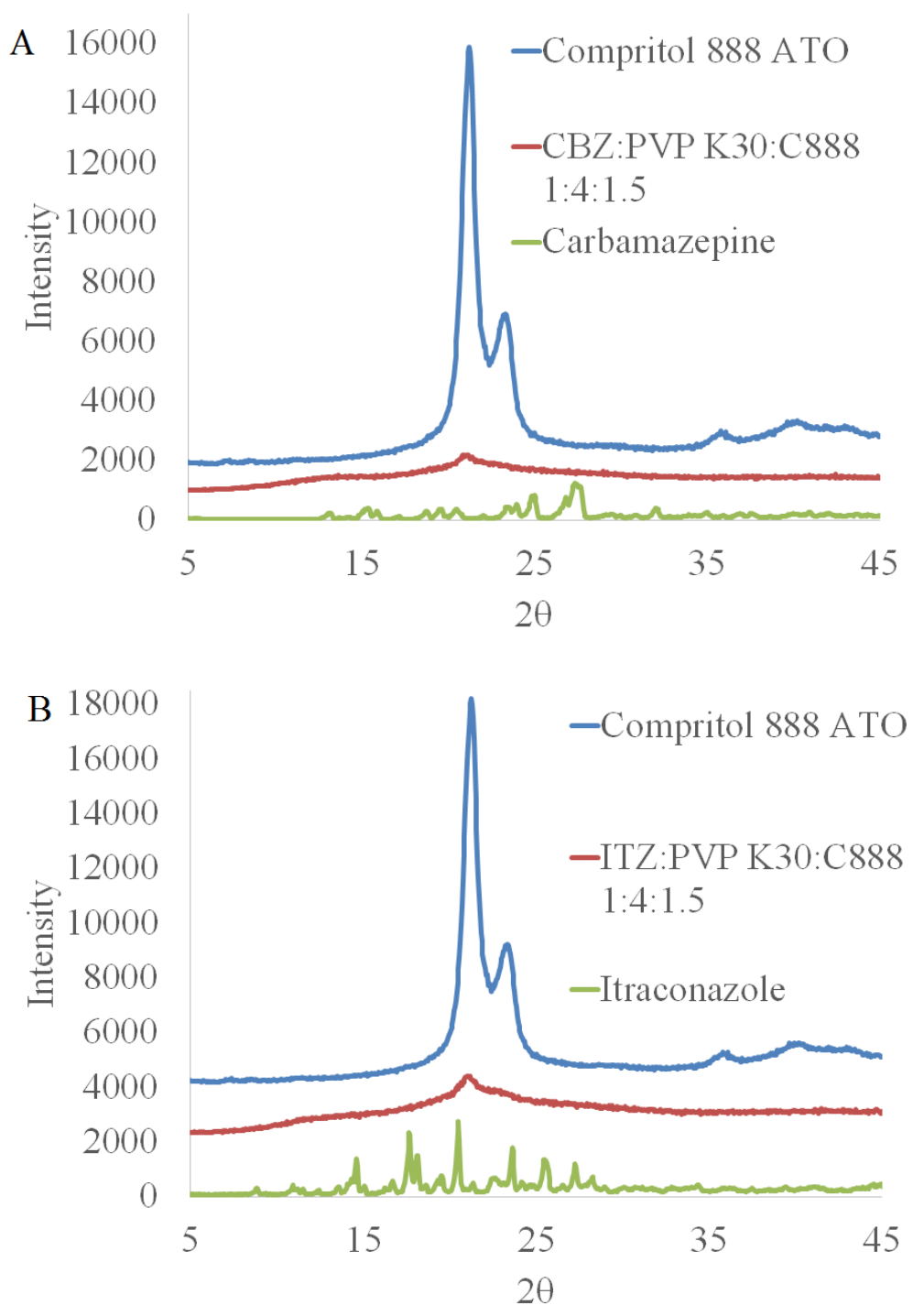


Figure 4.3 Powder x-ray diffractograms of A) CBZ and B) ITZ solid dispersion systems.

#### **4.4.4 *In Vitro* Release Studies**

Non-sink dissolution studies were performed in purified water to investigate the effect of PVP and C888 on the rate and extent of CBZ and ITZ supersaturation Figure 4.4. Inspection of Figure 4.4 indicates that the surface area to volume ratio of tablets containing CBZ affected the dissolution kinetics as would be expected. Tablets exhibiting a low surface area to volume ratio eroded more slowly and released drug at a slower rate. Based on visual observations, the tablets eroded slowly, often sloughing of granules and eventually disintegrated, preventing a complete analysis of the dissolution mechanism.

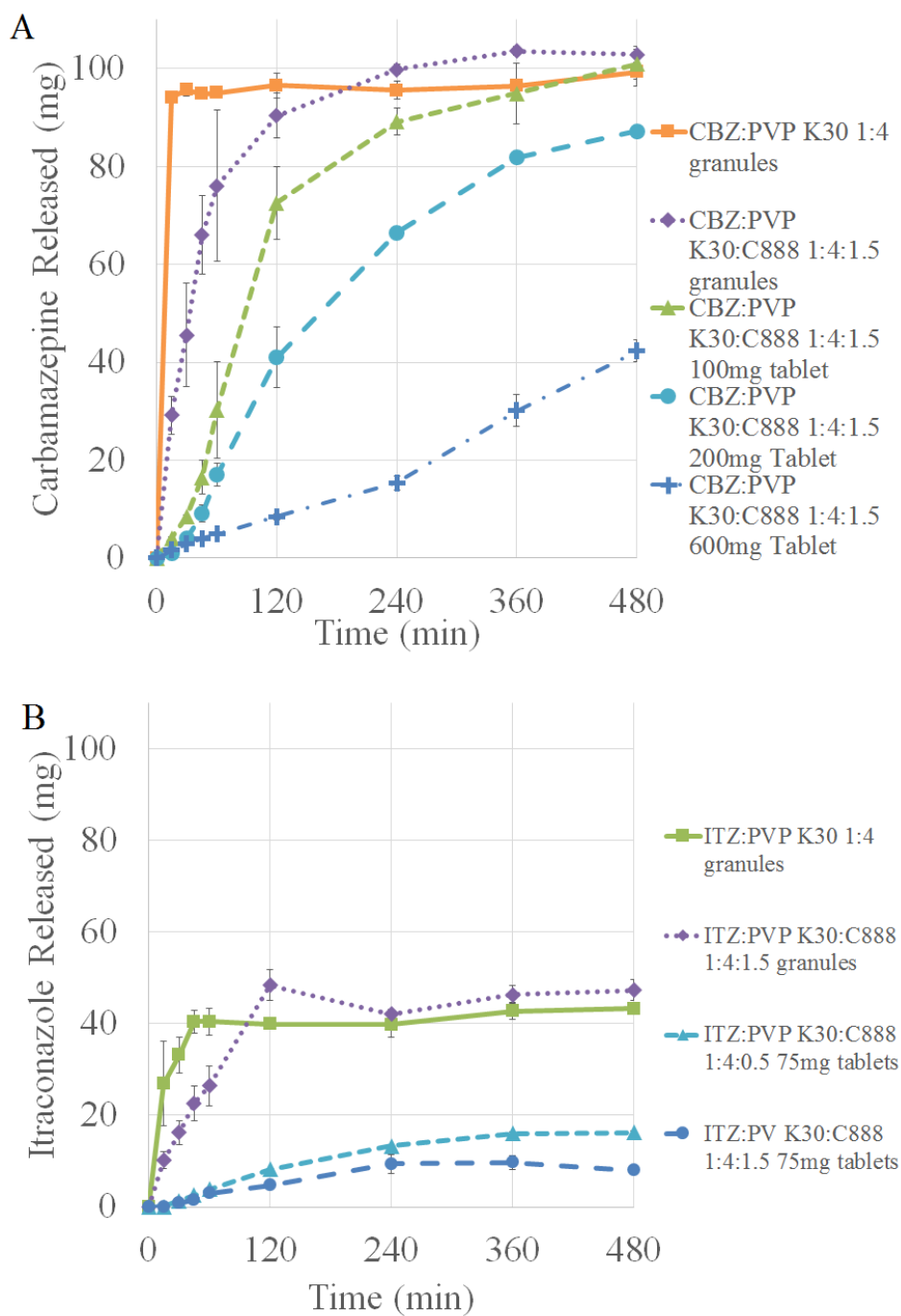


Figure 4.4 Non-sink dissolution of A)CBZ solid dispersions in 1000 ml purified water and B)ITZ solid dispersions in 1000 mL of 0.1 N HCl, USP Apparatus II at 50 RPM. Each vessel contains approximately 100 mg of drug. Weights indicate total tablet weight, with multiple tablets added as necessary to achieve target drug loading.

The amount of solubilized CBZ after 8 hours was roughly equivalent for solid dispersions, in granular form, with and without C888. In addition, tablets compressed to a total weight of 100 mg completely release drug. However, as the tablets were increased further in size to 200 mg and finally to 600 mg, the drug was slowly released and not completely liberated from the tablet during the same time.

In the case of ITZ, the granules performed similarly to those formulated with CBZ, drug release was slower when C888 was included in the composition. Similar amounts were dissolved into the solution for both ITZ granule formulations at concentrations well above the equilibrium solubility of ITZ. However, when the ITZ granules were compacted into small 75 mg total weight tablets, the drug was not released to the same extent. A reduction of the amount of C888 in the solid dispersions did not substantially improve the amount dissolved. A likely explanation is that ITZ was precipitating in the dosage form when the surface area to volume ratio was low. For these large tablets, the surface was observed to whiten and tablet disintegration/erosion did not occur. As further evidence, a sample of tablets observed to whiten in this manner were evaluated under polarized light microscopy and crystalline particles were observed (data not shown).

These results confirm that crystallization of drug within the tablet drastically alters the release rate and inhibits complete release. The mechanism of recrystallization cannot be ascertained from the data collected in Figure 4. Recrystallization may be the result of surface recrystallization due to supersaturated conditions in the media. Alternatively, water ingress, which upon absorption by PVP results in a glass-to-rubber transition, may increase molecular mobility within the dosage form prior to

disintegration/erosion. In addition, drug that is solubilized within the pores internal to the tablet is likely to be present in significant concentrations which may exceed solubility in that environment. In the case where diffusion from the pores to the bulk solution is slow, precipitation within the tablet pores is likely. To this effect, the compressed porous structures of the tablets is believed to contribute to the crystallization of the drug, inhibiting release. A cartoon of the proposed process and a more desirable mechanism of release are depicted in Figure 4.5.

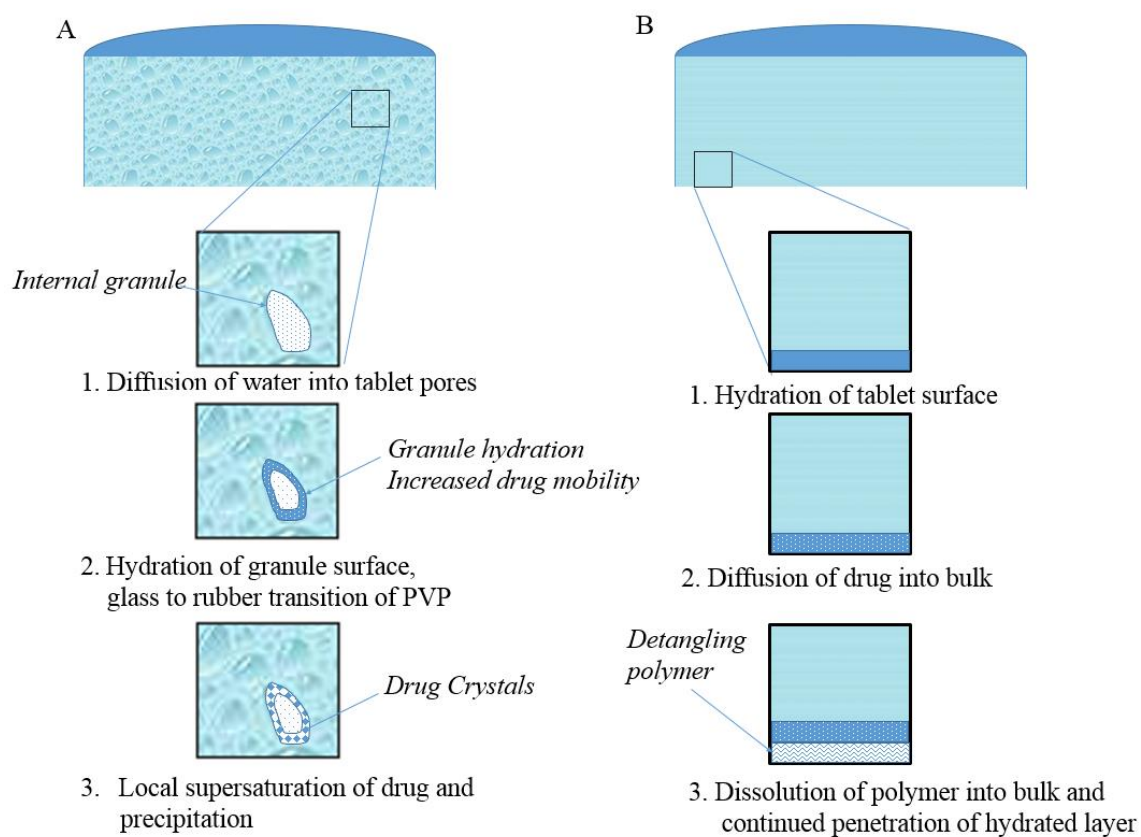


Figure 4.5 A cartoon depiction of the fate of drug in an amorphous solid dispersion containing tablet. A) A porous compressed tablet. B) A monolithic, molded tablet.

To probe this phenomena further, it was desirable to evaluate the CBZ compositions both above and below the saturation concentration of CBZ. Granules, porous tablets (compressed), and non-porous tablets (monolithic, molded) were prepared to study at these conditions. These geometries signify various conditions: 1) granules – polymer dissolution is on a similar timescale as the rate of penetration to the core due to high surface area to volume ratio; 2) compressed tablets – water diffusion to the core of the tablet occurs faster than tablet erosion/disintegration; 3) directly shaped monolithic tablets – water diffusion to the core of the eroding tablet will occur at a slow rate due to lack of pores prevalent in compressed tablets. In addition to evaluating each geometry at concentrations above and below the saturation concentration of CBZ, the solid dispersions were prepared with and without the inclusion of C888 to alter matrix hydrophobicity and reduce rate of water diffusion into the matrix. For these studies, fusion processing by KSD was performed, primarily due to the ability to shape a non-porous monolithic tablet having the same geometry as that prepared by standard tablet compression tools. Due to the small surface area to volume ratio of these tablets, the amount of C888 in the formulations was reduced from 1.5 parts to 0.5 parts to ensure drug diffusion rates in the tablets occurred over relevant experimental timescales. The results of this analysis are presented in Figure 4.6.

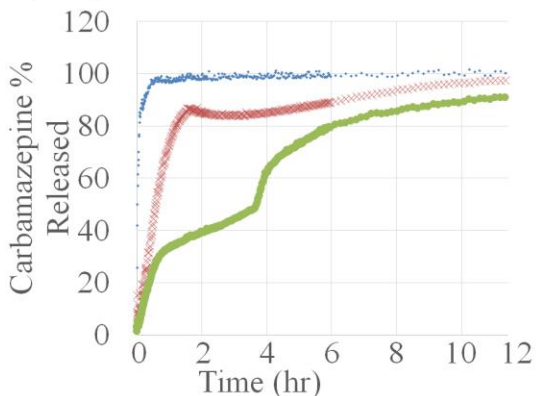
A) CBZ:PVP K30 1:4 Molded Tablet



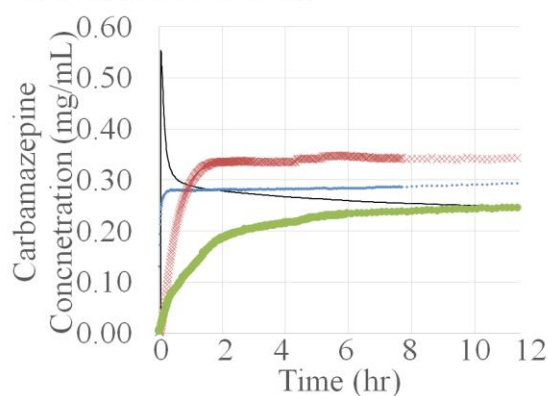
B) CBZ:PVP K30:C888 1:4:0.25 Molded Tablet



C) 0.2 mg/ml CBZ: PVP K30 1:4



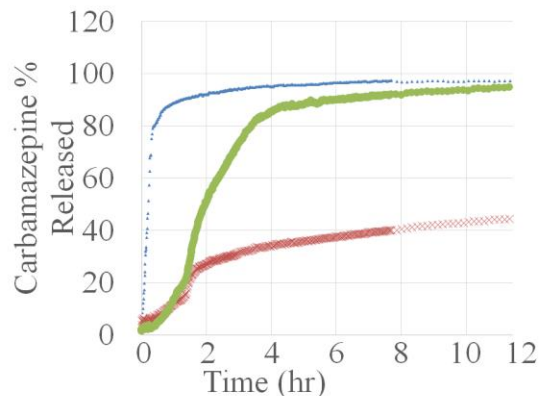
D) 0.4 mg/ml CBZ:PVP K30 1:4



· Granules    × Compressed Tablet

• Molded Tablet    – Solution Spike

E) 0.2 mg/ml CBZ:PVP K30:C888 1:4:0.25



F) 0.4 mg/ml CBZ:PVP K30:C888 1:4:0.25

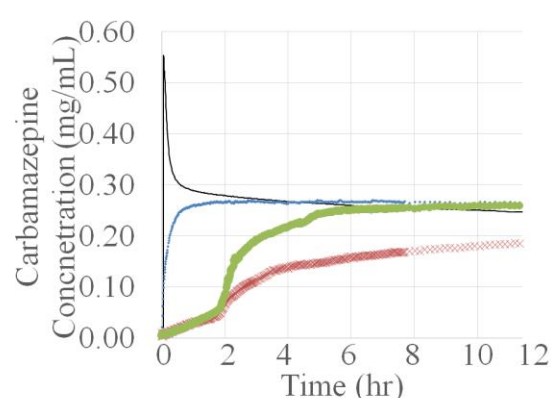


Figure 4.6 A) Molded tablet containing CBZ and PVP, B) Molded tablet containing CBZ, PVP and C888. C-F) Dissolution of granules (small blue dot), compressed tablets (red x) and molded tablets (large green circle), C) CBZ and PVP formulations below the solubility of CBZ (0.2 mg/ml) D) CBZ and PVP formulations above the solubility of CBZ (0.4 mg/ml) as compared to a solution spike of CBZ (black line) E) CBZ, PVP and C888 at 0.2 mg/ml F) CBZ, PVP and C888 at 0.4 mg/ml. USP I apparatus, 100 rpm, 37 °C in purified water (volume adjusted to dosage form weight).

The equilibrium concentration of crystalline CBZ dissolved under the experimental conditions was determined to be 0.23 mg/ml (Figure 4.6d) and confirmed by spiking the dissolution bath with excess CBZ dissolved in a small volume of acetonitrile. Based on this result, the dosage forms were studied at 0.2 mg/ml and 0.4 mg/ml to determine if and when supersaturated conditions in the media directly resulted in crystallization of CBZ within the dosage form. The molding process employed for this study produces tablets having an approximate weight of 1.15g. Following milling of the excess material, granules were appropriately sized and a portion was used to compress tablets of the same dimensions as monolithic tablets. For tablets containing C888, total drug content was reduced in order to maintain the correct surface area to volume ratio. However, dissolution media volumes were reduced to maintain the target final drug concentrations in the dissolution vessel.

Inspection of Figure 4.6 also provides insight to a significant potential advantage of controlled release solid dispersion tablets. The granules released rapidly in the non-sink conditions and rapidly reached an equilibrium concentration around 0.3 mg/ml. However, the tablet released at a slower rate and achieved a higher equilibrium concentration of 0.35 mg/ml. It is well known that the rate of nucleation formation in the supersaturated state increases when the extent of supersaturation increases. While this study design cannot confirm this possibility, it is likely that the rapidly formed free CBZ, concentrations of which exceeded the saturation concentration in 3 minutes, resulted in rapid nucleation, when compared to the tablet.

The dissolution curves resulting from the CBZ/PVP system (Figure 4.6c), along with visual observations indicated that supersaturated conditions in the dissolution media

were not a requirement for crystallization of CBZ in the dosage form. In the case of milled granules, drug release was rapid and complete at a CBZ concentration of 0.2 mg/ml. In the case of the compressed tablet, greater than 80% of the drug was released up until 1 hour and 45 minutes when the mostly disintegrated tablet was observed to whiten along with a corresponding change in release rate. It is believed that water penetrated the intergranular spaces and the portion of the tablet that did not disintegrate was hydrated below the surface. CBZ was mobilized by the corresponding reduction of the PVP glass transition temperature, yet unable to immediately enter the bulk solution. When the micro environmental concentration exceeded the solubility, it precipitated. The crystalline drug containing portion of the tablet, which did not completely disintegrate, then slow dissolved over the next 10 to 11 hours. In the case of the monolithic tablet, no tablet disintegration occurred. Drug release occurred in three phases: 1) rapid release of amorphous drug from the tablet surface - 0 to 30 minutes; 2) crystallization of drug in the tablet and slow drug release - 30 minutes to 3 hours and 30 minutes; 3) crystalline drug dissolution and diffusion from the matrix - 3 hours and 30 minutes to completion. The same study conducted at non-sink conditions, 0.4 mg/ml (Figure 4.6d), indicated that the first and second phases of drug release occurred on the same timescales. However, the third phase was incomplete due to saturated drug conditions in the media.

When C888 was included in the solid dispersions, the onset of crystallization in the different geometries contrasted the previous results (Figure 4.6e,f). In this case, the monolithic tablet exhibited a steady release over 3.5 hours at sink conditions while the compressed porous tablet exhibited incomplete release over this same time frame. The addition of C888 slowed the rate of water uptake into the tablet, allowing for polymer hydration and dissolution at the surface to occur at a rate sufficient to allow mobilized

amorphous drug to diffuse into the media. The porous compressed tablet exhibited inter-granule spaces that water freely penetrates, resulting in drug crystallization within the tablet before significant erosion/disintegration occurs, effectively stopping drug release.

On the whole, these data indicated the hydrophobicity of the tablet must be controlled in order to reduce the rate of water uptake into the solid dispersion matrix such that surface drug and polymer is dissolved into the media at a rate similar to water ingress. This finding was confirmed by studying similar systems containing ITZ at non-sink conditions. As demonstrated in Figure 4.7, porous compressed tablets with and without C888 all exhibited dissolution phases. The molded monolithic tablets released ITZ in a zero order fashion for 24 hours (the first 12 hours are shown in the figure), indicating that the water uptake rate into the tablet was slower than the rate of surface hydration and erosion. It is notable that ITZ is more hydrophobic than CBZ, based on analysis of their respective partition coefficients. In this case, ITZ itself acts as release modifier for PVP in the monolith and the addition of C888 simply further increased the hydrophobicity and slowed the rate of hydration and release.

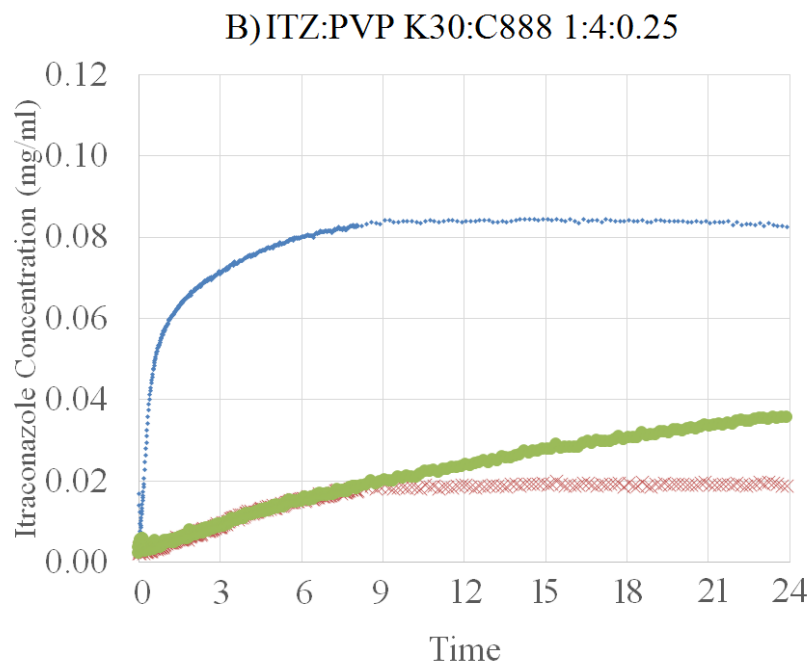
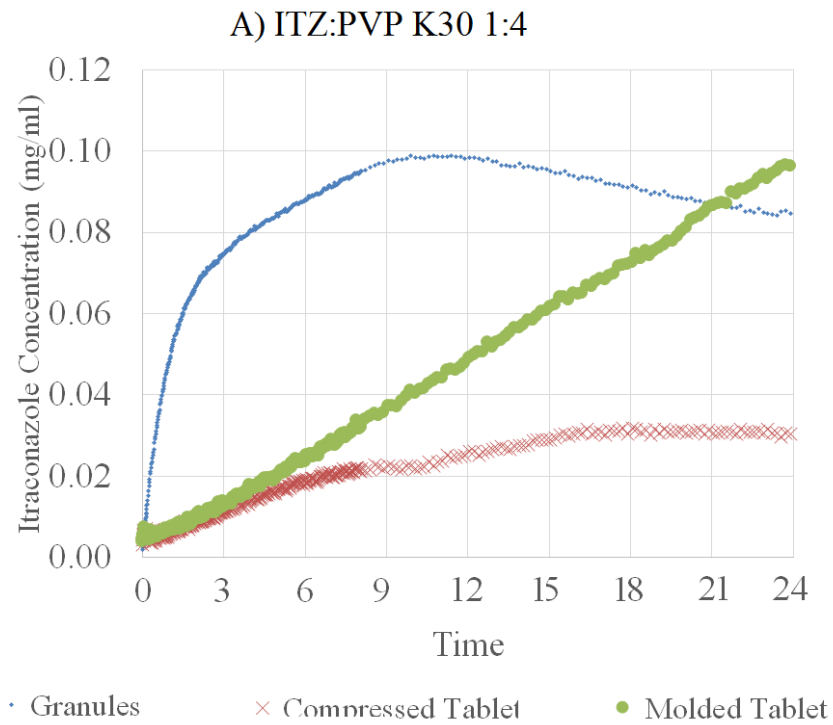


Figure 4.7 A) ITZ dissolution rates measured by USP Method II at 50rpm at 37 °C in 0.1 N HCl A) ITZ and PVP solid dispersions at 0.2mg/ml ITZ concentration B) ITZ, PVP and C888 solid dispersions at 0.2mg/ml ITZ concentration.

#### **4.5 CONCLUSIONS**

Formulation of controlled release tablets containing amorphous solid dispersions is challenging due to the tendency of the drug to recrystallize within the tablet during tablet hydration. Amorphous solid dispersions containing C888 were successfully prepared by HME and KSD. C888 was an effective processing aid and enabled HME processing of high molecular weight PVP. Using high density dissolution data, distinct phases of drug release were observed from tablets containing the drugs ITZ and CBZ in PVP and PVP/C888 matrices. The hydrophobicity, which was modulated by the inclusion of the C888 lipid, and geometry of the dosage form were observed to be the primary controlling factors in preventing crystallization and incomplete drug release. Rapid water ingress into hydrophilic or porous dosage forms resulted in crystallization when dissolution conditions were below the saturation solubility CBZ. Formulations prepared from CBZ, PVP and C888 were successfully formulated into controlled release tablets.

#### 4.6 REFERENCES

Breitenbach J (2002) Melt extrusion: from process to drug delivery technology. *European Journal of Pharmaceutics & Biopharmaceutics* **54**, 107-17.

Brouwers J, Brewster ME, and Augustijns P (2009) Supersaturating drug delivery systems: The answer to solubility-limited oral bioavailability? *Journal of Pharmaceutical Sciences* **98**, 2549-72.

Chiou WL and Riegelman S (1971) Pharmaceutical applications of solid dispersion systems. *Journal of Pharmaceutical Sciences* **60**, 1281-302.

Craig DQM (2002) The mechanisms of drug release from solid dispersions in water-soluble polymers. *International Journal of Pharmaceutics* **231**, 131-44.

Crowley MM, Zhang F, Repka MA, Thumma S, Upadhye SB, Kumar Battu S et al. (2007) Pharmaceutical Applications of Hot-Melt Extrusion: Part I. *Drug Development & Industrial Pharmacy* **33**, 909-26.

DiNunzio JC, Brough C, Hughey JR, Miller DA, Williams Iii RO, and McGinity JW (2010a) Fusion production of solid dispersions containing a heat-sensitive active ingredient by hot melt extrusion and Kinetisol® dispersing. *European Journal of Pharmaceutics & Biopharmaceutics* **74**, 340-51.

DiNunzio JC, Brough C, Miller DA, Williams Iii RO, and McGinity JW (2010b) Applications of KinetiSol® Dispersing for the production of plasticizer free amorphous solid dispersions. *European Journal of Pharmaceutical Sciences* **40**, 179-87.

DiNunzio JC, Miller DA, Yang W, McGinity JW, and Williams RO (2008) Amorphous Compositions Using Concentration Enhancing Polymers for Improved Bioavailability of Itraconazole. *Molecular Pharmaceutics* **5**, 968-80.

Friesen DT, Shanker R, Crew M, Smithey DT, Curatolo WJ, and Nightingale JAS (2008) Hydroxypropyl Methylcellulose Acetate Succinate-Based Spray-Dried Dispersions: An Overview. *Molecular Pharmaceutics* **5**, 1003-19.

Hancock BC, Shamblin SL, and Zografi G (1995) Molecular Mobility of Amorphous Pharmaceutical Solids Below Their Glass Transition Temperatures. *Pharmaceutical Research* **12**, 799-806.

Hancock BC, York P, and Rowe RC (1997) The use of solubility parameters in pharmaceutical dosage form design. *International Journal of Pharmaceutics* **148**, 1-21.

Hancock BC and Zografi G (1997) Characteristics and significance of the amorphous state in pharmaceutical systems. *Journal of Pharmaceutical Sciences* **86**, 1-12.

Hughey JR, Keen JM, Miller DA, Brough C, and McGinity JW (2012) Preparation of Viscous Solid Dispersion Systems by Hot-Melt Extrusion and KinetiSol® Dispersing: Polymer Screening and Thermal Stability. *International Journal of Pharmaceutics* **438**, 11-9.

Janssens S and Van den Mooter G (2009) Review: physical chemistry of solid dispersions. *Journal of Pharmacy & Pharmacology* **61**, 1571-86.

Keen JM, Martin C, Machado A, Sandhu H, McGinity JW, and DiNunzio JC (2013) Investigation of process temperature and screw speed on properties of a pharmaceutical

solid dispersion using corotating and counter-rotating twin-screw extruders. *Journal of Pharmacy & Pharmacology* n/a-n/a.

Kolter K, Karl M, Nalawade S, and Rottmann N (2010) Hot-Melt Extrusion with BASF Pharma Polymers: Extrusion Compendium. In BASF (ed.), (ed.), Vol. pp. Ludwigshafen, Germany.

Miller D, DiNunzio J, Yang W, McGinity J, and Williams R (2008a) Targeted Intestinal Delivery of Supersaturated Itraconazole for Improved Oral Absorption. *Pharmaceutical Research* **25**, 1450-9.

Miller DA, DiNunzio JC, Yang W, McGinity JW, and Williams RO (2008b) Enhanced In Vivo Absorption of Itraconazole via Stabilization of Supersaturation Following Acidic-to-Neutral pH Transition. *Drug Development & Industrial Pharmacy* **34**, 890-902.

Repka MA, Battu SK, Upadhye SB, Thumma S, Crowley MM, Zhang F et al. (2007) Pharmaceutical Applications of Hot-Melt Extrusion: Part II. *Drug Development & Industrial Pharmacy* **33**, 1043-57.

Serajuddin ATM (1999) Solid dispersion of poorly water-soluble drugs: Early promises, subsequent problems, and recent breakthroughs. *Journal of Pharmaceutical Sciences* **88**, 1058-66.

Tran P, Tran T, Park J, and Lee B-J (2011) Controlled Release Systems Containing Solid Dispersions: Strategies and Mechanisms. *Pharmaceutical Research* **28**, 2353-78.

Vasconcelos T, Sarmiento B, and Costa P (2007) Solid dispersions as strategy to improve oral bioavailability of poor water soluble drugs. *Drug Discovery Today* **12**, 1068-75.

## **Chapter 5: Development of Itraconazole Tablets Containing Viscous KinetiSol® Solid Dispersions: *in vitro* and *in vivo* Analysis in Dogs**

### **5.1 ABSTRACT**

The formulation factors relevant to developing immediate and controlled release dosage forms containing poorly soluble drugs dispersed in amorphous systems are poorly understood. While the utility of amorphous solid dispersions is becoming apparent in the pharmaceutical marketplace, literature reports tend to report on the development of solid dispersion particulates, which then must be formulated into a tablet. Amorphous solid dispersions of itraconazole in high molecular weight hydroxypropyl methylcellulose were prepared by KinetiSol® Dispersing and tablets were formulated to immediately disintegrate or control the release of itraconazole. Formulated tablets were evaluated by two non-sink dissolution methodologies and the dosage form properties that controlled the gelling tendency of the dispersion carrier, hydroxypropyl methylcellulose, were investigated. Selected candidates were evaluated in beagle dogs and compared to a commercially marketed composition. Tablets containing viscous dispersions were found to enhance the bioavailability of itraconazole.

### **5.2 INTRODUCTION**

Development of amorphous solid dispersions using glassy pharmaceutical polymers and poorly water soluble drugs has rapidly become a routine approach for improving the bioavailability of these drugs. The industrial application of this technology, which was first realized over 40 years ago (Sekiguchi et al., 1964, Chiou and Riegelman, 1971), has increased rapidly over the last decade. Not surprisingly, the

increased industrial relevance corresponds with an increased need due to the changing properties of new chemical entities (NCEs), which are becoming larger, more lipophilic, more complex and exhibit high melting points (Keseru and Makara, 2009). Likewise, development of these systems has benefitted from continued research into the properties of these systems relevant to drug release (Alonzo et al., 2011) and the thermodynamic and kinetic factors relevant to stability (Janssens and Van den Mooter, 2009), although there is still much to learn (Van den Mooter, 2012).

Spray drying (Friesen et al., 2008) and hot-melt extrusion (HME) (Repka et al., 2008) processes are well established in the production of amorphous solid dispersions. While many compositions may be produced by both technologies, the thermal properties and solubility of drugs and adjuvants may be particularly amenable to one process over the other. More recently, KinetiSol® Dispersing (KSD) has also been demonstrated in the literature to produce amorphous solid dispersions (DiNunzio et al., 2010c, Hughey et al., 2010). This novel fusion process is extremely rapid and limits thermal exposure (DiNunzio et al., 2010a); yet, KinetiSol® is capable of producing compositions containing viscous, high molecular weight polymers (Hughey et al., 2012) and high melting point compounds (Hughey et al., 2011). Viscous polymers present challenges in droplet formation (Broadhead et al., 1992) during spray drying and require plasticization to be extruded (Kolter et al., 2010). From an industrial perspective, high melting point compounds may not be dissolved in the polymer melt at temperatures and timescales suitable for HME. Furthermore, more challenging candidates have poor solubility in organic solvents and the resulting dilute solvent solutions are inefficient for spray drying. It follows that KinetiSol® Dispersing may enable new classes of solid dispersions with challenging drugs through formulation with viscous polymers.

The present study was constructed to investigate the utility of dosage forms prepared from viscous solid dispersions prepared by KSD on the pharmacokinetics of itraconazole (ITZ) in a beagle dog model, which has been identified as a suitable preclinical model to humans (Yoo et al., 2002). ITZ is a weak base (pKa 3.7) that is insoluble at the pH of the intestines. In fact, ITZ may be considered a worst case weakly basic model drug due to a high log P and extremely low solubility. Evidence to this effect are the large number of investigations intended to investigate the utility of formulations approaches using the drug (Francois et al., 2003, Six et al., 2005, Hoeben et al., 2006, Vaughn et al., 2006, DiNunzio et al., 2008, Mellaerts et al., 2008, Miller et al., 2008a). An exhaustive list of these studies is beyond the scope of this discussion. However, it is notable that bioavailability is not predictable based on sink dissolution (Six et al., 2005).

ITZ is marketed as an extruded amorphous solid dispersion, which is milled and compressed into tablets and sold under the brand name Onmel (Baert et al., 2003, 2006). Hypromellose 2910 5 cps (hydroxypropyl methylcellulose - Methocel™ E5 chemistry) (HPMC E5) is the carrier polymer in the solid dispersion based on a review of the prescribing information and patents listed in the FDA Orange Book. Patent coverage for the composition is not extended to high molecular weight grades of HPMC, such as Methocel™ E4M, which is considered anecdotally as evidence that the viscous compositions are not amenable to HME. Our research group has previously evaluated the improvement of higher molecular weight HPMC solid dispersion particles on oral bioavailability in rats (Miller et al., 2008b) and for improved stabilization in neutral

media (Hughey et al., 2012). For reference, the properties of the relevant various grades of HPMC, as determined by Keary (2001), are included for comparison in Table 5.1.

Table 5.1 Properties of hydroxypropyl methylcellulose Type 2910 (Methocel™ E).

Grade	Viscosity of 2 % Aqueous Solution (cps)	Weight-Average Molecular Weight [Mw] (g/mol)	Number-Average Molecular Weight [Mn] (g/mol)	Polydispersity	Intrinsic viscosity [η] (dl/g)
E5	5	28,700	11,100	2.5	0.81
E50	50	86,700	33,800	2.6	2.45
E4M	4000	323,200	78,700	4.1	7.32

While investigations into the utility of solid dispersion particles are necessary initially, formulation into a tablet is desirable for distribution. However, due to the gelling tendencies of solid dispersion carriers, drugs have a tendency to recrystallize in the dosage form prior to release and lack the same performance as the dispersion particles. Various investigators have described approaches to solve this problem. Tanaka et al. (2006) developed eroding matrix tablets that shielded particles from dissolution prior to release from the tablet. Srinarong et al. (2009) demonstrated enhanced dissolution through inclusion of super-disintegrants in the tablet and within the solid dispersion to promote rapid dispersion and wetting of the particles. However, high dose drugs require high loadings of solid dispersions to yield a dosage form of manageable size, and high loadings of super-disintegrants are not capable of overcoming the gelling tendency of dispersion carriers. Hughey et al. (2013) manipulated the gel-sol transition of the carrier polymer through the inclusion of salts to reduce gelling strength and promote disintegration.

The specific objectives of this investigation were to develop high molecular weight solid dispersions of itraconazole in HPMC E50 and EPMC E4M. A drug loading of 2:3 based on the HPMC E5 based comparator, Onmel, was selected. Tablets containing these solid dispersions were to be formulated such that rapid dissolution, similar to Onmel, and a controlled release profile could be evaluated by oral administration to beagle dogs. This design was intended to evaluate two hypotheses: 1) that viscous solid dispersions, exhibiting improved supersaturation maintenance at intestinal pH (Hughey et al., 2012), improve bioavailability; and 2) that the inclusion of salts to improve dissolution of tablets was realized in vivo (Hughey et al., 2013).

### **5.3 MATERIALS AND METHODS**

#### **5.3.1 Materials**

Itraconazole (ITZ) was purchased from Letco Medical (Decatur, Alabama). Hydroxypropyl methylcellulose (HPMC, Methocel<sup>TM</sup>) was kindly donated by The DOW Chemical Company (Midland, MI). Spray dried lactose (Flowlac<sup>®</sup> 90, Meggle AG, Wasserburg, Germany) and hydrogenated vegetable oil (Sterotex<sup>®</sup>, Abitec, Columbus, OH) was donated by Mutchler Inc. (Harrington Park, NJ). Microcrystalline cellulose (Ceolus<sup>TM</sup> KG-1000 was donated by Asahi Kasei America Inc. (New York, NY). Colloidal anhydrous silica (Cab-O-Sil M5P) was donated by Cabot (Boston, MA). Crospovidone (Kollidon<sup>®</sup> CL) was donated by BASF (Tarrytown, NY). Magnesium stearate, potassium bicarbonate, talc and croscarmellose sodium were purchased from Spectrum Chemicals and Laboratory Products (New Brunswick, NJ). Analytical reagents

were of ACS grade or higher and purchased from Fisher Scientific (Pittsburg, PA). Simulated intestinal powder (SIF) was purchased from Biorelevant.com (Croydon, UK).

## **5.3.2 Methods**

### ***5.3.2.1 KinetiSol® Dispersing***

Solid dispersions were formed using a KinetiSol® compounder (DisperSol Technologies, Georgetown, TX). Blends were hand mixed in a polyethylene bag and loaded into the processing chamber of the compounder. A shaft within the processing chamber, having protruding blades, was rotated at 2200 rpm using an online control module. Through a combination of high frictional and shearing forces imparted by the rotating blades, without the use of external heat, the temperature of the composition was rapidly increased until a molten mass was achieved. Realtime temperature of the material within the processing chamber was monitored. Once reaching the desired temperature of 140 °C, the mass was automatically ejected from the processing chamber. The material was briefly pressed between two metal plates to flatten, then manually cut while still hot into pieces of suitable size for feeding to the hammer mill.

### ***5.3.2.2 Milling and Sizing***

Solid dispersions were milled in two stages with a Laboratory Fitzmill L1A hammer mill (Fitzpatrick) operating at 9000 RPM in a hammer/impact forward position. Initially, a 0.125 in round-hole screen size was installed in the in the milling chamber to prepare course particles. Subsequently, a 0.020 in round-hole screen was installed and the previously discharged material was milled. For Formulations 1 and 2, the powder fractions between 75 µm and 150 µm were collected for blending and compression.

Subsequent formulations were prepared from the 75  $\mu\text{m}$  to 250  $\mu\text{m}$  fraction. Particle size fractions were separated following 15 agitations using a RX-24 Ro-Tap (W.S. Tyler Industrial Group, Mentor, OH).

### ***5.3.2.3 Blending and Compression***

For Formulations 1 and 2, sized solid dispersion was blended with spray dried lactose, MCC, and crospovidone for 15 min in a P-K Blend Master V-Shell blender (Patterson-Kelley Co., East Stroudsburg, PA) followed by an additional 5 minutes of blending with the talc, magnesium stearate, hydrogenated vegetable oil and colloidal anhydrous silica. Individual portions of the blend were weighed and compressed into 16mm flat faced round tablets at 1 kN compression force using a Manual Tablet Compaction Machine (MTCM-1, Globe Pharma, Inc., New Brunswick, NJ). Subsequent formulations were prepared by twice sieving all the materials together through a 20 mesh sieve and blending in one step for 15 minutes, followed by compression at 10 kN. The rationale for the selected compression forces is discussed later.

### ***5.3.2.4 Differential Scanning Calorimetry***

Differential scanning calorimetry (DSC) was performed on desiccated 8.0 mg  $\pm$  0.5 mg samples of milled KSD dispersions in crimped aluminum pans. The temperature range studied was from -10  $^{\circ}\text{C}$  to 300  $^{\circ}\text{C}$  with a ramp rate of 10  $^{\circ}\text{C}/\text{min}$ . A Model Q20 DSC (TA Instruments, New Castle, DE) was used for this analysis. For comparison and interpretation of the solid dispersion results, crystalline ITZ was also studied using a three step heat-cool-heat cycle: 1) 35  $^{\circ}\text{C}$  to 210  $^{\circ}\text{C}$  ramped at 10  $^{\circ}\text{C}/\text{min}$  2) 210  $^{\circ}\text{C}$  to 0  $^{\circ}\text{C}$

ramped at 40 °C/min 3) 0 °C to 225 °C to determine the melting point and glass transition temperature.

#### ***5.3.2.5 Powder X-Ray Diffraction***

An Equinox 100 standalone bench top X-ray diffractometer (INEL, Inc., Stratham NH) was used to analyze ITZ and milled solid dispersions. Samples were placed in an aluminum crucible and loaded in a rotating sample holder. Samples were analyzed for 300 seconds using a Cu K radiation source ( $\lambda = 1.5418 \text{ \AA}$ ) operating at 42 kV and 0.81 mA.

#### ***5.3.2.6 Non-Sink Dissolution Analysis***

Non-sink dissolution analysis was performed with a VK 7010 dissolution tester (Varian, Inc., Palo Alto, CA, USA) configured for USP Method A (paddles). 200 mg ITZ tablets were placed in dissolution vessels containing 750 mL of 0.1 N HCl ( $\sim 20\times$  equilibrium solubility) equilibrated at  $37.0 \pm 0.5 \text{ }^\circ\text{C}$  with paddles rotating at 100 rpm ( $n = 3$ ). After 2 h, 250 mL of 0.2 M  $\text{Na}_3\text{PO}_4$ , preheated to  $37.0 \pm 0.5 \text{ }^\circ\text{C}$ , was added to the dissolution vessels in order to adjust the pH to  $6.80 \pm 0.05$  and achieve a final volume of 1000 mL. 5 mL were manually removed, without media replacement, after 15, 60, 120, 125, 130, 135, 150, 180, 240, 300 and 360 min. All samples were immediately filtered through 0.2  $\mu\text{m}$  17-mm PVDF Target2 syringe filters (Thermo Scientific, Waltham, MA), and immediately diluted 1:1 with mobile phase. Samples were then transferred without further treatment to 1-mL HPLC vials (VWR International, West Chester, PA, USA) for HPLC analysis.

A small volume, pH-dilution analysis was also performed, based on the methodology presented Gao et al. intended to simulate the dynamic conditions of the gastrointestinal tract (Gao et al., 2010). This model as described was designed to mimic the gastrointestinal tract (GIT) of fasted rats. The volumes and time points were adjusted for this analysis. Dissolution was performed in vials at 37 °C in an orbital shaker operating at 100 rpm. 200 mg ITZ tablets were added to 30 mL of 0.01 N HCl. After 30 minutes 30 mL of concentrated FaSSIF, prepared by adding 4.45 g/L of SIF to pH 6.8, 80 mM phosphate buffer, was added. Subsequent dilutions were made by adding 10 ml of FaSSIF, prepared by adding 2.24 g/L of SIF to pH 6.8, 80 mM phosphate buffer, at 40, 60, 80, 100, and 120 min. A final dilution of 50 mL of FaSSIF was made at 140 min. 500 µL samples were collected at 5, 15, 30, 40, 60, 100, 140, 220 and 330 min. Immediately following sampling, samples were centrifuged (Eppendorf 5415C, Hamburg, Germany) at 18,000 RCF for 2 mins. 300 µL samples of the supernatant were diluted 1:1 with acetonitrile for quantification.

#### ***5.3.2.7 High Performance Liquid Chromatography***

High performance liquid chromatography (HPLC) was used to analyze the dissolution test samples. A 717 autosampler (Waters Corporation, Milford, MA) configured with a Luna 5 µm CN 100 Å, 150 x 4.6 mm column (Phenomenex, Torrance, CA). The mobile phase was a mixture of acetonitrile:water:diethanolamine 70:30:5 flowing at 1.00 mL/min. A Waters 2996 photodiode array detector, extracting at 263 nm, was used to quantify the results. The retention time of ITZ was approximately 6 min. All analyses maintained linearity ( $R^2 = 0.999$ ) in the range tested and a relative standard deviation of less than 0.6%. Empower 3 was utilized to process all chromatography data.

#### **5.3.2.8 *In Vivo* Analysis**

Preclinical analysis was performed at Charles River Laboratories (Wilmington, MA), Institutional Animal Care and Use Committee (IACUC) approval number P06092010. A pre-study health status check was performed on non-naïve animals, which included a physical exam, serum chemistry and hematology evaluations. 12 male beagle dogs were placed into three groups of four and fasted overnight prior to dosing. Food was returned after the 4 hour post dose blood collection. Each animal, weight 8 to 12 kg, was dosed with a 200 mg ITZ containing tablet and 40 mL of acidified water (pH 2) to assist dosing.

Sodium heparin was used as an anti-coagulant for 1 mL blood samples that were collected by direct venipuncture of a cephalic vein and placed at 2-8 °C on wet ice. Samples were collected at 0.25, 0.5, 1, 1.5, 2, 3, 5, 8, 12, 24, and 48 hr post dose. Samples were centrifuged at 3500 rpm to isolate plasma for 10 minutes at 2 to 8 °C. Plasma samples were transferred to polypropylene tubes in a 96-well plate stored on dry ice. ITZ was quantitated in the plasma samples using diclofenac as an internal standard by LC MS/MS demonstrating a linear range from 1 to 10,000 ng/mL ( $R^2 > 0.98$ ). Linear Trapezoidal non-compartmental pharmacokinetic analysis was performed in WinNonlin Version 2.1.

## **5.4 RESULTS AND DISCUSSION**

### **5.4.1 Highly Viscous Solid Dispersions**

Binary blends of ITZ and HPMC were blended and processed by KSD to a target temperature of 140 °C in order to dissolve the crystalline drug in the polymer. Example processing temperature vs time profiles for both molecular weight (MW) grades evaluated, E50 and E4M, are plotted in Figure 5.1. After approximately 4 seconds in the machine, the temperature was sufficient to be registered by the temperature sensor. The temperature increased rapidly until the target temperature was achieved and the viscous mass was ejected from the machine.

During initial process development, compositions were cooled completely while pressed between two chilled plates. However, the resulting cooled dispersions were extremely difficult to subdivide for feeding to the mill. When impacted with a large hammer, only occasionally was a piece broken from the mass. In order to facilitate milling, subsequent KSD batches were only pressed with room temperature plates, then cut into pieces of suitable size to feed into the laboratory L1A Fitzmill, which has a narrow throat. In addition, this model Fitzmill does not have a jacket for recirculating cooling water. To minimize heat buildup in the mill, a two stage milling process was performed and the mill allowed to cool between operations.

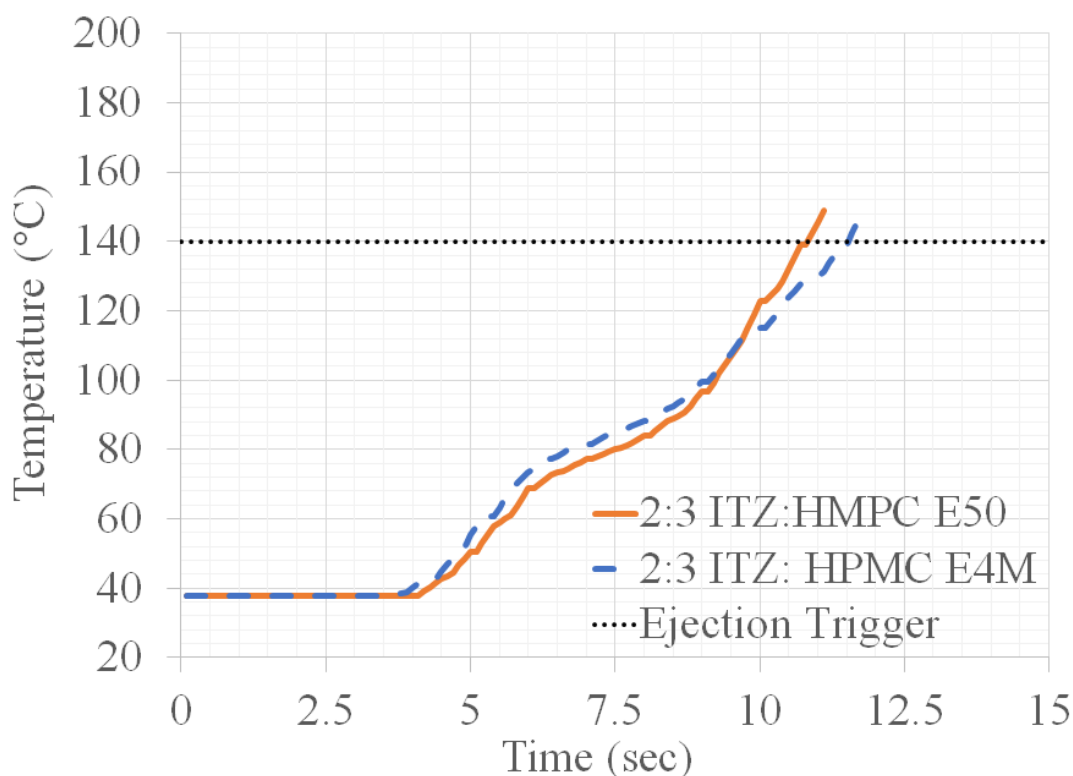


Figure 5.1 KSD processing profiles for ITZ and HPMC viscous solid dispersions.

Milled dispersions were desiccated, then analyzed by DSC to investigate the glass transition temperature ( $T_g$ ). The E50 and E4M dispersions were determined to have a single  $T_g$  as observed in Figure 5.2, indicating a single phase composition was prepared and that ITZ was molecularly dispersed in the polymer. In addition, there is no evidence of a crystalline ITZ phase as characterized by the lack of an endotherm around 169 °C, characteristic of the melting point of ITZ. The  $T_g$  of the E50 and E4M dispersions was determined to be 72.5 °C and 83.4 °C, respectively. The increase in  $T_g$  with MW of linear chain HPMC is expected as longer chain lengths increase the relative number of monomers restricted in conformational and rotation (Gibbs and DiMarzio, 1958). The number of chain terminations, which have conformational freedom and lack the stiffness

of their bound counterparts, decreases in a given sample mass as the MW increases. Correspondingly, increasing the MW of the system increases the excess free volume, enthalpy, viscosity and entropy of the system at a given temperature (Fox and Flory, 1950).

From an industrial pharmacy perspective, the increased  $T_g$  is desirable because molecular motion is restricted and may improve the shelf life of the amorphous form. According to Hancock et al. (1995), molecular motion relevant to a pharmaceutical shelf life is restricted sufficiently to kinetically stabilize the amorphous form at 50 °C below the glass transition temperature. Based on the measured  $T_g$  for the E50 and E4M ITZ dispersions, they should be expected to be kinetically stable at the typical stability storage conditions of 25 °C and 30 °C, respectively, provided that they are protected from moisture. While a thermodynamic assessment of the stability of this system is beyond the scope of this work, it is notable that the 40% ITZ HPMC dispersions may also be thermodynamically stable. In fact, neat glassy ITZ has been reported to have good stability (Six et al., 2001); however, the present discussion is relevant to the utility of viscous solid dispersions beyond the model drug used in the present study.

An observation, which will be mentioned but not investigated in this work, are the endotherms observed between 200 °C and 260 °C. According to a recently issued patent listed by the FDA Orange Book for ITZ, the magnitude of this melting endotherm correlates inversely with the oral bioavailability of ITZ in humans (Berndl et al., 2013). More specifically, it is reported that in 40% ITZ in HPMC E5 extruded solid dispersion systems prepared at increasingly aggressive conditions, this endotherm was observed to decrease in a set of samples from 0.49 J/g to 0.29 J/g and finally to 0.10 J/g. A

corresponding improvement of 10% and 50% in bioavailability was observed for the latter two samples when compared to the sample having an endotherm of 0.49 J/g. Endotherms reported for the KSD dispersions are 1.68 J/g and 3.31 J/g for the E50 and E4M under the same testing conditions. This trend would predict a decrease in the oral bioavailability of the KSD dispersions compared to Onmel, which is discussed later.

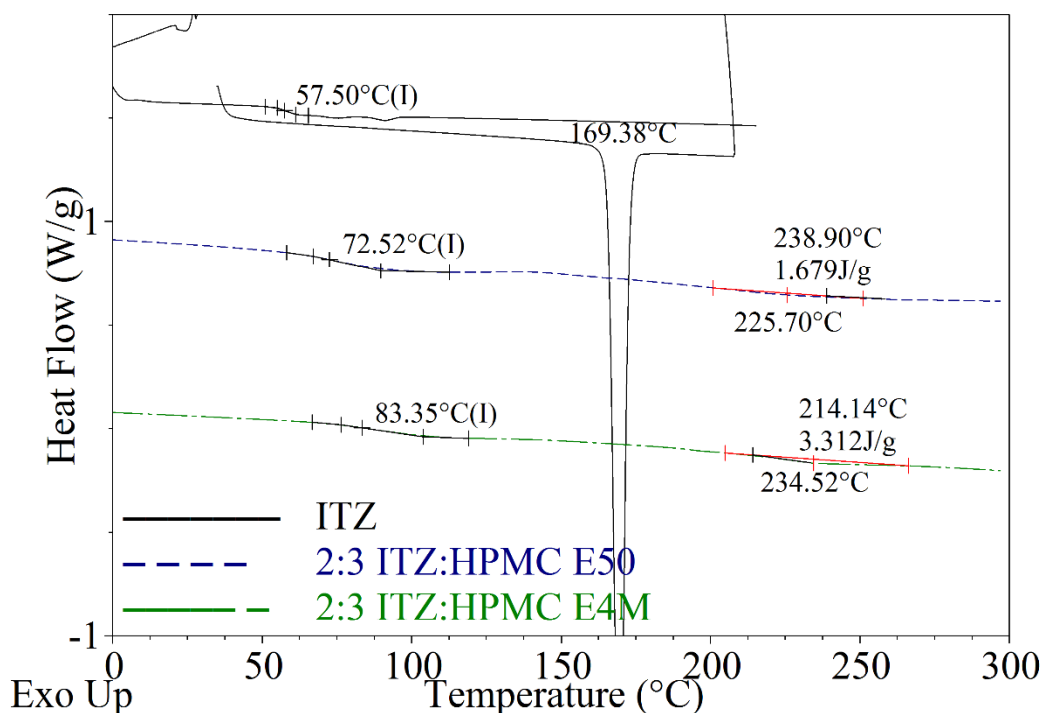


Figure 5.2 DSC thermograms of ITZ and HPMC viscous solid dispersions.

In order to confirm the amorphous nature of the E50 and E4M solid dispersions, wide angle powder X-Ray diffraction analysis was performed. As presented in Figure 5.3, crystalline ITZ exhibits a diffraction pattern having several characteristic peaks between  $10^\circ$  and  $30^\circ 2\theta$ . Overlaid diffraction patterns of the KSD solid dispersions

exhibit a halo in the region characteristic of amorphous materials. These results confirm the thermal analysis results for lack of substantial crystalline ITZ.

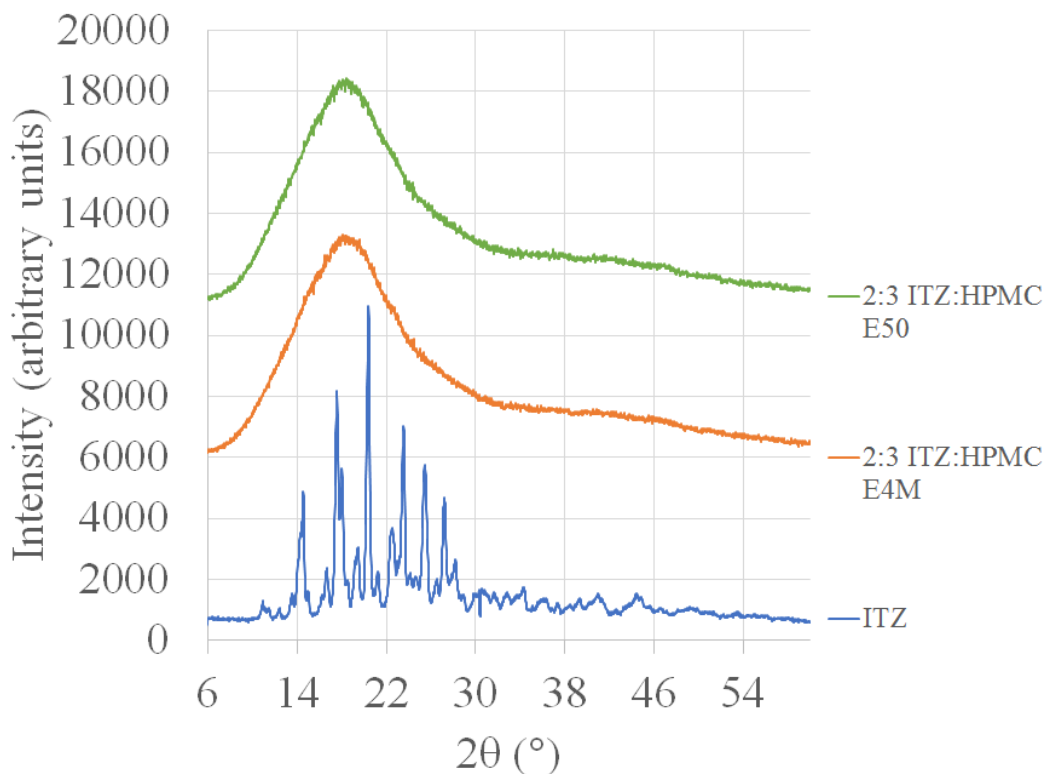


Figure 5.3 X-Ray diffractograms of ITZ and HPMC viscous solid dispersions.

#### 5.4.2 Tablet Compositions and *in Vitro* Analysis

Viscous KSD dispersions of HPMC and ITZ were previously evaluated and determined to inhibit precipitation of ITZ following an acid to neutral transition intended to simulate a transition of the stomach contents to the intestine (Hughey et al., 2012). This magnitude of supersaturation maintenance was observed to increase with an increase in HPMC MW. The next step in investigating the utility of these viscous systems and

ultimately understanding their importance *in vivo* was to develop tablet compositions. Experience and literature (Tanaka et al., 2006, Srinarong et al., 2009, Hughey et al., 2013) indicate that dissolution from tablets containing solid dispersions must be carefully controlled to ensure complete release without crystallization in the dosage form. Considering the comparator in our study, Onmel, disintegrates and contains a low viscosity HPMC dispersion, the initial tablet formulations that were investigated were selected based on Onmel's composition. Formulations 1 and 2, listed in Table 5.2, were prepared initially based on this composition although the exact grades of excipients were unknown. Preliminary disintegration studies (data not shown) indicated that at low compression forces (<5 kN), tablets containing KSD dispersions did not disintegrate, at least up to 20 min when the experiments were stopped. Tablets were compressed at ~ 1kN to achieve some tablet disintegration in less than 5 min. However, as visually observed in the disintegration apparatus, a large portion of the tablet was observed to form a viscous, non-disintegrating gel.

Table 5.2 ITZ solid dispersion containing tablet compositions.

<b>Ingredient</b>	<b>Form 1 (w/w%)</b>	<b>Form 2 (w/w%)</b>	<b>Form 3 (w/w%)</b>	<b>Form 4 (w/w%)</b>	<b>Form 5 (w/w%)</b>	<b>Form 6 (w/w%)</b>
ITZ: METHOCEL™ E50 2:3 solid dispersion	55.55	-	55.55	-	50.9	-
ITZ: METHOCEL™ E4M 2:3 solid dispersion	-	55.55	-	55.55	-	50.9
Spray Dried Lactose	24.0	24.0	24.0	24.0	22.0	22.0
Microcrystalline Cellulose	7.8	7.8	7.8	7.8	7.1	7.1
Crospovidone	9.0	9.0	4.5	4.5	4.1	4.1
Croscarmellose sodium	-	-	4.5	4.5	4.1	4.1
Talc	3.0	3.0	3.0	3.0	2.7	2.7
Hydrogenated vegetable oil type I	0.1	0.1	0.1	0.1	0.1	0.1
Colloidal anhydrous silica	0.3	0.3	0.3	0.3	0.3	0.3
Magnesium stearate	0.3	0.3	0.3	0.3	0.2	0.2
Potassium Bicarbonate(KHCO <sub>3</sub> )	-	-	-	-	8.3	8.3

The dissolution results for Formulations 1 and 2 were sub-optimal compared to Onmel, as seen in Figure 5.4. Less than 25% of the ITZ was dissolved in the acid phase for the E50 formulation, which rapidly precipitated in the 30 minutes following neutralization. The E4M formulation released less than 12.5% of the ITZ in the acid phase. These results directly contrast the solubility enhancement capabilities of ITZ and viscous HPMC solid dispersion particles previously evaluated (although at a lower concentration) (Hughey et al., 2012). However, the results for Onmel confirm Hughey's results that HPMC E5 does not substantially inhibit precipitation of Onmel following the pH change.

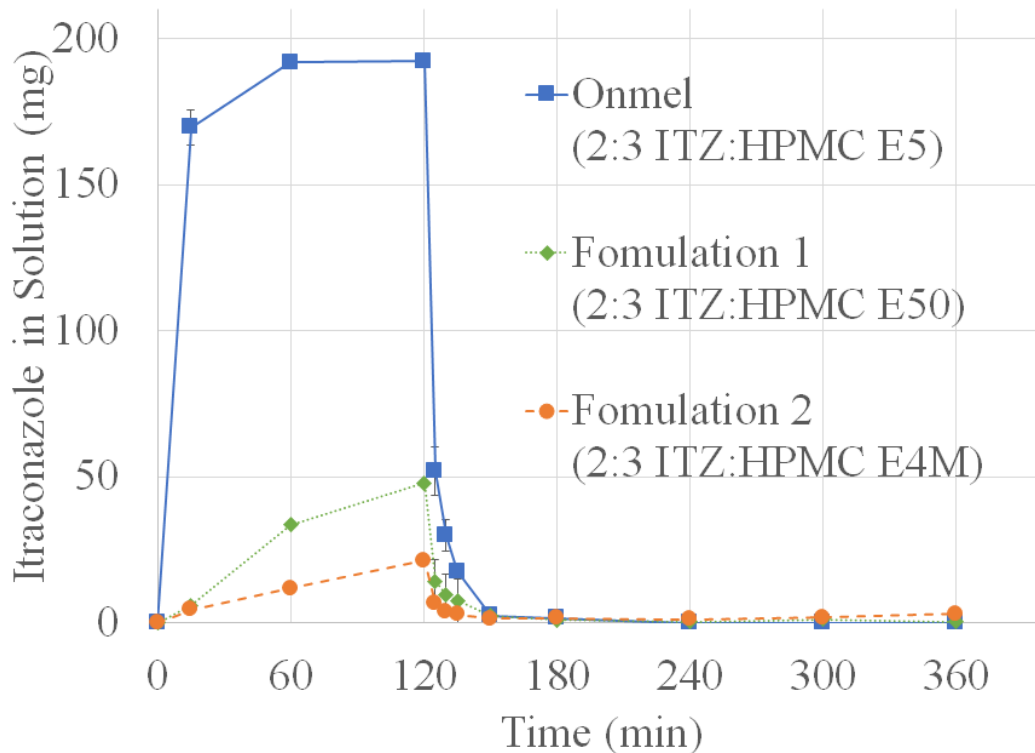


Figure 5.4 *In vitro* release profiles of non-disintegrating tablets containing viscous ITZ solid dispersions. USP Apparatus II 750 ml of 0.1 N HCL for 2 hours and 4 hours in 1000 pH 6.8 phosphate buffer at 37 °C, 100 rpm n=3.

Analysis of the tablet composition and properties yielded several possible explanations for the poor performance of Formulations 1 and 2. The tablets were compressed at a low compression force, which yields a low density compact (Denny, 2002). The low density of the superstructure may have negated the action of the included super-disintegrant, which acts to wick water into the dosage form and swells to break apart the tablet (Augsburger et al., 2006). Disintegrant effectiveness is known to improve with increasing compaction of powders in two-piece hard gelatin capsules (Botzolakis and Augsburger, 1984). Furthermore, high concentrations of super-disintegrants (>5%)

are not recommended by chemical manufacturers due to tendencies to gel. Based on these reasons, subsequent tablets compositions, Formulations 3-6 were compressed at a higher compression force and the super-disintegrant allotment of the composition was split between crospovidone and croscarmellose sodium. Croscarmellose sodium was selected due to its comparatively large swelling capability versus crospovidone.

Analysis of the tablet composition and properties should also include a discussion of the particle size distribution (PSD) and distribution of lubricants. Initially, a small and narrow PSD, 75  $\mu\text{m}$  to 150  $\mu\text{m}$ , was selected to formulate tablets. This distribution, compared to a large PSD, would have a larger surface area. A reduction of this surface area would decrease the magnitude of solid dispersion particle to particle contacts. It is known that the compressibility index of HPMC decreases with decreasing particle size (Malamataris et al., 1994). Furthermore, a decrease in the surface area while maintaining the lubricant levels may decrease the tensile strength of tablets while maintaining a desirable compact density (Pingali et al., 2011). To this end, it was desirable to increase the PSD and intentionally over blend the lubricants with the viscous KSD dispersions to allow for densification of the compact at a reduced tensile strength.

Based on the above rational, Formulations 3 and 4 were prepared at a higher compression force, one-half of the crospovidone was replaced with croscarmellose sodium, the PSD was modified to include the larger 150  $\mu\text{m}$  to 250  $\mu\text{m}$  fraction and the lubricants/glidants were included in the main blending steps. Formulations 5 and 6 were selected to investigate the impact of an effervescent salt on dissolution of HPMC. Hughey et al. (2013) reported this approach for rapid dissolution of Soluplus based solid dispersion compacts. The use of ions, particularly the anion, to manipulate the sol-gel

transition was demonstrated to improve dissolution. Additional improvement was realized when the ionic strength modifier was potassium bicarbonate, which releases carbon dioxide gas in the presence of acid, the volume expansion upon gas generation also acts to disintegrate the tablet. The anions evaluated for Soluplus were observed to generally follow the trend predicted by the Hofmeister series, the relevance of which is discussed later. Although the carbonate ion was not specifically evaluated, the cloud point of HPMC is also lowered consistently with the Hofmeister series (Joshi, 2011). Based on these investigations, potassium bicarbonate was added to Formulations 5 and 6 to generate disintegrating tablets.

Formulations 5 and 6 were observed to completely disintegrate in < 10 minutes. Based on visual observations, Formulations 3 and 4 disintegrated more significantly over the 20 minute observational period than Formulations 1 and 2 did, yet a viscous mass was still formed in the apparatus. The dissolution results from the pH change method are presented in Figure 5.5. The culmination of the changes made to the tablets produced the desired results. Tablets from Formulations 3 and 4 were observed to slowly erode, and exhibited controlled release in acid with substantial improvement of supersaturation in neutral media following pH change. Furthermore, inclusion of potassium bicarbonate produces visually effervescent tablets that rapidly disintegrated in the dissolution vessel. The resulting dissolution profiles for Formulations 5 and 6 resulted in greater than 75% release for both E50 and E4M viscous dispersions by 15 minutes. In addition, Formulation 6 exhibited the greatest area under the dissolution curve (AUDC) in neutral media, tabulated for all compositions in Table 5.3. The neutral phase AUDC was substantially improved versus Onmel for Formulations 3, 4, 5 and 6.

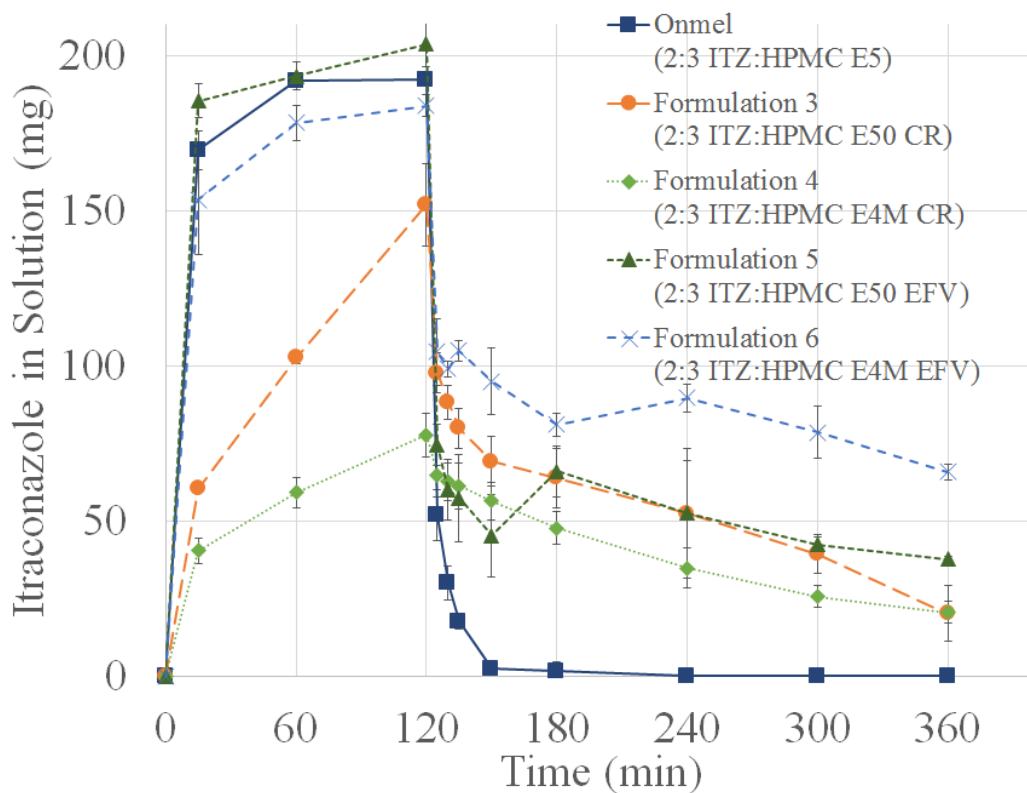


Figure 5.5 *In vitro* release profiles of slow and rapidly disintegrating tablets containing viscous ITZ solid dispersions. USP Apparatus II 750 ml of 0.1 N HCL for 2 hours and 4 hours in 1000 pH 6.8 phosphate buffer at 37 °C, 100 rpm n=3.

Table 5.3 Area under the dissolution curves for ITZ solid dispersion containing tablet compositions, n=3.

<b>Formulation</b>	<b>AUDC Acid (mg min)</b>	<b>AUDC Neutral (mg min)</b>	<b>AUDC Total (mg min)</b>	<b>AUDC pH Dilution (µg min/ml)</b>
Formulation 1 (E50)	2.6 ± 0.1	21.4 ± 8.1	24.1 ± 8.1	
Formulation 2 (E4M)	1.2 ± 0.1	9.6 ± 0.5	10.8 ± 0.6	
Formulation 3 (E50 CR)	314.9 ± 15.3	510.6 ± 72.6	825.5 ± 87.9	237.1 ± 32.9
Formulation 4 (E4M CR)	177.2 ± 16.1	374.1 ± 45.2	551.3 ± 61.3	173.0 ± 32.0
Formulation 5 (E50 EFV)	582.5 ± 17.3	435.9 ± 72.7	1018.4 ± 90.0	
Formulation 6 (E4M EFV)	515.6 ± 26.8	718.6 ± 46.4	1234.2 ± 73.2	693.1 ± 140.5
Onmel	25.7 ± 0.6	76.2 ± 5.7	101.9 ± 6.3	

While disintegration is an important step in the drug release process of immediate release dosage forms, drug release from HPMC containing tablets may occur by erosion (Conti et al., 2007) or a combination of erosion or diffusion (Lee, 2011). Provided that water does not rapidly penetrate the tablet and create a supersaturated micro environment amenable to drug recrystallization, eroding systems may be desirable for poorly water soluble drugs to promote drug absorption in the later stages of the intestinal tract (Tanaka et al., 2006). The potential benefits of and strategies for such systems were recently reviewed by (Tran et al., 2011). In order to better understand the dissolution of the

formulations demonstrating a controlled acid phase release, a dissolution methodology more closely mimicking gastrointestinal transit was desired. The previously employed pH-change method provides valuable insight into the mechanisms of release and factors improving precipitation inhibition in neutral media, there are several differences from the GIT that could be improved: 1) the volume of the acid phase (750 ml) is too large, 2) the media does not effectively simulate bile due to lack of phospholipids and bile salts, 3) the pH change is too abrupt and 4) there is no donor compartment to simulate absorption of the drug.

The pH-dilution model, the rationale for which is clearly described by Gao et al. (Gao et al., 2010), was selected to more closely mimic the gastrointestinal conditions. Briefly, the method utilizes a starting volume of 30 mL at pH 2, which is then diluted with fasted simulated intestinal fluid (FaSSIF) (Galia et al., 1998) in small increments over the period of hours, with the initial neutralization occurring at 30 min. This method was scaled to simulate a large animal species and a lower centrifugal force was utilized to accommodate available instrumentation. This methodology addresses several of the limitations of the pH-change methodology. While this method does not employ a donor compartment, the results are still of interest and are reported in Figure 5.6. A comparison of the controlled release formulations indicates that the E50 composition (Formulation 3) is more effective and supersaturating ITZ in small volumes than the equivalent E4M composition (Formulation 4).

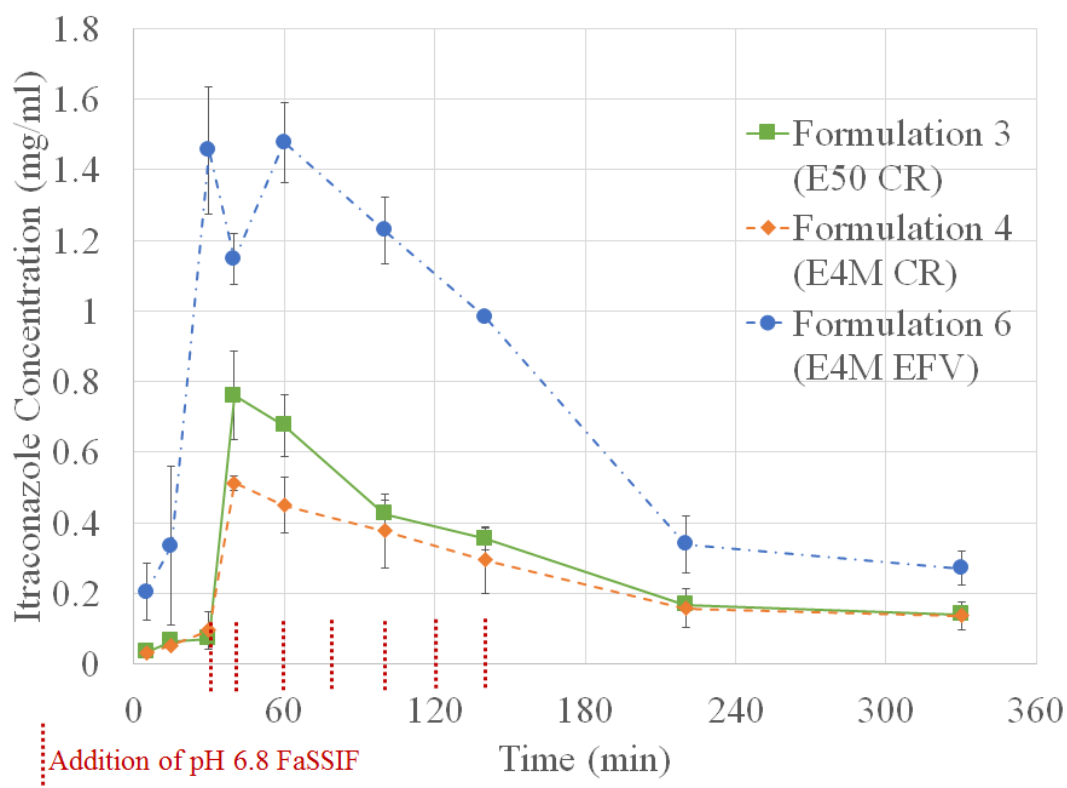


Figure 5.6 Small volume pH dilution model. *In vitro* release profiles of 200 mg ITZ tablets containing viscous solid dispersions. Initial conditions 30 ml pH 2 HCl at 37 °C, rotated at 100 rpm in an orbital shaker.

Formulation 6, the E4M effervescent immediate release composition was also evaluated by the pH-dilution model. An interesting observation was made starting at the 30 min time point for this formulation. Following centrifugation for 2 min at 18,000 RCF, suspended particles were still apparent. Samples from time points for all the formulations were observed to produce milky suspensions. However, suspended species from Formulation 6 were not removed by the centrifugation process to the extent that was observed for Formulations 3 and 4, which appeared clear post centrifugation. Prior to centrifugation, media samples from all compositions appeared to be milky

white. According to Stokes law, these results indicate the suspended species in the presence of potassium bicarbonate were smaller. When diluted with acetonitrile, these centrifuged samples went clear. Viscosity contributions in the media were immediately ruled out as Formulations 3 and 4 did not completely liberate HPMC and were assessed during sample collection as less viscous than Formulation 6.

Centrifugation is a known alternative to filtration in removing particulates during non-sink dissolution analysis. Curatolo et al. (2009) reported methodologies utilized to screen a variety of drug candidates that included combinations of filtration and centrifugation to separate different species. Drug polymer species generated from amorphous solid dispersions are poorly understood in the literature, although Freisen et al. (Friesen et al., 2008) present an interesting discussion on the topic. The formation of nano/micro-dispersions during dissolution of a marketed extruded dispersion of ritanovir has also been reported (Tho et al., 2010). In this case, the evidence suggests that the carbonate anion is inducing a particle size and/or otherwise altering the nature of the drug/polymer/bile species that is formed during dissolution. While the Hofmeister series is well known for over 120 years, and the impact of the anion on HPMC cloud point was predicted, the mechanisms of action is still debated. Of particular interest are recent research linking the effects of anions from the Hofmeister series directly to interactions between ions and macromolecules (Zhang and Cremer, 2006). This treatment supports the observation that the suspended species may be altered by the presence of a Hofmeister ion.

A comparison of Formulations 4 and 6 based on the pH-dilution method is complicated by the observation that different size species were generated, likely due to

the presence of a strong Hofmeister anion. The free drug concentration is unknown based on the present sample handling procedure. Nevertheless, it is unlikely that only free drug is bioavailable. This is corroborated by the ritanovir results, which reports the formation of colloidal species (Tho et al., 2010). While the pH-dilution method, with samples centrifuged at 18,000 RCF, provides valuable information that can be used to narrow candidates, inevitably, an *in vivo* analysis is warranted.

#### **5.4.3 *In Vivo* Analysis in Beagle Dogs**

Based on the previous presented results, Formulations 3 and 6 were chosen for evaluation in the Beagle dog model. These formulations would evaluate the utility of a controlled release viscous solid dispersion and a more viscous immediate release solid dispersion in the presence a strong Hofmeister anion. Prior to discussing the results, some brief statements on rational for the study design are warranted. ITZ is known to have over 30 metabolites, with the major active metabolite being hydroxyitraconazole (Yoo et al., 2002). A review of pharmacokinetic (pK) reports for itraconazole in Beagle dogs and humans indicated that this metabolite closely followed the parent compound plasma concentration and therefore was not primary to understanding the absorption of itraconazole (Yoo et al., 2002, Six et al., 2005, Mellaerts et al., 2008). Individual beagle dogs are genetically similar to other individuals due to selective breeding and thus more amenable to direct comparison than humans. In addition, due to the lipophilicity of ITZ, the wash out period makes it difficult to minimize the time the dog is withheld from the colony in a three –way cross-over design. As such, a cross-over study was not chosen to evaluate the compositions. Finally, an acid flush was utilized to provide the dosage form with a starting acid pH vs pre-treatment with pentagastrin. The effects of pentagastrin

may last several hours, which would negate discrimination of formulations based on precipitation tendency at neutral pH (Akimoto et al., 2000).

The plasma concentration profiles of ITZ following oral administration of 200 mg ITZ containing tablets prepared as Formulations 3 and 6 are presented in Figure 5.7 along with the plasma concentration profile of the commercially marked control formulation, Onmel. Evaluation of the average curves up to 3 hr indicate that both viscous dispersions prolonged the absorption of itraconazole compared to Onmel. Further evidence of prolonged absorption phase is the location of the slope change between 4 and 24 hours for the viscous dispersions, which occurs later than Onmel and can be explained by prolonged distribution of the drug.

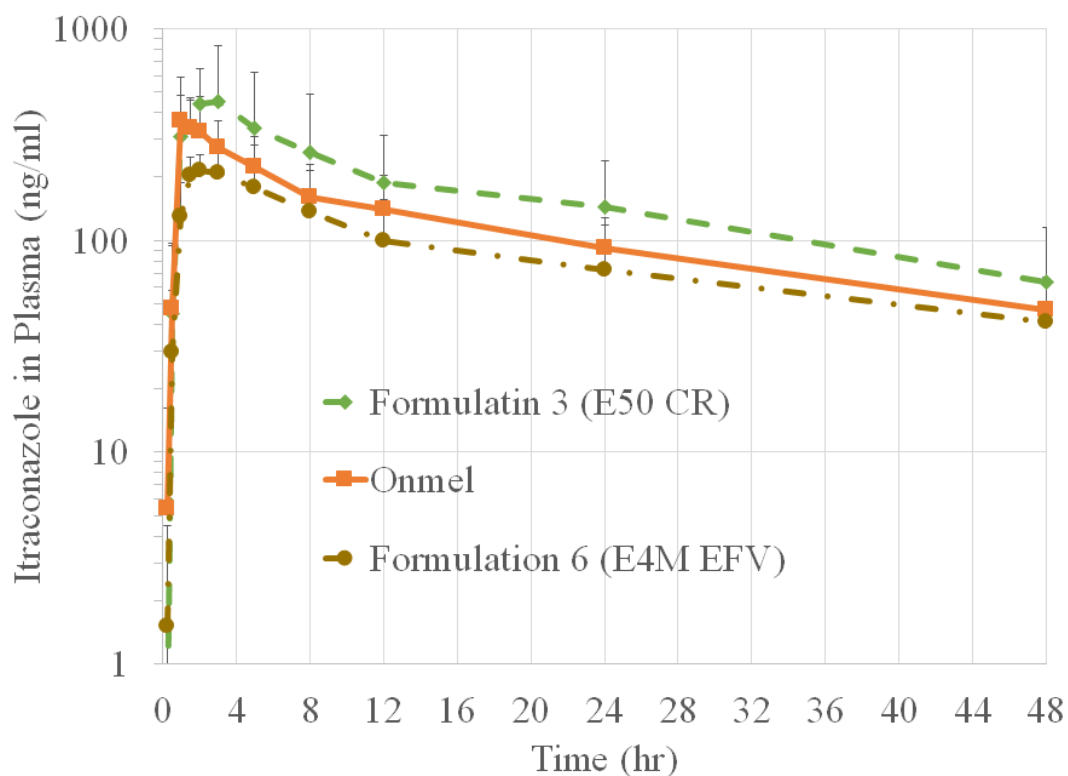


Figure 5.7 *In vivo* plasma concentrations of ITZ following oral administration of tablets in beagle dogs, n=4 dose = 200 mg ITZ.

Selected pharmacokinetic parameters for the three cohorts are summarized in Table 5.4. Analysis of variance indicate that the results are not statistically significant and confirms the hypothesis that viscous solid dispersions can be formulated into tablets for bioavailability enhancement. The  $T_{max}$ ,  $C_{max}$  and AUC results contradict the predictions from the *in vitro* methodologies. It is plausible that the pH-change methodology over predicts the AUC of Formulation 6 due to volume effects. The volume of media required to completely disintegrate the tablet as observed in the pH-change methodology is much higher than that in the dog, this is corroborated by the slower release profile observed in acid by the small volume pH-dilution method.

Furthermore, pH-dilution methodology, which employed centrifugation at 18,000 RCF, most likely did not separate the bio relevant species formed by the dispersion in the presence of the Hofmeister anion. However, the variability of Cmax for Formulation 6 was noted to be reduced in comparison with the other cohorts.

The weakly basic drug, ritonavir, which is also marketed as an extruded solid dispersion, including innovator and several generic solid formulations, was reviewed to investigate the suitability of the dog as a preclinical model for bioequivalence in humans (Garren et al., 2010). The results indicated that the dog may occasionally over predict bioequivalence in humans. Alternatively, when the dog model predicted poor bioavailability (F <60), human bioavailability was also poor. If these results can be extrapolated to ITZ, which is not guaranteed, the results established collected in this study would not exclude either formulation from evaluation in an appropriately powered human bioequivalence study.

Table 5.4 Pharmacokinetic parameters for ITZ solid dispersion containing tablet compositions following oral administration to beagle dogs, n=4.

<b>Formulation</b>	<b>Cmax (ng/ml)</b>	<b>Tmax (hr)</b>	<b>AUC<sub>0-48</sub> (ng hr/ml)</b>	<b>F (%)</b>
Formulation 3 (E50 CR)	561 ± 331	1.75 ± 0.96	7968 ± 5537	146
Formulation 6 (E4M EFV)	244 ± 62	2.88 ± 1.55	4165 ± 2166	76
Onmel (E5)	406 ± 193	1.63 ± 0.95	5470 ± 2213	-

## 5.5 CONCLUSIONS

Viscous ITZ solid dispersions prepared from high molecular weight HPMC were successfully prepared into tablets exhibiting supersaturated concentrations of ITZ at basic pH for physiologically relevant time periods. The release rate from tablets could be adjusted for controlled or immediate release through the manipulation of compression adjuvants while maintaining supersaturation maintenance in release media, which was greatly improved compared to the commercial control. Manipulation of the cloud point of HPMC through the addition of anionic species to the formulation was observed to alter the size of the suspended species produced upon dissolution of the formulation. When administered to dogs, the KSD compositions enhanced bioavailability similar to the commercially extruded control, yet the tablets have properties desirable for stability and controlled release applications.

## 5.6 REFERENCES

Akimoto M, Nagahata N, Furuya A, Fukushima K, Higuchi S, and Suwa T (2000) Gastric pH profiles of beagle dogs and their use as an alternative to human testing. *European Journal of Pharmaceutics & Biopharmaceutics* **49**, 99-102.

Alonzo DE, Gao Y, Zhou D, Mo H, Zhang GGZ, and Taylor LS (2011) Dissolution and precipitation behavior of amorphous solid dispersions. *Journal of Pharmaceutical Sciences* **100**, 3316-31.

Augsburger LL, Brzeczko AW, Shah U, and Hahm HA (2006) Super Disintegrants: Characterization and Function. In *Encyclopedia of Pharmaceutical Technology*. Vol. 1, pp. 3553-67.

Baert L, Verreck G, and Thone D (2003) Antifungal Compositions with Improved Bioavailability. US6509038B2.

Baert L, Verreck G, and Thone D (2006) Antifungal Compositions with Improved Bioavailability. US7081255B2.

Berndl G, Degenhardt M, Maegerlein M, and Dispersyn G (2013) Itraconazole Compositions with Improved Bioavailability. US8486456B2.

Botzolakis JE and Augsburger LL (1984) The role of disintegrants in hard-gelatin capsules. *Journal of Pharmacy & Pharmacology* **36**, 77-84.

Broadhead J, Edmond Rouan SK, and Rhodes CT (1992) The spray drying of pharmaceuticals. *Drug Development & Industrial Pharmacy* **18**, 1169-206.

Chiou WL and Riegelman S (1971) Pharmaceutical applications of solid dispersion systems. *Journal of Pharmaceutical Sciences* **60**, 1281-302.

Conti S, Maggi L, Segale L, Ochoa Machiste E, Conte U, Grenier P et al. (2007) Matrices containing NaCMC and HPMC: 1. Dissolution performance characterization. *International Journal of Pharmaceutics* **333**, 136-42.

Curatolo W, Nightingale J, and Herbig S (2009) Utility of Hydroxypropylmethylcellulose Acetate Succinate (HPMCAS) for Initiation and Maintenance of Drug Supersaturation in the GI Milieu. *Pharmaceutical Research* **26**, 1419-31.

Denny PJ (2002) Compaction equations: a comparison of the Heckel and Kawakita equations. *Powder Technology* **127**, 162-72.

DiNunzio JC, Brough C, Hughey JR, Miller DA, Williams Iii RO, and McGinity JW (2010a) Fusion production of solid dispersions containing a heat-sensitive active ingredient by hot melt extrusion and Kinetisol® dispersing. *European Journal of Pharmaceutics & Biopharmaceutics* **74**, 340-51.

DiNunzio JC, Brough C, Miller DA, Williams RO, and McGinity JW (2010c) Fusion processing of itraconazole solid dispersions by kinetisol® dispersing: A comparative study to hot melt extrusion. *Journal of Pharmaceutical Sciences* **99**, 1239-53.

DiNunzio JC, Miller DA, Yang W, McGinity JW, and Williams RO (2008) Amorphous Compositions Using Concentration Enhancing Polymers for Improved Bioavailability of Itraconazole. *Molecular Pharmaceutics* **5**, 968-80.

Fox TG and Flory PJ (1950) Second-Order Transition Temperatures and Related Properties of Polystyrene. I. Influence of Molecular Weight. *Journal of Applied Physics* **21**, 581-91.

Francois M, Snoeckx E, Putteman P, Wouters F, De Proost E, Delaet U et al. (2003) A mucoadhesive, cyclodextrin-based vaginal cream formulation of itraconazole. *The AAPS Journal* **5**, 50-4.

Friesen DT, Shanker R, Crew M, Smithey DT, Curatolo WJ, and Nightingale JAS (2008) Hydroxypropyl Methylcellulose Acetate Succinate-Based Spray-Dried Dispersions: An Overview. *Molecular Pharmaceutics* **5**, 1003-19.

Galia E, Nicolaides E, Hörter D, Löbenberg R, Reppas C, and Dressman JB (1998) Evaluation of Various Dissolution Media for Predicting In Vivo Performance of Class I and II Drugs. *Pharmaceutical Research* **15**, 698-705.

Gao Y, Carr RA, Spence JK, Wang WW, Turner TM, Lipari JM et al. (2010) A pH-Dilution Method for Estimation of Biorelevant Drug Solubility along the Gastrointestinal Tract: Application to Physiologically Based Pharmacokinetic Modeling. *Molecular Pharmaceutics* **7**, 1516-26.

Garren KW, Rahim S, Marsh K, and Morris JB (2010) Bioavailability of generic ritonavir and lopinavir/ritonavir tablet products in a dog model. *Journal of Pharmaceutical Sciences* **99**, 626-31.

Gibbs JH and DiMarzio EA (1958) Nature of the Glass Transition and the Glassy State. *The Journal of Chemical Physics* **28**, 373-83.

Hancock BC, Shamblin SL, and Zografi G (1995) Molecular Mobility of Amorphous Pharmaceutical Solids Below Their Glass Transition Temperatures. *Pharmaceutical Research* **12**, 799-806.

Hoeben BJ, Burgess DS, McConville JT, Najvar LK, Talbert RL, Peters JI et al. (2006) In Vivo Efficacy of Aerosolized Nanostructured Itraconazole Formulations for Prevention of Invasive Pulmonary Aspergillosis. *Antimicrobial Agents & Chemotherapy* **50**, 1552-4.

Hughey J, DiNunzio J, Bennett R, Brough C, Miller D, Ma H et al. (2010) Dissolution Enhancement of a Drug Exhibiting Thermal and Acidic Decomposition Characteristics by Fusion Processing: A Comparative Study of Hot Melt Extrusion and KinetiSol® Dispersing. *AAPS PharmSciTech* **11**, 760-74.

Hughey JR, Keen JM, Brough C, Saeger S, and McGinity JW (2011) Thermal processing of a poorly water-soluble drug substance exhibiting a high melting point: The utility of KinetiSol® Dispersing. *International Journal of Pharmaceutics* **419**, 222-30.

Hughey JR, Keen JM, Miller DA, Brough C, and McGinity JW (2012) Preparation of Viscous Solid Dispersion Systems by Hot-Melt Extrusion and KinetiSol® Dispersing: Polymer Screening and Thermal Stability. *International Journal of Pharmaceutics* **438**, 11-9.

Hughey JR, Keen JM, Miller DA, Kolter K, Langley N, and McGinity JW (2013) The use of inorganic salts to improve the dissolution characteristics of tablets containing Soluplus®-based solid dispersions. *European Journal of Pharmaceutical Sciences* **48**, 758-66.

Janssens S and Van den Mooter G (2009) Review: physical chemistry of solid dispersions. *Journal of Pharmacy & Pharmacology* **61**, 1571-86.

Joshi SC (2011) Sol-Gel Behavior of Hydroxypropyl Methylcellulose (HPMC) in Ionic Media Including Drug Release. *Materials* **4**, 1861-905.

Keary CM (2001) Characterization of METHOCEL cellulose ethers by aqueous SEC with multiple detectors. *Carbohydrate Polymers* **45**, 293-303.

Keseru GM and Makara GM (2009) The influence of lead discovery strategies on the properties of drug candidates. *Nature Reviews. Drug Discovery* **8**, 203-12.

Kolter K, Karl M, Nalawade S, and Rottmann N (2010) Hot-Melt Extrusion with BASF Pharma Polymers: Extrusion Compendium. In BASF (ed.), (ed.), Vol. pp. Ludwigshafen, Germany.

Lee PI (2011) Modeling of drug release from matrix systems involving moving boundaries: Approximate analytical solutions. *International Journal of Pharmaceutics* **418**, 18-27.

Malamataris S, Karidas T, and Goidas P (1994) Effect of particle size and sorbed moisture on the compression behaviour of some hydroxypropyl methylcellulose (HPMC) polymers. *International Journal of Pharmaceutics* **103**, 205-15.

Mellaerts R, Mols R, Jammaer JAG, Aerts CA, Annaert P, Van Humbeeck J et al. (2008) Increasing the oral bioavailability of the poorly water soluble drug itraconazole with ordered mesoporous silica. *European Journal of Pharmaceutics & Biopharmaceutics* **69**, 223-30.

Miller D, DiNunzio J, Yang W, McGinity J, and Williams R (2008a) Targeted Intestinal Delivery of Supersaturated Itraconazole for Improved Oral Absorption. *Pharmaceutical Research* **25**, 1450-9.

Miller DA, DiNunzio JC, Yang W, McGinity JW, and Williams RO (2008b) Enhanced In Vivo Absorption of Itraconazole via Stabilization of Supersaturation Following Acidic-to-Neutral pH Transition. *Drug Development & Industrial Pharmacy* **34**, 890-902.

Pingali K, Mendez R, Lewis D, Michniak-Kohn B, Cuitino A, and Muzzio F (2011) Mixing order of glidant and lubricant – Influence on powder and tablet properties. *International Journal of Pharmaceutics* **409**, 269-77.

Repka MA, Majumdar S, Kumar Battu S, Srirangam R, and Upadhye SB (2008) Applications of hot-melt extrusion for drug delivery. *Expert Opinion on Drug Delivery* **5**, 1357-76.

Sekiguchi K, Obi N, and Ueda Y (1964) Studies on Absorption of Eutectic Mixture. II. Absorption of fused Conglomerates of Chloramphenicol and Urea in Rabbits. *Chemical & Pharmaceutical Bulletin* **12**, 134-44.

Six K, Daems T, de Hoon J, Van Hecken A, Depre M, Bouche M-P et al. (2005) Clinical study of solid dispersions of itraconazole prepared by hot-stage extrusion. *European Journal of Pharmaceutical Sciences* **24**, 179-86.

Six K, Verreck G, Peeters J, Augustijns P, Kinget R, and Van den Mooter G (2001) Characterization of glassy itraconazole: a comparative study of its molecular mobility below T<sub>g</sub> with that of structural analogues using MTDSC. *International Journal of Pharmaceutics* **213**, 163-73.

Srinarong P, Faber JH, Visser MR, Hinrichs WLJ, and Frijlink HW (2009) Strongly enhanced dissolution rate of fenofibrate solid dispersion tablets by incorporation of superdisintegrants. *European Journal of Pharmaceutics & Biopharmaceutics* **73**, 154-61.

Tanaka N, Imai K, Okimoto K, Ueda S, Tokunaga Y, Ibuki R et al. (2006) Development of novel sustained-release system, disintegration-controlled matrix tablet (DCMT) with solid dispersion granules of nilvadipine (II): In vivo evaluation. *Journal of Controlled Release* **112**, 51-6.

Tho I, Liepold B, Rosenberg J, Maegerlein M, Brandl M, and Fricker G (2010) Formation of nano/micro-dispersions with improved dissolution properties upon dispersion of ritonavir melt extrudate in aqueous media. *European Journal of Pharmaceutical Sciences* **40**, 25-32.

Tran P, Tran T, Park J, and Lee B-J (2011) Controlled Release Systems Containing Solid Dispersions: Strategies and Mechanisms. *Pharmaceutical Research* **28**, 2353-78.

Van den Mooter G (2012) The use of amorphous solid dispersions: A formulation strategy to overcome poor solubility and dissolution rate. *Drug Discovery Today: Technologies* **9**, e79-e85.

Vaughn JM, McConville JT, Burgess D, Peters JI, Johnston KP, Talbert RL et al. (2006) Single dose and multiple dose studies of itraconazole nanoparticles. *European Journal of Pharmaceutics & Biopharmaceutics* **63**, 95-102.

Yoo S, Kang E, Shin B, Jun H, Lee S-H, Lee K et al. (2002) Interspecies comparison of the oral absorption of itraconazole in laboratory animals. *Archives of Pharmacal Research* **25**, 387-91.

Zhang Y and Cremer PS (2006) Interactions between macromolecules and ions: the Hofmeister series. *Current Opinion in Chemical Biology* **10**, 658-63.

## **Chapter 6: Continuous Twin Screw Melt Granulation of Glyceryl Behenate: Evaluation of Critical Process Parameters and Development of Controlled Release Tramadol Hydrochloride Tablets for Improved Safety**

### **6.1 ABSTRACT**

Interest in granulation processes using twin screw extrusion machines is rapidly growing. The primary objectives of this study were to investigate the critical processing parameters for direct production of granules using this technique with glyceryl behenate as a binder, evaluate the properties of the resulting granules and develop controlled release tablets containing tramadol HCl. In addition, the granulation mechanism was probed and the polymorphic form of the lipid and drug release rate were evaluated on stability. Granules were prepared using a Leistritz NANO16 twin screw extruder operated without a constricting die. The solid state of the granules were characterized by differential scanning calorimetry and X-ray diffraction. Formulated tablets were studied in 0.1N HCl containing 0-40% ethanol to investigate propensity for alcohol induced dose dumping. The extrusion barrel temperature profile and feed rate were determined to be the primary factors influencing the particle size distribution. Granules were formed by a combination immersion/distribution mechanism, did not require subsequent milling, and were observed to contain desirable polymorphic forms of glyceryl behenate. Drug release from tablets was complete and controlled over 16 hours and the tablets were determined to be resistant to alcohol induced dose dumping. Following 3 months at 40°C and 75% relative humidity, no specific trends were observed for the drug release rate from tablets.

## 6.2 INTRODUCTION

Historically, pharmaceutical processes have been developed as batch unit operations, requiring batch specific release. A current industrial trend is to adapt or replace these batch processes with continuous processes, which corresponds to a changing regulatory environment (Plumb, 2005). The Food and Drug Administration's (FDA) question based review (QbR) is a shift in quality assessment focusing on critical quality attributes (CQAs) and quality by design (QbD) (Yu, 2008), which requires development and understanding of the formulation and process design space (Lionberger et al., 2008). This shift de-emphasizes the application of pharmaceutical batch operations and post-processing characterization and emphasizes the development of process analytical technologies (PAT) amenable to continuous processing and real-time release testing (Read et al., 2010). In addition to compliance with regulatory approaches and improved quality understanding, continuous processes have been demonstrated as a cost effective alternative to batch processing (Schaber et al., 2011).

Granulation, most broadly defined as a powder agglomeration, is applied in numerous pharmaceutical products for a variety of reasons, e.g. to facilitate compression (Lakshman et al., 2011), improve flow (Danish and Parrott, 1971), uniformity (Wan et al., 1992), and to enhance (Yang et al., 2007) or control (Ochoa et al., 2010) dissolution. Batch granulation processes may require complex analysis to scale up (Faure et al., 2001), suffer from variability (Sochon et al., 2010) and may require large investments in equipment. Continuous granulation processes are already known (Vervaeet and Remon, 2005) and reports focus on the application of twin-screw extruders operating without a die (Akiyama et al., 1995, Djuric and Kleinebudde, 2010, Dhenge et al., 2011, Lakshman

et al., 2011, Vasanthavada et al., 2011, Mu and Thompson, 2012). It is notable that the majority of these reports focus on the use of thermoplastic binders.

Commonly, continuous granulation binders are polymeric, which are suitable for wet or melt granulation. The range of polymers suitable for continuous melt granulation is still being explored. The majority of reports utilizing the twin screw extruder for continuous granulation describe wet granulation. Recent continuous melt granulation reports have employed polyethylene glycol (Van Melkebeke et al., 2006, Mu and Thompson, 2012) or the cellulose hydroxypropyl methylcellulose and hydroxypropyl cellulose (Vasanthavada et al., 2011). However, polymeric binders may be undesirable if the granulation process is developed for modified or controlled release applications due to solubility in ethanol and susceptibility to dose dumping in hydroalcoholic media (Fadda et al., 2008). Lipids, which are insoluble in ethanol, can be employed for modified and controlled release applications as a safer alternative. Continuous melt processes have been previously demonstrated to produce controlled release matrices. However, they require either downstream grinding (Liu et al., 2001) or specialized equipment for handling of liquid extrudate (Lo et al., 2009). The continuous production of granules, suitable for continuous blending/compression and for sustained release from a lipid matrix has not previously been demonstrated. At the binder concentrations required for sustained release, these low melting point binders tend to form a paste or a liquid.

The objective of this study was to develop a continuous granulation process for tramadol hydrochloride and glyceryl behenate (C888), which directly results in granules suitable for blending and compression. Tramadol hydrochloride is an analgesic that is

currently marketed as an oral controlled release dosage form. The FDA has issued a draft guidance requiring any new controlled release tramadol hydrochloride products be tested for propensity of dose dumping (FDA, 2007). In addition to conversion of the prepared granules into tablets having a safe hydroalcoholic dissolution profile, the granulation and drug release mechanisms were investigated. Finally, the stability of the polymorphic form was evaluated along with drug release following 3 months of storage at 40 °C, 75% relative humidity conditions.

### **6.3 MATERIALS AND METHODS**

#### **6.3.1 Materials**

Glyceryl behenate, Compritol® 888 ATO (C888), was kindly donated by Gattefossé (Saint Priest, France). Tramadol hydrochloride was purchased from Letco Medical (Decatur, AL). Microcrystalline cellulose (Avicel PH-102) donated by FMC Biopolymer (Philadelphia, PA). Magnesium stearate, USP/NF was purchased from Spectrum Chemicals Corporation (Gardena, CA). Spray dried lactose (Fast Flow 316) was donated by Foremost Farms (Baraboo, WI). Dicalcium phosphate (Emcompress®) was donated by JRS Pharma (Rosenberg, Germany). 40cc high density polyethylene (HDPE) packer white, boston round bottles and 33-400 P/P closures with Hs035 induction sealable liners were purchased from Tricorbraun (St. Louis, MO). Analytical reagents of ACS grade or higher were purchased from Fisher Scientific (Pittsburg, PA).

## **6.3.2 Methods**

### ***6.3.2.1 Milling***

The tramadol hydrochloride as received contained a substantial fraction of particles greater than 250  $\mu\text{m}$ . Prior to granulation, tramadol hydrochloride was milled using a Fitzmill Laboratory L1A (Fitzpatrick Inc., Elmhurst, IN) operating at 9000 rpm, knives forward, using a 0.020 in screen. The fraction less than 100  $\mu\text{m}$  was collected for further processing and analysis.

### ***6.3.2.2 Continuous Twin Screw Granulation***

Continuous granulation was performed using a NANO16 20:1 L:D 16 mm twin screw extruder (Liestritz, Somerville, NJ) operating at 200 rpm. The feeding zone was maintained at approximately 25 °C using recirculating ambient water. The subsequent control zones (Zone-1, Zone-2, Zone-3 and Endplate) and feed rate were adjusted to control the granulation process. Materials were manually pre-blended in polyethylene bags and charged to a Model 102M screw feeder (Schenck AccuRate Inc., Whitewater, WI). As needed, the material was manually agitated in the hopper to prevent bridging and maintain a constant flow rate. For all experiments, the extruder was operated without a die or transfer plate.

### ***6.3.2.3 Melt Mixing Granulation***

C888 was added to a beaker and melted at 80 °C on a hot plate with the aid of a stir bar. When molten, tramadol hydrochloride was added to disperse. The mixture was

then poured onto a glass plate to cool and solidify. The solidified dispersion was then manually ground through a No. 20 mesh sieve for further processing and analysis.

#### ***6.3.2.4 Blending and Compression***

Tramadol hydrochloride granules and a pore former were blended for 15 min in a P-K Blend Master V-Shell blender (Patterson-Kelley Co., East Stroudsburg, PA) followed by an additional 5 minutes of blending with the tableting lubricant, magnesium stearate. Individual portions of the blend were weighed and compressed into 11mm flat faced round tablets at 20 kN compression force using a Manual Tablet Compaction Machine (MTCM-1, Globe Pharma, Inc., New Brunswick, NJ).

#### ***6.3.2.5 Particle Size Characterization***

The granulation particle size distributions were determined by sieve analysis using a RX-24 Ro-Tap (W.S. Tyler Industrial Group, Mentor, OH). 25 g samples were agitated for 15 minutes using the following sieve mesh No.: 20, 30, 40, 60, 100, 230, Pan (850  $\mu\text{m}$ , 600  $\mu\text{m}$ , 425  $\mu\text{m}$ , 250  $\mu\text{m}$ , 150  $\mu\text{m}$ , 63  $\mu\text{m}$ , respectively). Each sieve was tarred prior to addition of the sample and the amount retained on each sieve was determined following agitation.

#### ***6.3.2.6 Scanning Electron Microscopy***

Granules were imaged using a Quanta 650 FEG scanning electron microscope (FEI company, Inc., Hillsboro, OR). Samples were analyzed under vacuum with the electron beam operating at 20 kV. Samples were distributed onto adhesive carbon tape

affixed to an aluminum stage. Samples were sputter coated with a 60/40 mixture of palladium/gold under argon for 30 seconds prior to imaging.

#### ***6.3.2.7 Thermal Analysis***

Differential scanning calorimetry (DSC) was performed on 6.0 mg  $\pm$  0.5 mg samples granules in crimped aluminum pans. The temperature range studied was from 30 °C to 230 °C with a ramp rate of 4 °C/min. A Model Q20 DSC (TA Instruments, New Castle, DE) was used for this analysis.

#### ***6.3.2.8 Powder X-Ray Diffraction***

An Equinox 100 standalone bench top X-ray diffractometer (INEL, Inc., Stratham NH) was used to analyze granules for polymorphic form. Samples were placed in an aluminum crucible and loaded in a rotating sample holder. Samples were analyzed for 300 seconds using a Cu K radiation source ( $\lambda = 1.5418 \text{ \AA}$ ) operating at 42 kV and 0.81 mA.

#### ***6.3.2.9 Sink Dissolution Analysis***

Dissolution analysis was performed using a VK7000 Dissolution Tester (Vankel Technology Group, Cary, NC) USP Type I apparatus operated with at VK8000 autosampler. The dissolution medium was 900 mL of 0.1 N HCl, optionally containing 5%, 20% or 40% v/v ethanol. Tablets or granules containing 100 mg of tramadol hydrochloride were studied at 75 rpm and 37 °C. 6 ml samples were collected with the timepoints varying based on the experiment. 300  $\mu$ L aliquots were quantitated in

triplicate at 271 nm using a MTZ-200 Plate UV-Vis plate reader (Biotek Instruments, Winooski, VT).

#### **6.3.2.10 Stability**

Stability studies were conducted on samples of granules and tablets at 40 °C and 75% relative humidity conditions. 15 g samples of granules or 6 tablets were dispensed into 40cc HDPE bottles and induction sealed for 4 sec using a Compak Jr Induction Cap Sealing System (Enercon Ind., Menomonee Falls) set to high. Packaged tablets were separated into two groups, with one group placed in an oven at 50 °C for 24 hours prior to being placed on stability. A sealed unopened bottle was collected and evaluated initially, at 2 weeks, 1 month, 2 months and 3 months.

### **6.4 RESULTS AND DISCUSSION**

#### **6.4.1 Continuous Granulation Process Development**

In preliminary studies, the lipid binder and release modifier, C888, was evaluated in binary mixtures with microcrystalline cellulose (MCC), which was included to serve as a model for crystalline drug. Avicel PH102 was selected due to the particle size similarity with hammer milled tramadol. These mixtures were processed through the extruder with all temperature control points set at 80 °C, above the melting temperature of C888. The particle size distributions of these experiments, data not shown, revealed some notable observations. First, the concentration of C888 in the binary blend that resulted produced substantial granule fractions in the range of 150 to 600 µm was narrow,

with a 25% C888 producing >30% fines (less than 63 $\mu$ m) and 40% C888 producing a paste.

Additionally, experiments with low binder concentrations, <25% C888, and MCC having a starting particle size fraction in the range of 150 to 250  $\mu$ m, resulted in granules that were smaller than the starting particle size. This indicated that friable particles might actually be milled by the action of the twin screws rotating in the barrel. This observation was surprising and resulted in a shift of the objectives. A hypothesis formed that it may be possible to stage the unit operations traversing the twin screw such that granulation, cooling, and sizing would occur prior to exiting the barrel.

In order to probe this possibility, tramadol hydrochloride and C888 blends were evaluated at a throughput rate of 7.5 g/min using the temperature profiles depicted in Figure 6.1a and tabulated in Table 6.1. A high concentration of binder, 85%, was selected for these studies to represent an extreme binder loading. Profile 1 served as a control with all control points along the barrel length adjusted to 80 °C, which was selected to be above the melting range of C888. This condition resulted in the formation of a paste, depicted in Figure 6.1c. Following 15 minutes agitation in the RoTap, greater than 60% of this composition was retained on a 20 mesh sieve, Figure 6.1b. Profiles 2 and 3 were selected to cool the granulation below the melting range of C888 at increasingly aggressive rates prior to discharge. As depicted in Figure 6.1d, granules flowed directly from the screws under these conditions. The particle size distribution of Profile 3 was of particular interest as >96% of the granules were observed to have a particle size between 63 and 850  $\mu$ m and 73% of the granules were between 150 and 600

$\mu\text{m}$ . Profile 3 represented a gradual temperature decrease from the initial melting zone, set at 80 °C, to discharge at 50 °C.

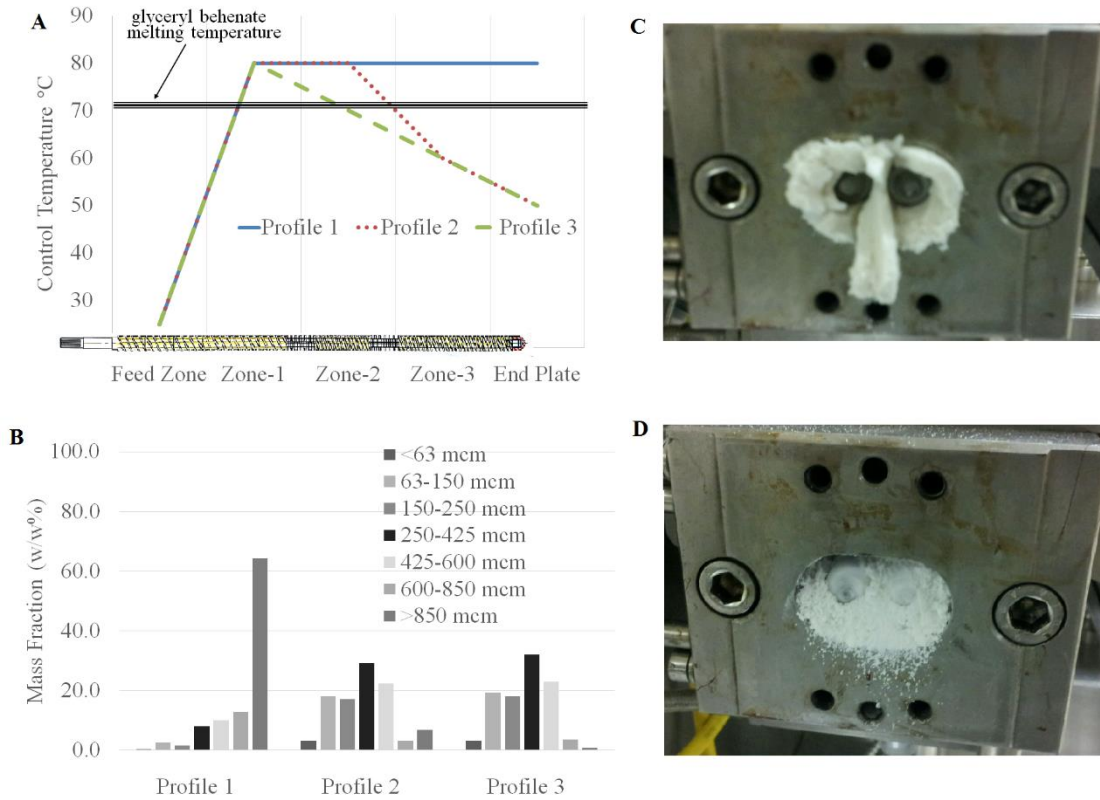


Figure 6.1 A) Continuous twin screw granulation temperatures encountered by the granulation while traversing the extruder barrel. B) Particle size distributions of granules produced at each temperature profile. C) Granulation output from temperature profile 1. D) Granulation output from temperature profile 3.

Table 6.1 Granulation temperature profiles used in the NANO16 twin screw extruder

<b>Zone</b>	<b>Profile 1 (°C)</b>	<b>Profile 2 (°C)</b>	<b>Profile 3 (°C)</b>
Feed Zone	~25	~25	~25
Zone-1	80	80	80
Zone-2	80	80	70
Zone-3	80	60	60
End Plate	80	50	50

While these experiments confirmed the potential utility of a decreasing barrel temperature profile for particle size control, the mechanism of granulation was not immediately apparent. Fundamentally, this experiment could not distinguish if the mixture was forming a paste within the melting zone and subsequently being milled by the kneading blocks or if a more conventional granulation mechanism was involved. As discussed later, experiments were constructed to investigate further.

Preliminary investigation of drug release from tablets prepared from the 15% tramadol hydrochloride granules demonstrated the ability of the melt granulation process to produce matrices suitable for controlled release (data not shown). Based on these preliminary results the drug concentration was increased to 35% for development of the final dosage form. The decreasing temperature profile 3 was also found to acceptable for direct formation of granules. However, growth of the particle size distribution was determined to be inversely proportional to the feed rate, as shown in Figure 6.2. These results are meaningful in determining the processing design space for particle size control; however, detailed evaluation of these results would benefit from an understanding of the granulation mechanism, which is discussed later. Because the throughput was the only variable changed in this experiment, the reduction in throughput

rate directly corresponds to an increase in specific energy input into the granulation. It follows that growth of the particle size distribution is proportional to specific energy input.

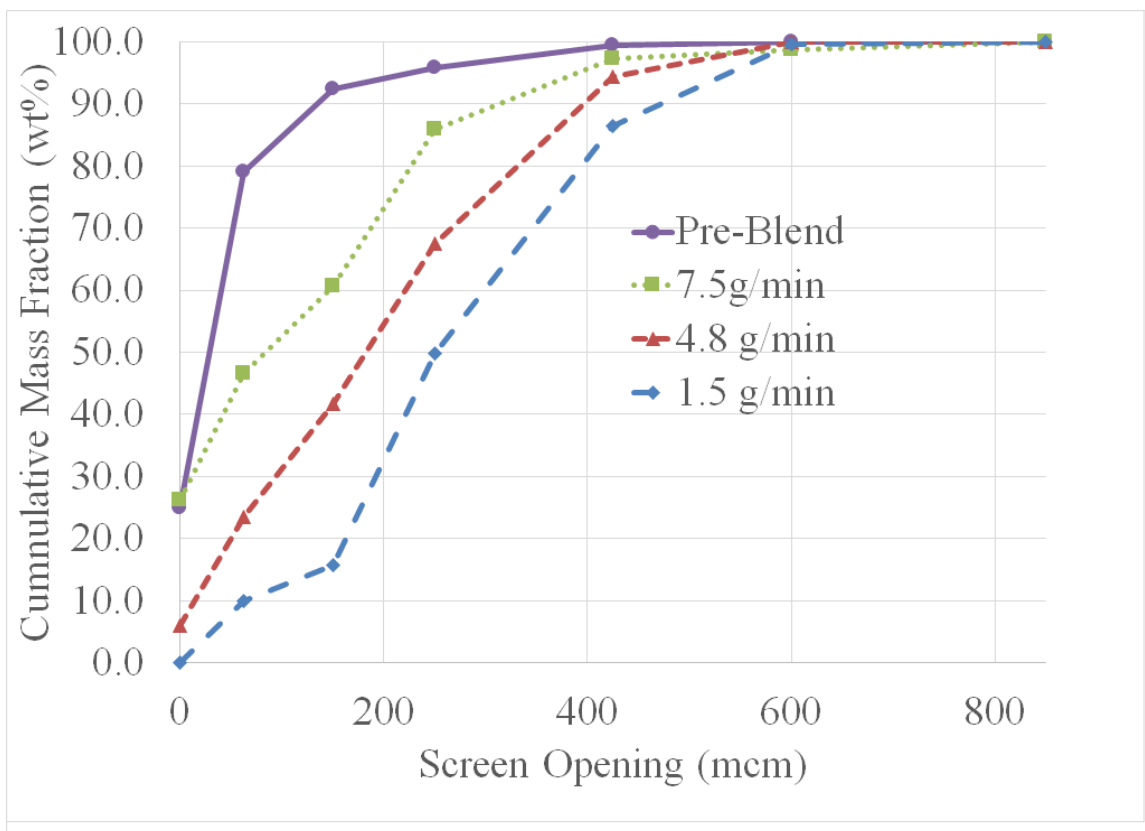


Figure 6.2 Cumulative particle size distributions of the pre-blend and 35% tramadol hydrochloride granulations prepared using temperature profile 3 at various throughput rates.

## 6.4.2 Granule Characterization and Stability

The particle size distribution of the continuously prepared granulation is not only critical for process control of subsequent unit operations such as blending and compression, but likely plays a critical role in controlling the drug release rate, which is discussed later. In addition, the particle morphology as well as the polymorphic forms of C888 and tramadol hydrochloride in the granulation should be understood as factors in subsequent processes and for controlling drug release.

As previously discussed, granulation with C888 at concentrations greater than 40% tends to produce a paste, unless the temperature profile is controlled as described in this work. At high lipid binder concentrations, granulation can be achieved by simply melting the lipid in a beaker or tank and dispersing the active ingredient. This batch melt mixing process is followed by cooling of the mass and grinding. For comparison, a 15% tramadol hydrochloride granulation was prepared by melt mixing and grinding through a 20 mesh sieve. Figure 6.3 depicts scanning electron micrographs of 15% tramadol hydrochloride granules prepared by continuous twin screw granulation and by melt mixing/grinding. The surface of the particles prepared by continuous twin screw granulation are observed to be smoother and the particles themselves have a more spherical shape when compared to the conventional batch process. As a consequence of this morphology, granules prepared by continuous twin screw granulation were found to have excellent flowability as defined by the USP angle of repose analysis (data not shown).

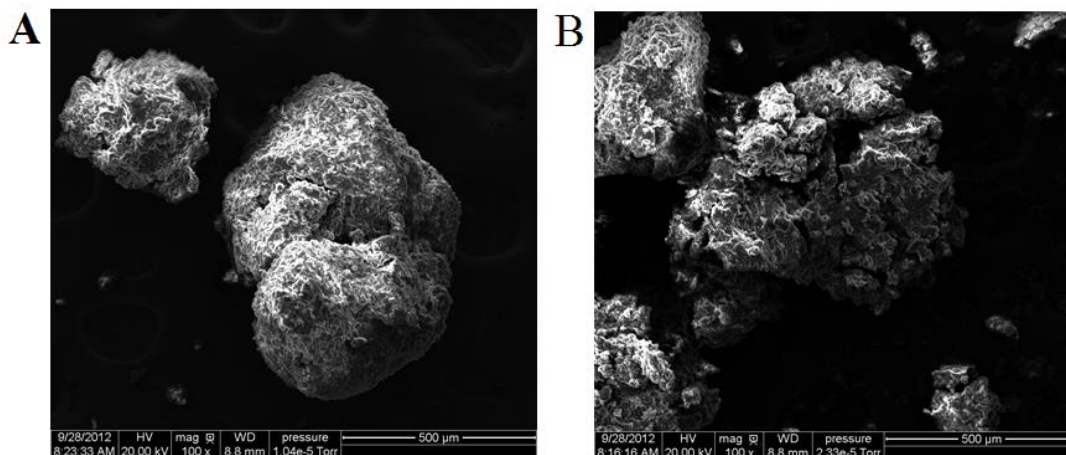


Figure 6.3 Scanning electron micrographs of 15% tramadol hydrochloride in glyceryl behenate granules prepared by A) continuous twin screw granulation B) melt mixing and grinding.

Polymorphic changes in lipid based dosage forms are known to alter drug release and such phenomena were critical to understanding early pharmaceutical dosage forms, such as suppositories and solid lipid matrices (Windbergs et al., 2009). Preliminary experiments were performed to ensure that the mDSC and XRD methodologies were capable of detecting the various polymorphs of C888. Neat C888 was evaluated by second fusion experiments, which validated the ability of the DSC methodology to detect the  $\alpha_2$  polymorph, characterized by a melting endotherm around 67.5 °C and previously characterized and noted to be unstable by Brubach et al. (2007). In addition, 24 hour curing of freshly quenched C888 samples at 50 °C resulted in the emergence of an XRD diffraction peak at 19.2° 2 $\theta$ . This peak is normally associated with a triclinic phase, or  $\beta$  polymorph, which was observed but not identified by Hamdani et al. (Hamdani et al., 2003). Supporting this identification is the diffraction peak at 19.4° 2 $\theta$  identified by

Windbergs et al. (2009) to be characteristic of  $\beta$  tristearin. However, this phase has also previously been described for glyceryl behenate as both triclinic and orthorhombic phases, or  $\beta$ i (Jenning et al., 2000). While the emergence of this peak is notable, C888 is supplied as a stable hexagonal phase (sub  $\alpha$  polymorph) comprising a mixture of glyceryl mono-, di-, and tribehenate. The mixture precludes the formation of a single  $\beta$  polymorph. Furthermore, curing was observed to result in the appearance of a small endotherm having a peak at approximately 75 °C, which is associated with a  $\beta$ form. The melting endotherm of tramadol hydrochloride observed around 178 °C following continuous melt granulation was also compared to that of a physical mixture and determined to be similar. This indicates the twin screw granulation process did not impact the polymorphic form of tramadol hydrochloride.

While the previous observations related to the polymorphic form of C888 are of note, what is of primary importance is that the polymorphic form can be detected by the methods employed here and the stability of the formed polymorphic mixture can be assessed. Continuously produced granules containing 35% tramadol hydrochloride were packaged into induction sealed HDPE bottles and analyzed over the course of 3 months during storage at 40°C/75%RH. The initial results, as determined by DSC and XRD, are plotted along with the stability time points are plotted in Figure 6.4 and Figure 6.5, respectively.

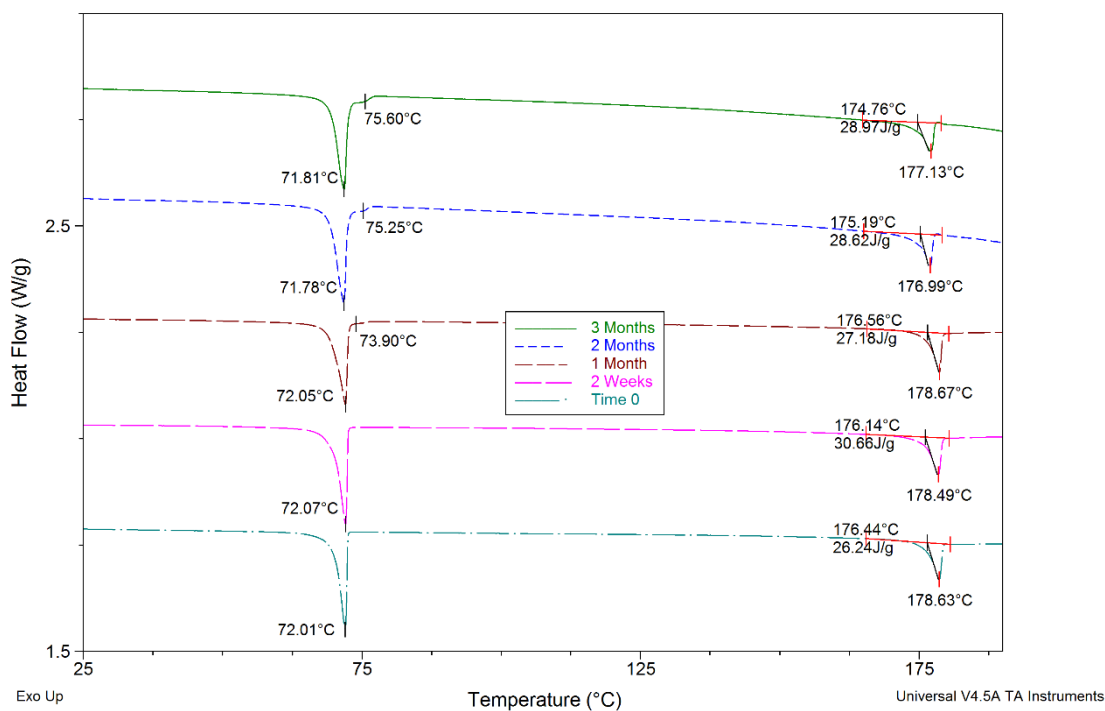


Figure 6.4 DSC thermograms of 35% tramadol HCl granules during 3 months of storage at 40 °C 75% relative humidity conditions in induction sealed HDPE bottles.

The DSC results, lacking low melting temperature endotherms indicate that the unstable sub  $\alpha$  and  $\alpha_2$  polymorphs observed following rapid quenching are not present. The melting endotherms of tramadol hydrochloride appear to be stable over this timescale as well, indicating a stable crystalline form of the drug is present in the granules formed by twin screw extrusion. Starting at 1 month, a small endotherm characteristic of a higher melting point polymorph, which is believed to be the triclinic form, becomes evident and grows over the remaining months. XRD corroborates the observation that the tramadol hydrochloride crystalline structure is stable. However, the intensity of several tramadol hydrochloride peaks are masked by the emergence of triclinic associated peaks around  $19.2^\circ$  and  $23^\circ 2\theta$ .

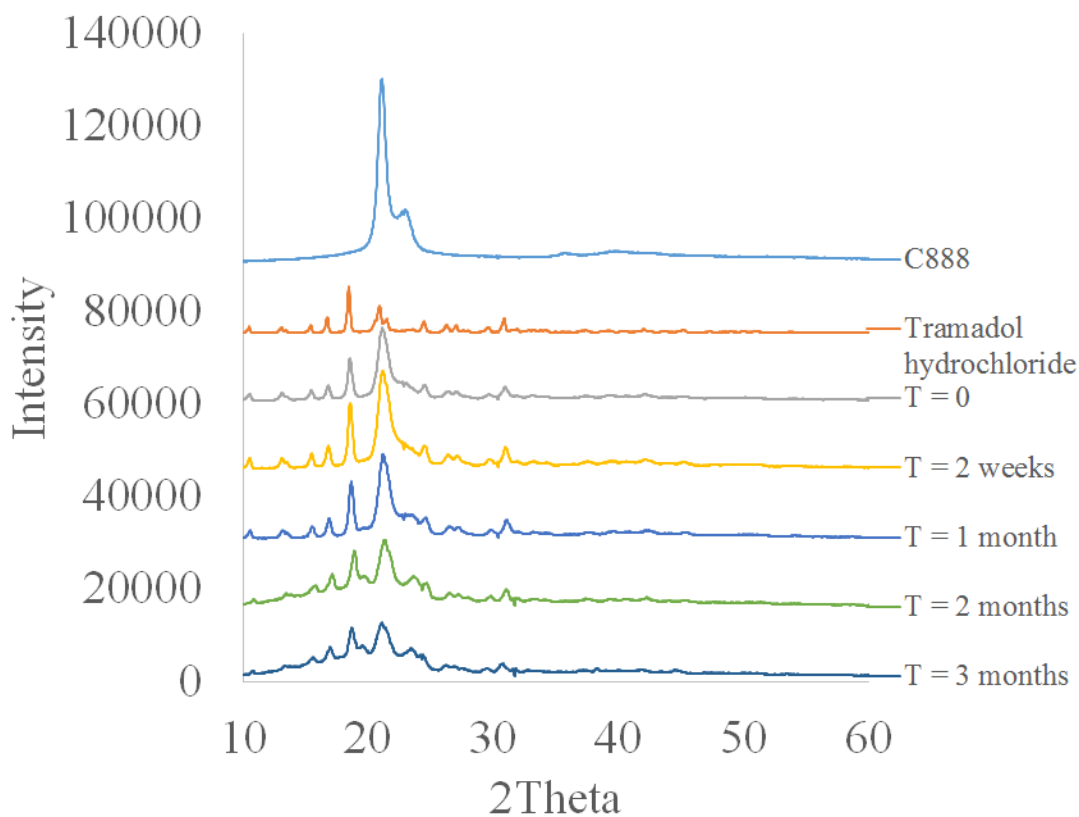


Figure 6.5 X-Ray diffractograms of 35% tramadol HCl granules during 3 months of storage at 40 °C 75% relative humidity conditions in induction sealed HDPE bottles.

### 6.4.3 Mechanism of Granulation

As previously described, continuous granulation with the barrel temperature profile decreasing from above the melting point of C888 to below the melting point of C888 prior to discharge resulted in the direct production of granules with a desirable particle size distribution. Controlling at 80 °C in all zones resulted in the formation of a paste. In addition, the process was observed to reduce the particle size distribution of

MCC (Avicel PH-102). Together these observations indicate two possible granulation mechanisms. The first possibility being that the C888 is completely melted and forms a paste with dispersed tramadol hydrochloride. While cooling, the mixing action of the screws may separate and grind this material. Alternatively and what will be demonstrated as likely, the residence time of the mixture in the 80 °C section of the extruder is too short for complete melting to occur. This would likely involve immersion and distribution nucleation mechanisms, the relative contribution of which would depend on the starting particle size as discussed by Mu and Thompson (2012). Determining the relative contributions of the granulation mechanisms is confounded by potential milling effects of the cooled granules. However, if the C888 portion of the blend is completely melted in the heated section of the extruder, changes in the C888 feed particle size would not have an impact on the resulting particle size distribution. Once a paste is formed and the drug dispersed, subsequent cooling and grinding would be independent of the starting particle size of the binder.

To investigate the granulation mechanism, C888 was pre-processed by melting at 80 °C, cooling and grinding through a 14 mesh sieve. The particles were cured at 50 °C for 24 hours as a precaution to ensure low melting point polymorphs were not present. The particles were classified into three sizes 50 to 60 mesh, 60 to 120 mesh and 120 to 200 mesh. Each size fraction was individually blended with tramadol hydrochloride, The particle size distributions of these pre-blends are charted in Figure 6.6a. Following granulation at 4.8 g/min, the resulting particle size distributions were determined as presented in Figure 6.6b. A control granulation of the neat, unprocessed material is included for comparison. These results are sufficient to rule out the formation of a paste in the 80 °C section of the extruder barrel. Each sieve cut was assayed for tramadol

hydrochloride and the results were found to be  $35\% \pm 5\%$ , indicating intimate mixing occurred at all particle sizes regardless of initial binder size.

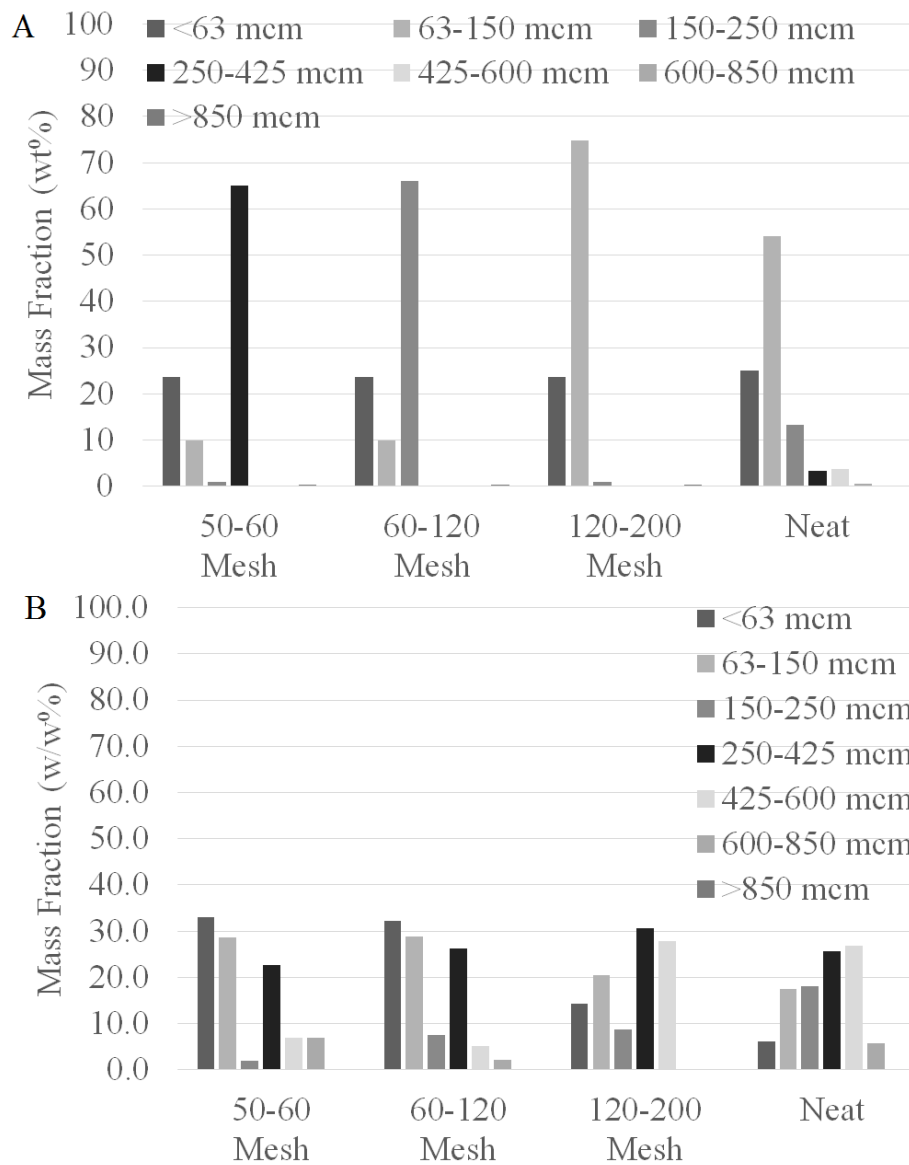


Figure 6.6 Impact of binder (glyceryl behenate) feed particle size. Cumulative particle size distributions of 35% tramadol hydrochloride blends and granulations prepared using neat glyceryl behenate and pre-processed glyceryl behenate of various sieve cuts. A) Pre-blends prior to granulation B) granules prepared at 4.8 g/minute using temperature profile 3.

Granule dissolution provides further evidence that the C888 portion of the granulation is not completely melted in the 80 °C section of the extruder barrel. When compared to melt mixed and ground granulation, continuous twin screw granules appear to have different release mechanisms, as shown in Figure 6.7. Melt mixed and ground granules appear to have a large, >30%, burst effect which is not present in the twin screw granules. The melt mixing and grinding process resulted in particles having a rough surface morphology, which exposes tramadol hydrochloride to the release medium. The twin screw granules are better encapsulated by the portion of C888 that melted during the process, which mitigates the burst. This highlights a benefit of the twin screw granulation process as bursts are typically undesirable in controlled release applications. Following the burst from the melt mixed granules, an additional 40% of the drug was released over the next 15 hours. Tramadol HCl in granules prepared by continuous twin screw granulation was released within 4 hours.

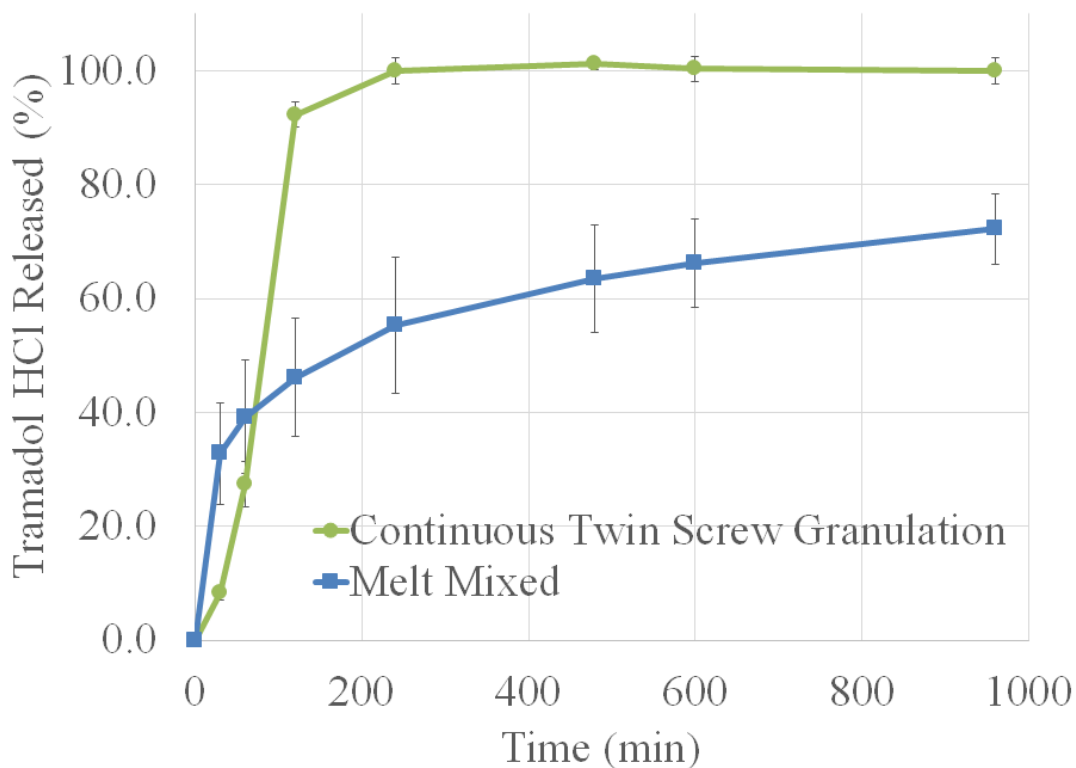


Figure 6.7 Sink dissolution of 35% tramadol hydrochloride granules prepared by continuous twin screw granulation and melt mixing. n=3, USP Apparatus I, 75 rpm, 900 ml 0.1N HCl at 37 °C.

The release profile of continuous twin screw granules is very interesting in that there is minimal burst, yet complete release is still achieved in a short timescale. A likely explanation, supported by the evidence that not all the C888 is melted during the process, is that the granules contain agglomerated particles of tramadol hydrochloride and C888 held together and coated by a thin layer of C888. This geometry prevents a burst due to lack of surface drug. Release is controlled, yet rapid compared to fully melted particles.

#### 6.4.4 Tablet Formulation and Stability

A safe controlled release tramadol hydrochloride dosage form would ideally meter drug release over a period of 12 to 24 hours, completely release the drug, exhibit near zero order release, and resist changes in release rate during the first few hours when exposed to alcohol. Five tablet compositions were studied to investigate how the granulation process and the presence of pore formers impact the release kinetics, see Table 6.2. Formulation 1 serves as a direct compression control and has an equivalent composition to Formulation 3. Formulation 2 contains an insoluble and slightly swellable pore former. While Formulations 3 and 4 represent the inclusion of a soluble and insoluble pore formers, respectively. Formulation 5 represents a negative control, comprising the compacted granules and no pore former.

Table 6.2 Tablet Formulations

<b>Ingredient</b>	<b>Form 1</b>	<b>Form 2</b>	<b>Form 3</b>	<b>Form 4</b>	<b>Form 5</b>
35% tramadol hydrochloride in glyceryl behenate <b>blend</b>	286 mg	-	-	-	-
35% tramadol hydrochloride in glyceryl behenate twin screw <b>granules</b>	-	286 mg	286 mg	286 mg	286 mg
Lactose (Fast Flo 316)	200 mg		200 mg		
Microcrystalline cellulose (Avicel PH-102)		200 mg			
Dicalcium phosphate (Emcompress)				200 mg	
Magnesium Stearate	5 mg				

Formulation 5, containing only the compacted granules released drug at very slow rate compared to the experimental timescale of 16 hours, as shown in Figure 6.8. This result is expected based on the release rate of the granules themselves, which controlled

release for 4 hours. It is known that release from lipid based matrix tablets can be controlled by inclusion of pore formers and that release occurs by diffusion through the matrix and through pores in the matrix (Kato et al., 1994, Sato et al., 1997). The soluble pore former lactose, Formulation 3, creates an improved network of pores within the matrix tablet following solubilization, which increases the porous diffusion component. Dicalcium phosphate, Formulation 4, also increases the porous diffusion component, yet not to the same extent as would be expected and is observed for lactose. Of particular interest, is the dissolution profile from Formulation 2 containing microcrystalline cellulose. Only tablets of this formulation were observed to crack during the dissolution process. This cracking is the result of the swelling of microcrystalline cellulose in the presence of water. This effect is subtle compared to commercially available disintegrants and superdisintegrants, as the tablet remains intact following dissolution. However, these cracks alter the tortuosity of the porous network which is known to alter the drug release from matrix tablets (Crowley et al., 2004). This changes the tortuosity of the network and results in a drug release profile that more closely resembles a zero order release. A first order release profile is normally associated with crystalline matrix tablets, for which complex mathematic models have been developed to describe drug dissolution and release (Siepmann and Siepmann, 2011).

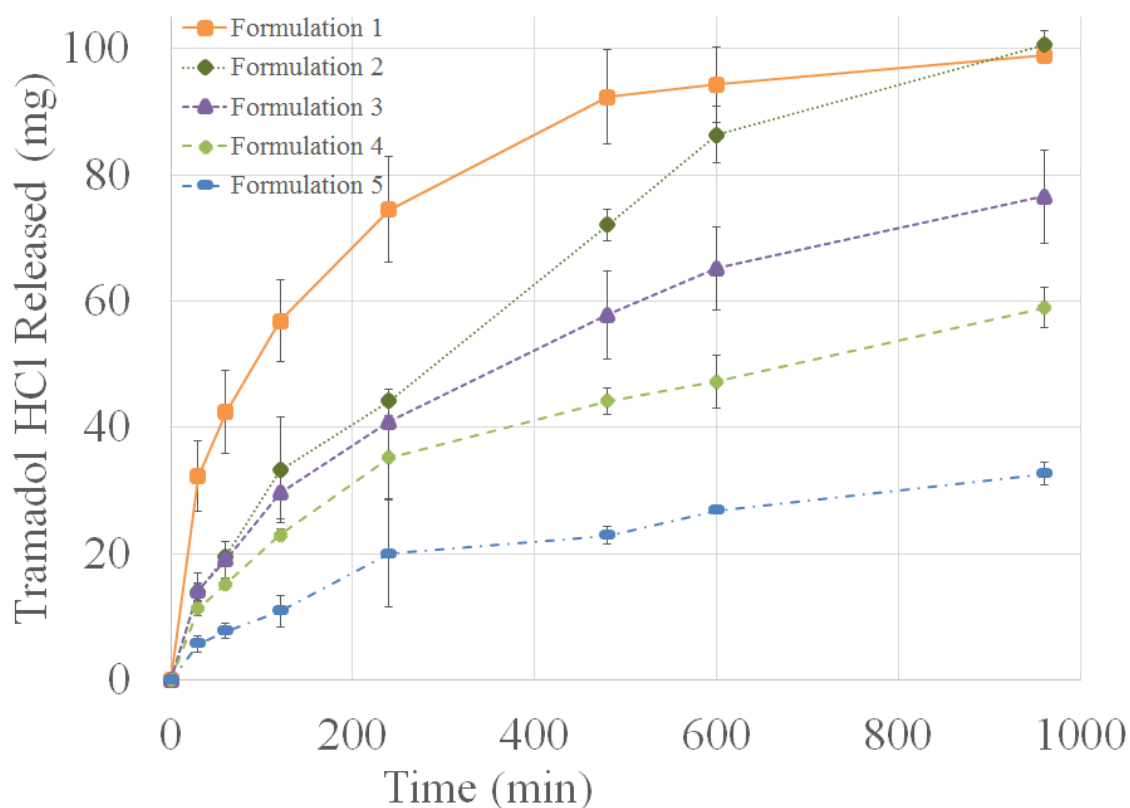


Figure 6.8 Sink dissolution profiles of 100 mg tramadol hydrochloride tablets. n=3, USP Apparatus I, 75 rpm, 900 ml 0.1N HCl at 37 °C.

The compressed twin screw granules, when formulated with a pore former, have been demonstrated to meet the formulation objectives of complete release, sustained release, and near zero order release rate. For the dosage form to have an optimal safety profile, dose dumping in the presence of alcohol must be prevented. The hydroalcoholic dissolution tests recommended by the FDA draft guidance were performed on Formulation 3, as shown in Figure 6.9. As a comparison, the impact of the twin screw granulation process was determined by evaluating Formulation 1, the directly compressed control. An additional 20% of drug was released over the 2 hours for the control.

However, the twin screw granulation present in Formulation 3 tablets inhibited direct access of ethanol to the drug and no significant change in the dissolution profile was observed. These results indicate that the C888 layer present on the particles presents a diffusion barrier for ethanol and provides for a safe dosage form.

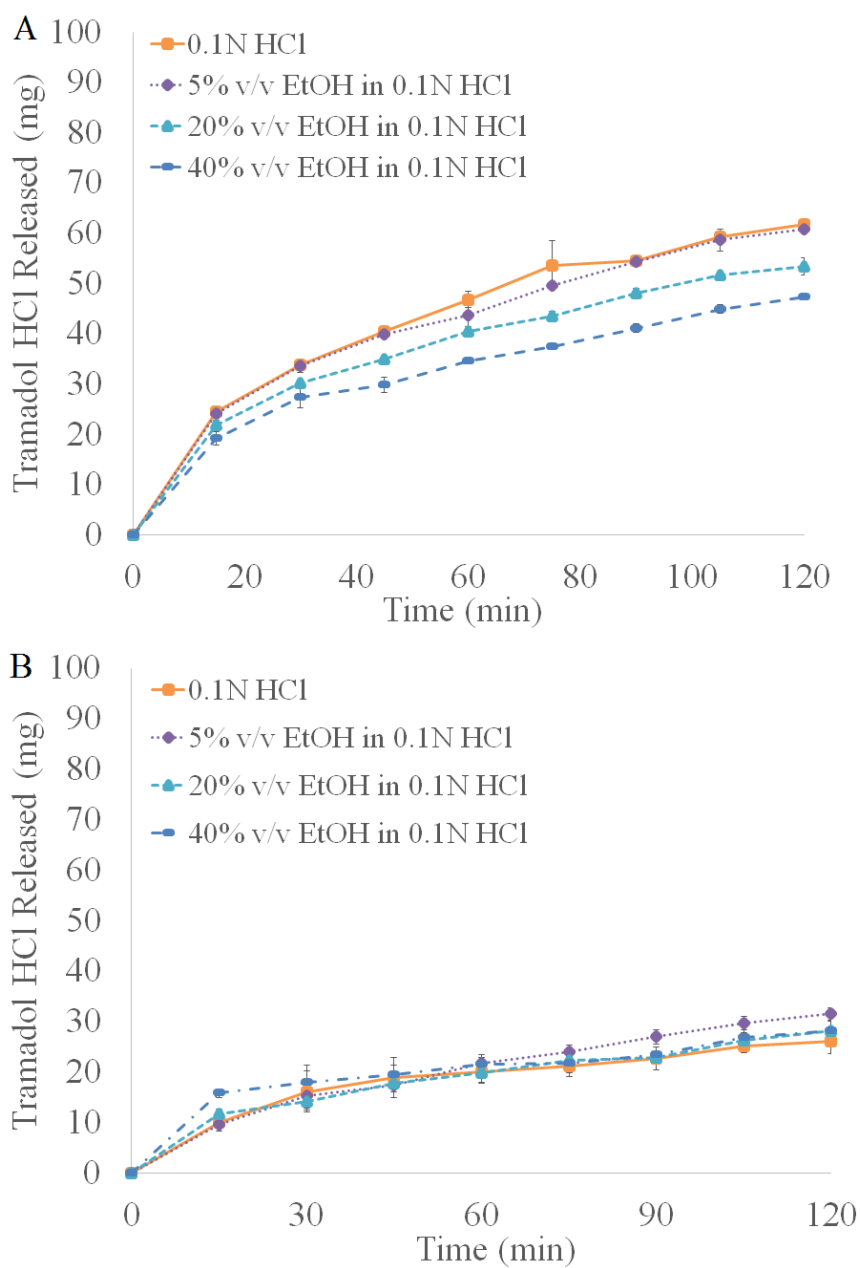


Figure 6.9 Hydroalcoholic dissolution profiles of 100 mg tramadol hydrochloride tablets prepared by A) direct compression (Formulation 1) or B) continuous twin screw granulation and compression (Formulation 3). n=3, USP Apparatus I, 75 rpm, 900 ml 0.1N HCl containing 0%, 5%, 20% or 40% ethanol at 37 °C.

Tablets from Formulation 2 were packaged into HDPE bottles and induction sealed for evaluation on stability at 40 °C and 75% relative humidity conditions. Immediately after compression and packaging, the bottles were separated into two groups. One group, designated as “cured” was placed at 50 °C for 24 hours while the uncured group was held at ambient conditions prior to placing in the stability chamber. This curing process is recommended by the supplier of C888 following melt processing and is intended to provide the necessary activation energy needed to convert any low melting point polymorphs to more stable forms. When low melting point polymorphs are present, the lipid matrix may rearrange and substantially alter drug release (Singh et al., 2007). As observed in Figure 6.10, the dissolution profiles of cured and uncured tablets were nearly identical. This result was expected based on the previously reported polymorphic form of the twin screw granules, which were not observed to have unstable sub  $\alpha$  or  $\alpha_2$  phases. Furthermore, the growth of the triclinic phase observed during stability of the granules did not result in a corresponding dissolution trend. However, it is possible that variability associated with the formation of the tortuous network might obfuscate any drug release impact of this polymorphic shift on stability.

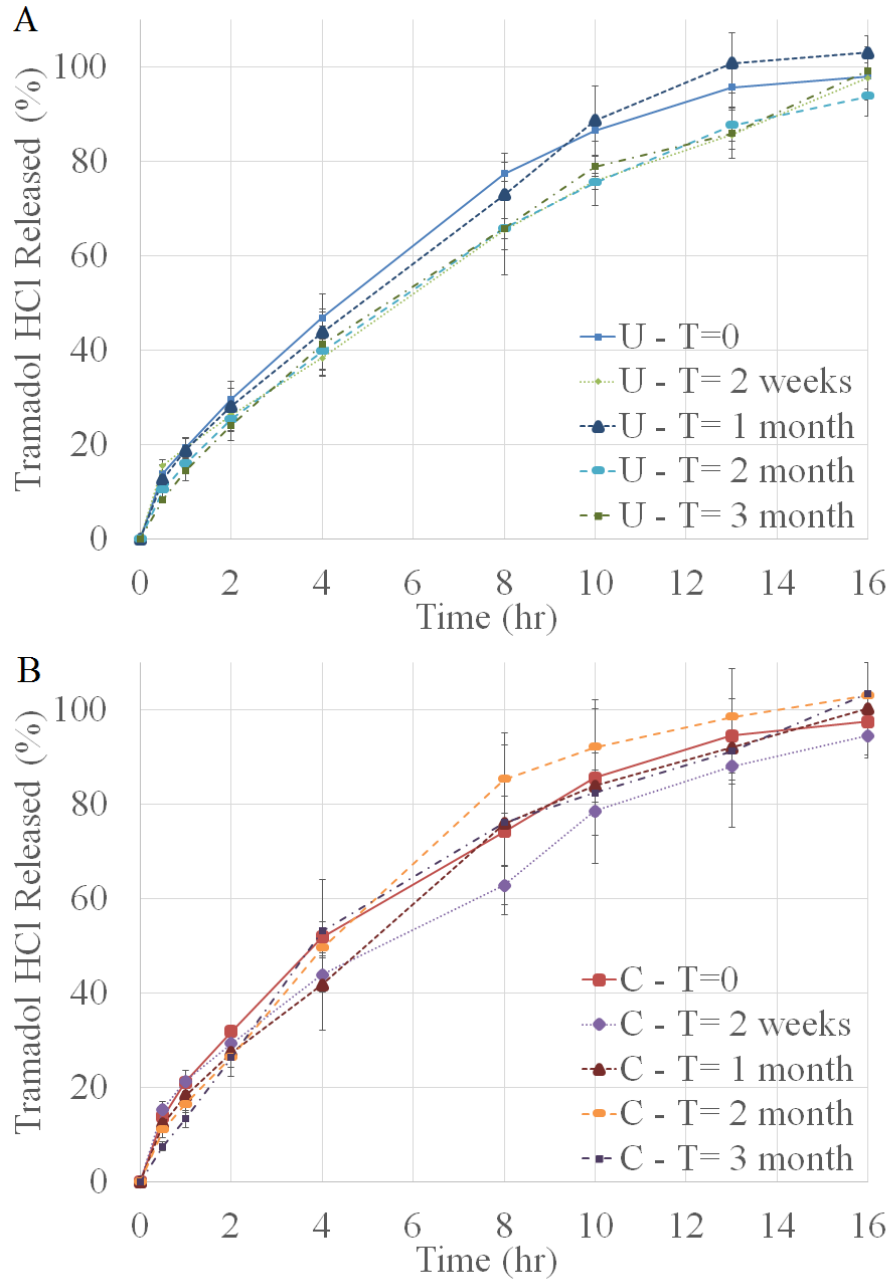


Figure 6.10 Dissolution profiles of 100 mg tramadol hydrochloride tablets (formulation 2) during 3 months storage at 40 °C/75%RH A) uncured tablets or B) tablets cured for 24 hours at 50 °C. n=3, USP Apparatus I, 75 rpm, 900 ml 0.1N HCl.

## **6.5 CONCLUSIONS**

Twin screw granulation using a NANO16 twin screw extruder has been demonstrated as a viable process for the direct production of granules, which exhibit a desirable particle shape and morphology. A controlled decreasing barrel temperature profile, the throughput rate and starting lipid binder size were determined to be CQAs. Tramadol HCl and glyceryl behenate granules were successfully prepared into controlled release tablets that did not dose dump in alcohol. The granulation process did not involve complete melting of glyceryl behenate due to a short residence time above the melting temperature, therefore the mechanism likely involves a combination of immersion and distribution. Continuous twin screw granulation results in a mixture of stable polymorphs of glyceryl behenate and resulting tablets exhibit a stable dissolution profile without the need for curing.

## 6.6 REFERENCES

Akiyama Y, Nagahara N, Kashihara T, Hirai S, and Toguchi H (1995) In Vitro and in Vivo Evaluation of Mucoadhesive Microspheres Prepared for the Gastrointestinal Tract Using Polyglycerol Esters of Fatty Acids and a Poly(acrylic acid) Derivative. *Pharmaceutical Research* **12**, 397-405.

Brubach JB, Jannin V, Mahler B, Bourgaux C, Lessieur P, Roy P et al. (2007) Structural and thermal characterization of glyceryl behenate by X-ray diffraction coupled to differential calorimetry and infrared spectroscopy. *International Journal of Pharmaceutics* **336**, 248-56.

Crowley MM, Schroeder B, Fredersdorf A, Obara S, Talarico M, Kucera S et al. (2004) Physicochemical properties and mechanism of drug release from ethyl cellulose matrix tablets prepared by direct compression and hot-melt extrusion. *International Journal of Pharmaceutics* **269**, 509-22.

Danish FQ and Parrott EL (1971) Flow rates of solid particulate pharmaceuticals. *Journal of Pharmaceutical Sciences* **60**, 548-54.

Dhenge RM, Cartwright JJ, Doughty DG, Hounslow MJ, and Salman AD (2011) Twin screw wet granulation: Effect of powder feed rate. *Advanced Powder Technology* **22**, 162-6.

Djuric D and Kleinebudde P (2010) Continuous granulation with a twin-screw extruder: Impact of material throughput. *Pharmaceutical Development & Technology* **15**, 518-25.

Fadda HM, Mohamed MAM, and Basit AW (2008) Impairment of the in vitro drug release behaviour of oral modified release preparations in the presence of alcohol. *International Journal of Pharmaceutics* **360**, 171-6.

Faure A, York P, and Rowe RC (2001) Process control and scale-up of pharmaceutical wet granulation processes: a review. *European Journal of Pharmaceutics & Biopharmaceutics* **52**, 269-77.

FDA (2007) Draft Guidance on Tramadol. In (ed.), Vol. pp. Center for Drug Evaluation and Research (CDER).

Hamdani J, Moës AJ, and Amighi K (2003) Physical and thermal characterisation of Precirol® and Compritol® as lipophilic glycerides used for the preparation of controlled-release matrix pellets. *International Journal of Pharmaceutics* **260**, 47-57.

Jenning V, Schäfer-Korting M, and Gohla S (2000) Vitamin A-loaded solid lipid nanoparticles for topical use: drug release properties. *Journal of Controlled Release* **66**, 115-26.

Kato Y, Sunada H, Yonezawa Y, and Ishino R (1994) Sustained release mechanisms of wax matrix system for controlled release. *Chemical & Pharmaceutical Bulletin* **42**, 1646-50.

Lakshman JP, Kowalski J, Vasanthavada M, Tong W-Q, Joshi YM, and Serajuddin ATM (2011) Application of melt granulation technology to enhance tableting properties of poorly compactible high-dose drugs. *Journal of Pharmaceutical Sciences* **100**, 1553-65.

Lionberger R, Lee S, Lee L, Raw A, and Yu L (2008) Quality by Design: Concepts for ANDAs. *The AAPS Journal* **10**, 268-76.

Liu J, Zhang F, and McGinity JW (2001) Properties of lipophilic matrix tablets containing phenylpropanolamine hydrochloride prepared by hot-melt extrusion. *European Journal of Pharmaceutics & Biopharmaceutics* **52**, 181-90.

Lo JB, Appel LE, Herbig SM, McCray SB, and Thombre AG (2009) Formulation design and pharmaceutical development of a novel controlled release form of azithromycin for single-dose therapy. *Drug Development & Industrial Pharmacy* **35**, 1522-9.

Mu B and Thompson MR (2012) Examining the mechanics of granulation with a hot melt binder in a twin-screw extruder. *Chemical Engineering Science* **81**, 46-56.

Ochoa L, Igartua M, Hernández RM, Solinís MÁ, Gascón AR, and Pedraz JL (2010) In vivo evaluation of two new sustained release formulations elaborated by one-step melt granulation: Level A in vitro–in vivo correlation. *European Journal of Pharmaceutics & Biopharmaceutics* **75**, 232-7.

Plumb K (2005) Continuous Processing in the Pharmaceutical Industry: Changing the Mind Set. *Chemical Engineering Research and Design* **83**, 730-8.

Read EK, Park JT, Shah RB, Riley BS, Brorson KA, and Rathore AS (2010) Process analytical technology (PAT) for biopharmaceutical products: Part I. concepts and applications. *Biotechnology & Bioengineering* **105**, 276-84.

Sato H, Miyagawa Y, Okabe T, Miyajima M, and Sunada H (1997) Dissolution mechanism of diclofenac sodium from wax matrix granules. *Journal of Pharmaceutical Sciences* **86**, 929-34.

Schaber SD, Gerogiorgis DI, Ramachandran R, Evans JMB, Barton PI, and Trout BL (2011) Economic Analysis of Integrated Continuous and Batch Pharmaceutical Manufacturing: A Case Study. *Industrial & Engineering Chemistry Research* **50**, 10083-92.

Siepmann J and Siepmann F (2011) Mathematical modeling of drug release from lipid dosage forms. *International Journal of Pharmaceutics* **418**, 42-53.

Singh R, Poddar S, and Chivate A (2007) Sintering of wax for controlling release from pellets. *AAPS PharmSciTech* **8**, E175-E83.

Sochon RPI, Zomer S, Cartwright JJ, Hounslow MJ, and Salman AD (2010) The variability of pharmaceutical granulation. *Chemical Engineering Journal* **164**, 285-91.

Van Melkebeke B, Vermeulen B, Vervaet C, and Remon JP (2006) Melt granulation using a twin-screw extruder: A case study. *International Journal of Pharmaceutics* **326**, 89-93.

Vasanthavada M, Wang Y, Haefele T, Lakshman JP, Mone M, Tong W et al. (2011) Application of melt granulation technology using twin-screw extruder in development of high-dose modified-release tablet formulation. *Journal of Pharmaceutical Sciences* **100**, 1923-34.

Vervaet C and Remon JP (2005) Continuous granulation in the pharmaceutical industry. *Chemical Engineering Science* **60**, 3949-57.

Wan LSC, Heng PWS, and Muhuri G (1992) Incorporation and distribution of a low dose drug in granules. *International Journal of Pharmaceutics* **88**, 159-63.

Windbergs M, Strachan CJ, and Kleinebudde P (2009) Understanding the solid-state behaviour of triglyceride solid lipid extrudates and its influence on dissolution. *European Journal of Pharmaceutics & Biopharmaceutics* **71**, 80-7.

Yang D, Kulkarni R, Behme RJ, and Kotiyan PN (2007) Effect of the melt granulation technique on the dissolution characteristics of griseofulvin. *International Journal of Pharmaceutics* **329**, 72-80.

Yu L (2008) Pharmaceutical Quality by Design: Product and Process Development, Understanding, and Control. *Pharmaceutical Research* **25**, 781-91.

## Chapter 7: Concluding Remarks

### 7.1 DISSERTATION CONCLUSION

The research described herein was undertaken to investigate novel thermal processing modes and formulations intended to enhance bioavailability. When carefully combined with suitable pharmaceutical grade materials, thermal processes enable the preparation of superstructures and molecular dispersions that can be tailored for a broad range of applications. Several examples were investigated by applying thermodynamics, kinetics and by probing mechanics of action. For example, a counter-rotating twin screw extrusion geometry was demonstrated for the first time as a favorable alternative to the commonly applied co-rotation twin screw geometry for more efficiently arriving at the thermodynamically limited drug loading of an amorphous solid dispersions. A novel approach of including a lipid in a glassy dispersion was demonstrated to alter the mechanism of release from an amorphous solid dispersion improving the control of drug release. The relatively new thermal process, KinetiSol<sup>®</sup> Dispersing, was applied to generate a viscous solid dispersion, and significant challenges associated with controlling the release of formulated tablets were overcome and the tablets were verified *in vivo* to enhance the bioavailability of a poorly soluble drug. A new processing mode, utilizing a novel temperature profile in a modified twin screw extruder, was developed for manufacturing controlled release granulations of a lipid and demonstrated to produce effective, yet safe controlled release properties.

## Bibliography

Abberger T, Seo A, and Schæfer T (2002) The effect of droplet size and powder particle size on the mechanisms of nucleation and growth in fluid bed melt agglomeration.

*International Journal of Pharmaceutics* **249**, 185-97.

Akimoto M, Nagahata N, Furuya A, Fukushima K, Higuchi S, and Suwa T (2000) Gastric pH profiles of beagle dogs and their use as an alternative to human testing.

*European Journal of Pharmaceutics & Biopharmaceutics* **49**, 99-102.

Akiyama Y, Nagahara N, Kashihara T, Hirai S, and Toguchi H (1995) In Vitro and in Vivo Evaluation of Mucoadhesive Microspheres Prepared for the Gastrointestinal Tract Using Polyglycerol Esters of Fatty Acids and a Poly(acrylic acid) Derivative.

*Pharmaceutical Research* **12**, 397-405.

Al-Obaidi H, Ke P, Brocchini S, and Buckton G (2011) Characterization and stability of ternary solid dispersions with PVP and PHPMA. *International Journal of Pharmaceutics* **419**, 20-7.

Alonzo DE, Gao Y, Zhou D, Mo H, Zhang GGZ, and Taylor LS (2011) Dissolution and precipitation behavior of amorphous solid dispersions. *Journal of Pharmaceutical Sciences* **100**, 3316-31.

Amidon GL, Lennernäs H, Shah VP, and Crison JR (1995) A Theoretical Basis for a Biopharmaceutic Drug Classification: The Correlation of in Vitro Drug Product Dissolution and in Vivo Bioavailability. *Pharmaceutical Research* **12**, 413-20.

Appel LE, Ray RJR, Lyon DK, West JB, McCray SB, Crew MD et al. (2011) Multiparticulate crystalline drug compositions having controlled release profiles. US7887844B2.

Augsburger LL, Brzezczko AW, Shah U, and Hahm HA (2006) Super Disintegrants: Characterization and Function. In *Encyclopedia of Pharmaceutical Technology*. Vol. 1, pp. 3553-67.

Aungst BJ (2000) Intestinal permeation enhancers. *Journal of Pharmaceutical Sciences* **89**, 429-42.

Baert L, Verreck G, and Thone D (2003) Antifungal Compositions with Improved Bioavailability. US6509038B2.

Baert L, Verreck G, and Thone D (2006) Antifungal Compositions with Improved Bioavailability. US7081255B2.

Baker R (1987) In *Controlled Release of Biologically Active Agents*. Vol. pp. John Wiley & Sons, New York.

Bellantone RA, Patel P, Sandhu H, Choi DS, Singhal D, Chokshi H et al. (2012) A method to predict the equilibrium solubility of drugs in solid polymers near room temperature using thermal analysis. *Journal of Pharmaceutical Sciences* **101**, 4549-58.

Berndl G, Degenhardt M, Maegerlein M, and Dispersyn G (2013) Itraconazole Compositions with Improved Bioavailability. US8486456B2.

Bikiaris DN (2011a) Solid dispersions, Part I: recent evolutions and future opportunities in manufacturing methods for dissolution rate enhancement of poorly water-soluble drugs. *Expert Opinion on Drug Delivery* **8**, 1501-19.

Bikiaris DN (2011b) Solid dispersions, Part II: new strategies in manufacturing methods for dissolution rate enhancement of poorly water-soluble drugs. *Expert Opinion on Drug Delivery* **8**, 1663-80.

Blagden N, de Matas M, Gavan PT, and York P (2007) Crystal engineering of active pharmaceutical ingredients to improve solubility and dissolution rates. *Advanced Drug Delivery Reviews* **59**, 617-30.

Botzolakis JE and Augsburger LL (1984) The role of disintegrants in hard-gelatin capsules. *Journal of Pharmacy & Pharmacology* **36**, 77-84.

Breitenbach J (2002) Melt extrusion: from process to drug delivery technology. *European Journal of Pharmaceutics & Biopharmaceutics* **54**, 107-17.

Broadhead J, Edmond Rouan SK, and Rhodes CT (1992) The spray drying of pharmaceuticals. *Drug Development & Industrial Pharmacy* **18**, 1169-206.

Brouwers J, Brewster ME, and Augustijns P (2009) Supersaturating drug delivery systems: The answer to solubility-limited oral bioavailability? *Journal of Pharmaceutical Sciences* **98**, 2549-72.

Brubach JB, Jannin V, Mahler B, Bourgaux C, Lessieur P, Roy P et al. (2007) Structural and thermal characterization of glyceryl behenate by X-ray diffraction coupled to

differential calorimetry and infrared spectroscopy. *International Journal of Pharmaceutics* **336**, 248-56.

Cao Q-R, Liu Y, Xu W-J, Lee B-J, Yang M, and Cui J-H (2012) Enhanced oral bioavailability of novel mucoadhesive pellets containing valsartan prepared by a dry powder-coating technique. *International Journal of Pharmaceutics* **434**, 325-33.

Carcaboso ÁM, Chiappetta DA, Höcht C, Blake MG, Boccia MM, Baratti CM et al. (2008) In vitro/in vivo characterization of melt-molded gabapentin-loaded poly(epsilon-caprolactone) implants for sustained release in animal studies. *European Journal of Pharmaceutics & Biopharmaceutics* **70**, 666-73.

Cavallari C, Rodriguez L, Albertini B, Passerini N, Rosetti F, and Fini A (2005) Thermal and fractal analysis of diclofenac/Gelucire 50/13 microparticles obtained by ultrasound-assisted atomization. *Journal of Pharmaceutical Sciences* **94**, 1124-34.

Cerea M, Zheng W, Young CR, and McGinity JW (2004) A novel powder coating process for attaining taste masking and moisture protective films applied to tablets. *International Journal of Pharmaceutics* **279**, 127-39.

Chiou WL and Riegelman S (1971) Pharmaceutical applications of solid dispersion systems. *Journal of Pharmaceutical Sciences* **60**, 1281-302.

Clark M, Kiser P, Loxley A, McConville C, Malcolm R, and Friend D (2011) Pharmacokinetics of UC781-loaded intravaginal ring segments in rabbits: a comparison of polymer matrices. *Drug Delivery and Translational Research* **1**, 238-46.

Conti S, Maggi L, Segale L, Ochoa Machiste E, Conte U, Grenier P et al. (2007) Matrices containing NaCMC and HPMC: 1. Dissolution performance characterization.

*International Journal of Pharmaceutics* **333**, 136-42.

Craig DQM (2002) The mechanisms of drug release from solid dispersions in water-soluble polymers. *International Journal of Pharmaceutics* **231**, 131-44.

Craig DQM, Royall PG, Kett VL, and Hopton ML (1999) The relevance of the amorphous state to pharmaceutical dosage forms: glassy drugs and freeze dried systems. *International Journal of Pharmaceutics* **179**, 179-207.

Crowley MM, Schroeder B, Fredersdorf A, Obara S, Talarico M, Kucera S et al. (2004) Physicochemical properties and mechanism of drug release from ethyl cellulose matrix tablets prepared by direct compression and hot-melt extrusion. *International Journal of Pharmaceutics* **269**, 509-22.

Crowley MM, Zhang F, Repka MA, Thumma S, Upadhye SB, Kumar Battu S et al. (2007) Pharmaceutical Applications of Hot-Melt Extrusion: Part I. *Drug Development & Industrial Pharmacy* **33**, 909-26.

Curatolo W, Nightingale J, and Herbig S (2009) Utility of Hydroxypropylmethylcellulose Acetate Succinate (HPMCAS) for Initiation and Maintenance of Drug Supersaturation in the GI Milieu. *Pharmaceutical Research* **26**, 1419-31.

Danish FQ and Parrott EL (1971) Flow rates of solid particulate pharmaceuticals. *Journal of Pharmaceutical Sciences* **60**, 548-54.

Dave VS, Fahmy RM, Bensley D, and Hoag SW (2012) Eudragit® RS PO/RL PO as rate-controlling matrix-formers via roller compaction: Influence of formulation and process variables on functional attributes of granules and tablets. *Drug Development & Industrial Pharmacy* **0**, 1-14.

Davis SS (2005) Formulation strategies for absorption windows. *Drug Discovery Today* **10**, 249-57.

Denny PJ (2002) Compaction equations: a comparison of the Heckel and Kawakita equations. *Powder Technology* **127**, 162-72.

Dhenge RM, Cartwright JJ, Doughty DG, Hounslow MJ, and Salman AD (2011) Twin screw wet granulation: Effect of powder feed rate. *Advanced Powder Technology* **22**, 162-6.

Dierickx L, Saerens L, Almeida A, De Beer T, Remon JP, and Vervaet C (2012) Co-extrusion as manufacturing technique for fixed-dose combination mini-matrices. *European Journal of Pharmaceutics & Biopharmaceutics* **81**, 683-9.

DiNunzio JC, Brough C, Hughey JR, Miller DA, Williams Iii RO, and McGinity JW (2010a) Fusion production of solid dispersions containing a heat-sensitive active ingredient by hot melt extrusion and Kinetisol® dispersing. *European Journal of Pharmaceutics & Biopharmaceutics* **74**, 340-51.

DiNunzio JC, Brough C, Miller DA, Williams Iii RO, and McGinity JW (2010b) Applications of KinetiSol® Dispersing for the production of plasticizer free amorphous solid dispersions. *European Journal of Pharmaceutical Sciences* **40**, 179-87.

DiNunzio JC, Brough C, Miller DA, Williams RO, and McGinity JW (2010c) Fusion processing of itraconazole solid dispersions by kinetisol® dispersing: A comparative study to hot melt extrusion. *Journal of Pharmaceutical Sciences* **99**, 1239-53.

DiNunzio JC, Miller DA, Yang W, McGinity JW, and Williams RO (2008) Amorphous Compositions Using Concentration Enhancing Polymers for Improved Bioavailability of Itraconazole. *Molecular Pharmaceutics* **5**, 968-80.

Djuric D and Kleinebudde P (2010) Continuous granulation with a twin-screw extruder: Impact of material throughput. *Pharmaceutical Development & Technology* **15**, 518-25.

Eise K, Herrmann H, Jakopin S, Burkhardt U, and Werner H (1981) An analysis of twin-screw extruder mechanisms. *Advances in Polymer Technology* **1**, 18-39.

Fadda HM, Mohamed MAM, and Basit AW (2008) Impairment of the in vitro drug release behaviour of oral modified release preparations in the presence of alcohol. *International Journal of Pharmaceutics* **360**, 171-6.

Faure A, York P, and Rowe RC (2001) Process control and scale-up of pharmaceutical wet granulation processes: a review. *European Journal of Pharmaceutics & Biopharmaceutics* **52**, 269-77.

FDA (2007) Draft Guidance on Tramadol. In (ed.), Vol. pp. Center for Drug Evaluation and Research (CDER).

FDA (2008) Guidance for Industry: Q3A Impurities in New Drug Substances. In *Revision 2*. (ed.), Vol. pp. Center for Drug Evaluation and Research (CDER).

Feng J, Xu L, Gao R, Luo Y, and Tang X (2012) Evaluation of polymer carriers with regard to the bioavailability enhancement of bifendate solid dispersions prepared by hot-melt extrusion. *Drug Development & Industrial Pharmacy* **38**, 735-43.

Fini A, Moyano JR, Ginés JM, Perez-Martinez JI, and Rabasco AM (2005) Diclofenac salts, II. Solid dispersions in PEG6000 and Gelucire 50/13. *European Journal of Pharmaceutics & Biopharmaceutics* **60**, 99-111.

Flory PJ (1942) Thermodynamics of High Polymer Solutions. *Journal of Chemical Physics* **10**, 51-61.

Forster A, Hempenstall J, and Rades T (2001) Characterization of glass solutions of poorly water-soluble drugs produced by melt extrusion with hydrophilic amorphous polymers. *Journal of Pharmacy & Pharmacology* **53**, 303-15.

Fox TG and Flory PJ (1950) Second-Order Transition Temperatures and Related Properties of Polystyrene. I. Influence of Molecular Weight. *Journal of Applied Physics* **21**, 581-91.

Francois M, Snoeckx E, Putteman P, Wouters F, De Proost E, Delaet U et al. (2003) A mucoadhesive, cyclodextrin-based vaginal cream formulation of itraconazole. *The AAPS Journal* **5**, 50-4.

Friesen DT, Shanker R, Crew M, Smithey DT, Curatolo WJ, and Nightingale JAS (2008) Hydroxypropyl Methylcellulose Acetate Succinate-Based Spray-Dried Dispersions: An Overview. *Molecular Pharmaceutics* **5**, 1003-19.

Fukuda M, Peppas NA, and McGinity JW (2006) Floating hot-melt extruded tablets for gastroretentive controlled drug release system. *Journal of Controlled Release* **115**, 121-9.

Galia E, Nicolaides E, Hörter D, Löbenberg R, Reppas C, and Dressman JB (1998) Evaluation of Various Dissolution Media for Predicting In Vivo Performance of Class I and II Drugs. *Pharmaceutical Research* **15**, 698-705.

Gao Y, Carr RA, Spence JK, Wang WW, Turner TM, Lipari JM et al. (2010) A pH-Dilution Method for Estimation of Biorelevant Drug Solubility along the Gastrointestinal Tract: Application to Physiologically Based Pharmacokinetic Modeling. *Molecular Pharmaceutics* **7**, 1516-26.

Garren KW, Rahim S, Marsh K, and Morris JB (2010) Bioavailability of generic ritonavir and lopinavir/ritonavir tablet products in a dog model. *Journal of Pharmaceutical Sciences* **99**, 626-31.

Gazzaniga A, Cerea M, Cozzi A, Foppoli A, Maroni A, and Zema L (2011) A Novel Injection-Molded Capsular Device for Oral Pulsatile Delivery Based on Swellable/Erodible Polymers. *AAPS PharmSciTech* **12**, 295-303.

Ghimire M, Hodges LA, Band J, Lindsay B, O'Mahony B, McInnes FJ et al. (2011) Correlation between in vitro and in vivo erosion behaviour of erodible tablets using gamma scintigraphy. *European Journal of Pharmaceutics & Biopharmaceutics* **77**, 148-57.

Gibbs JH and DiMarzio EA (1958) Nature of the Glass Transition and the Glassy State. *The Journal of Chemical Physics* **28**, 373-83.

Hamdani J, Moës AJ, and Amighi K (2003) Physical and thermal characterisation of Precirol® and Compritol® as lipophilic glycerides used for the preparation of controlled-release matrix pellets. *International Journal of Pharmaceutics* **260**, 47-57.

Hancock BC, Shamblin SL, and Zografi G (1995) Molecular Mobility of Amorphous Pharmaceutical Solids Below Their Glass Transition Temperatures. *Pharmaceutical Research* **12**, 799-806.

Hancock BC, York P, and Rowe RC (1997) The use of solubility parameters in pharmaceutical dosage form design. *International Journal of Pharmaceutics* **148**, 1-21.

Hancock BC and Zografi G (1997) Characteristics and significance of the amorphous state in pharmaceutical systems. *Journal of Pharmaceutical Sciences* **86**, 1-12.

Hancock BC and Zografi G (1994) The Relationship Between the Glass Transition Temperature and the Water Content of Amorphous Pharmaceutical Solids. *Pharmaceutical Research* **11**, 471-7.

Hasanzadeh D, Ghaffari S, Monajjemzadeh F, Al-Hallak M-K, Soltani G, and Azarmi S (2009) Thermal Treating of Acrylic Matrices as a Tool for Controlling Drug Release. *Chemical & Pharmaceutical Bulletin* **12**, 1356-62.

Hoeben BJ, Burgess DS, McConville JT, Najvar LK, Talbert RL, Peters JI et al. (2006) In Vivo Efficacy of Aerosolized Nanostructured Itraconazole Formulations for Prevention of Invasive Pulmonary Aspergillosis. *Antimicrobial Agents & Chemotherapy* **50**, 1552-4.

Hoffman AS (2008) The origins and evolution of “controlled” drug delivery systems. *Journal of Controlled Release* **132**, 153-63.

Huggins ML (1942) Thermodynamics Properties of Solutions of Long-Chain Compounds. *Annals of the New York Academy of Sciences* **43**, 1-32.

Hughey J, DiNunzio J, Bennett R, Brough C, Miller D, Ma H et al. (2010) Dissolution Enhancement of a Drug Exhibiting Thermal and Acidic Decomposition Characteristics by Fusion Processing: A Comparative Study of Hot Melt Extrusion and KinetiSol® Dispersing. *AAPS PharmSciTech* **11**, 760-74.

Hughey JR, Keen JM, Brough C, Saeger S, and McGinity JW (2011) Thermal processing of a poorly water-soluble drug substance exhibiting a high melting point: The utility of KinetiSol® Dispersing. *International Journal of Pharmaceutics* **419**, 222-30.

Hughey JR, Keen JM, Miller DA, Brough C, and McGinity JW (2012) Preparation of Viscous Solid Dispersion Systems by Hot-Melt Extrusion and KinetiSol® Dispersing: Polymer Screening and Thermal Stability. *International Journal of Pharmaceutics* **438**, 11-9.

Hughey JR, Keen JM, Miller DA, Kolter K, Langley N, and McGinity JW (2013) The use of inorganic salts to improve the dissolution characteristics of tablets containing Soluplus®-based solid dispersions. *European Journal of Pharmaceutical Sciences* **48**, 758-66.

Ilić I, Dreu R, Burjak M, Homar M, Kerč J, and Srčič S (2009) Microparticle size control and glimepiride microencapsulation using spray congealing technology. *International Journal of Pharmaceutics* **381**, 176-83.

Jannin V, Musakhanian J, and Marchaud D (2008) Approaches for the development of solid and semi-solid lipid-based formulations. *Advanced Drug Delivery Reviews* **60**, 734-46.

Janssens S and Van den Mooter G (2009) Review: physical chemistry of solid dispersions. *Journal of Pharmacy & Pharmacology* **61**, 1571-86.

Jenning V, Schäfer-Korting M, and Gohla S (2000) Vitamin A-loaded solid lipid nanoparticles for topical use: drug release properties. *Journal of Controlled Release* **66**, 115-26.

Joshi HN, Tejwani RW, Davidovich M, Sahasrabudhe VP, Jemal M, Bathala MS et al. (2004) Bioavailability enhancement of a poorly water-soluble drug by solid dispersion in polyethylene glycol–polysorbate 80 mixture. *International Journal of Pharmaceutics* **269**, 251-8.

Joshi SC (2011) Sol-Gel Behavior of Hydroxypropyl Methylcellulose (HPMC) in Ionic Media Including Drug Release. *Materials* **4**, 1861-905.

Kablitz CD, Harder K, and Urbanetz NA (2006) Dry coating in a rotary fluid bed. *European Journal of Pharmaceutical Sciences* **27**, 212-9.

Kablitz CD and Urbanetz NA (2007) Characterization of the film formation of the dry coating process. *European Journal of Pharmaceutics & Biopharmaceutics* **67**, 449-57.

Kato Y, Sunada H, Yonezawa Y, and Ishino R (1994) Sustained release mechanisms of wax matrix system for controlled release. *Chemical & Pharmaceutical Bulletin* **42**, 1646-50.

Kawabata Y, Wada K, Nakatani M, Yamada S, and Onoue S (2011) Formulation design for poorly water-soluble drugs based on biopharmaceutics classification system: Basic approaches and practical applications. *International Journal of Pharmaceutics* **420**, 1-10.

Keary CM (2001) Characterization of METHOCEL cellulose ethers by aqueous SEC with multiple detectors. *Carbohydrate Polymers* **45**, 293-303.

Keen JM, Martin C, Machado A, Sandhu H, McGinity JW, and DiNunzio JC (2013) Investigation of process temperature and screw speed on properties of a pharmaceutical solid dispersion using corotating and counter-rotating twin-screw extruders. *Journal of Pharmacy & Pharmacology* n/a-n/a.

Keseru GM and Makara GM (2009) The influence of lead discovery strategies on the properties of drug candidates. *Nature Reviews. Drug Discovery* **8**, 203-12.

Kolašinac N, Kachrimanis K, Homšek I, Grujić B, Đurić Z, and Ibrić S (2012) Solubility enhancement of desloratadine by solid dispersion in poloxamers. *International Journal of Pharmaceutics* **436**, 161-70.

Kolter K, Karl M, Nalawade S, and Rottmann N (2010) Hot-Melt Extrusion with BASF Pharma Polymers: Extrusion Compendium. In BASF (ed.), (ed.), Vol. pp. Ludwigshafen, Germany.

Lakshman JP, Kowalski J, Vasanthavada M, Tong W-Q, Joshi YM, and Serajuddin ATM (2011) Application of melt granulation technology to enhance tableting properties of poorly compactible high-dose drugs. *Journal of Pharmaceutical Sciences* **100**, 1553-65.

Lee PI (2011) Modeling of drug release from matrix systems involving moving boundaries: Approximate analytical solutions. *International Journal of Pharmaceutics* **418**, 18-27.

Leuner C and Dressman J (2000) Improving drug solubility for oral delivery using solid dispersions. *European Journal of Pharmaceutics & Biopharmaceutics* **50**, 47-60.

Lin D and Huang Y (2010) A thermal analysis method to predict the complete phase diagram of drug-polymer solid dispersions. *International Journal of Pharmaceutics* **399**, 109-15.

Lionberger R, Lee S, Lee L, Raw A, and Yu L (2008) Quality by Design: Concepts for ANDAs. *The AAPS Journal* **10**, 268-76.

Liu H, Wang P, Zhang X, Shen F, and Gogos CG (2010) Effects of extrusion process parameters on the dissolution behavior of indomethacin in Eudragit® E PO solid dispersions. *International Journal of Pharmaceutics* **383**, 161-9.

Liu J, Zhang F, and McGinity JW (2001) Properties of lipophilic matrix tablets containing phenylpropanolamine hydrochloride prepared by hot-melt extrusion. *European Journal of Pharmaceutics & Biopharmaceutics* **52**, 181-90.

Lo JB, Appel LE, Herbig SM, McCray SB, and Thombre AG (2009) Formulation design and pharmaceutical development of a novel controlled release form of azithromycin for single-dose therapy. *Drug Development & Industrial Pharmacy* **35**, 1522-9.

Luo Y, Zhu J, Ma Y, and Zhang H (2008) Dry coating, a novel coating technology for solid pharmaceutical dosage forms. *International Journal of Pharmaceutics* **358**, 16-22.

Malamataris S, Karidas T, and Goidas P (1994) Effect of particle size and sorbed moisture on the compression behaviour of some hydroxypropyl methylcellulose (HPMC) polymers. *International Journal of Pharmaceutics* **103**, 205-15.

Malcolm RK, Edwards K-L, Kiser P, Romano J, and Smith TJ (2010) Advances in microbicide vaginal rings. *Antiviral Research* **88, Supplement**, S30-S9.

Manas-Zloczower I (2009) Continuous Process Visualization: Visual Observation, On-Line Monitoring, Model-Fluid Extrusion and Simulation. In *Mixing and Compounding of Polymers*. Manas-Zloczower I (ed.), 2nd Edition (ed.), Vol. pp. 473-572. Hanser Publications, Munich.

Marsac P, Li T, and Taylor L (2009) Estimation of Drug–Polymer Miscibility and Solubility in Amorphous Solid Dispersions Using Experimentally Determined Interaction Parameters. *Pharmaceutical Research* **26**, 139-51.

Marsac P, Shamblin S, and Taylor L (2006) Theoretical and Practical Approaches for Prediction of Drug–Polymer Miscibility and Solubility. *Pharmaceutical Research* **23**, 2417-26.

Martin C (2004) Counter-Rotating Twin-Screw Extruders. In (ed.), Vol. pp. 101-6, RonJon Publishing, Denton, TX, SPE Plastics Technician’s Toolbox – Extrusion, Drawer 4: Single & Twin-Screw Extruders, Section: Twin Screw Extruders.

Mehuys E, Remon JP, Korst A, Van Bortel L, Mols R, Augustijns P et al. (2005) Human bioavailability of propranolol from a matrix-in-cylinder system with a HPMC-Gelucire® core. *Journal of Controlled Release* **107**, 523-36.

Mehuys E, Vervaet C, Gielen I, Van Bree H, and Remon JP (2004a) In vitro and in vivo evaluation of a matrix-in-cylinder system for sustained drug delivery. *Journal of Controlled Release* **96**, 261-71.

Mehuys E, Vervaet C, and Remon JP (2004b) Hot-melt extruded ethylcellulose cylinders containing a HPMC-Gelucire® core for sustained drug delivery. *Journal of Controlled Release* **94**, 273-80.

Mellaerts R, Mols R, Jammaer JAG, Aerts CA, Annaert P, Van Humbeeck J et al. (2008) Increasing the oral bioavailability of the poorly water soluble drug itraconazole with ordered mesoporous silica. *European Journal of Pharmaceutics & Biopharmaceutics* **69**, 223-30.

Miller D, DiNunzio J, Yang W, McGinity J, and Williams R (2008a) Targeted Intestinal Delivery of Supersaturated Itraconazole for Improved Oral Absorption. *Pharmaceutical Research* **25**, 1450-9.

Miller DA, DiNunzio JC, Yang W, McGinity JW, and Williams RO (2008b) Enhanced In Vivo Absorption of Itraconazole via Stabilization of Supersaturation Following Acidic-to-Neutral pH Transition. *Drug Development & Industrial Pharmacy* **34**, 890-902.

Miller DA, McConville JT, Yang W, Williams RO, and McGinity JW (2007) Hot-melt extrusion for enhanced delivery of drug particles. *Journal of Pharmaceutical Sciences* **96**, 361-76.

Minnich CB, Greiner L, Reimers C, Uerdingen M, and Liauw MA (2011) Bridging the gap: A nested-pipe reactor for slow reactions in continuous flow chemical synthesis. *Chemical Engineering Journal* **168**, 759-64.

Monti D, Burgalassi S, Rossato MS, Albertini B, Passerini N, Rodriguez L et al. (2010) Poloxamer 407 microspheres for orotransmucosal drug delivery. Part II: In vitro/in vivo evaluation. *International Journal of Pharmaceutics* **400**, 32-6.

Mu B and Thompson MR (2012) Examining the mechanics of granulation with a hot melt binder in a twin-screw extruder. *Chemical Engineering Science* **81**, 46-56.

Nair R, Nyamweya N, Gönen S, Martínez-Miranda LJ, and Hoag SW (2001) Influence of various drugs on the glass transition temperature of poly(vinylpyrrolidone): a thermodynamic and spectroscopic investigation. *International Journal of Pharmaceutics* **225**, 83-96.

Newa M, Bhandari KH, Li DX, Kwon T-H, Kim JA, Yoo BK et al. (2007) Preparation, characterization and in vivo evaluation of ibuprofen binary solid dispersions with poloxamer 188. *International Journal of Pharmaceutics* **343**, 228-37.

Newman A, Knipp G, and Zografi G (2012) Assessing the performance of amorphous solid dispersions. *Journal of Pharmaceutical Sciences* **101**, 1355-77.

Nukala R, Boyapally H, Slipper I, Mendham A, and Douroumis D (2010) The Application of Electrostatic Dry Powder Deposition Technology to Coat Drug-Eluting Stents. *Pharmaceutical Research* **27**, 72-81.

Ochoa L, Igartua M, Hernández RM, Solinís MÁ, Gascón AR, and Pedraz JL (2010) In vivo evaluation of two new sustained release formulations elaborated by one-step melt granulation: Level A in vitro–in vivo correlation. *European Journal of Pharmaceutics & Biopharmaceutics* **75**, 232-7.

Passerini N, Albertini B, Perissutti B, and Rodriguez L (2006) Evaluation of melt granulation and ultrasonic spray congealing as techniques to enhance the dissolution of praziquantel. *International Journal of Pharmaceutics* **318**, 92-102.

Passerini N, Calogerà G, Albertini B, and Rodriguez L (2010) Melt granulation of pharmaceutical powders: A comparison of high-shear mixer and fluidised bed processes. *International Journal of Pharmaceutics* **391**, 177-86.

Pingali K, Mendez R, Lewis D, Michniak-Kohn B, Cuitino A, and Muzzio F (2011) Mixing order of glidant and lubricant – Influence on powder and tablet properties. *International Journal of Pharmaceutics* **409**, 269-77.

Plumb K (2005) Continuous Processing in the Pharmaceutical Industry: Changing the Mind Set. *Chemical Engineering Research and Design* **83**, 730-8.

Poulesquen A and Vergnes B (2003) A study of residence time distribution in co-rotating twin-screw extruders. Part I: Theoretical modeling. *Polymer Engineering & Science* **43**, 1841-8.

Poulesquen A, Vergnes B, Cassagnau P, Michel A, Carneiro OS, and Covas JA (2003) A study of residence time distribution in co-rotating twin-screw extruders. Part II: Experimental validation. *Polymer Engineering & Science* **43**, 1849-62.

Qiao M, Zhang L, Ma Y, Zhu J, and Chow K (2010) A novel electrostatic dry powder coating process for pharmaceutical dosage forms: Immediate release coatings for tablets. *European Journal of Pharmaceutics & Biopharmaceutics* **76**, 304-10.

Quinten T, Beer TD, Vervaet C, and Remon JP (2009a) Evaluation of injection moulding as a pharmaceutical technology to produce matrix tablets. *European Journal of Pharmaceutics & Biopharmaceutics* **71**, 145-54.

Quinten T, De Beer T, Onofre FO, Mendez-Montealvo G, Wang YJ, Remon JP et al. (2011) Sustained-release and swelling characteristics of xanthan gum/ethylcellulose-based injection moulded matrix tablets: in vitro and in vivo evaluation. *Journal of Pharmaceutical Sciences* **100**, 2858-70.

Quinten T, Gonnissen Y, Adriaens E, Beer TD, Cnudde V, Masschaele B et al. (2009b) Development of injection moulded matrix tablets based on mixtures of ethylcellulose and low-substituted hydroxypropylcellulose. *European Journal of Pharmaceutical Sciences* **37**, 207-16.

Rao M, Ranpise A, Borate S, and Thanki K (2009) Mechanistic Evaluation of the Effect of Sintering on Compritol® 888 ATO Matrices. *AAPS PharmSciTech* **10**, 355-60.

Read EK, Park JT, Shah RB, Riley BS, Brorson KA, and Rathore AS (2010) Process analytical technology (PAT) for biopharmaceutical products: Part I. concepts and applications. *Biotechnology & Bioengineering* **105**, 276-84.

Reitz C and Kleinebudde P (2007) Solid lipid extrusion of sustained release dosage forms. *European Journal of Pharmaceutics & Biopharmaceutics* **67**, 440-8.

Repka MA, Battu SK, Upadhye SB, Thumma S, Crowley MM, Zhang F et al. (2007) Pharmaceutical Applications of Hot-Melt Extrusion: Part II. *Drug Development & Industrial Pharmacy* **33**, 1043-57.

Repka MA, Gutta K, Prodduturi S, Munjal M, and Stodghill SP (2005) Characterization of cellulosic hot-melt extruded films containing lidocaine. *European Journal of Pharmaceutics & Biopharmaceutics* **59**, 189-96.

Repka MA, Majumdar S, Kumar Battu S, Srirangam R, and Upadhye SB (2008) Applications of hot-melt extrusion for drug delivery. *Expert Opinion on Drug Delivery* **5**, 1357-76.

Sammoura F, Kang J, Heo Y-M, Jung T, and Lin L (2007) Polymeric microneedle fabrication using a microinjection molding technique. *Microsystem Technologies* **13**, 517-22.

Sato H, Miyagawa Y, Okabe T, Miyajima M, and Sunada H (1997) Dissolution mechanism of diclofenac sodium from wax matrix granules. *Journal of Pharmaceutical Sciences* **86**, 929-34.

Sauer D, Zheng W, Coots LB, and McGinity JW (2007) Influence of processing parameters and formulation factors on the drug release from tablets powder-coated with Eudragit® L 100-55. *European Journal of Pharmaceutics & Biopharmaceutics* **67**, 464-75.

Sax G, Feil F, Schulze S, Jung C, Bräuchle C, and Winter G (2012) Release pathways of interferon  $\alpha$ 2a molecules from lipid twin screw extrudates revealed by single molecule fluorescence microscopy. *Journal of Controlled Release*

Schaber SD, Gerogiorgis DI, Ramachandran R, Evans JMB, Barton PI, and Trout BL (2011) Economic Analysis of Integrated Continuous and Batch Pharmaceutical

Manufacturing: A Case Study. *Industrial & Engineering Chemistry Research* **50**, 10083-92.

Schulze S and Winter G (2009) Lipid extrudates as novel sustained release systems for pharmaceutical proteins. *Journal of Controlled Release* **134**, 177-85.

Sekiguchi K, Obi N, and Ueda Y (1964) Studies on Absorption of Eutectic Mixture. II. Absorption of fused Conglomerates of Chloramphenicol and Urea in Rabbits. *Chemical & Pharmaceutical Bulletin* **12**, 134-44.

Serajuddin ATM (1999) Solid dispersion of poorly water-soluble drugs: Early promises, subsequent problems, and recent breakthroughs. *Journal of Pharmaceutical Sciences* **88**, 1058-66.

Shah A and Gupta M (2004) Comparison of the Flow in Co-Rotating and Counter-Rotating Twin-Screw Extruders. In *ANTEC, Conference Proceedings*. (ed.), Vol. 1, pp. 443-7,

Siepmann J and Siepmann F (2011) Mathematical modeling of drug release from lipid dosage forms. *International Journal of Pharmaceutics* **418**, 42-53.

Singh R, Poddar S, and Chivate A (2007) Sintering of wax for controlling release from pellets. *AAPS PharmSciTech* **8**, E175-E83.

Six K, Daems T, de Hoon J, Van Hecken A, Depre M, Bouche M-P et al. (2005) Clinical study of solid dispersions of itraconazole prepared by hot-stage extrusion. *European Journal of Pharmaceutical Sciences* **24**, 179-86.

Six K, Verreck G, Peeters J, Augustijns P, Kinget R, and Van den Mooter G (2001) Characterization of glassy itraconazole: a comparative study of its molecular mobility below T<sub>g</sub> with that of structural analogues using MTDSC. *International Journal of Pharmaceutics* **213**, 163-73.

Sochon RPJ, Zomer S, Cartwright JJ, Hounslow MJ, and Salman AD (2010) The variability of pharmaceutical granulation. *Chemical Engineering Journal* **164**, 285-91.

Srinarong P, Faber JH, Visser MR, Hinrichs WLJ, and Frijlink HW (2009) Strongly enhanced dissolution rate of fenofibrate solid dispersion tablets by incorporation of superdisintegrants. *European Journal of Pharmaceutics & Biopharmaceutics* **73**, 154-61.

Streubel A, Siepmann J, and Bodmeier R (2006) Drug delivery to the upper small intestine window using gastroretentive technologies. *Current Opinion in Pharmacology* **6**, 501-8.

Sudha B, Sridhar B, and Srinatha A (2010) Modulation of Tramadol Release from a Hydrophobic Matrix: Implications of Formulations and Processing Variables. *AAPS PharmSciTech* **11**, 433-40.

Tadmor Z and Gogos CG (2006) Principles of Polymer Processing. In 2 (ed.), Vol. pp. Wiley-Interscience, Hoboken.

Tanaka N, Imai K, Okimoto K, Ueda S, Tokunaga Y, Ibuki R et al. (2006) Development of novel sustained-release system, disintegration-controlled matrix tablet (DCMT) with solid dispersion granules of nilvadipine (II): In vivo evaluation. *Journal of Controlled Release* **112**, 51-6.

Tang B, Cheng G, Gu J-C, and Xu C-H (2008) Development of solid self-emulsifying drug delivery systems: preparation techniques and dosage forms. *Drug Discovery Today* **13**, 606-12.

Tayel S, Soliman I, and Louis D (2010) Formulation of Ketotifen Fumarate Fast-Melt Granulation Sublingual Tablet. *AAPS PharmSciTech* **11**, 679-85.

Terife G, Wang P, Faridi N, and Gogos CG (2012) Hot melt mixing and foaming of soluplus® and indomethacin. *Polymer Engineering & Science* **52**, 1629-39.

Tho I, Liepold B, Rosenberg J, Maegerlein M, Brandl M, and Fricker G (2010) Formation of nano/micro-dispersions with improved dissolution properties upon dispersion of ritonavir melt extrudate in aqueous media. *European Journal of Pharmaceutical Sciences* **40**, 25-32.

Tian Y, Booth J, Meehan E, Jones DS, Li S, and Andrews GP (2012) Construction of Drug–Polymer Thermodynamic Phase Diagrams Using Flory–Huggins Interaction Theory: Identifying the Relevance of Temperature and Drug Weight Fraction to Phase Separation within Solid Dispersions. *Molecular Pharmaceutics* **10**, 236-48.

Tran P, Tran T, Park J, and Lee B-J (2011) Controlled Release Systems Containing Solid Dispersions: Strategies and Mechanisms. *Pharmaceutical Research* **28**, 2353-78.

Tucker III C (2009) Mixing of Miscible Liquids. In *Mixing and Compounding of Polymers*. Manas-Zloczower I (ed.), 2nd Edition (ed.), Vol. pp. 5-38. Hanser Publications, Munich.

Urbanetz NA and Lippold BC (2005) Solid dispersions of nimodipine and polyethylene glycol 2000: dissolution properties and physico-chemical characterisation. *European Journal of Pharmaceutics & Biopharmaceutics* **59**, 107-118.

Van den Mooter G (2012) The use of amorphous solid dispersions: A formulation strategy to overcome poor solubility and dissolution rate. *Drug Discovery Today: Technologies* **9**, e79-e85.

Van Melkebeke B, Vermeulen B, Vervaet C, and Remon JP (2006) Melt granulation using a twin-screw extruder: A case study. *International Journal of Pharmaceutics* **326**, 89-93.

Vasanthavada M, Wang Y, Haeefele T, Lakshman JP, Mone M, Tong W et al. (2011) Application of melt granulation technology using twin-screw extruder in development of high-dose modified-release tablet formulation. *Journal of Pharmaceutical Sciences* **100**, 1923-34.

Vasconcelos T, Sarmento B, and Costa P (2007) Solid dispersions as strategy to improve oral bioavailability of poor water soluble drugs. *Drug Discovery Today* **12**, 1068-75.

Vaughn JM, McConville JT, Burgess D, Peters JI, Johnston KP, Talbert RL et al. (2006) Single dose and multiple dose studies of itraconazole nanoparticles. *European Journal of Pharmaceutics & Biopharmaceutics* **63**, 95-102.

Verhoeven E, De Beer TRM, Schacht E, Van den Mooter G, Remon JP, and Vervaet C (2009) Influence of polyethylene glycol/polyethylene oxide on the release characteristics of sustained-release ethylcellulose mini-matrices produced by hot-melt extrusion: in vitro

and in vivo evaluations. *European Journal of Pharmaceutics & Biopharmaceutics* **72**, 463-70.

Verhoeven E, Vervaet C, and Remon JP (2006) Xanthan gum to tailor drug release of sustained-release ethylcellulose mini-matrices prepared via hot-melt extrusion: in vitro and in vivo evaluation. *European Journal of Pharmaceutics & Biopharmaceutics* **63**, 320-30.

Verreck G, Decorte A, Heymans K, Adriaensen J, Cleeren D, Jacobs A et al. (2005) The effect of pressurized carbon dioxide as a temporary plasticizer and foaming agent on the hot stage extrusion process and extrudate properties of solid dispersions of itraconazole with PVP-VA 64. *European Journal of Pharmaceutical Sciences* **26**, 349-58.

Vervaet C and Remon JP (2005) Continuous granulation in the pharmaceutical industry. *Chemical Engineering Science* **60**, 3949-57.

Vilhelmsen T and Schæfer T (2005) Agglomerate formation and growth mechanisms during melt agglomeration in a rotary processor. *International Journal of Pharmaceutics* **304**, 152-64.

Wan LSC, Heng PWS, and Muhuri G (1992) Incorporation and distribution of a low dose drug in granules. *International Journal of Pharmaceutics* **88**, 159-63.

Windbergs M, Haaser M, McGoverin CM, Gordon KC, Kleinebudde P, and Strachan CJ (2010) Investigating the relationship between drug distribution in solid lipid matrices and dissolution behaviour using raman spectroscopy and mapping. *Journal of Pharmaceutical Sciences* **99**, 1464-75.

Windbergs M, Strachan CJ, and Kleinebudde P (2009) Understanding the solid-state behaviour of triglyceride solid lipid extrudates and its influence on dissolution. *European Journal of Pharmaceutics & Biopharmaceutics* **71**, 80-7.

Yang D, Kulkarni R, Behme RJ, and Kotiyani PN (2007) Effect of the melt granulation technique on the dissolution characteristics of griseofulvin. *International Journal of Pharmaceutics* **329**, 72-80.

Yoo S, Kang E, Shin B, Jun H, Lee S-H, Lee K et al. (2002) Interspecies comparison of the oral absorption of itraconazole in laboratory animals. *Archives of Pharmacal Research* **25**, 387-91.

Yu L (2008) Pharmaceutical Quality by Design: Product and Process Development, Understanding, and Control. *Pharmaceutical Research* **25**, 781-91.

Zema L, Loreti G, Melocchi A, Maroni A, and Gazzaniga A (2012) Injection Molding and its application to drug delivery. *Journal of Controlled Release* **159**, 324-31.

Zhang X-M, Feng L-F, Hoppe S, and Hu G-H (2008) Local residence time, residence revolution, and residence volume distributions in twin-screw extruders. *Polymer Engineering & Science* **48**, 19-28.

Zhang Y and Cremer PS (2006) Interactions between macromolecules and ions: the Hofmeister series. *Current Opinion in Chemical Biology* **10**, 658-63.

Zhao Y, Inbar P, Chokshi HP, Malick AW, and Choi DS (2011) Prediction of the thermal phase diagram of amorphous solid dispersions by flory–huggins theory. *Journal of Pharmaceutical Sciences* **100**, 3196-207.

Zheng X, Yang R, Zhang Y, Wang Z, Tang X, and Zheng L (2007) Part II:  
Bioavailability in Beagle Dogs of Nimodipine Solid Dispersions Prepared by Hot-Melt  
Extrusion. *Drug Development & Industrial Pharmacy* **33**, 783-9.

## **Vita**

Justin Martin Keen was born on October 31, 1979 in Idaho Falls, Idaho to Charles and Velda Keen where his father was an instructor at the Navy Nuclear Power Training Unit. His family relocated to Bay City, TX where Justin graduated from Bay City High School in 1998. Justin studied Chemical Engineering at the University of Texas at Austin, where he earned his Bachelor of Science degree in December of 2002 and held an undergraduate research position under the supervision of Dr. James W. McGinity and Dr. Robert O Williams, III. Justin began his career as a Formulation Scientist at DPT Laboratories in San Antonio in January 2003. In the summer of 2004, Justin returned to Austin where he joined PharmaForm and eventually became Director of Manufacturing for their facility, which operated primarily in the development and initial scale up of solid oral pharmaceuticals for human clinical trials. In these roles, Justin worked on several current commercial pharmaceutical products, both over the counter and prescription, and developed processing expertise in hot-melt extrusion. Justin married his wife Kelly Danielle Kutch in December of 2005. They welcomed their daughter, Kinsley Denise, in 2008 and are currently expecting their son, Bennett Myrl, in December 2013. In the fall of 2010, he joined the College of Pharmacy as a graduate student under the supervision of Dr. James W. McGinity and Dr. Robert O. Williams, III. Justin is a coauthor of three issued patents and six patent applications, all related to hot-melt extrusion of pharmaceuticals. Justin has presented his work in the form of posters at national and international conferences and is the first author on two publications, reproduced here as Chapters 1 and 3. The remaining research chapters will be submitted to high impact pharmaceutical journals. Justin is a coauthor of three publications resulting from collaborations with graduate students during graduate school. In addition, Justin has one published first author book chapter and is a coauthor for a book chapter currently in

press. Justin has also given two invited presentations at national and international conferences.

Permanent Address: 608 S. Lake Creek Dr., Round Rock, TX, 78681

This dissertation was typed by the author.